NUREG/CP-0149
Vol. 3

Proceedings of the U.S. Nuclear Regulatory Commission

Twenty-Third Water Reactor Safety Information Meeting

Volume 3

- Structural & Seismic Engineering
- Primary Systems Integrity
- Equipment Operability and Aging
- ECCS Strainer Blockage Research & Regulatory Issues

Held at
Bethesda Marriott Hotel
Bethesda, Maryland
October 23–25, 1995

U.S. Nuclear Regulatory Commission

Office of Nuclear Regulatory Research

Proceedings prepared by
Brookhaven National Laboratory

AVAILABILITY NOTICE

Availability of Reference Materials Cited in NRC Publications

Most documents cited in NRC publications will be available from one of the following sources:

1. The NRC Public Document Room, 2120 L Street, NW., Lower Level, Washington, DC 20555-0001

2. The Superintendent of Documents, U.S. Government Printing Office, P. O. Box 37082, Washington, DC 20402-9328

3. The National Technical Information Service, Springfield, VA 22161-0002

Although the listing that follows represents the majority of documents cited in NRC publications, it is not intended to be exhaustive.

Referenced documents available for inspection and copying for a fee from the NRC Public Document Room include NRC correspondence and internal NRC memoranda; NRC bulletins, circulars, information notices, inspection and investigation notices; licensee event reports; vendor reports and correspondence; Commission papers; and applicant and licensee documents and correspondence.

The following documents in the NUREG series are available for purchase from the Government Printing Office: formal NRC staff and contractor reports, NRC-sponsored conference proceedings, international agreement reports, grantee reports, and NRC booklets and brochures. Also available are regulatory guides, NRC regulations in the *Code of Federal Regulations*, and *Nuclear Regulatory Commission Issuances*.

Documents available from the National Technical Information Service include NUREG-series reports and technical reports prepared by other Federal agencies and reports prepared by the Atomic Energy Commission, forerunner agency to the Nuclear Regulatory Commission.

Documents available from public and special technical libraries include all open literature items, such as books, journal articles, and transactions. *Federal Register* notices, Federal and State legislation, and congressional reports can usually be obtained from these libraries.

Documents such as theses, dissertations, foreign reports and translations, and non-NRC conference proceedings are available for purchase from the organization sponsoring the publication cited.

Single copies of NRC draft reports are available free, to the extent of supply, upon written request to the Office of Administration, Distribution and Mail Services Section, U.S. Nuclear Regulatory Commission, Washington, DC 20555-0001.

Copies of industry codes and standards used in a substantive manner in the NRC regulatory process are maintained at the NRC Library, Two White Flint North, 11545 Rockville Pike, Rockville, MD 20852-2738, for use by the public. Codes and standards are usually copyrighted and may be purchased from the originating organization or, if they are American National Standards, from the American National Standards Institute, 1430 Broadway, New York, NY 10018-3308.

DISCLAIMER NOTICE

NUREG/CP-0149
Vol. 3

Proceedings of the U.S. Nuclear Regulatory Commission

Twenty-Third Water Reactor Safety Information Meeting

Volume 3

- Structural & Seismic Engineering
- Primary Systems Integrity
- Equipment Operability and Aging
- ECCS Strainer Blockage Research & Regulatory Issues

Held at
Bethesda Marriott Hotel
Bethesda, Maryland
October 23–25, 1995

Manuscript Completed: February 1996
Date Published: March 1996

Compiled by: Susan Monteleone

C. Bonsby, NRC Project Manager

Office of Nuclear Regulatory Research
U.S. Nuclear Regulatory Commission
Washington, DC 20555–0001

Proceedings prepared by
Brookhaven National Laboratory

NUREG/CP-0149, Vol. 3, has been reproduced from the best available copy.

ABSTRACT

This three-volume report contains papers presented at the Twenty-Third Water Reactor Safety Information Meeting held at the Bethesda Marriott Hotel, Bethesda, Maryland, October 23-25, 1995. The papers are printed in the order of their presentation in each session and describe progress and results of programs in nuclear safety research conducted in this country and abroad. Foreign participation in the meeting included papers presented by researchers from France, Italy, Japan, Norway, Russia, Sweden, and Switzerland. The titles of the papers and the names of the authors have been updated and may differ from those that appeared in the final program of the meeting.

PROCEEDINGS OF THE
23rd WATER REACTOR SAFETY INFORMATION MEETING

October 23-25, 1995

Published in Three Volumes

GENERAL INDEX

VOLUME 1

VOLUME 2

VOLUME 3

REGISTERED ATTENDEES (NON-NRC)
23RD WATER REACTOR SAFETY INFORMATION MEETING

D. AGARWAL
U.S. DEPARTMENT OF ENERGY
NE-50/GTN-E478
WASHINGTON, DC 20585 USA

M. AHMED
WESTINGHOUSE ELECTRIC CORP.
4350 NORTHERN PIKE
MONROEVILLE, PA 15146-2886 USA

T. AL-H ISSAINI
DUKE POWER CO.
1010 SHORELINE CO.
STANLEY, NC 28164 USA

M. ALLEN
SANDIA NATIONAL LABORATORY
PO BOX 5800
ALBUQUERQUE, NM 87185-1137 USA

C. ALLISON
IDAHO NATIONAL ENGINEERING LAB
PO BOX 1625, MS 3840
IDAHO FALLS, ID 83415 USA

A. ALONSO
SONSEJO DE SEGURIDAD NUCLEAR
JUSTO DORADO, 11
MADRID, 28040 SPAIN

R. ANDERSON
NORTHERN STATES POWER CO.
414 NICOLLET MALL
MINNEAPOLIS, MN 55401 USA

A. ANKRUM
PACIFIC NORTHWEST LAB
PO BOX 999, MS K828
RICHLAND, WA 99352 USA

K. ARAI
TOSHIBA NUCLEAR ENGINEERING LAB
4-1, UKISHIMA-CHI, KAWASAKI-KU
KAWASAKI, 210 JAPAN

P. ARNOLD
PJA ENGINEERING
FORCHHEIMERSTR. 31
ERLANGEN, 91056 GERMANY

V. ASMOLOV
RRC "KURCHATOV INSTITUTE"
KURCHATOV SQUARE 1
MOSCOW, 123182 RUSSIA

S. AZUMI
KANSAI ELECTRIC POWER CO., INC.
2001 L ST., N.W., SUITE 801
WASHINGTON, DC 20036 USA

M. BALE
B&W FUEL COMPANY
3315 OLD FOREST RD
LYNCHBURG, VA 24506-0935 USA

A. BARATTA
PENN STATE UNIVERSITY
231 SACKETT
UNIVERSITY PARK, PA 16803 USA

J. BARDELAY
IIPSN/CEA
60-68 AV. DU GEN. LECLERC PG6
FONTENAY AUX ROSES, 92265 FRANCE

R. BARI
BROOKHAVEN NATIONAL LABORATORY
BLDG. 197C, PO BOX 5000
UPTON, NY 11973-5000 USA

M. BEAUMONT
WESTINGHOUSE ELECTRIC CORPORATION
11921 ROCKVILLE PIKE - SUITE 450
ROCKVILLE, MD 20852 USA

J. BECKHAM
SOUTHERN NUCLEAR-GEORGIA POWER CO.
PO BOX 1295
BIRMINGHAM, AL 35201 USA

L. BELBLIDIA
SCANDPOWR, INC.
101 LAKE FOREST BLVD, #340
GAITHERSBURG, MD 20877 USA

D. BERRY
SANDIA NATIONAL LABORATORY
P.O. BOX 5800
ALBUQUERQUE, NM 87185-0744 USA

C. BEYER
BATTELLE PNL
11300 W. COURT
PASCO, WA 99302 USA

D. BHARGAVA
VIRGINIA POWER
5000 DOMINION BLVD.
GLEN ALLEN, VA 23060 USA

N. BIXLER
SANDIA NATIONAL LABORATORY
P.O. BOX 5800
ALBUQUERQUE, NM 87185-0739 USA

T. BJORLO
OECD HALDEN REACTOR PROJECT
P.O. BOX 173, OS ALLE 4
N-1751 HALDEN, NORWAY

J. BLASS
OAK RIDGE NATIONAL LABORATORY
236 GUM HOLLOW ROAD
OAK RIDGE, TN 37830 USA

J. BOCCIO
BROOKHAVEN NATIONAL LABORATORY
BLDG. 130, PO BOX 5000
UPTON, NY 11973-5000 USA

L. BOLSHOV
RUSSIAN ACADEMY OF SCIENCES
B. TULSKAYA, 52
MOSCOW, 113191 RUSSIA

M. BONNER
BROOKHAVEN NATIONAL LABORATORY
BLDG. 197C, PO BOX 5000
UPTON, NY 11973-5000 USA

B. BOYACK
LOS ALAMOS NATIONAL LABORATORY
P.O. BOX 1663
LOS ALAMOS, NM 87575 USA

U. BREDOLT
ABB ATOM
ABB ATOM AKTIEBOLAG
VASTERAS S72163 SWEDEN

G. BROWN
AEA TECHNOLOGY
TH5C8, RISLEY WARRINGTON
CHESHIRE, WA36A5 ENGLAND

T. BROWN
SANDIA NATIONAL LABORATORY
PO BOX 5800
ALBUQUERQUE, NM 87185-0748 USA

R. BUDNITZ
FUTURE RESOURCES ASSOCIATES INC.
2039 SHATTUCK AVENUE, SUITE 402
BERKELEY, CA 94704 USA

S. CALPENA
DIR. FOR SAFETY OF NUCLEAR INSTALLATIONS
60-64 AV. DE LA DIVISION LECLERC
FONTENAY AUX ROSES, 92265 FRANCE

A. CAMP
SANDIA LABS.
P.O. BOX 5800, MS 0747
ALBUQUERQUE, NM 87185 USA

G. CAPPONI
ANPA
VIA VITALIANO BRANCATI, 48
ROME, 00144 ITALY

R. CARLSON
LAWRENCE LIVERMORE NATIONAL LAB.
PO BOX 808, L634
LIVERMORE, CA 94551 USA

M. CARLSSON
STUDSVIK NUCLEAR AB
S-611 82 NYKOPING
NYKOPING, S-611 82 SWEDEN

D. CASADA
OAK RIDGE NATIONAL LABORATORY
P.O. BOX 2009
OAK RIDGE, TN 37831-8065 USA

N. CAVLINA
U. OF ZAGREB, ELECT. ENG'G & COMPUTING
UNSKA 3
ZAGREB, 10000 CROATIA

S. CHAKRABORTY
SWISS FEDERAL NUCLEAR SAFETY
INSPECTORATE
VILLIGEN, CH-5232 SWITZERLAND

W. CHEN
ENERGY TECHNOLOGY ENGIN. CENTER
6633 CANOGA AVENUE
CANOGA PARK, CA 91304 USA

F.B. CHEUNG
PENNSYLVANIA STATE UNIVERSITY
304 REBER BLDG.
UNIVERSITY PARK, PA 16802 USA

D. CHO
ARGONNE NATIONAL LABORATORY
9700 CO. CASS AVE., BLDG. 208
ARGONNE, IL 60439 USA

J.S. CHOI
KOREA INSTITUTE OF NUCLEAR SAFETY
PO BOX 114
YUSUNG, TAEJON, 305-600 KOREA

T. CHU
SANDIA NATIONAL LABORATORY
PO BOX 5800
ALBUQUERQUE, NM 87185-1137 USA

H. CHUNG
ARGONNE NATIONAL LAB
9700 S. CASS AVE
ARGONNE, IL 60439 USA

G. CICCARELLI
BROOKHAVEN NATIONAL LABORATORY
BLDG. 130, PO BOX 5000
UPTON, NY 11973-5000 USA

J. CLAUSS
SANDIA NATIONAL LABORATORY
PO BOX 5800, MS-0741
ALBUQUERQUE, NM 87185-0741 USA

P. COLAIANNI
DUKE POWER CO.
MAIL STOP EC12R P.O. BOX 1006
CHARLOTTE, NC 28201-1006 USA

R. COLE
SANDIA NATIONAL LABORATORY
SANDIA NATIONAL LAB, DEPT. 6421
ALBUQUERQUE, NM 87185-0739 USA

L. CONNOR
STS, INC.
3 METRO CENTER - SUITE 610
BETHESDA, MD 20814 USA

S. COOPER
SCIENCE APPLICATIONS INTERNATIONAL CORP.
11251 ROGER BACON D, M/S E-3-1
RESTON, VA 22090 USA

B. CORWIN
OAK RIDGE NATIONAL LABORATORY
P.O. BOX 2008
OAK RIDGE, TN 37831-6151 USA

M. COURTAUD
COMMISSARIAT A L'ENERGIE ATOMIQUE
CEA/GRENOBLE - 17, RUE DES MARTYRS
GRENOBLE CEDEX 9, 38054 FRANCE

M. CUNNINGHAM
PACIFIC NORTHWEST LAB.
PO BOX 999
RICHLAND, WA 99352 USA

C. CZAJKOWSKI
BROOKHAVEN NATIONAL LABORATORY
BLDG. 130, PO BOX 5000
UPTON, NY 11973-5000 USA

J. DAVIS
BROOKHAVEN NATIONAL LABORATORY
BLDG. 130, PO BOX 5000
UPTON, NY 11973-5000 USA

J. DAVIS
NEI
1776 I ST NW
WASHINGTON, DC 20002 USA

D. DIAMOND
BROOKHAVEN NATIONAL LABORATORY
BLDG. 130, PO BOX 5000
UPTON, NY 11973-5000 USA

S. DINGMAN
SANDIA NATIONAL LABORATORY
PO BOX 5800, MS 0747
ALBUQUERQUE, NM 87185-0747 USA

S. DOROFEEV
RRC "KURCHATOV INSTITUTE"
KURCHATOV SQUARE 1
MOSCOW, 123182 RUSSIA

A. DRAKE
WESTINGHOUSE ELECTRIC CORP.
P.O. BOX 350
PITTSBURGH, PA 15239 USA

J-L. DROULAS
ELECTRICITE DE FRANCE-SEPTEN
12-14, AVENUE DUTRIEVOZ
VILLEURBANNE CEDEX, 69628 FRANCE

J. DUCO
IPSN/DPEI CEA-FAR
BP6
FONTENAY-AUX-ROSES, 92265 FRANCE

M. EL-HAWARY
ATOMIC ENERGY CONTROL BOARD, CANADA
280 SLATER STREET
OTTAWA, ONT K1P 5S9 CANADA

Z. ELAWAR
PALO VERDE NUCLEAR PLANT
PO BOX 52034
PHOENIX, AZ 85072-2034 USA

R. ENNIS
TENERA
1901 RESEARCH BLVD.
ROCKVILLE, MD 20850 USA

P. EWING
OAK RIDGE NATIONAL LABORATORY
PO BOX 2008, MS 6006
OAK RIDGE, TN 37831 USA

R. FENECH
NUCLEAR OPERATIONS, PALISADES PLANT
27780 BLUE STAR MEMORIAL HWY.
COVERT, MI 49043 USA

D. FERETIC
U. OF ZAGREB, ELECT. ENG'G & COMPUTING
UNSKA 3
ZAGREB, 10000 CROATIA

R. FIELDHACK
WISCONSIN ELECTRIC POWER CO.
231 W. MICHIGAN
MILWAUKEE, WI 53201 USA

I. FIERO
ABB COMBUSTION ENGINEERING
1000 PROSPECT HILL RD
WINDSOR, CT 06095 USA

L. FISCHER
LAWRENCE LIVERMORE NATIONAL LAB.
PO BOX 808, L631
LIVERMORE, CA 94551 USA

M. FLETCHER
AECL TECHNOLOGIES
19041 RAINES DRIVE
DERWOOD, MD 20855 USA

K. FOLK
SOUTHER NUCLEAR
P.O. BOX 1295
BINMINGHAM, AL 35201 USA

J. FORESTER
SANDIA NATIONAL LABORATORY
PO BOX 5800, MS 0747
ALBUQUERQUE, NM 87185-0747 USA

E. FOX
OAK RIDGE NATIONAL LABORATORY
P.O. BOX 2009
OAK RIDGE, TN 37832-8063 USA

W. FRID
SWEDISH NUCLEAR POWER INSPECTORATE
UTLANDSGIRD 7, UT/S/
STOCKHOLM, S-10658 SWEDEN

T. FUKETA
JAPAN ATOMIC ENERGY RESEARCH INSTITUTE
TOKAI, IBARAKI 319-11
TOKAI, 319-11 JAPAN

W. GALYEAN
IDAHO NATIONAL ENGINEERING LAB
PO BOX 1625
IDAHO FALLS, ID 83415-3850 USA

R. GAMBLE
GE NUCLEAR ENERGY
75 CURTNER AVE., MC 781
SAN JOSE, CA 95125 USA

P. GANGO
IVO INTERNATIONAL LTD.
RAJATORPANTIE 8, VANTAA
IVO, 01019 FINLAND

R. GAUNTT
SANDIA NATIONAL LABORATORY
PO BOX 5800, MS 1139
ALBUQUERQUE, NM 87185 USA

G. GAUTHIER
INST. OF PROTECTION & NUCLEAR SAFETY
DES/SAMS BP 6F
FONTENAY-AUX-ROSES, 92265 FRANCE

R. GAZDZINSKI
OGDEN ENVIRONMENTAL & ENERGY SVCS.
1777 SENTRY PKWY W., STE 300
BLUE BELL, PA 19422 USA

N. GHADIALI
BATTELLE COLUMBUS LABORATORIES
505 KING AVE
COLUMBUS, OH 43201 USA

G. GIGGER
WESTINGHOUSE ELECTRIC
PO BOX 79
WEST MIFFLIN, PA 15122 USA

K. GILLEN
SANDIA NATIONAL LABORATORY
PO BOX 5800, MS 1407
ALBUQUERQUE, NM 87185-1407 USA

R. GILLILAND
OAK RIDGE NATIONAL LABORATORY
PO BOX 2009, MS 8063
OAK RIDGE, TN 37830-8063 USA

J. GLEASON
CONSULTANT TO BNL
1815 CROSS CREEK RD.
HUNTSVILLE, AL 35802 USA

L. GOLDSTEIN
S.M. STOLLER CORP.
485 WASHINTON AVENUE
PLEASANTVILLE, NY 10570 USA

M. GOMOLINSKI
IPSN - FRANCE
BP 6
FONTENAY AUX ROSES, 92265 FRANCE

S. GRAHAM
NAVAL SURFACE WARFARE CENTER
CODE 614, 3A LEGGETT CIR.
ANNAPOLIS, MD 21402 USA

D. GRAND
CEA DRN/DTP/STR
STR CEA-GRENOBLE 17, RUE DES MARTYRS
GRENOBLE-CEDEX 9, 38054 FRANCE

W. GRANT
ATOMIC ENERGY CONTROL BOARD - CANADA
P.O. BOX 1046, STN. B, 280 SLATER STREET
OTTAWA, ONT K1P 5S9 CANADA

M. GREGORIC
SLOVENIAN NUCLEAR SAFETY ADMIN.
VOJKOVA 59
LJUBLJANA, 61113 SLOVENIA

F. GRIFFIN
OAK RIDGE NATIONAL LABORATORY
PO BOX 2009
OAK RIDGE, TN 37831-8057 USA

M. GROUNES
STUDSVIK NUCLEAR AB
S-611 82 NYKOPING
NYKOPING, S-611 82 SWEDEN

K. HADDAD
PENNSYLVANIA STATE UNIVERSITY
215 REBER BLDG.
UNIVERSITY PARK, PA 16802 USA

L. HANES
EPRI
3412 HILLVIEW AVENUE
PALO ALTO, CA 94304 USA

A. HANEVIK
OECD HALDEN PROJECT
OS ALLE 13
1750 HALDEN, NORWAY

D. HARRISON
U.S. DEPT. OF ENERGY
NE-50
WASHINGTON, DC 20545 USA

G. HART
PERFORMANCE CONTRACTING INC.
4025 BONNE INDUSTRIAL
SHAWNEE, KS 66226 USA

H. HASHEMIAN
ANALYSIS & MEASUREMENT SERVICES CORP.
AMS 9111 CROSS PARK DR.
KNOXVILLE, TN 37923 USA

K. HASHIMOTO
JAPAN ATOMIC ENERGY RESEARCH INSTITUTE
TOKAI-MURA
IBARAKI-KEN, 319-11 JAPAN

G. HECKER
ALDEN RESEARCH LABORATORY, INC.
30 SHREWSBURY STREET
HOLDEN, MA 01520 USA

G. HEUSENER
FORSCHUNGSZENTRUM KARLSRUHE
POSTFACH 3640
KARLSRUHE, 76021 GERMANY

J. HIGGINS
BROOKHAVEN NATIONAL LABORATORY
BLDG. 130, PO BOX 5000
UPTON, NY 11973-5000 USA

L. HOCHREITER
WESTINGHOUSE ELECTRIC CORP.
P.O. BOX 355
PITTSBURGH, PA 15230 USA

P. HOFMANN
FORSCHUNGSZENTRUM KARLSRUHE
POSTFACH 3640
KARLSRUHE, 76021 GERMANY

S.W. HONG
SANDIA NATIONAL LABORATORY
PO BOX 5800, MS 1139
ALBUQUERQUE, NM 87185 USA

E. HONTANON
C.I.E.M.A.T. RESEARCH CENTER
AVDA. COMPLUTENSE, 22
MADRID, 28040 SPAIN

W. HORIN
WINSTON & STRAWN
1400 I ST. N.W.
WASHINGTON, DC 20005 USA

L. HORVATH
BROOKHAVEN NATIONAL LABORATORY
BLDG. 130, P.O. BOX 5000
UPTON, NY 11973 USA

R. HOUSER
WESTINGHOUSE BETTIS ATOMIC POWER LAB.
PO BOX 79
WEST MIFFLIN, PA 15122 USA

T. HSU
VIRGINIA POWER
5000 DOMINION BLVD.
GLEN ALLEN, VA 23060 USA

A. HUERTA
CNSNS
DR. BARRAGAN 779, COL. NARVARIC
MEXICO D.F., MEXICO 03020 MEXICO

J. HUTCHINSON
EPRI PLANT SUPPORT ENGINEERING
1300 W. HARRIS BLVD
CHARLOTTE, NC 28262 USA

Y.D. HWANG
KOREA ATOMIC ENERGY RESEARCH INSTITUTE
POWER REACTOR DEVELOPMENT TEAM
YUSUNG-GU, TAEJUN KOREA

T. HYRSKY
IVO INTERNATIONAL LTD.
RAJATORPANTLE 8, VANTAA
IVO, 01019 FINLAND

J. HYVARINEN
FINNISH CENTRE FOR RAD. & NUC. SAFETY
PO BOX 14
HELSINKI, FIN-00881 FINLAND

K. IDO
SHIKOKU ELECTRIC POWER CO., INC.
6-1-2 MINATOMACHI
MATSUYAMA, 790 JAPAN

J. IRELAND
LOS ALAMOS NATIONAL LABORATORY
PO BOX 1663, MS F606
LOS ALAMOS, NM 87545 USA

M. ISHII
PURDUE UNIVERSITY
1290 NUCLEAR ENGINEERING BLDG.
WEST LAFAYETTE, IN 47907-1290 USA

K. ISHIJIMA
JAPAN ATOMIC ENERGY RESEARCH INSTITUTE
TOKAI, IBARAKI 319-11
TOKAI, 319-11 JAPAN

R. ISLAMOV
RUSSIAN ACADEMY OF SCIENCES
B. TULSKAYA, 52
MOSCOW, 113191 RUSSIA

T. ITO
JAPAN INSTITUTE OF NUCLEAR SAFETY
FUJITA KANKO TORANOMON BLDG. 4F
MINATO-KU, TOKYO 105 JAPAN

R. JAMES
ELECTRIC POWER RESEARCH INSTITUTE
3412 HILLVIEW AVENUE
PALO ALTO, CA 94304 USA

F. JANSKY
BTB-JANSKY GMBH
GERLIUGER STR. 151
LEONBERG, 71229 GERMANY

M. JIMINEZ
FLORIDA POWER & LIGHT
700 UNIVERSE BLVD.
JUNO BEACH, FL 33408 USA

R. JOHNSON
PACIFIC GAS & ELECTRIC CO.
PO BOX 770000, MC A10A
SAN FRANCISCO, CA 94177 USA

W. JOHNSON
UNIVERSITY OF VIRGINIA
REACTOR BUILDING, UNIVERSITY OF VIRGINIA
CHARLOTTESVILLE, VA 22903 USA

S. KARIMIAN
PSE&G
PO BOX 236
HANCOCK'S BRIDGE, NJ 08038 USA

T. KASSNER
ARGONNE NATIONAL LAB
9700 S. CASS AVE
ARGONNE, IL 60439 USA

S. KERCEL
OAK RIDGE NATIONAL LABORATORY
PO BOX 2008, MS 6318
OAK RIDGE, TN 37831 USA

S. KIKKAWA
NUCLEAR POWER ENGINEERING CORP.
3-CHOME TORANOMON, 8F, 17-1
MINATO-KU, TOKYO 105 JAPAN

K. KILPI
VTT ENERGY
PO BOX 1604, FIN-02044 VTT
ESPOO 15, 02150 FINLAND

B. KIM
KOREA INSTITUTE OF NUCLEAR SAFETY
PO BOX 114
YUSUNG, TAEJON, 305-600 KOREA

H. KIM
KOREA INSTITUTE OF NUCLEAR SAFETY
PO BOX 114
YUSUNG, TAEJON, 305-600 KOREA

H.C. KIM
KOREA INSTITUTE OF NUCLEAR SAFETY
PO BOX 114
YUSUNG, TAEJON, 305-600 KOREA

H.Y. KIM
KOREA INSTITUTE OF NUCLEAR SAFETY
PO BOX 114
YUSUNG, TAEJON, 305-600 KOREA

S.B. KIM
KOREA ATOMIC ENERGY RESEARCH INSTITUTE
P.O. BOX 105, YUSEONG
TAEJON, KOREA

S. KINNERSLY
AEA TECHNOLOGY
UK WINFRITH
DORCITESTER, DORSET U.K.

A. KISSELEV
RUSSIAN ACADEMY OF SCIENCES
B. TULSKAYA, 52
MOSCOW, 113191 RUSSIA

M. KITAMURA
NUCLEAR POWER ENGINEERING CORP.
3-13, 4-CHOME TORANOMON, MINATO-KU
TOKYO, 105 JAPAN

J. KLAPPROTH
GENERAL ELECTRIC
PO BOX 780, MC J26
WILMINGTON, NC 28409 USA

L. KLEIN
ATOMIC ENERGY CONTROL BOARD CANADA
PO BOX 1046, STA. B, 280 SLATER ST.
OTTAWA, ONT K1P 5S9 CANADA

J. KLUGEL
SWISS FEDERAL NUC. SAFETY INSPECTORAT
VILLIGEN, CH-5232 SWITZERLAND

N. KOJIMA
MITSUBISHI HEAVY INDUSTRIES, LTD.
1-1, WADAMISAKI-CHO, 1-CHOME
HYOGO-KU, KOBW JAPAN

K. KORSAH
OAK RIDGE NATIONAL LABORATORY
PO BOX 2008, MS 6010
OAK RIDGE, TN 37831 USA

D. KOSS
PENNSYLVANIA STATE UNIVERSITY
202A STEIDLE BLDG.
UNIVERSITY PARK, PA 16802 USA

F. KRAMER
CONSULTANT TO MITSUBISHI HEAVY IND.
5427 FAIR OAKS ST.
PITTSBURGH, PA 15217 USA

B. KUJAL
NUCLEAR RESEARCH INSTITUTE
NUCLEAR POWER & SAFETY DIV.
REZ, 25068 CZECH REPUBLIC

Y. KUKITA
JAPAN ATOMIC ENERGY RESEARCH INSTITUTE
TOKAI, IBARAKI 319-11
TOKAI, 319-11 JAPAN

K. KURODA
NUCLEAR POWER ENGINEERING CORP
3-CHOME TORANOMON, 8F, 17-1
MINATO-KU, TOKYO 105 JAPAN

K. KUSSMAUL
MPA, UNIVERSITY OF STUTTGART
PFAFFENWALDRING 32
STUTTGART, 70569 GERMANY

J. LA CHANCE
SCIENCE APPLICATIONS INTERNATIONAL CORP.
2109 AIR PARK RD SE
ALBUQUERQUE, NM 87106 USA

P. LACY
UTILITY RESOURCE ASSOCIATES CORP.
51 MONROE ST., STE 1600
ROCKVILLE, MD 20850 USA

J. LAKE
IDAHO NATIONAL ENGINEERING LABORATORY
BOX 1625, MS 3860
IDAHO FALLS, ID 83415-3860 USA

S. LANGENBUCH
GRS - GERMANY
FORSCHUNGSGELANDE
GARCHING, 85748 GERMANY

H-K. LEE
NUCLEAR TECH DEPT.
ATOMIC ENERGY COUNCIL
TAIPEI, TAIWAN ROC

J. LEE
KOREA INSTITUTE OF NUC. SAFETY
P.O. BOX 114 YUSUNG
TAEJON, KOREA

S. LEE
ONTARIO HYDRO
700 UNIVERSITY AVENUE
TORONTO, ONTARIO M5G 1X6 CANADA

Y-W. LEE
KOREA INSTITUTE OF NUCLEAR SAFETY
PO BOX 114
YUSUNG, TAEJON, 305-600 KOREA

J. LEHNER
BROOKHAVEN NATIONAL LABORATORY
BLDG. 130, PO BOX 5000
UPTON, NY 11973-5000 USA

S. LEVINSON
B&W NUCLEAR TECHNOLOGIES
3315 OLD FOREST RD.
LYNCHBURG, VA 24501 USA

R. LICCIARDO
PROFESSIONAL ENGINEER & ECONOMIST
11801 ROCKVILLE PIKE, SUITE 1405
NO. BETHESDA, MD 20852 USA

M. LIVOLANT
IPSN
CE/FAR BP6
FONTENAY-AUX-ROSES CEDEX, 92265 FRANCE

K. LOCKWOOD
KNOLLS ATOMIC POWER LABORATORY
PO BOX 1072 (P3-172)
SCHENECTADY, NY 12301-1072 USA

R. LOFARO
BROOKHAVEN NATIONAL LABORATORY
BLDG. 130, PO BOX 5000
UPTON, NY 11973-5000 USA

J.-L. LUC
DIR. FOR SAFETY OF NUCLEAR INSTALLATIONS
4 IMPASSE MATHIEU
PARIS, 75015 FRANCE

W. LUCKAS
BROOKHAVEN NATIONAL LABORATORY
BLDG. 130, PO BOX 5000
UPTON, NY 11973-5000 USA

D. MAGALLON
CEC JRC-ISPRA
JRC-EURATOM ISPRA
ISPRA, 20120 ITALY

H. MAGLEBY
IDAHO NATIONAL ENGINEERING LAB
PO BOX 1625, MS 3870
IDAHO FALLS, ID 83415 USA

B. MAGONDEAUX
ELECTRICITE DE FRANCE-SEPTEN
12-14, AVENUE DUTRIEVOZ
VILLEURBANNE CEDEX, 69628 FRANCE

J. MARN
U. OF MARIBOR, FAC. OF MECHANICAL ENG'G.
PO BOX 224
MARIBOR, SI62000 SLOVENIA

R. MARTINEZ, JR.
JUPITER CORPORATION
STE 900, 2730 UNIVERSITY BLVD. W.
WHEATON, MD 20902 USA

T. MATSUMOTO
NUCLEAR POWER ENGINEERING CORP.
5F 17-1, TORANOMON, MINATO-KU
TOKYO, 105 JAPAN

G. MEYER
B&W FUEL COMPANY
3315 OLD FOREST RD
LYNCHBURG, VA 24506-0935 USA

P. MEYER
SWISS FEDERAL NUC. SAFETY INSPECTORATE
(HSK)
VILLIGEN, AG CH-5232 SWITZERLAND

T. MIEDA
ISHIKAWAJIMA-HARIMA HEAVY INDUSTRIES
1, SHIN-NAKAHARA-CHO, ISOGO-KU
YOKOHAMA, 235 JAPAN

P. MILELLA
ANPA
VIA VITALIANO BRANCATI 68
ROME, 00144 ITALY

J. MILLER
SCIENTECH
11140 ROCKVILLE PIKE, SUITE 500
ROCKVILLE, MD 20874 USA

R. MILLER
WESTINGHOUSE ELECTRIC CORP.
PO BOX 355
PITTSBURGH, PA 15230 USA

S. MIRSKY
SCIENCE APPLICATIONS INTERNATIONAL CORP.
20201 CENTURY BLVD.
GERMANTOWN, MD 20770 USA

S. MODRO
IDAHO NATIONAL ENGINEERING LABORATORY
P.O. BOX 1625, MS 3895
IDAHO FALLS, ID 83415 USA

S. MONTELEONE
BROOKHAVEN NATIONAL LABORATORY
BLDG. 130, PO BOX 5000
UPTON, NY 11973-5000 USA

M. MONTGOMERY
NUCLEAR FUEL INDUSTRIES, LTD.
3845 NORWOOD CT.
BOULDER, CO 80304 USA

D. MOON
WASHINGTON PUBLIC PWR SUPPLY SYS
PO BOX 968 (MD PE21)
RICHLAND, WA 99352 USA

E. MOREL
FRAMATOME
TOUR FIAT
PARIS LA DEFENSE, 92084 FRANCE

A. MOTTA
PENNSYLVANIA STATE UNIVERSITY
231 SACKETT BLDG.
UNIVERSITY PARK, PA 16802 USA

M. MUHLHEIM
OAK RIDGE NATIONAL LABORATORY
P.O. BOX 2009
OAK RIDGE, TN 37831-8065 USA

M. MUNTZING
MORGAN LEWIS & BOCKIUS LLP
1800 M ST., NW
WASHINGTON, DC 20036 USA

Y.W. NA
KOREA ATOMIC ENERGY RESEARCH INSTITUTE
PO BOX 105, YUSONG
TAEJON, 305-600 KOREA

A. NAKAMURA
NUCLEAR POWER ENGINEERING CORP.
3-13, 4-CHOME, TORANOMON MINATO-KU
TOKYO, 105 JAPAN

Y. NARUSE
TOSHIBA CORP.
8, SHINSUGITA-CHO, ISOGO-KU
YOKOHAMA, 235 JAPAN

D. NAUS
OAK RIDGE NATIONAL LABORATORY
P.O. BOX 2009
OAK RIDGE, TN 37831-8065 USA

U. NAYAK
WESTINGHOUSE ELECTRIC CORP.
PO BOX 355
PITTSBURGH, PA 15230 USA

G. NIEDERAUER
LOS ALAMOS NATIONAL LABORATORY
MS K575 LANL
LOS ALAMOS, NM 87545 USA

A. NUNEZ
CNSNS
DR. BARRAGAN 779; COL. NARVARIC
MEXICO D.F., MEXICO 03020 MEXICO

S. ONO
HITACHI WORKS, HITACHI LTD.
1-1 SAIWAI-CHO 3-CHOME, HIMCHI-SHI
IBARAKI-KEN, 317 JAPAN

N. ORTIZ
SANDIA NATIONAL LABORATORY
PO BOX 5800, MS 0736
ALBUQUERQUE, NM 87185-0736 USA

D. OSETEK
LOS ALAMOS TECHNICAL ASSOCIATES
BLDG. 1 SUITE 400, 2400 LOUISIANA BLVD. NE
ALBUQUERQUE, NM 87110 USA

F. OWRE
OECD HALDEN REACTOR PROJECT
OS ALLE 13
N 1751 HALDEN, NORWAY

O. OZER
EPRI
PO BOX 10412
PALO ALTO, CA 94303-0813 USA

J. PAPIN
IPSN
CE CADARACHE
ST PAUL LEZ DURANCE, 13108 FRANCE

K-B. PARK
KOREA ATOMIC ENERGY RESEARCH INST.
PO BOX 105, YUSONG
TAEJON, 305-600 KOREA

M. PARKER
IL DEPT. OF NUCLEAR SAFETY
1035 OUTER PARK DRIVE
SPRINGFIELD, IL 62704 USA

J. PELTIER
IPSN
C.E. FONTENAY - AUX - ROSES BP6
FONTENAY-AUX-ROSES, 92965 FRANCE

W. PENNELL
OAK RIDGE NATIONAL LABORATORY
PO BOX 2009, MS-8056
OAK RIDGE, TN 37830-8056 USA

A. PEREZ-NAVARRO
UNIV. ALFONSO X EL SABIO
AVDA D E LA UNIVERSIDAD, 1
MADRID, 28691 SPAIN

V. PETENYI
NUC. REG. AUTHORITY OF SLOVAK REPUBLIC
BAJKALSKA 27, PO BOX 24
BRATISLAVA, 820 07 SLOVAKIA

M. PILCH
SANDIA NATIONAL LABORATORY
PO BOX 5800
ALBUQUERQUE, NM 87185-1137 USA

A. POOLE
OAK RIDGE NATIONAL LABORATORY
Y12 PLANT, BLDG. 9102-1 BEAR CREEK RD.
OAK RIDGE, TN 37831-8038 USA

V. PROKLOV
RRC "KURCHATOV INSTITUTE"
KURCHATOV SQUARE 1
MOSCOW, 123182 RUSSIA

J. PUGA
UNESA
FRANCISCO GERVAS 3
MADRID, 28020 SPAIN

C. PUGH
OAK RIDGE NATIONAL LABORATORY
PO BOX 2009, MS 8063
OAK RIDGE, TN 37831 USA

E. PURVIS
10105 CLEAR SPRING ROAD
DAMASCUS, MD 20872 USA

L. RANEY
COMMONWEALTH EDISON CO.
1400 OPUS PL.
DOWNERS GROVE, IL 60515 USA

V. RANSOM
PURDUE UNIVERSITY
SCHOOL OF NUCLEAR ENGINEERING - NUCL 140
WEST LAFAYETTE, IN 47907 USA

D. RAPP
WESTINGHOUSE BETTIS ATOMIC POWER LAB.
PO BOX 79
WEST MIFFLIN, PA 15122 USA

J. RASHID
ANATECH RESEARCH CORP.
5435 OBERLIN DR.
SAN DIEGO, CA 92121 USA

S. RAY
WESTINGHOUSE ELECTRIC CORP.
PO BOX 355
PITTSBURGH, PA 15230 USA

P. REGNIER
INST. OF PROTECTION & NUCLEAR SAFETY
DES/SAMS BP 6F
FONTENAY-AUX-ROSES, 92265 FRANCE

K. REIL
SANDIA NATIONAL LABORATORY
PO BOX 5800, MS 1139
ALBUQUERQUE, NM 87185-1139 USA

M. REOCREUX
IPSN
CE CADARACHE
ST PAUL LEZ DURANCE, 13108 FRANCE

W. RETTIG
DEPARTMENT OF ENERGY
1574 LOLA STREET
IDAHO FALLS, ID 83402 USA

J. REYES, JR.
OREGON STATE UNIVERSITY
RADIATION CENTER C116
CORVALLIS, OR 97331-5902 USA

M. RHATIB-RAHBAR
ENERGY RESEARCH INC.
P.O. BOX 2034
ROCKVILLE, MD 20854 USA

U. ROHATGI
BROOKHAVEN NATIONAL LABORATORY
BLDG. 475B, PO BOX 5000
UPTON, NY 11973-5000 USA

P. ROTHWELL
HM NUCLEAR INSTALLATIONS INSPECTORATE
ST. PETER'S HOUSE, BALLIOL RD., BOOTLE
LIVERPOOL, L20 3LZ UNITED KINGDOM

J. ROYEN
OECD NUCLEAR ENERGY AGENCY
12 BLVD. DES ILES
ISSY-LES-MOULINEAUX, F-92130 FRANCE

K. RUSSELL
IDAHO NATIONAL ENGINEERING LABORATORY
PO BOX 1625, MS 3779
IDAHO FALLS, ID 83415 USA

O. SANDERVAG
SWEDISH NUCLEAR POWER INSPECTORATE
KLARABERGSVIADUKTEN 90
STOCKHOLM, 10658 SWEDEN

H. SASAJIMA
TOSHIBA CORP.
8, SHINSUGITA-CHO, ISOGO-KU
YOKOHAMA, 235 JAPAN

M. SATTISON
LOCKHEED IDAHO TECHNOLOGIES CO.
PO BOX 1625, MS 3850
IDAHO FALLS, ID 83415-3850 USA

N. SCHAUKI
SIEMENS/WYLE
445 UPSHIRE CIRC.
GAITHERSBURG, MD 20878 USA

P. SCHEINERT
WESTINGHOUSE BETTIS ATOMIC POWER LAB.
PO BOX 79
WEST MIFFLIN, PA 15122 USA

E. SCHMIDT
NUS CORP.
910 CLOPPER ROAD
GAITHERSBURG, MD 20878 USA

F. SCHMITZ
IPSN
CE CADARACHE
ST PAUL LEZ DURANCE, 13108 FRANCE

W. SCHOLTYSSEK
FORSCHUNGSZENTRUM KARLSRUHE
POSTFACH 3640
KARLSRUHE, 76021 GERMANY

M. SCHWARZ
IPSN
CE CADARACHE
ST PAUL LEZ DURANCE, 13108 FRANCE

M. SEITO
JAPAN INSTITUTE OF NUCLEAR SAFETY
FUJITA KANKO TORANOMON BLDG. 7F
MINATO-KU, TOKYO 105 JAPAN

P. SEONG
KOREA ADVANCED INST. OF SCIENCE & TECH.
373-1 GUSONG-DONG YUSONG-KU
TAEJON, 305-701 KOREA

S. SETH
THE MITRE CORPORATION
MS:W779, 7525 COLSHIRE DRIVE
MC LEAN, VA 22102 USA

W. SHA
ARGONNE NATIONAL LABORATORY
9700 S. CASS AVENUE
ARGONNE, IL 60439 USA

W. SHACK
ARGONNE NATIONAL LAB
BLDG. 212
ARGONNE, IL 60439 USA

J. SHEFFIELD
OAK RIDGE NATIONAL LABORATORY
PO BOX 2008
OAK RIDGE, TN 37831-6248 USA

S. SIM
KOREA ATOMIC ENERGY RESEARCH INSTITUTE
DUKJIN-DONG 150, KAERI
TAEJON, KOREA

L. SIMPSON
ATOMIC ENERGY OF CANADA LTD.
WHITESHELL LABORATORIES
PINAWA, MANITOBA ROE 1LO CANADA

W. SLAGLE
WESTINGHOUSE ELECTRIC CORP.
PO BOX 355
PITTSBURGH, PA 15230 USA

L. SLEGERS
SIEMENS-KWU
P.O. BOX 101063, BERLINER STR. 295
OFFENBACH, D63067 GERMANY

S. SLOAN
IDAHO NATIONAL ENGINEERING LABORATORY
PO BOX 1625
IDAHO FALLS, ID 83415-3895 USA

V. SMIRNOV
RRC "KURCHATOV INSTITUTE"
KURCHATOV SQUARE 1
MOSCOW, 123182 RUSSIA

F. SOUTO
SCIENCE & ENGINEERING ASSOCIATES, INC.
6100 UPTOWN BLVD. NE, STE 700
ALBUQUERQUE, NM 87110 USA

K. ST. JOHN
YANKEE ATOMIC ELECTRIC CO.
580 MAIN ST.
BOLTON, MA 01741 USA

R. STEELE, JR.
IDAHO NATIONAL ENGINEERING LAB
PO BOX 1625
IDAHO FALLS, ID 83415-3870 USA

P. STOOP
NETHERLANDS ENERGY RES. FOUNDATION
PO BOX 1, 1755 ZG PETTEN
WESTERDUINWEG 3, PETTEN,
THE NETHERLANDS

M. STRAND
SCIENTECH, INC.
11140 ROCKVILLE PIKE, SUITE 500
ROCKVILLE, MD 20852 USA

V. STRIZHOV
RUSSIAN ACADEMY OF SCIENCES
B. TULSKAYA, 52
MOSCOW, 113191 RUSSIA

E. STUBBE
TRACTEBEL ENERGY ENGINEERING
AVENUE ARIANE 7
BRUSSELS, 1200 BELGIUM

W. STUBLER
BROOKHAVEN NATIONAL LABORATORY
BLDG. 130, PO BOX 5000
UPTON, NY 11973-5000 USA

S. SUNG
KOREAN NUCLEAR FUEL CO.
HYUPSIN-MEMSION #101,
177-9 YONGDUZ-DONG JUNG-GU,
TAEJON, SOUTH KOREA

H. TAGAWA
NUPEC
BROOKHAVEN NAT. LAB., APT. 4C
UPTON, NY 11973 USA

M. TAKAYASU
NUCLEAR FUEL INDUSTRIES, LTD.
950, OHAZA NODA KUMATORI-CHO
SENNAN-GUN, OSAKA 590-04 JAPAN

T. TANAKA
SANDIA NATIONAL LABORATORY
PO BOX 5800, MS 0737
ALBUQUERQUE, NM 87185-0737 USA

J. TAYLOR
BROOKHAVEN NATIONAL LABORATORY
BLDG. 130, PO BOX 5000
UPTON, NY 11973-5000 USA

C. THIBAULT
WYLE LABORATORIES
7800 HIGHWAY 20 WEST
HUNTSVILLE, AL 35807-7777 USA

H. THORNBURG
CONSULTANT
901 S. WARFIELD DR.
MT. AIRY, MD 21771 USA

E. TITLAND
MATERIALS & ENERGY ASSOCIATES, INC.
512 IDLEWILD RD., PO BOX 1107
BEL AIR, MD 21014 USA

J. TONG
ATOMIC ENERGY CONTROL BOARD, CANADA
280 SLATER STREET
OTTAWA, ONT K1P 5S9 CANADA

I. TOTH
KFKI ATOMIC ENERGY RESEARCH INST.
PO BOX 49
BUDAPEST, H-1525 HUNGARY

R. TREGONING
NAVAL SURFACE WARFARE CENTER
CODE 614, 3A LEGGETT CIR.
ANNAPOLIS, MD 21402 USA

R. VALENTIN
ARGONNE NATIONAL LABORATORY
9700 S. CASS AVENUE - BLDG. 308
ARGONNE, IL 60439 USA

K. VALTONEN
FINNISH CENTRE FOR RAD. & NUC. SAFETY
PO BOX 14
HELSINKI, FIN-00881 FINLAND

T. VAN ETTEN
KNOLLS ATOMIC POWER LABORATORY
PO BOX 1072 (P3-172)
SCHENECTADY, NY 12301-1072 USA

M. VESCHUNOV
RUSSIAN ACADEMY OF SCIENCES
B. TULSKAYA, 52
MOSCOW, 113191 RUSSIA

Y. WAARANPERA
ABB ATOM
NUCLEAR SYSTEMS DIV.
VASTERAS, S-72163 SWEDEN

N. WAECKEL
EDF SEPTEN
12-14 AVENUE DUTRIEVOZ
VILLEURBANNE, 69628 FRANCE

J. WATKINS
IDAHO NATIONAL ENGINEERING LAB
PO BOX 1625
IDAHO FALLS, ID 83415-3870 USA

M. WETZEL
BECHTEL CORP.
9801 WASHINGTONIAN BLVD.
GAITHERSBURG, MD 20878 USA

K. WHITT
SOUTHERN NUCLEAR
40 INVERNESS CENTER PKWY.
BIRMINGHAM, AL 35201 USA

W. WIESENACK
OECD HALDEN REACTOR PROJECT
P.O. BOX 171
HALDEN, NORWAY

G. WILKOWSKI
BATTELLE COLUMBUS
505 KING AVENUE
COLUMBUS, OH 43201 USA

S. WILLIAMS
DOMINION ENGINEERING, INC.
6862 ELM ST.
MC LEAN, VA 22101 USA

R. WOOD
OAK RIDGE NATIONAL LABORATORY
PO BOX 2008, MS 6010
OAK RIDGE, TN 37831 USA

J. WREATHALL
WREATHWOOD GROUP
4157 MACDUFF WAY
DUBLIN, OH 43016 USA

J. WRIGHT
MODELING & COMPUTING SERVICES
6400 LOOKOUT ROAD
BOULDER, CO 80301 USA

G. WROBEL
ROCHESTER GAS & ELECTRIC CORP.
89 EAST AVENUE
ROCHESTER, NY 14649 USA

L. WUNDERLICH
KNOLLS ATOMIC POWER LABORATORY
PO BOX 1072 (D2-221)
SCHENECTADY, NY 12301-1072 USA

G. YADIGAROGLU
SWISS FED. INST. OF TECH. &
PAUL SCHERRER INST.
ETH-ZENTRUM, CLT
ZURICH, CH-8092 SWITZERLAND

L. YEGOROVA
RRC "KURCHATOV INSTITUTE"
KURCHATOV SQUARE 1
MOSCOW, 123182 RUSSIA

K.J. YOO
KOREA ATOMIC ENERGY RESEARCH INST.
PO BOX 105, YUSONG
TAEJON, 305-600 KOREA

M. YOUNG
SANDIA NATIONAL LABORATORY
PO BOX 5800
ALBUQUERQUE, NM 87185-0748 USA

T. ZAMA
TOKYO ELECTRIC POWER CO., INC.
1901 L ST., NW, SUITE 720
WASHINGTON, DC 20036 USA

G. ZIGLER
SCIENCE & ENGINEERING ASSOCIATES, INC.
6100 UPTOWN BLVD. NE, STE 700
ALBUQUERQUE, NM 87110 USA

PROCEEDINGS OF THE
23rd WATER REACTOR SAFETY INFORMATION MEETING
October 23-25, 1995

CONTENTS - VOLUME 3

EQUIPMENT OPERABILITY AND AGING
J. Vora, Chair

ECCS STRAINER BLOCKAGE RESEARCH & REGULATORY ISSUES
C. Serpan, Chair

AN ASSESSMENT OF SEISMIC MARGINS IN NUCLEAR PLANT PIPING*

W. P. Chen, K. R. Jaquay
Energy Technology Engineering Center, Canoga Park, CA, USA

N. C. Chokshi**, D. Terao**
U.S. Nuclear Regulatory Commission, Washington, DC, USA

ABSTRACT

Interim results of an ongoing program to assist the U.S. Nuclear Regulatory Commission (NRC) in developing regulatory positions on the seismic analyses of piping and overall safety margins of piping systems are reported. Results of: 1) reviews of seismic testing of piping components performed as part of the Electric Power Research Institute (EPRI)/NRC Piping and Fitting Dynamic Reliability (PFDR) Program, and 2) assessments of safety margins inherent in the ASME Code, Section III, piping seismic design criteria as revised by the 1994 Addenda are reported. The reviews indicate that the margins inherent in the revised criteria may be less than acceptable and that modifications to these criteria may be required.

1. INTRODUCTION

The Energy Technology Engineering Center (ETEC) is providing assistance to the U.S. NRC in developing regulatory positions on the seismic analysis of piping. As part of this effort, ETEC performed reviews of the ASME Code, Section III, piping seismic design criteria as revised by the 1994 Addenda (revised criteria). These revised criteria were based on the results of the PFDR Program (Guzy, 1988; EPRI, 1994).

The PFDR Program was implemented by General Electric (GE) and included simulated dynamic seismic, hydrodynamic, and water hammer testing and analyses of piping components and/or systems. Seismic tests were performed on 33 simple cantilever configurations of piping components and two prototypic piping systems. Material specimen fatigue-ratcheting tests were also performed. Based on these analyses and tests, revised criteria for the seismic design of ASME Code, Section III, Class 1, 2, and 3 piping systems were developed by EPRI and GE (Tagart & Ranganath, 1992; EPRI, 1994).

The revised ASME Code piping seismic design criteria were based on the rules developed by EPRI and GE (EPRI, 1994), and on evaluations by the ASME Special Task Group on Integrated Piping Criteria (STGIPC)*** and the Technical Core Group (TCG) of the Advanced Reactor Corporation (ARC)***. The results of the PFDR Program were included in these evaluations.

---

* Research sponsored by the Office of Nuclear Regulatory Research, U.S. Nuclear Regulatory Commission and performed at the Energy Technology Engineering Center which is operated for the U.S. Department Energy under Contract Number DE-AC03-76-SF00700.

** The views expressed in this paper and those of the authors and should not be construed to reflect the NRC position.

*** These ASME/STGIPC and ARC/TCG evaluations are documented in reports of limited distribution.

This paper summarizes the current status of ETEC reviews of the revised ASME Code piping seismic design criteria in the 1994 Addenda and some of their bases. In addition, interim reviews by the Peer Review Group (PRG), which was established to provide an overview of the results of the ETEC reviews, are also summarized.

2. OVERVIEW OF PFDR PIPING COMPONENT TESTING

The objectives of the PFDR program were:

1. To identify failure mechanisms and failure levels of piping components and systems under dynamic loading.
2. To provide a data base that will improve the prediction of piping system response and failure due to high level dynamic loads.
3. To develop an improved, realistic and defensible set of piping design rules for inclusion into the ASME Code.

As previously indicated, piping component, piping system and materials specimen fatigue-ratchet testing were performed as part of this program.

The component testing was performed by ANCO Engineers, Inc. (ANCO). During testing, piping components including elbows, tees, reducers, nozzles and supports were subjected to simulated dynamic seismic, hydrodynamic and water hammer (low-, mid- and high-frequency, respectively) loadings. Failure occurred during the seismic and water hammer loading tests, but not in the hydrodynamic loading tests. The current review is limited to the seismic loading tests only; the hydrodynamic and water hammer tests were not included. Components ranged between four- and eight-inches in diameter, were between Schedule 10 and 80 in thickness, and were fabricated from stainless or carbon steel.

A total of 41 pipe components were tested. Of these tests, 33 were simulated high level seismic tests, 2 were quasi-static tests on elbows, and the remaining 6 were mid- and high-frequency tests. These last 6 tests are not included in the review. Results for 27 of the 33 PFDR seismic component tests were reevaluated by ETEC during this review. These 27 tests are identified in the load margin Tables 1 and 2 and involved 6-inch diameter, stainless and carbon steel components of varying thicknesses (Schedules 10 through 80).

Typical test configurations are shown in Figures 1 and 2 (EPRI, 1994) and a typical targeted test time history and response spectra are shown in Figures 3 and 4, respectively. During testing a single time history was utilized but the amplitude of the input was uniformly scaled to adjust the input load level and the time scale stretched or compressed to adjust the frequency of the peak response acceleration to be approximately 90% of the fundamental frequency of the test configuration. Typical test sequences involved initial low level characterization and verification tests and subsequent high level tests. Typically, the high level input was applied up to ten times or until a through-wall crack developed in the tested component. Some tests were terminated due to incipient instability of the test configuration as a result of ratcheting.

Results of the two PFDR seismic system tests were reevaluated by ETEC for the U.S. NRC as part of a separate program. Results of this reevaluation and other system tests are reported elsewhere.

The PFDR materials specimen tests were intended to assess the effects of ratcheting on low cycle fatigue. Testing concluded that for low cyclic strains, shakedown occurred and failures were essentially due to fatigue. However, for large cyclic strains, sustained ratchet failures were observed.

3. REVISED ASME CODE PIPING SEISMIC DESIGN CRITERIA

The 1994 Addenda to the ASME Code, Section III, provide revised seismic design criteria for Class 1, 2, and 3 piping in Code Subsections NB/NC/ND-3600, respectively. The Addenda also provide alternate criteria in Code Subsection NB-3200. For piping, the 1994 Addenda introduce the concepts of reversing and nonreversing dynamic loads. For nonreversing dynamic loads and reversing dynamic loads in combination with nonreversing dynamic loads, the previous criteria are unchanged. However, conditionally higher allowable stresses are specified for reversing dynamic loads not required to be combined with nonreversing dynamic loads. Reversing dynamic loads include seismic loads.

Revised criteria are provided for both ASME Code Service Level B Operating Basis Earthquake (OBE) and Service Level D Safe Shutdown Earthquake (SSE) loads. The revised OBE criteria are not included in this review since regulatory changes in process will essentially eliminate the OBE from design considerations.

For the SSE, the revised Subsections NB/NC/ND-3600 criteria are the same for Class 1, 2, and 3 piping and require that the Code Equation (9) primary membrane plus bending stress load combination be less than 4.5 S_m. This criterion is similar to the previous Service Level D criterion except that: 1) the method of analysis to determine the seismic bending moments is specified, 2) the previous S_y-based allowable limit is eliminated, and 3) the previous S_m-based allowable limit of 3 S_m is increased by 50%. The replacement of the previous S_h-based allowable stress for Code Class 2 and 3 systems by a S_m-based allowable stress is noteworthy.

Conditions for application of the higher allowable stress limit require, in part, that:

1. The analysis be based on an elastic response spectrum solution utilizing 5% damping and peak broadening of no less than ±15%.
2. B_2-based stresses due to weight effects be limited to 0.5 S_m.
3. C_2-based stress ranges due to SSE anchor motion effects be limited to 6 S_m.
4. Average axial stresses due to SSE relative anchor motion effects be limited to S_m.
5. Ratios of the outside diameter to wall thickness be limited to 50.
6. The ratio of the dominant load driving frequency to the lowest piping system natural frequency is greater than 0.5

The alternate piping criteria of Subsection NB-3200 of the revised criteria provide that, for the SSE, the average through-wall ratchet strain due to all simultaneously applied loads be limited to 5%, and the effective peak strain range due to all simultaneously applied loads be limited on the basis of the alternating stress intensity value at 10 cycles from the applicable Code Appendix I design fatigue curve.

4. TECHNICAL BASES FOR REVISED CRITERIA

The technical bases for the revised criteria provided in the 1994 EPRI, STGIPC and TCG reports concluded that the failure mode in piping systems due to reversing dynamic loads is ratchet-fatigue and not collapse and, consequently, that elimination of reversing dynamic loads from the ASME

Code collapse criterion is justified. However, stresses due to these loads need to be limited to prevent failures due to ratcheting and/or fatigue. Thus, the limitation of the average through-wall ratchet strain as specified in revised Subsection NB-3200 is intended to provide that ratcheting effects on low cycle fatigue are negligible. In turn, empirical studies are claimed to demonstrate that the increased allowable stress limits in revised Subsection NB/NC/ND-3600 also provide that the ratchet strain limit of revised Subsection NB-3200 is satisfied.

The TCG and STGIPC evaluations were based primarily on the load margins, denoted by Fm_r in the STGIPC report, demonstrated during PFDR component testing, where the load margin for a given set of design criteria is defined as the ratio of the minimum level of the seismic load expected to provide a through-wall crack in the piping system during one application of the load to the maximum level of the load permitted under the given set of design criteria. For the PFDR tests, FM_r was determined assuming that the fatigue failure stress was inversely proportional to $\sqrt{N}$ where N is the number of stress cycles. Load margins as evaluated by the STGIPC/TCG, ignoring weight and pressure stresses, are provided in column H of the nominal load margin Table 1.

5. REVIEW OF STGIPC/TCG LOAD MARGINS

Reviews of the revised piping design criteria and their bases identified issues relating to the STGIPC/TCG evaluations of load margins demonstrated during PFDR component testing and the applicability of these margins to piping systems in general. Other issues included the inadequate technical support for the elimination from consideration of the collapse failure mode and the revised NB-3200 criteria, the inadequate consideration of concurrent seismic anchor motion and thermal expansion effects, and the underprediction of support loads by linear analysis methods.

However, in the following, only issues relating to the STGIPC/TCG load margins will be presented. These issues include the effects of:

1. R_w, the ratio of the frequency of the peak of the test input to the natural frequency of the test configuration (R_w values are provided in Column J of load margin Table 1).
2. Broadening the peak of response spectrum of the test input in the load margin calculations.
3. The test temperatures.

In addition, ETEC reviews found that the B_2 stress indices utilized to obtain the STGIPC/TCG load margins for some of the straight-through piping products were based on failure characterizations which were inconsistent with Markl's tests (Markl, 1952). B_2 indices utilized by ETEC and by GE, if different, are provided in columns B and C, respectively, of Table 1. Corresponding stresses utilizing GE calculated response moments using 5% damping (M5) are provided in column D of Table 1. Further, the number of high level tests to cause failure utilized by ETEC and by GE, if different, are provided in columns E and F, respectively, of Table 1. Finally, load margins calculated by ETEC and the TCG for PFDR component tests are provided in columns G and H, respectively, of Table 1.

Extrapolation of the results of PFDR testing to more critical conditions not tested were based on correction factors. Factors to account for the effects of test temperature, and the incorrect use of broadened vs. unbroadened input spectra for load margin evaluations are provided in columns I and K, respectively, of Table 1. These R_w and unbroadened vs. broadened correction factors are based on STGIPC/TCG evaluations reported during the September, 1993 ASME Code meetings. Resulting extrapolated load margins due to consideration of the above effects are provided in column L of Table 1. The minimum margin of 0.91 for Test No. 11 in column L is less than the

minimum margins (approximately 2) for Test No. 36 reported during the September meetings. Moreover, many of the margins in Table 1 are less than the preliminary value proposed by a PRG reviewer necessary to assume the validity of the current seismic PRG evaluation methodology.

The margins in column L of Table 1 were based in part on STGIPC/TCG procedures for extrapolations for failure in a single event and STGIPC/TCG nonlinear analyses for corrections for R_w ratio effects. Use of these procedures and analyses in this review was to evaluate the significance of the effects only and should not be construed to imply their acceptance. However, independent assessments of these effects are ongoing.

Further, the margins in Table 1 do not include other effects evaluated by ETEC such as concurrent pressure and weight stresses and the actual geometry and material properties of the components tested. Consideration of these effects will result in the corrected load margins shown in Table 2. In this table the ratios of the actual to nominal Code Equation (9) stress values are provided in the column labeled "INFO D/A"; the ratios of the ETEC load margins to the STGIPC and ARC/TCG margins based on single load event adjustments are provided in the column labeled "INFO H/I"; adjusted load margins due to Code Section III vs. actual yield strength differences are provided in column K; adjusted load margins due to temperature adjustments in column M; and correction factors for the use of broadened spectra and frequency ratio effects are in columns O and Q, respectively. Finally, the corrected margins are provided in column S. Details of these adjustments are provided elsewhere.

6. PEER REVIEW GROUP REVIEWS

Based on its preliminary reviews, there was consensus in the Peer Review Group that, even with resolution of obvious problems (e.g., limit on pressure during SSE, and use of S_m instead of S_h for Class 2 and 3 systems), the seismic margins associated with the 1994 Addenda design criteria may be too low to be deemed acceptable from a design standpoint.

Issues identified during these reviews included:

1. The inadequate technical basis for the revised Subsection NB-3200 rules.
2. The questionable elimination of the collapse failure mode from consideration and the use of the collapse failure criterion in NB/NC/ND-3600 to control fatigue failure.
3. The acceptability of the analytically derived margin correction factors for off-resonance conditions.
4. The definition of seismic margin utilized in the STGIPC and TCG evaluations and the lack of an established acceptable value for this margin.
5. The under-prediction of seismic system response by linear analysis method in piping systems designed in accordance with the revised rules.
6. The effects on failure modes of the presence of Code-allowed imperfections in piping systems designed in accordance with the revised criteria.

The Peer Review Group identified the need to resolve issues relating to:

1. The effects of input variability on margin, the effect of input scaling, and the true nature of the response of low frequency systems.
2. Component vs. system failure modes.
3. The under-prediction of system response by linear analysis in the evaluation of piping systems with increased allowable stresses.

4. Material related issues including dynamic strain aging and Code Section XI-allowed imperfection issues.

7. CONCLUSIONS

Results of the ETEC evaluations indicated that margins associated with the revised seismic design criteria in the 1994 Addenda to the ASME Code, Section III, may be too low to be acceptable from a design standpoint and that some modifications to these criteria may be appropriate.

REFERENCES

EPRI 1994. *EPRI TR-102792-V1 through V5, Piping and Fitting Dynamic Reliability Program, Volume 1 through Volume 5.*

Guzy, D. 1988. Piping Design Criteria and Research, Current NRC Activities in Dynamic Design. *Nuclear Engineering and Design. 107: 161-167.*

Markl, A. R. C. 1952. Fatigue Tests of Piping Components. *ASME Transactions. 74:287-303.*

Tagart, Jr., S.W. & Ranganath, S. 1992. Proposed Dynamic Stress Criteria for Piping. *PVP 237-1: 133-137*

ACKNOWLEDGMENTS: The authors would like to express their gratitude to members of the Peer Review Group and the NRC Offices of Nuclear Reactor Regulation and Nuclear Regulatory Research staff for their contributions to this program.

TABLE 1

EXTRAPOLATED NOMINAL LOAD MARGINS FOR PFDR TESTS
BASED ON REVISED CRITERION B2M/Z < 4.5 SM

PFDR COMPONENT TEST MARGINS									EXTRAPOLATED TEST MARGINS			
NOMINAL B2M5/Z				NO. TEST		SINGLE EVENT ADJ			TEMP ADJ	FREQ ADJ		MARGIN
A	B	C	D	E	F	G	H	I	J	K	L	M
PFDR	ETEC	GE B2	B2M5	ETEC	GE NO.	EVENT	UNADJUST	TCG	ER(T)	RW	UNBR/BR	ADJUSTED
ELBOWS												
1	2.37		544	5.50		1276	14.18	14.00	0.82	0.833	0.34	3.90
2	2.37		499	9.50		1538	17.09	18.50	0.82	0.859	0.31	4.31
3	5.51		752	3.25	3.50	1356	15.07	15.70	0.76	0.900	0.33	3.75
4	3.27		645	2.50		1020	11.33	11.40	0.82	0.806	0.37	3.44
5	3.27		670	3.50		1254	13.94	15.70	0.82	0.900	0.33	3.75
6	3.27		631	3.50		1180	13.11	14.20	0.76	0.900	0.33	3.27
7	3.27		752	4.50		1596	17.73	19.50	0.76	0.714	0.44	5.97
8	3.27		772	4.87	5.00	1703	18.92	21.40	0.76	0.917	0.34	4.92
13	4.29		679	4.41	2.50	1425	15.83	13.90	0.82	0.897	0.33	4.23
19	3.27		704	2.65	3.00	1145	12.73	15.20	0.76	0.956	0.37	3.59
30	5.51		354	3.33	3.00	645	7.17	6.90	0.76	0.972	0.38	2.08
31	5.51		740	3.92	3.50	1463	16.26	17.20	0.76	0.875	0.30	3.74
35	3.27		584	4.58	5.00	1250	13.89	16.10	0.82	0.932	0.35	4.03
37	5.51		373	4.85	2.00	507	5.64	5.60	0.76	0.972	0.38	1.63
41	3.27		811	2.00		1146	12.74	14.10	0.82	0.929	0.25	3.67
STRAIGHT THROUGH PIPING PRODUCTS												
9	1.00	2.03	331	1.50		405	4.50	10.30	0.76	0.900	0.33	1.12
10	1.00	2.02	336	2.50		531	5.90	13.30	0.76	0.900	0.33	1.47
11	3.35		599	0.35	0.50	353	3.93	4.50	0.76	0.862	0.30	0.91
12	1.00	2.02	402	2.50		635	7.06	17.00	0.76	0.875	0.30	1.62
14	1.00	2.02	304	1.50		373	4.14	8.80	0.82	0.875	0.30	1.03
15	1.00		428	5.24	5.00	980	10.89	11.60	0.76	0.875	0.30	2.51
16	1.00		1009	0.99	0.50	1005	11.17	8.50	0.82	0.905	0.33	3.05
34	1.00		419	6.75	4.00	1089	12.10	9.60	0.82	0.914	0.34	3.37
36	1.00	2.52	242	1.01	0.50	243	2.70	4.20	0.82	0.770	0.43	0.95
38	2.52	2.02	817	3.60		1551	17.23	15.10	0.76	0.929	0.35	4.60
39	2.52	2.02	841	3.74	4.00	1627	18.08	16.80	0.76	0.956	0.37	5.09
40	1.00		785	1.37	2.00	918	10.20	12.40	0.76	0.929	0.35	2.72

TABLE 2

EXTRAPOLATED CORRECTED LOAD MARGINS FOR PFDR TESTS BASED ON REVISED CRITERION B2M/Z < 4.5 SM

	EQ 9 W/THK ADJ						SINGLE EVENT ADJ							SY ADJ		TEMP ADJ		BRD RS ADJ			REMS RW ADJ		
	A	B		C	D		E	F		G	H	I		J	K	L	M	N	O	P	Q	R	S
PFDR ID	B2M5 /Z NOM T	B2M5 /Z ACT T	INFO B/A	P.WT STRS ACT T	TOT STRS ACT T	INFO D/A	GE # OF EVNT	MM N/23	INFO F/E	EVNT CORR D	4.5SM LOAD MRGN	TCG LOAD MRGN	INFO H/I	III/T SY	LOAD MRGN	650F /70F	LOAD MRGN	RW	UNBR /BR @RW	LOAD MRGN	MRF/ MRF @ 0.5	INFO O*Q	LOAD MRGN
ELBOWS																							
1	544	544	1.00	2	546	1.00	5.50	2.20	1.00	1280	14.22	14.00	1.02	0.88	12.44	0.82	10.20	0.833	0.51	5.20	0.66	0.34	3.42
2	499	499	1.00	2	501	1.00	9.50	9.50	1.00	1543	17.14	18.50	0.93	0.88	15.00	0.82	12.30	0.859	0.51	6.27	0.60	0.31	3.78
3	752	752	1.00	1	754	1.00	3.50	3.25	0.93	1358	15.09	15.70	0.96	0.88	13.32	0.76	10.12	0.900	0.62	6.31	0.53	0.33	3.32
4	645	645	1.00	0	646	1.00	2.50	2.50	1.00	1021	11.34	11.40	0.99	0.73	8.30	0.82	6.81	0.806	0.51	3.47	0.73	0.37	2.62
5	670	670	1.00	0	671	1.00	3.50	3.50	1.00	1255	13.95	15.70	0.89	0.73	10.21	0.82	8.37	0.900	0.62	5.22	0.53	0.33	2.74
6	631	631	1.00	1	631	1.00	3.50	3.50	1.00	1181	13.12	14.20	0.92	0.55	7.26	0.76	5.52	0.900	0.62	3.44	0.53	0.33	1.81
7	752	752	1.00	1	753	1.00	4.50	4.50	1.00	1597	17.74	19.50	0.91	0.55	9.82	0.76	7.46	0.714	0.51	3.81	0.87	0.44	3.31
8	772	699	0.91	1	700	0.91	5.00	4.87	0.97	1544	17.15	21.40	0.80	0.55	9.49	0.76	7.22	0.917	0.69	4.95	0.50	0.34	2.47
13	679	679	1.00	1	680	1.00	2.50	4.41	1.76	1427	15.86	13.90	1.14	0.74	11.81	0.82	9.68	0.897	0.61	5.94	0.53	0.33	3.15
19	704	704	1.00	1	704	1.00	3.00	2.65	0.88	1146	12.76	15.20	0.84	0.56	7.08	0.76	5.38	0.956	0.83	4.48	0.44	0.37	1.99
30	354	329	0.93	11	340	0.96	3.00	3.33	1.11	619	6.88	6.90	1.00	0.88	6.07	0.76	4.61	0.972	0.90	4.13	0.43	0.38	1.76
31	740	740	1.00	2	741	1.00	3.50	3.92	1.12	1467	16.30	17.20	0.95	0.78	12.66	0.76	9.63	0.875	0.53	5.09	0.57	0.30	2.92
35	584	547	0.94	3	550	0.94	5.00	4.58	0.92	1178	13.09	16.10	0.81	0.83	10.83	0.82	8.88	0.932	0.74	6.60	0.48	0.35	3.14
37	373	547	0.87	11	336	0.90	2.00	1.85	0.93	457	5.08	5.60	0.91	0.88	4.49	0.76	3.41	0.972	0.90	3.05	0.43	0.38	1.30
41	811	325	1.00	0	811	1.00	2.00	2.00	1.00	1147	12.75	14.10	0.90	0.80	10.14	0.82	8.31	0.929	0.73	6.08	0.48	0.35	2.92
STRAIGHT THROUGH PRODUCTS																							
9	331	331	1.00	11	341	1.03	1.50	1.50	1.00	418	4.65	10.30	0.45	0.74	3.42	0.76	2.60	0.900	0.62	1.62	0.53	0.33	0.85
10	336	336	1.00	7	342	1.02	2.50	2.50	1.00	541	6.01	13.30	0.45	0.74	4.42	0.76	3.36	0.900	0.62	2.09	0.53	0.33	1.10
11	599	582	0.97	6	589	0.98	0.50	0.35	0.70	348	3.86	4.50	0.86	0.75	2.92	0.76	2.22	0.862	0.51	1.13	0.60	0.30	0.68
12	402	402	1.00	11	412	1.03	2.50	2.50	1.00	652	7.25	17.00	0.43	0.74	5.33	0.76	4.05	0.875	0.53	2.14	0.57	0.30	1.23
14	304	304	1.00	11	315	1.04	1.50	1.50	1.00	386	4.29	8.80	0.49	0.84	3.62	0.82	2.97	0.875	0.53	1.57	0.57	0.30	0.90
15	428	428	1.00	10	438	1.02	5.00	5.24	1.05	1003	11.15	11.60	0.96	0.81	9.04	0.76	6.87	0.875	0.53	3.63	0.57	0.30	2.08
16	1009	1016	1.01	10	1026	1.02	0.50	0.99	1.98	1022	11.35	8.50	1.34	0.71	8.03	0.82	6.58	0.905	0.64	4.23	0.52	0.33	2.19
34	419	423	1.01	6	430	1.02	4.00	6.75	1.69	1116	12.40	9.60	1.29	0.79	9.75	0.82	8.00	0.914	0.68	5.40	0.50	0.34	2.72
36	242	242	1.00	12	255	1.05	0.50	1.01	2.01	255	2.84	4.20	0.68	0.77	2.18	0.82	1.79	0.770	0.51	0.91	0.84	0.43	0.77
38	817	817	1.00	12	830	1.01	3.60	3.60	1.00	1574	17.49	15.10	1.16	0.75	13.09	0.76	9.95	0.929	0.73	7.27	0.48	0.35	3.50
39	841	834	0.99	2	835	0.99	4.00	3.74	0.94	1615	17.95	16.80	1.07	0.75	13.43	0.76	10.21	0.956	0.83	8.51	0.44	0.37	3.78
40	785	849	1.08	2	851	1.08	2.00	1.37	0.68	995	11.05	12.40	0.89	0.81	8.96	0.76	6.81	0.929	0.73	4.98	0.48	0.35	2.39

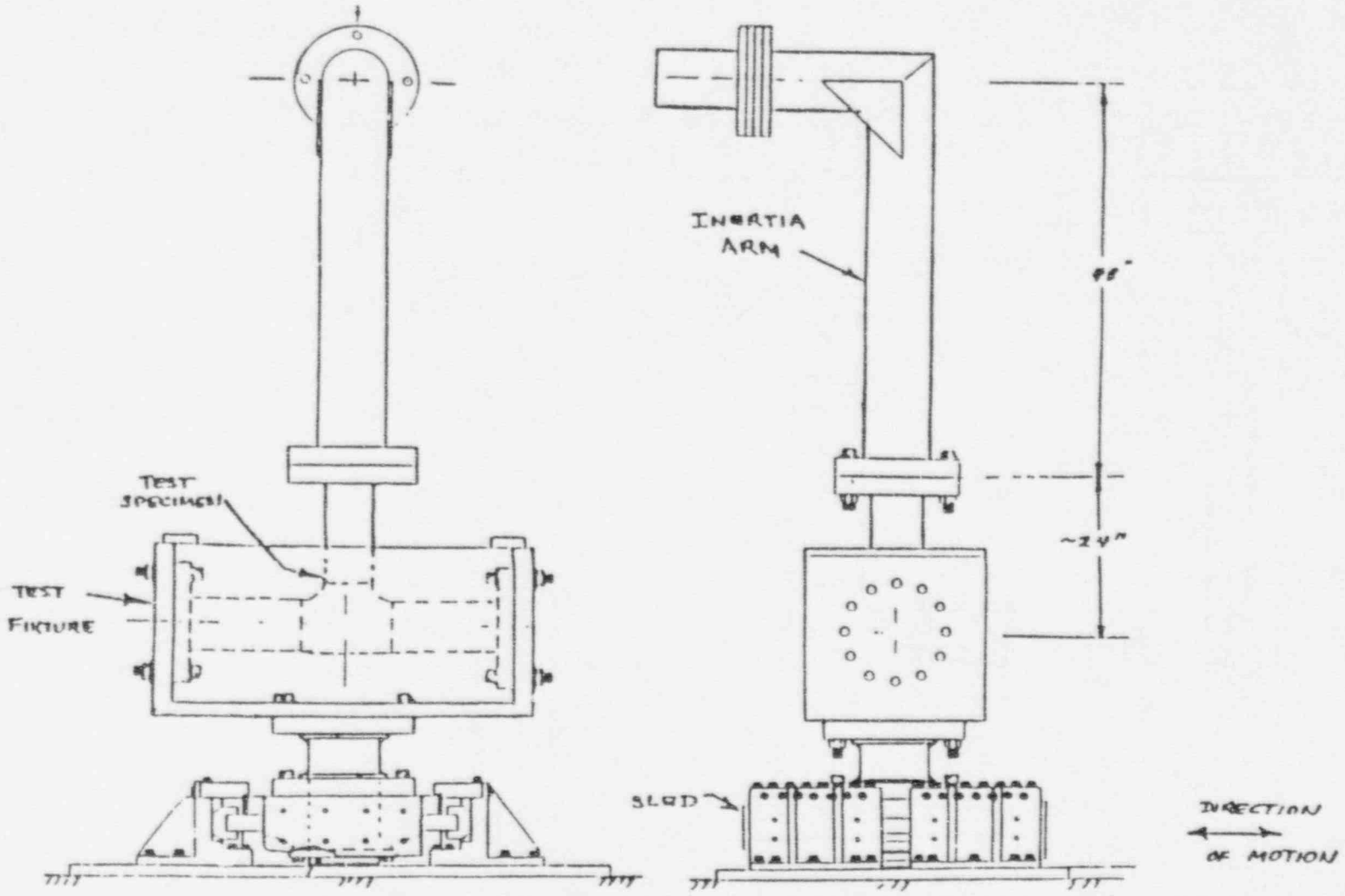

FIGURE 1. TEST 11 CONFIGURATION

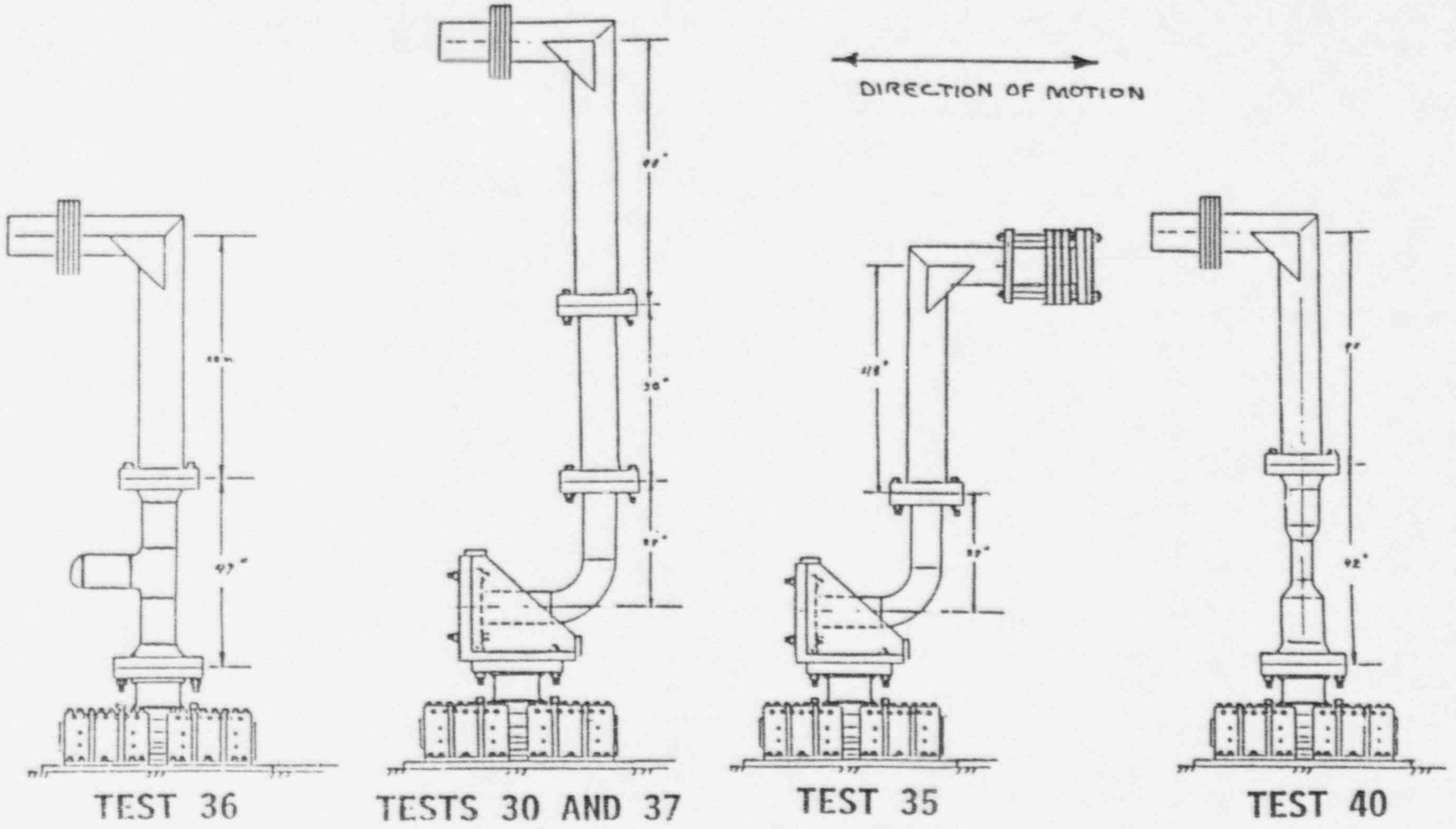

FIGURE 2. VARIOUS TEST CONFIGURATIONS

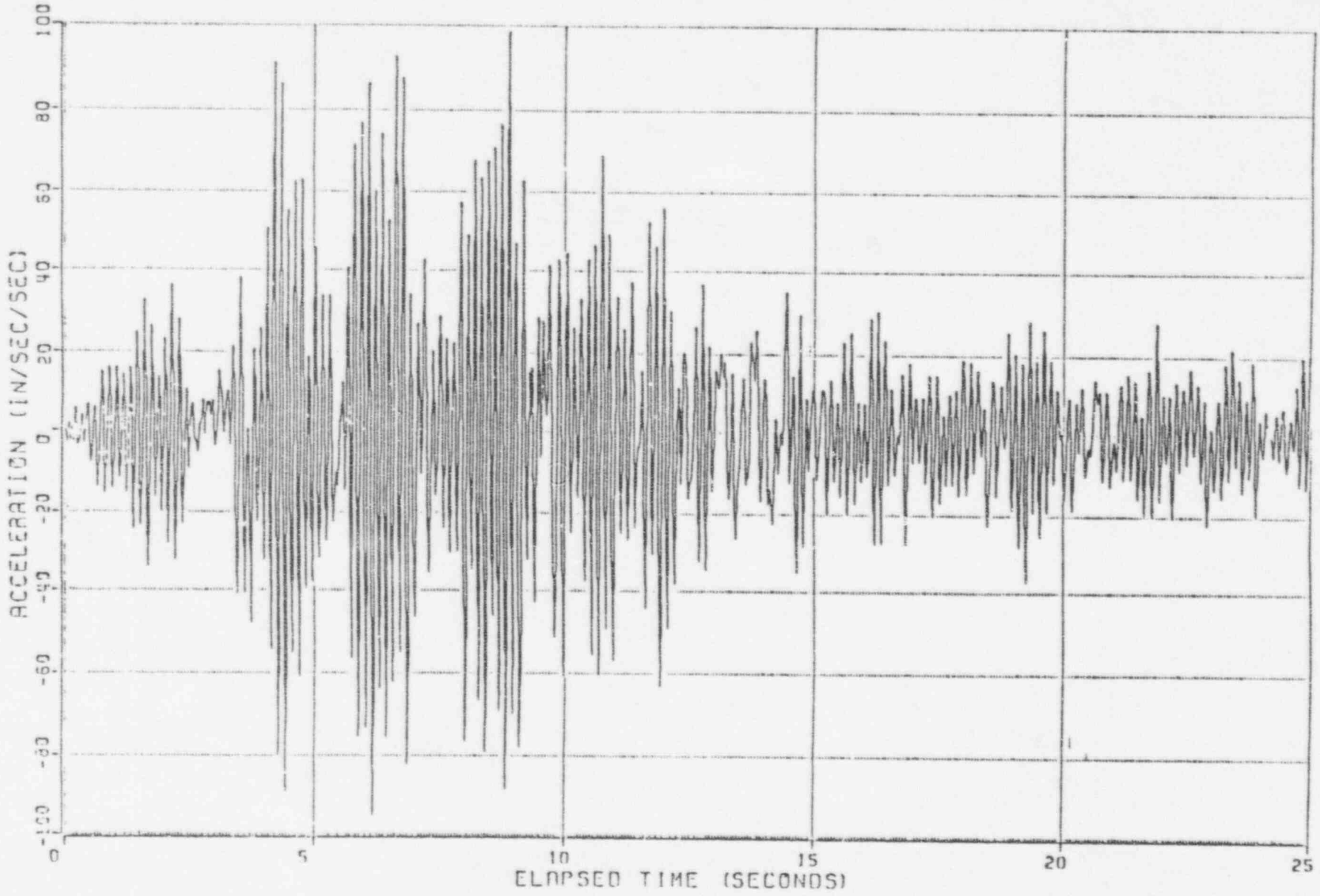

FIGURE 3. TYPICAL TARGETED INPUT TIME HISTORY

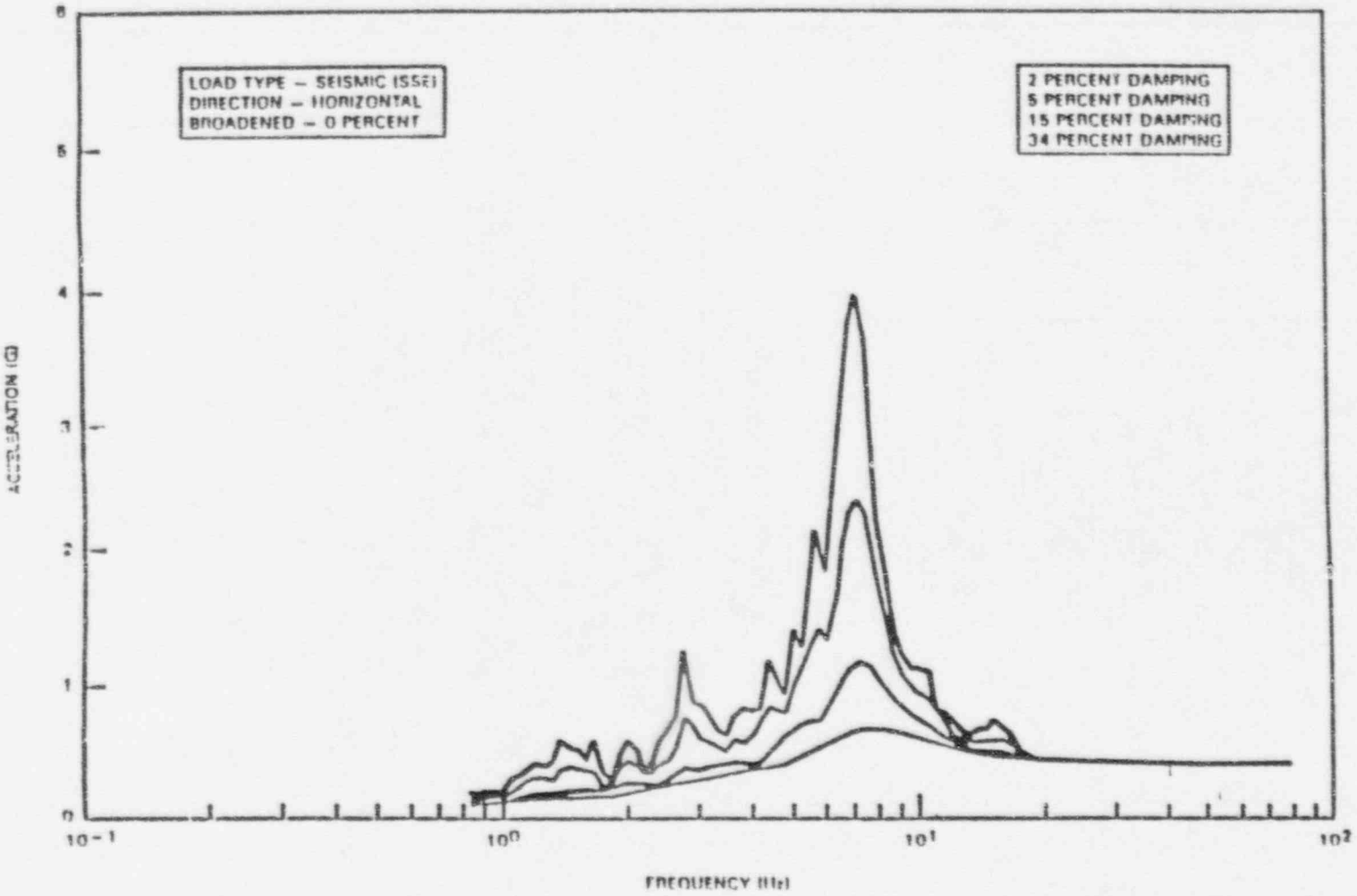

FIGURE 4. TYPICAL TARGETED INPUT RESPONSE SPECTRA

RPV AND STEAM GENERATOR PRESSURE BOUNDARY

Jack Strosnider
Materials & Chemical Engineering Branch Chief
Office of Nuclear Reactor Regulation, USNRC

STEAM GENERATOR RULE MAKING

The move to performance and risked based regulation is resulting in some interesting changes in regulatory philosophy and raising some interesting technical issues. This trend is illustrated in work underway to develop a new rule for regulating steam generator tube degradation. Supporting this new approach to regulation will present some significant challenges to researchers.

As the types of SG tube degradation affecting PWR SGs has changed, and improvements in tube inspection and repair technology have occurred, current SG regulatory requirements and guidance have become increasingly out of date. This regulatory situation has been dealt with on a plant-specific basis, however to resolve this problem in the long term, the NRC has begun development of a performance-based rule.

As currently structured, the proposed steam generator rule would require licensees to implement SG programs that monitor the condition of the steam generator tubes against accepted performance criteria to provide reasonable assurance that the steam generator tubes remain capable of performing their intended safety functions. Currently the staff is developing three performance criteria that will ensure the tubes can continue to perform their safety function (i.e. ensure adequate leakage and structural integrity) and therefore satisfy the SG rule requirements. The staff, in developing the criteria, is striving to ensure that the performance criteria have the two key attributes of being (1) measurable (enabling the tube condition to be "measured" against the criteria) and (2) tolerable (ensuring that failures to meet the criteria do not result in unacceptable consequences. A general description of the criteria are:

(1) Structural integrity criteria: Ensures that the structural integrity of the SG tubes is maintained for the operating cycle consistent with the margins intended by the ASME Code.

(2) Leakage integrity criteria: Ensures that postulated accident leakages and the associated dose releases are limited relative to 10 CFR Part 50 guidelines and 10 CFR Part 50 Appendix A GDC 19.

(3) Operational leakage criteria: Ensures that the operating unit will be shut down as a defense-in depth measure when operational SG tube leakage exceeds established leakage limits.

The rule will establish a flexible framework that allows steam generator tube integrity to be addressed using a degradation specific management approach. As currently envisioned, the staff would not need to review and approve SG tube repair criteria, i.e. the current practice. Instead, licensees would have to ensure that the performance criteria (and therefore SG rule) continue to be met. For the performance-based rule approach to be successful the staff believes licensees must: (1) perform adequate SG tube inspections that sufficiently detect and characterize the degradation in the SGs and, (2) perform sound engineering evaluations or in situ pressure tests that assess detected degradation against the SG rule performance criteria.

Since the SG tubes function as the containment boundary following postulated severe accidents to prevent a large release from bypassing containment, a major task of the SG rulemaking effort is assessing the current risk associated with SG tube integrity and ensuring that the SG rule maintains an acceptable level of risk when considering tube performance under severe accident scenarios.

The results of ongoing and planned research will play an important role in implementing the new approach to regulating steam generator tube integrity. Potential change in steam generator tube rupture risk must be assessed as part of the rule making process. Information on the behavior of steam generator tubes and other primary system components under severe accident temperature and pressure conditions will be essential in this evaluation. Research to establish the capability and reliability of nondestructive examination methods and tube structural and leakage assessment models for steam generator tubes will be critical in the actual implementation of the rule. As indicated above, a good understanding of the reliability with which tube degradation can be characterized is essential to assuring that the specified performance criteria are met.

GENERIC LETTER 92-01 SUPPLEMENT 1: "REACTOR VESSEL STRUCTURAL INTEGRITY"

As a result of the review of responses to Generic Letter (GL) 9201 and the Palisades PTS the NRC staff concluded that licensees may not have been aware of or considered all relevant information and data in previous assessments that they have performed of their RPVS. This conclusion was based on observations that licensee responses to GL 92-01 did not, in all cases, include or consider all data available for specific weld heats and that in some cases licensees reported different data, e.g., best-estimate chemistries, for the same weld heat. The staff determined that original fabrication records, surveillance information and research results are in the possession of various vendors, utilities, institutes and laboratories. For some RPVS, particularly those of older vintage, it was concluded that neither the licensee nor any other single organization, e.g., vendor, possesses all the information relevant to performing an RPV integrity assessment.

Based on the above finding, the staff concluded that the most effective way to resolve this issue was through a supplement to GL 92-01 requiring the licensees to collect all the data relevant to their RPVS, and if there are data that they had not previously considered, to perform a reassessment of their RPV.

The supplement to GL 92-01 was issued on May 19, 1995. Within 90 days of the issue date of the supplement, licensees are to provide to the NRC a description of those actions taken or planned to locate all data relevant to the determination of RPV integrity, or an explanation of why the existing data base is considered complete as previously submitted. Within 6 months of the issue date of the supplement, licensees are to provide the NRC: (a) an assessment of any changes in best-estimate chemistry based on consideration of all relevant data; (b) a determination of the need for the use of the ratio procedure in accordance with the established Position 2.1 of Regulatory Guide 1.99, Revision 2, for those licensees that use surveillance data to provide a basis for the RPV integrity evaluation; and (c) a written report providing any newly acquired data as specified above and (1) the results of any necessary revisions to the evaluation of RPV integrity in accordance with the requirements of 10 CFR 50.60, 10 CFR 50.61, Appendices G and H to 10 CFR Part 50, and any potential impact on the LTOP or P-T limits in the technical specifications or (2) a certification that previously submitted evaluations remain valid.

REACTOR VESSEL ANNEALING

The staff issued a safety evaluation on April 12, 1995, for the Palisades RPV, which concluded that the margins of safety intended by the PTS rule, 10 CFR 50 61, will be satisfied through the 14th refueling outage, scheduled for late 1999. To increase the fracture toughness of the RPV so that it can meet the margins of safety intended by the PTS rule after 1999, the licensee proposes to anneal the RPV during the 13th refueling outage. The Palisades reactor vessel would be the first commercial nuclear vessel annealed in the U.S.

The licensee's annealing plan calls for the annealing to be performed using an indirect gas-fired heating method which would heat the reactor vessel beltline region (area surrounding the effective height of the core) to 850°F - 900°F for approximately 168 hours. The licensee projects that this annealing treatment should result in recovery of 80% to 90% of the fracture toughness lost due to radiation embrittlement.

The Department of Energy is planning to conduct to reactor vessel annealing demonstrations. The first demonstration at the Marble Hill site will use a gas-fired heating method and is tentatively scheduled for April - June, 1996. The licensee for Palisades has informed the staff that they will be relying heavily on the results of the Marble Hill demonstration for their planned anneal of the Palisades vessel (late 1998 to 1999). A major objective of the annealing demonstration is to use instrumentation on the unirradiated vessel to verify the accuracy of the computer programs used to perform the thermal analysis of the annealing process; thereby, providing the basis for using reduced instrumentation during the actual anneal at Palisades. There is a desire to minimize the instrumentation that must be installed on an irradiated reactor because of the high radiation exposures involved. The second demonstration at the Midland site will employ an electric resistance heating approach and is tentatively scheduled for late 1996.

Environmentally Assisted Cracking of LWR Materials*

O. K. Chopra, H. M. Chung, T. F. Kassner, and W. J. Shack
Argonne National Laboratory
Argonne, Illinois

Abstract

Research on environmentally assisted cracking (EAC) of light water reactor materials has focused on (a) fatigue initiation in pressure vessel and piping steels, (b) crack growth in cast duplex and austenitic stainless steels (SSs), (c) irradiation-assisted stress corrosion cracking (IASCC) of austenitic SSs, and (d) EAC in high-nickel alloys. The effect of strain rate during different portions of the loading cycle on fatigue life of carbon and low-alloy steels in 289°C water was determined. Crack growth studies on wrought and cast SSs have been completed. The effect of dissolved-oxygen concentration in high-purity water on IASCC of irradiated Type 304 SS was investigated and trace elements in the steel that increase susceptibility to intergranular cracking were identified. Preliminary results were obtained on crack growth rates of high-nickel alloys in water that contains a wide range of dissolved oxygen and hydrogen concentrations at 289 and 320°C.

The program on Environmentally Assisted Cracking of Light Water Reactor Materials is currently focused on four tasks: fatigue initiation in pressure vessel and piping steels, fatigue and environmentally assisted crack growth in cast duplex and austenitic SS, irradiation-assisted stress corrosion cracking of austenitic SSs, and environmentally assisted crack growth in high-nickel alloys. Measurements of corrosion-fatigue crack growth rates (CGRs) of wrought and cast stainless steels has been essentially completed. Recent progress in these areas is outlined in the following sections.

Irradiation Assisted Stress Corrosion Cracking

Failures of reactor-core internal components in both BWRs and PWRs have occurred after accumulation of relatively high fluence (>5 x 10^{20} n·cm^{-2}, E >1 MeV). As neutron fluence increases, initially nonsensitized austenitic SSs can become susceptible to intergranular failure. This type of degradation is commonly referred to as irradiation-assisted stress corrosion cracking (IASCC). Although most failed components can be replaced, some components would be very difficult or impractical to replace.

Heat-to-heat variations in susceptibility to IASCC have been observed to be very significant, even among high-purity (HP) materials containing virtually identical chemical compositions. Although radiation-induced grain-boundary Cr depletion is believed by most investigators to play an important role in IASCC, additional deleterious processes may be associated with trace impurities that are not usually identified in material specifications. Such trace elements could be introduced during steelmaking processes or during fabrication and welding.

---

* Job Code A2212; NRC Program Manager: Dr. M. McNeil

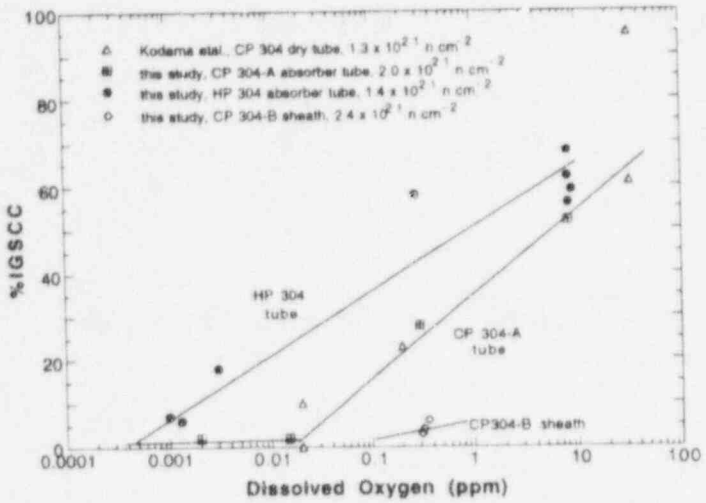

Figure 1.
Percent IGSCC vs. DO for HP and CP Type 304 SS neutron–absorber tubes (this study) and CP Type 304 SS dry tubes (Kodama et al.). Three distinct trends in DO dependence are evident.

Slow–strain–rate–tensile (SSRT) tests in simulated BWR environments on high- and commercial-purity (HP and CP) Type 304 SS were performed to determine the effects of water chemistry on susceptibility to IASCC. To obtain some insight into the mechanism(s) of IASCC, we attempted to correlate the susceptibility to intergranular cracking determined by SSRT tests with results of microchemical analysis of grain boundaries by Auger electron spectroscopy (AES).

The effect of dissolved oxygen (DO) in HP water on the susceptibility of irradiated materials to IASCC is shown in Fig. 1 for HP and CP neutron–absorber tubes and a control–blade sheath (fabricated from another CP–grade heat). Negligible IGSCC was observed in specimens from the control–blade sheath for all fluence levels; therefore, no tests were conducted to investigate the effect of DO, other than at ≈0.3 ppm. Results obtained by Kodama et al.,[1,2] are also shown for comparison. The effect of electrochemical potential (ECP) on the susceptibility of irradiated materials to IASCC is shown in Fig. 2 along with some results by Indig et al.[3] The effect of DO level and ECP on IASCC appears to be different for the HP and CP materials. The HP heats were less sensitive to DO level and ECP and were more susceptible to IASCC than the CP heats for all DO and fluence levels. No IASCC was observed in the CP heats for ECP <–140 mV SHE and DO <0.01 ppm.

The HP absorber specimen that exhibited a surprisingly high susceptibility to IGSCC of ≈18% at a very low DO of ≈0.002 ppm (Fig. 1) and ECP of ≈–320 mV SHE (Fig. 2) was examined in detail by AES. An intergranular (IG) region on the fracture surface was sputtered to a depth of ≈60 nm, and AES spectra were obtained as a function of depth from the fracture surface. Unexpected concentrations of F, Ca, B, Zn, and Al were observed in the AES spectra. Al was used as a deoxidizer during melting of the HP–grade SS and Ca could have originated from CaF_2 that may have been used as flux in melting HP SS. The B and Zn on the fracture surface was probably picked up from the water.

As shown in Fig. 3, a higher level of fluorine on grain boundaries may be associated with higher susceptibility to IASCC.[4] Inadvertent contamination of reactor components by fluorine could occur during pickling (in a solution containing HF) in the case of tubular components such as neutron–absorber–rod tubes, and by an F–containing weld flux in the case of large welded components such as BWR core shrouds and certain older top guides. A synergistic effect of a lower concentration of Cr and a higher concentration of fluorine on grain boundaries on susceptibility to IGSCC is consistent with IGSCC results by Ward et al.[5]

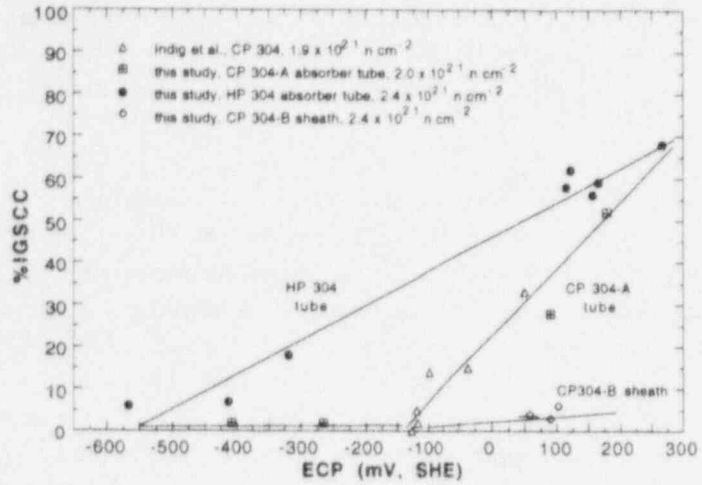

Figure 2.
Percent IGSCC vs. ECP of HP and CP Type 304 SS neutron–absorber tubes (this study) and CP Type 304 SS BWR sheet material (Indig et al.)

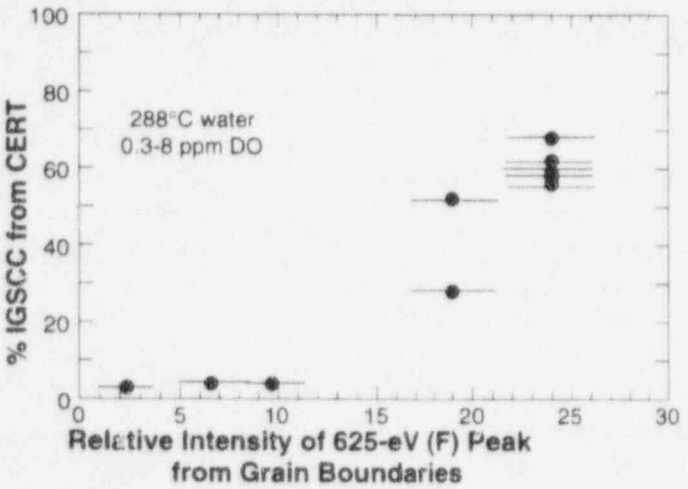

Figure 3.
Percent IGSCC vs. average intensity of fluorine signal from grain boundaries of HP and CP Type 304 SS BWR components

They reported fluorine–accelerated IGSCC of nonirradiated thermally sensitized bend specimens and weldments of CP–grade Type 304 SS that were contaminated with a fluorine–containing weld flux. They also reported that fluorine–assisted IGSCC was less sensitive to DO compared to classical IGSCC of thermally sensitized fluorine–free specimens, which is consistent with our present results.

Halide impurities play a catalytic role in accelerating aqueous corrosion of Fe and Fe–base alloys but their influence can be strongly mitigated by the concentration of Cr ions in water.[6] The corrosion acceleration has been attributed to the rate of formation of ligand complex between Fe–halide (i.e., halide anion chemisorbed on Fe) and H_2O molecules, which has rate several orders of magnitude higher than the rate of formation of a similar ligand complex between halide–free Fe atoms and H_2O molecules.[6] A similar effect can be postulated for relative reaction rates to form fluorine–containing and fluorine–free ligand complexes of $FeF(H_2O)_5$ and $Fe(H_2O)_5$, respectively. A halide atom is released from the labile ligand complex [e.g., $FeF(H_2O)_5$] dissolved in water when H_2O replaces the halide atom in the complex, thus leading to a classical catalysis by halides. However, this reaction chain is broken when the concentration of Cr ions in water is high (e.g., at a crack tip in which grain boundaries exhibit minimal Cr depletion), because Cr–halide–H_2O ligand complex [e.g., $CrF(H_2O)_5$] forms rapidly but remains inert in water. This inhibits a catalytic role of the halide atoms (e.g., fluorine atoms). According to this model, several key

factors that could influence susceptibility to IASCC are: the concentration of free halide atoms (e.g., fluorine) available on grain boundaries (i.e., those not trapped by stable precipitates[7] or compounds), the concentration of Cr ions in water at the crack tip, and the lability of $FeF_x(H_2O)_y$ complex under irradiation in LWR water.

The above hypotheses seems to be consistent not only with the behavior of HP–grade neutron–absorber tubes (high susceptibility) and CP–grade control–blade sheath (negligible susceptibility) observed in our study but also with increased susceptibility to IGSCC of fluorine–contaminated welds of either nonirradiated or irradiated Type 304 SS. However, it is too early to make a conclusive statement regarding its validity and applicability to cracking of LWR core–internal components. Nonetheless, irradiation–induced grain–boundary depletion of Cr and contamination and segregation of halides (most likely fluorine) during component fabrication appear to be the two key processes that may produce synergistic effects leading to increased susceptibility to IASCC. Compared to nonirradiated and solution–annealed material, the synergistic effect will be undoubtedly more pronounced for materials in which yielding in the grain matrix is relatively more difficult as a result of hardening by either irradiation or cold work.

Fatigue of LWR Structural Materials

The ASME Boiler and Pressure Vessel Code provides rules for the construction of nuclear power plant components. Appendix I to Section III of the Code specifies fatigue design curves for structural materials. The effects of reactor coolant environments are not explicitly addressed by these design curves, although test data illustrate potentially significant effects of LWR environments on the fatigue resistance of carbon and low–alloy steels.

Interim fatigue design curves that account for environmental effects were presented in NUREG/CR–5999. A more rigorous statistical analysis of the available data was developed in NUREG/CR–6335. One important conclusion derived from our test program and a rigorous review of the available data is that a minimum strain appears to be required for environmentally assisted decrease in fatigue life. This threshold strain may vary with material and loading conditions such as steel type, temperature, DO, strain ratio, mean stress, etc., but for both A106–Gr B carbon steel and A533–Gr B low–alloy steel used in our present study, the threshold strain range is ≈0.36%.

Although the correlations in NUREG/CR–5999 and NUREG/CR–6335 are in excellent agreement with available laboratory data for loading histories with constant strain amplitudes and constant strain rates during the tensile portion of the loading cycle, actual loading histories are far more complex. Exploratory fatigue tests are being conducted with waveforms where the slow strain rate is applied during only a fraction of the tensile loading cycle. The results of such tests will be used to develop a "damage rule" that can be used to predict life under complex loading histories.

The results of tests on A106–Gr B steel at ≈0.75% strain range under a variety of loading waveforms are summarized in Fig. 4. The histories consist of segments of loading and unloading at fast and slow strain rates. The variation in fatigue life of A106–Gr B and A533–Gr B steels as a function of the fraction of loading strain at slow strain rate is shown in Fig. 5; results from tests conducted at Ishikawajima–Harima Heavy Industries Co. (IHI) on the ANL heat of A106–Gr B steel are also included in the figure. Open symbols indicate tests where the slow portions occurred near the maximum tensile strain. Closed symbols indicate tests where the slow portions occurred near the maximum compressive strain. In stroke–controlled

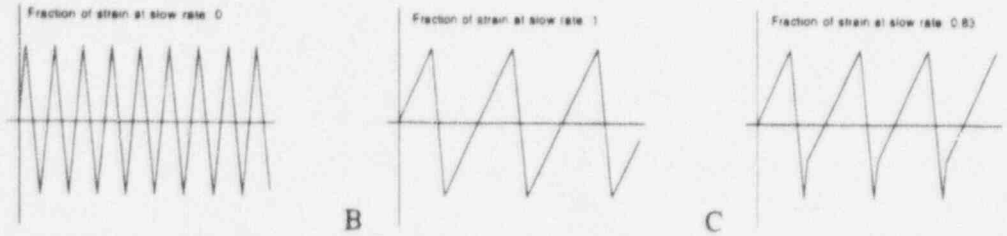

A

Air: 3,253; 3,753
PWR: 2,230; 1,525
Hi DO: 2,077; 1,756

B

Air: 3,721; 3,424; 6,275
PWR: 2,141
Hi DO: 303; 469

C

Air: 3,893
PWR: –
Hi DO: 340

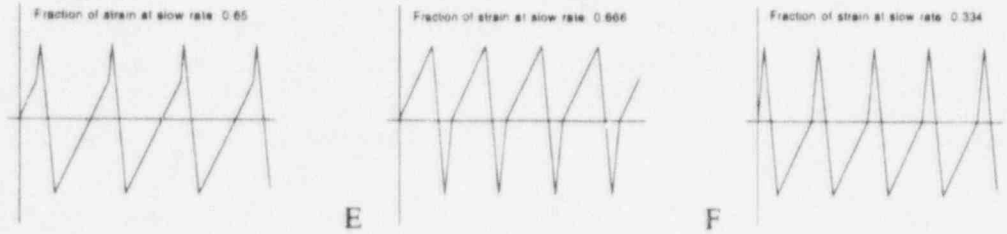

D

Air: 4,356
PWR: –
Hi DO: 615

E

Air: 5,261

F

Air: –
PWR: –
Hi DO: 1,935

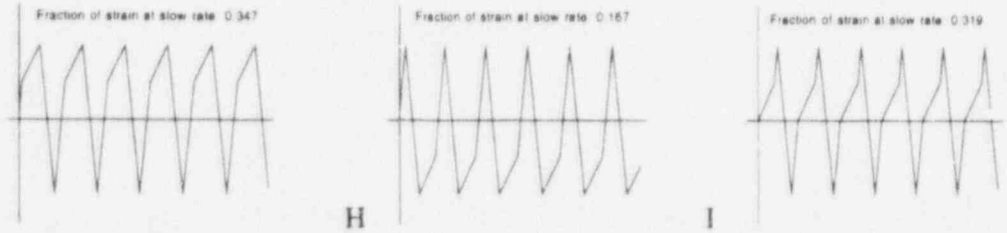

G

Air: 5,139
PWR: –
Hi DO: 615; 553

H

Air: 4,087
PWR: –
Hi DO: 1,649; 2,080

I

Air: 5,240
PWR: –
Hi DO: 1,306

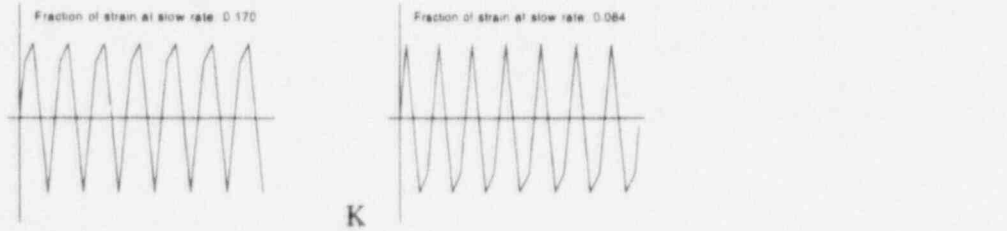

J

Air: 4,122
PWR: –
Hi DO: 888

K

Air: 4,105
PWR: –
Hi DO: 2,093

Figure 4. Fatigue life of A106–Gr B carbon steel at 288°C and 0.75% strain range in air and water under different loading waveforms

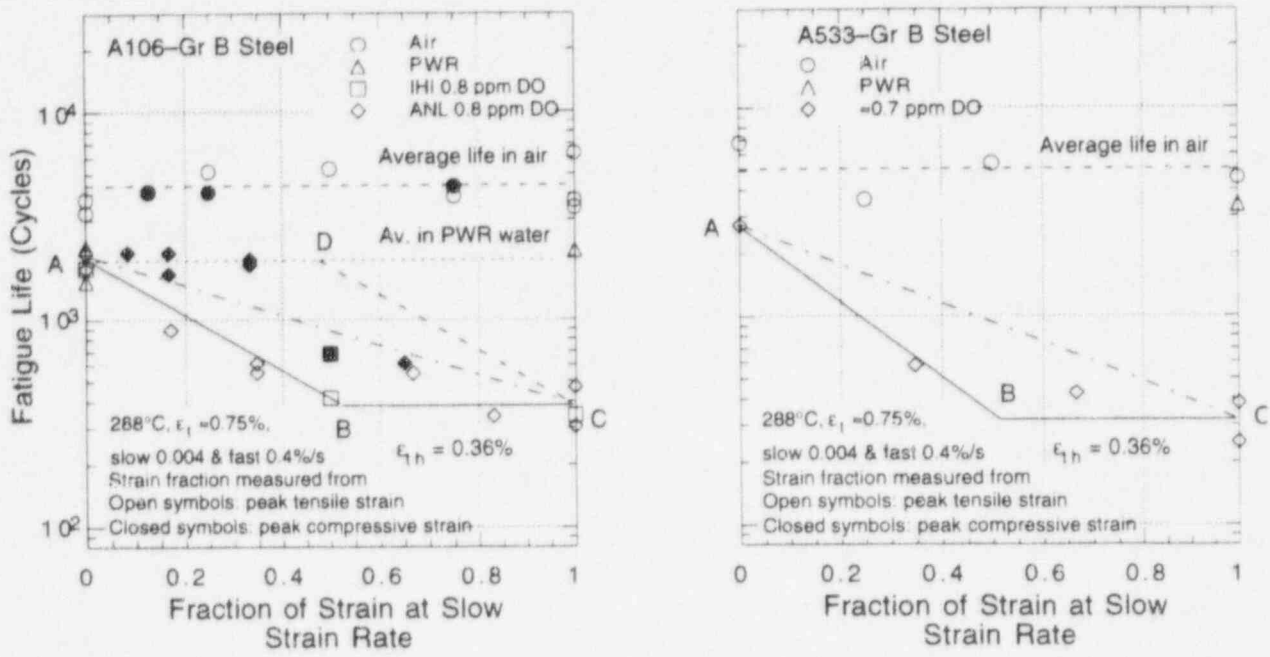

Figure 5. Fatigue life of A106–Gr B and A533–Gr B steels tested with loading waveforms where slow strain rate is applied during a fraction of tensile loading cycle

tests, the fraction of loading strain that is actually applied to the specimen gage section is not constant but varies during the cycle. For example, for waveforms E and F, although 0.5 of the applied displacement is at a slow rate, the actual fractions of strain at slow rate in the specimen gage section are 0.666 and 0.334, respectively.

The results to date suggest that a slow strain rate applied during any portion of the loading cycle above the threshold strain is equally effective in decreasing fatigue life, i.e., the relative damage due to the slow strain rate is independent of the strain amplitude once the amplitude exceeds the threshold value.[8–10] This can be demonstrated using the results shown in Fig. 5. If the relative damage were totally independent of strain amplitude, the life should decrease linearly from A to C along the chain–dot line in Fig. 5. Instead, loading histories where the slow strain rate occurs near the maximum compressive strain (waveforms F, H, or K) produce little damage (i.e., they follow the horizontal line AD in Fig. 5, until the fraction of the strain history is sufficiently large that slow strain rates are occurring for strain amplitudes greater than the threshold. In contrast, for loading histories where the slow strain rate occurs near the maximum tensile strain (waveforms E, G, or H), life decreases continuously with the fraction of strain applied at the slow strain rate (line AB in Fig. 5), and then saturates as the fraction increases so that a portion of the slow strain rate now occurs at amplitudes less than the threshold value (line BC in Fig. 5). Thus, the hypothesis that each portion of the loading cycle above the threshold strain is equally damaging implies the decrease in fatigue life should follow line ABC when a slow rate occurs near the maximum tensile strain, and line ADC when it occurs near the maximum compressive strain.

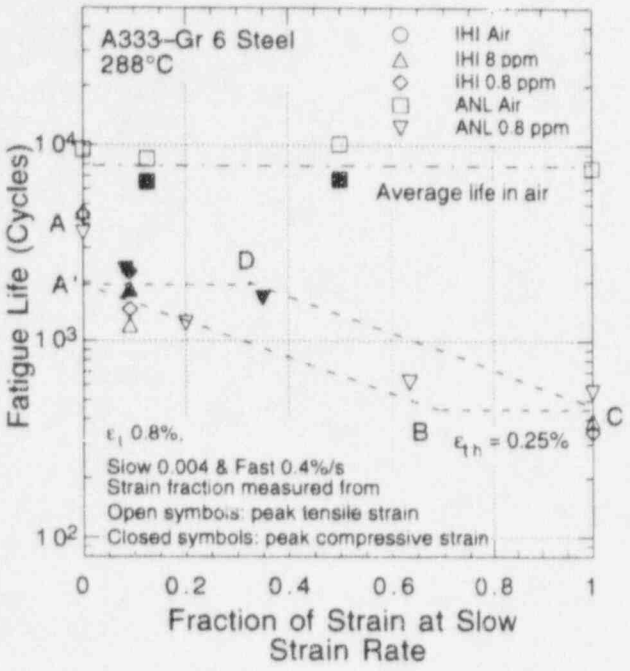

Figure 6.
Fatigue life of A333–Gr 6 carbon steel tested in air and water with loading waveforms where slow strain rate is applied during a fraction of the tensile cycle

Our conclusions appear to be in conflict with results from studies at IHI in Japan* that indicate that all portions of the tensile loading cycle are equally damaging, even the portion of the loading cycle that has only elastic strain. Fatigue tests were conducted on an IHI heat of A333–Gr 6 steel to try to resolve this issue.

The change in fatigue life of the IHI heat of A333–Gr 6 steel with fraction of loading strain at slow strain rate is shown in Fig. 6. Tests conducted at IHI in water containing 8 or 0.8 ppm DO are also included in the figure. The ANL and IHI test results are in good agreement. However, the data for this A333–Gr 6 steel appear to have a different trend than observed for the A106–Gr B steel used for the tests summarized in Fig. 5. For A333–Gr 6 steel, a slow strain rate near peak compressive strain appears to cause a significant reduction in fatigue life, whereas as discussed previously, steel slow strain rates only had a significant effect on fatigue of A106–Gr B when they occurred at strains greater than the threshold strain, which for this steel is ≈0.36%. We believe this apparent disagreement may be attributed to the effect of strain rate on fatigue life. A302–Gr B low-alloy steel and A333–Gr 6 carbon steel exhibit a strain rate effect in air, e.g., the fatigue life of both steels in air decreased ≈20% when the strain rate decreases from 0.4 to 0.004 %/s. In ' ', we believe that the decrease in fatigue life from A to A' is most likely caused by a strain rate effect that is independent of the environment. Further decreases in strain rate are unlikely to have a significant effect on fatigue life in air. If the hypothesis that each portion of the loading cycle above the threshold strain is equally damaging is valid, the decrease in fatigue life due to environmental effects should follow line A'BC when a slow rate is applied near peak tensile strain and line A'DC when it is applied near peak compressive strain.

Progress Report on Experimental Research on Fatigue Life in LWR Environment, May 1993 to September 1994, prepared by Japanese EFD Committee, Thermal and Nuclear Power Engineering Society, presented at the Pressure Vessel Research Council meetings in New York, October 10–13, 1994.

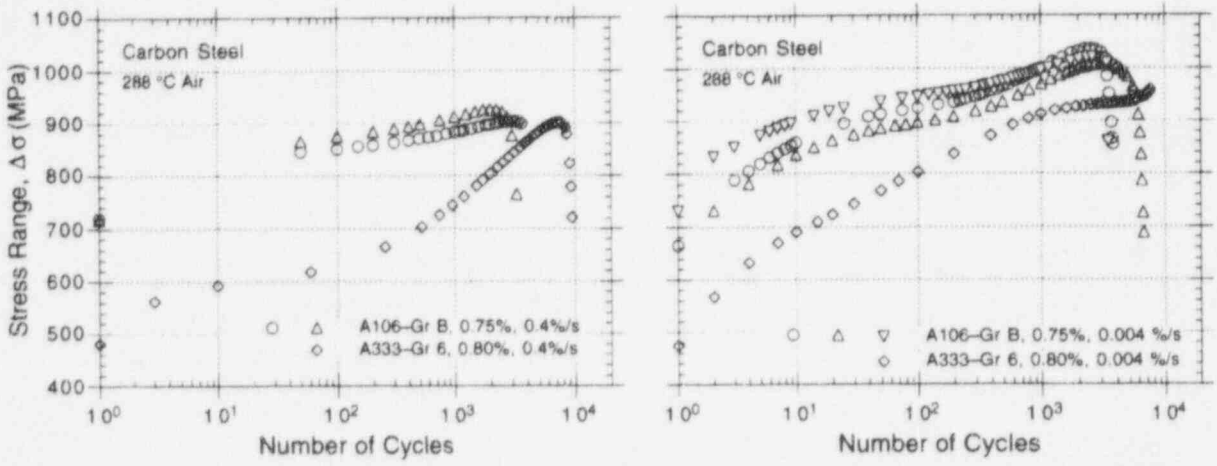

Figure 7. Effect of strain rate on cyclic strain–hardening behavior of A106–Gr B and A333–Gr 6 steels in air at 288°C and 0.75% strain range

Additional evidence of differences in behavior of the A106–Gr B and A333–Gr 6 steels is evident from the cyclic–hardening behavior. In Fig. 7, cyclic stress range is shown as function of the fatigue cycles for the two steels tested in air at 288°C, total strain range of 0.75 or 0.80%, and strain rates of 0.4 and 0.004 %/s. The A333–Gr 6 steel has a very low yield stress and shows significant cyclic hardening during the entire test. The A106–Gr B steel has a higher yield stress and exhibits a rapid cyclic hardening only during the initial 100 cycles. The latter also shows some dynamic strain aging at slow strain rates.

Environmentally Assisted Cracking of Alloy 600 and SSs in Simulated LWR Water

Besides its widespread use for steam generator tubing, Alloy 600 is used for a variety of structural elements in reactor systems. Cracking has been observed in a number of these components, e.g., instrument nozzles and heater thermal sleeves in the pressurizer,† penetrations for control–rod–drive mechanisms in reactor vessel closure heads in the primary system of PWRs,†† and in shroud–support–access–hole covers§ in BWRs. Experience strongly suggests that materials that are susceptible to SCC are also susceptible to environmental degradation of fatigue life and fatigue–crack–growth properties. Preliminary information on the effect of temperature, load ratio, and stress intensity on environmentally assisted cracking (EAC) of Alloys 600 and 690 in simulated BWR and PWR water has been obtained, and the crack growth rates (CGRs) of these materials have been compared with those of Type 316NG and sensitized Type 304 SS under conditions where EAC occurs in all materials.

The effect of water chemistry on CGRs of mill–annealed Alloy 600 and sensitized Type 304 SS was explored at a load ratio of 0.95 in water that contained ≈200 ppb DO. Small amounts of chromate and sulfate (<200 ppb) and two amines (1–5 ppm) produced small but measurable changes in the CGRs of the sensitized Type 304 SS specimens but had virtually no effect on the CGR of the Alloy 600 specimen. The CGR data for the three specimens are plotted in Fig. 8 versus the CGRs for wrought SSs in air predicted by the ASME Code Section XI correlation at the K_{max} and load ratio values used in the tests. The dashed and

†USNRC Information Notice No. 90–10, "Primary Water Stress Corrosion Cracking (PWSCC) of Inconel 600," Feb. 1990.

††INPO Document SER 20–93 "Intergranular Stress Corrosion Cracking of Control Rod Drive Mechanism Penetrations," Sept.1993.

§USNRC Information Notice No. 92–57, "Radial Cracking of Shroud Support Access Hole Cover Welds," Aug. 1992.

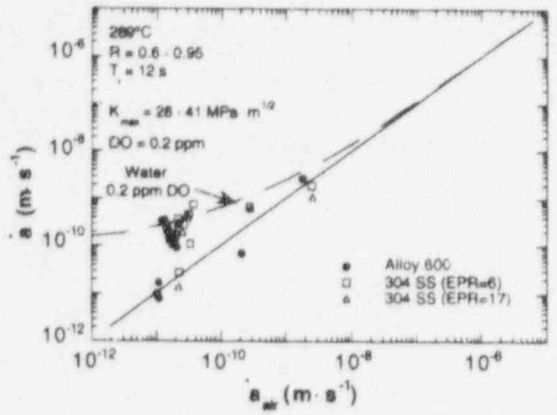

Figure 8.
Corrosion fatigue data for specimens of Alloy 600 and sensitized Type 304 SS in oxygenated water at 289°C. Dashed line represents ANL model predictions for austenitic SSs in water containing 0.2 ppm DO. Diagonal line corresponds to crack growth of SSs in air.

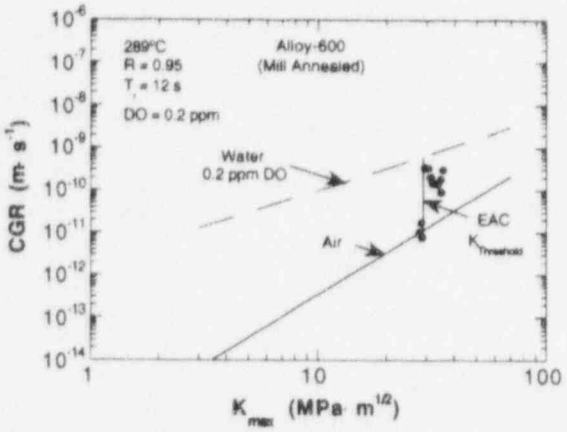

Figure 9.
Dependence of CGR of Alloy 600 specimen on K_{max} in oxygenated water at 289°C. Dashed and solid lines represent ANL model predictions for austenitic SSs in water containing 0.2 ppm DO and in air, respectively, at an R value of 0.95 and rise time of 12 s.

solid lines represent ANL model predictions for crack growth in water[11] and the "air line" predicted by the ASME Code, respectively. The data for all materials are bounded by the two curves. There appears to be a transition between the "air" curve and EAC behavior at a threshold corresponding to $\dot{a}_{air} \approx 2 \times 10^{11}$ m·s^{-1}. This threshold behavior can also be expressed in terms of K_{max} as shown in Fig. 9, which suggests a threshold K_{max} for EAC of ≈26 MPa·m$^{1/2}$ at an R of 0.95.

Corrosion–fatigue experiments were conducted on mill–annealed Alloy 600 and mill–annealed plus thermally treated Alloy 690 specimens to investigate the effects of temperature and dissolved oxygen and hydrogen in HP water on CGRs of these materials. The results are summarized in Fig. 10. At load ratios of 0.2 and 0.6, the CGRs are virtually independent of DO concentration or the ECP, which is not surprising, because at this load ratio, the CGRs are dominated by the mechanical cycling. At a higher load ratio of 0.9 where the environmental contribution is more significant, the CGRs decrease as the DO concentration or ECP decreases at 289 and 320°C. In all cases, the CGRs of both materials lie near or below the "air" curve for austenitic SSs. At an R ratio of 0.6, CGRs were typically higher in Alloy 690 than in Alloy 600. However, at an R ratio of 0.9, where the CGR dependence on DO concentration and ECP suggest that environmental enhancement is significant, CGRs in Alloy 600 were generally greater than those in the Alloy 690.

Experiments were also performed in simulated PWR primary–system water containing 450 ppm B and 2.25 ppm Li (added to the feedwater as H_3BO_3 and LiOH), 3–58 cm^3 H_2·kg^{-1} H_2O, and 750 ppb hydrazine,

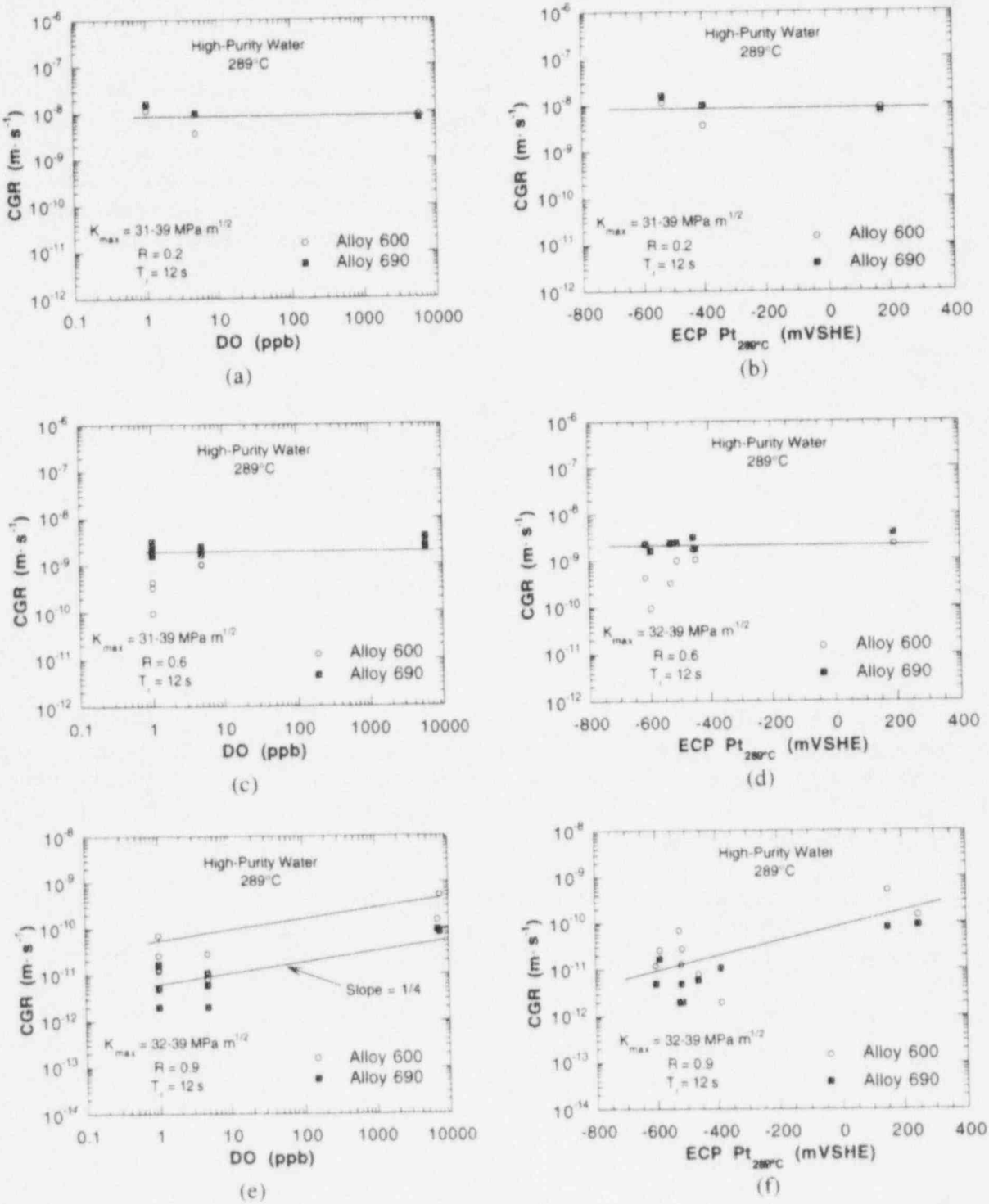

Figure 10. Dependence of CGRs of Alloy 600 and 690 specimens at 289°C on DO concentration in HP water and ECP of Pt electrode at 289°C at load ratios (R) of 0.2 (a and b), 0.6 (c and d), and 0.9 (e and f), respectively

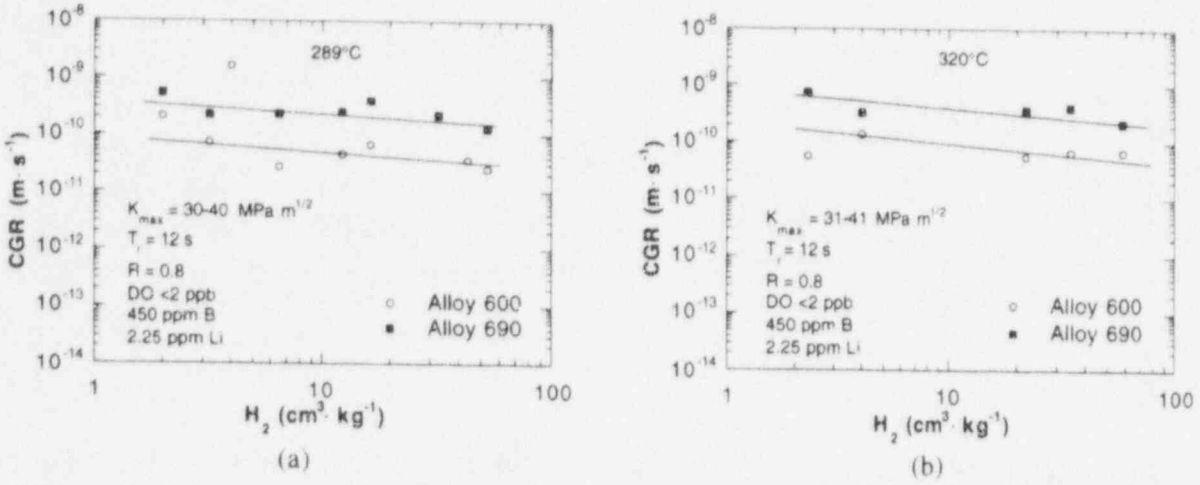

Figure 11. Dependence of CGRs of Alloy 600 and 690 specimens at (a) 289 and (b) 320°C on dissolved–H_2 concentration in simulated PWR water at load ratio of 0.8

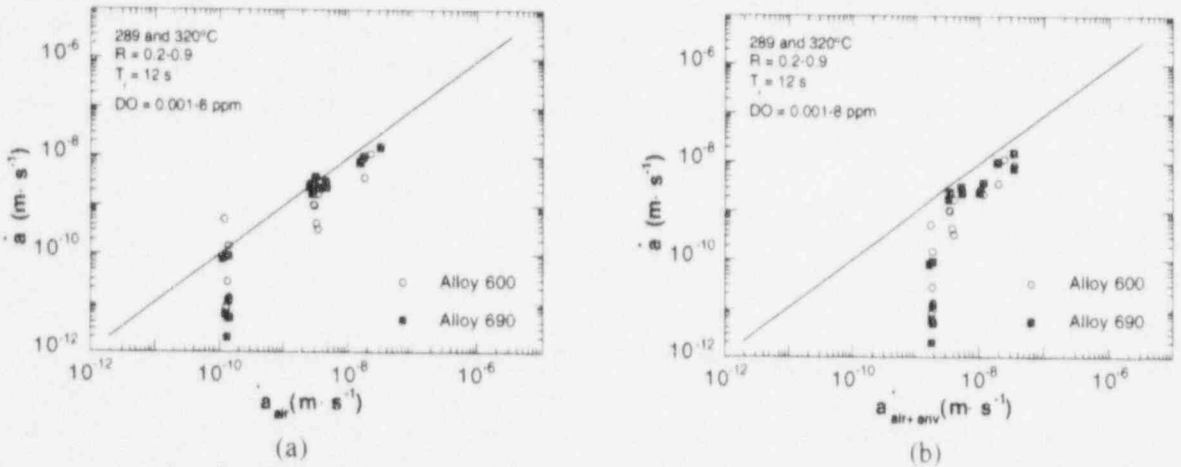

Figure 12. Corrosion fatigue data for Alloy 600 and 690 specimens in HP water at 289 and 320°C vs. (a) CGRs for SSs in air predicted by ASME Code, and (b) CGRs for SSs in water from ANL model, both under same loading conditions as in experiments. Lines represent identical CGRs for these alloys in test environments and for SSs (a) in air and (b) in water.

which was added to scavenge the residual DO to a very low level (≈1 ppb). The results of these tests are summarized in Fig. 11. At the load ratio R = 0.8 and water chemistry conditions used for these tests, the Alloy 690 specimen exhibited a higher CGR by a factor of ≈3 than Alloy 600 at both 289 and 320°C. Crack growth experiments will be conducted at higher load ratios, including constant load (R = 1.0), to determine whether Alloy 690 exhibits lower rates than Alloy 600 at higher R values. The CGRs decreased slightly as dissolved H_2 concentration increased from 3 to 58 $cm^3 \cdot kg^{-1}$. A somewhat larger decrease in the CGRs was expected based on a predicted change in the thermodynamic stability of NiO corrosion product on the alloys as the H_2 concentration of water increased, or as the temperature decreased in these experiments.

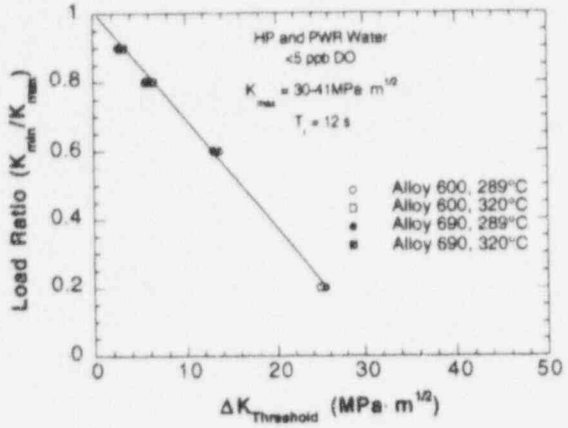

Figure 13.
Dependence of ΔK_{th} for Alloy 600 and 690 specimens in simulated PWR and de-oxygenated HP water on load ratio at 289 and 320°C

The CGRs for R ratios from 0.2–0.9 and DO concentrations from 0.001–8 ppm are plotted in Fig. 12 in terms of the CGR rate predicted by the ASME Section XI curve for SSs in air and the environmentally enhanced CGRs for SSs in water predicted by the correlations presented in Ref. 11. At very low CGRs the correlations are very conservative compared to the observed CGRs. The threshold values of ΔK as a function of load ratio R, corresponding to the threshold CGRs in Fig. 12, are shown in Fig. 13. Although only data at low DO are plotted in the figure, the results in Fig. 12 suggest that the results are valid even at higher DO levels. The dependence of $\Delta K_{Threshold}$ on load ratio can be expressed by a simple linear equation:

$$\Delta K_{th} = 32.0\,(1-R). \qquad (1)$$

SCC and Corrosion Fatigue of Austenitic and Aged Cast Stainless Steels

Most of the available data on corrosion fatigue of austenitic SSs in aqueous environments have been developed in support of LWR technology in the United States and abroad. Because Section XI of the ASME Code currently provides only an in-air design curve, corrosion fatigue data from the literature were analyzed to develop corrosion fatigue curves for SSs in aqueous environments. The results of this review were published in NUREG/CR-6176. At that time, there were few data available on CGRs in deaerated water at CGRs of 10^{-10} m·s^{-1} or less, which are of most interest in actual applications. Therefore, a conservative recommendation was made, i.e., correlations based on data obtained in water that contained ≈0.2 ppm DO should also be applied to low-oxygen environments characteristic of PWRs. Additional CGR tests on cast duplex and austenitic SSs have been performed to provide a technical basis for updating the correlations given in NUREG/CR-6176.

These tests indicated that CGRs in thermally aged cast SSs are similar to those in wrought SSs. In Fig. 14, measured CGRs for aged and nonaged cast SSs are compared with the predictions based on correlations for wrought SSs in NUREG/CR-6176. Tests in low-DO water show lower CGRs than in water with 0.2 ppm DO. Ford et al.[12] developed a detailed CGR model that includes the effects of DO (through changes in ECP). Based on SSRT tests, Kassner et al.[13] suggested that CGRs exhibit an $\approx[O_2]^{1/4}$ dependence on DO concentration. Predictions of both models are in reasonable agreement with the observed decreases in CGR corresponding to a decrease from 8 ppm to 200 ppb, but the model of Ford et al. predicts a significantly

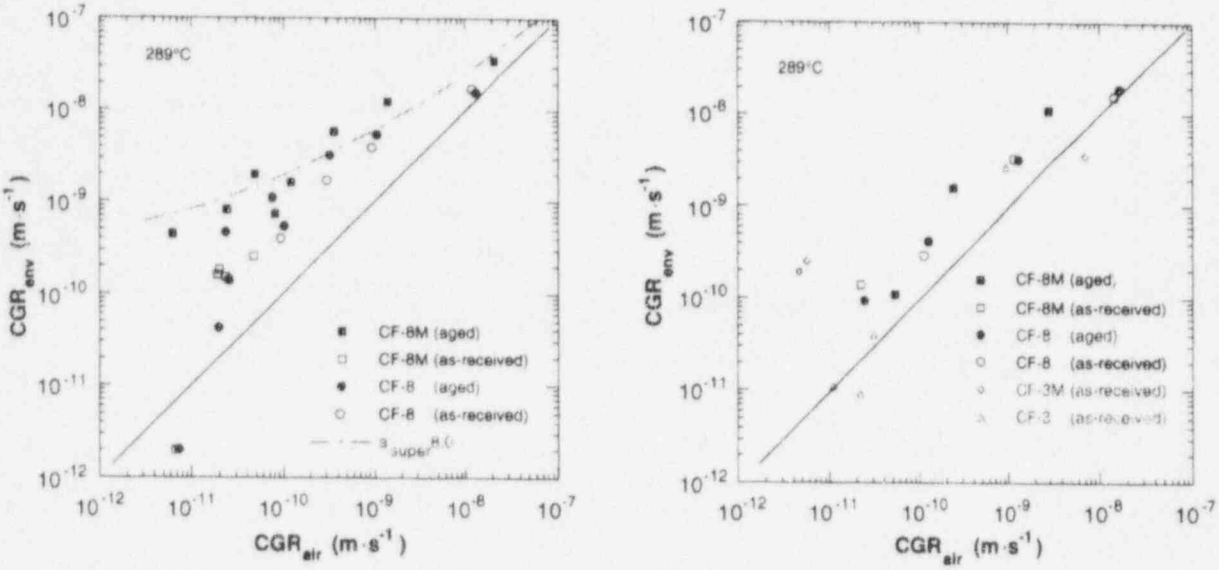

Figure 14. Corrosion fatigue data for as–received CF–3, –3M, and –8M and aged CF–8M and –8 cast SS in water containing 8 (left) and 0.2 (right) ppm DO at 289°C. Diagonal lines correspond to crack growth in air in Section XI of the ASME Code. Dashed lines indicate predictions from correlations in NUREG/CR–6176.

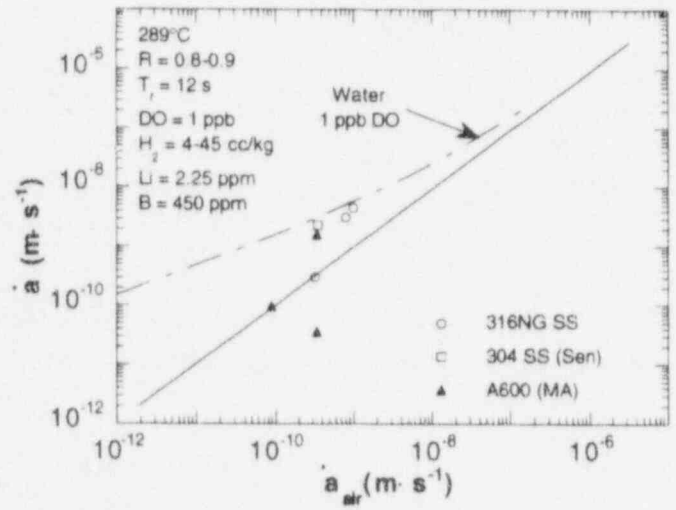

Figure 15.
Corrosion fatigue data for specimens of Alloy 600, Type 316NG and sensitized Type 304 SS in simulated PWR primary water at 289°C. Dashed line represents model predictions for austenitic SSs in water containing 1 ppb DO. Diagonal line corresponds to crack growth of SSs in air.

larger decrease in CGR than that of Kassner et al. when the DO decreases to ≈ 1 ppb. Revised correlations based on the latter model[13] are in good agreement with observed CGRs, as shown in Fig. 15.

Tests were also performed on Types 316NG and 304 SS and as–received and thermally aged CF–3 cast SS to investigate threshold stress intensity factors ΔK_{th}^{EAC} for EAC. Threshold behavior was clearly observed, as shown in Fig. 16, and the dependence of ΔK_{th}^{EAC} on load ratio for Types 347, 316NG, and sensitized 304 SS, and for thermally aged CF–3 and CF–8 grades of cast SS, was determined (Fig. 17). As in the case of Alloys 600 and 690, a simple linear relationship was observed:

$$\Delta K_{th}^{EAC} = 25.0(1 - R). \qquad (2)$$

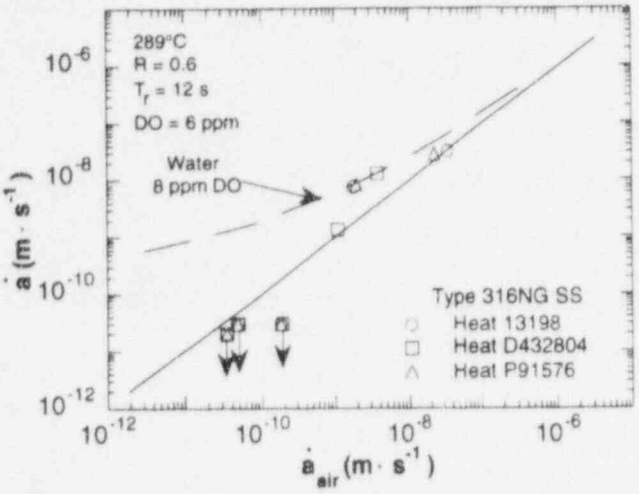

Figure 16.
Corrosion fatigue data for specimens from three heats of Type 316NG SS in HP oxygenated water at 289°C. Dashed line represents model predictions at an R value of 0.6 and rise time of 12 s in water containing 8 ppm DO. Solid line corresponds to crack growth of SSs in air.

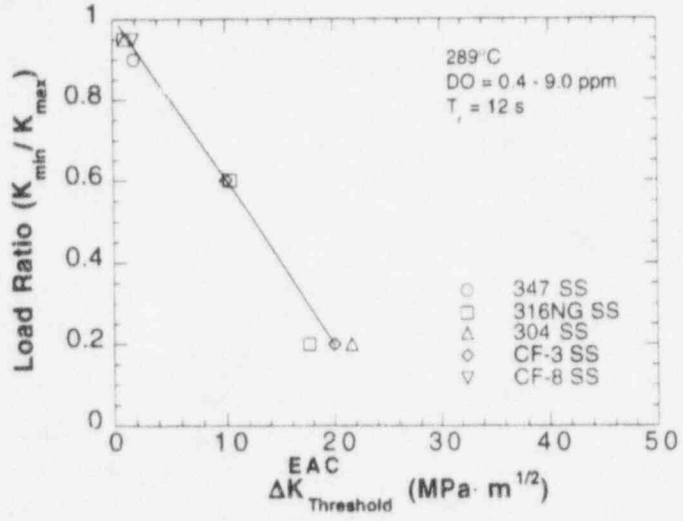

Figure 17.
Dependence of ΔK_{th} for EAC of wrought and cast austenitic SSs in HP oxygenated water at 289°C on load ratio

The correlations in NUREG/CR-6176 are being revised to include some "credit" for low DO in PWR environments. The data are being reviewed to determine whether thresholds can be included in the revised correlations.

References

1. M. Kodama, S. Nishimura, J. Morisawa, S. Shima, S. Suzuki, and M. Yamamoto, *Effects of Fluence and Dissolved Oxygen on IASCC in Austenitic Stainless Steels*, Proc. 5th Int. Symp. on Environmental Degradation of Materials in Nuclear Power Systems – Water Reactors, D. Cubicciotti, E. P. Simonen, and R. Gold, eds., American Nuclear Society, La Grange Park, IL, pp. 948-954 (1992).

2. M. Kodama, R. Katsura, J. Morisawa, S. Nishimura, S. Suzuki, K. Asano, K. Fukuya, and K. Nakata, *IASCC Susceptibility of Austenitic Stainless Steels Irradiated to High Neutron Fluence*, Proc. 6th Int.l Symp. on Environmental Degradation of Materials in Nuclear Power Systems - Water Reactors, R. E. Gold and E. P. Simonen, eds., The Minerals, Metals, and Materials Society, Warrendale, PA, pp. 583–588 (1993).

3. M. E. Indig, J. L. Nelson, and G. P. Wozadlo, *Investigation of the Protection Potential Against IASCC*, Proc. 5th Int. Symp. on Environmental Degradation of Materials in Nuclear Power Systems – Water Reactors, D. Cubicciotti, E. P. Simonen, and R. Gold, eds., American Nuclear Society, La Grange Park, IL, pp. 941–947 (1992).

4. H. M. Chung, W. E. Ruther, and J. E. Sanecki, in *Environmentally Assisted Cracking in Light Water Reactors: Semiannual Report, October 1993–March 1994*, NUREG/CR–4667 Vol. 18, ANL–95/2, pp. 27–35 (March 1995).

5. C. T. Ward, D. L. Mathis, and R. W. Staehle, *Intergranular Attack of Sensitized Austenitic Stainless Steel by Water Containing Fluoride Ions*, Corrosion **25**, 394–396 (1969).

6. N. C. Huang and Z. Nagy, *Kinetics of the Ferrous/Ferric Electrode Reaction in the Absence of Chloride Catalysis*, J. Electrochem. Soc. **134**, 2215–2220 (1987).

7. S. Kasahara, K. Nakata, K. Fukuya, S. Shima, A. J. Jacobs, G. P. Wozadlo, and S. Suzuki, *The Effects of Minor Elements on IASCC Susceptibility in Austenitic Stainless Steels Irradiated with Neutrons*, in Proc. 6th Int. Symp. on Environmental Degradation of Materials in Nuclear Power Systems - Water Reactors, R. E. Gold and E. P. Simonen, eds., The Minerals, Metals, and Materials Society, Warrendale, PA, pp. 615–622 (1993).

8. O. K. Chopra, W. F. Michaud, and W. J. Shack, in *Environmentally Assisted Cracking in Light Water Reactors, Semiannual Report, April–September 1994*, NUREG/CR–4667 Vol. 19, ANL–95/25, pp. 3–18 (Sept. 1995).

9. O. K. Chopra and W. J. Shack, *Effects of LWR Environments on Fatigue Life of Carbon and Low-Alloy Steels*, in Fatigue and Crack Growth: Environmental Effects, Modeling Studies, and Design Considerations, PVP Vol. 306, S. Yukawa, ed., American Society of Mechanical Engineers, New York, pp. 95–109 (1995).

10. O. K. Chopra and W. J. Shack, *Effects of Material and Loading Variables on Fatigue Life of Carbon and Low-Alloy Steels in LWR Environments*, in Transactions of the 13th Int. Conf. on Structural Mechanics in Reactor Technology (SMiRT 13), Vol. II, M. M. Rocha and J. D. Riera, eds., Escola de Engenharia – Universidade Federal do Rio Grande do Sul, Porto Alegre, Brazil, pp. 551–562 (1995).

11. W. J. Shack and T. F. Kassner, *Review of Environmental Effects on Fatigue Crack Growth of Austenitic Stainless Steels*, NUREG/CR–6176, ANL–94/1, (May 1994).

12. F. P. Ford, D. F. Taylor, P. L. Andresen, and R. Ballinger, *Corrosion-Assisted Cracking of Stainless and Low-Alloy Steels*, EPRI NP-5064s, Electric Power Research Institute, Palo Alto, CA (February 1987).

13. T. F. Kassner, W. E. Ruther, and W. K. Soppet, *Mitigation of Stress Corrosion Cracking of AISI 304 Stainless Steel by Organic Species at Low Concentrations in Oxygenated Water*, Corrosion 90, Paper No. 489, Las Vegas, NV (April 1990).

Steam Generator Tube Integrity Program*

D. R. Diercks,† J. Muscara,** and W. J. Shack†
†Argonne National Laboratory
Argonne, Illinois
**Office of Nuclear Regulatory Research, USNRC

Abstract

A new research program on steam generator tubing degradation is being sponsored by the U.S. Nuclear Regulatory Commission (NRC) at Argonne National Laboratory. This program is intended to support a performance-based steam generator tube integrity rule. Critical areas addressed by the program include evaluation of the processes used for the in-service inspection of steam generator tubes and recommendations for improving the reliability and accuracy of inspections; validation and improvement of correlations for evaluating integrity and leakage of degraded steam generator tubes, and validation and improvement of correlations and models for predicting degradation in steam generator tubes as aging occurs. The studies will focus on mill-annealed Alloy 600 tubing, however, tests will also be performed on replacement materials such as thermally-treated Alloy 600 or 690. An overview of the technical work planned for the program is given.

Introduction

Steam generators have historically been among the most troublesome of the major components in commercial pressurized water reactor (PWR) nuclear power plants around the world. Corrosion problems have afflicted steam generators from the very introduction of PWR technology. Shippingport, the first commercial PWR operated in the United States, developed leaking cracks in two Type 304 stainless steel (SS) steam generator tubes in 1957, after only 150 h of full-power operation. Other early incidents of stress corrosion cracking (SCC) in austenitic SS steam generator tubes occurred at the Savannah River Heavy Water Plutonium Production Reactor, the USS Nautilus Reactor, the Hanford New Production Reactor, the Yankee Rowe PWR, and the Indian Point Unit 1 PWR. The first three failures were attributed to halide-induced SCC and the latter two to free caustic.

Because austenitic SS steam generator tubes were found to be susceptible to SCC from both chlorides and free caustic, the decision was made in the late 1960s to use Alloy 600 tubes in the U.S. and most of Europe and Alloy 800 tubes in Germany. However, these changes did not eliminate corrosion-related degradation in steam generator tubing, and a succession of failures has continued to afflict steam generators in the U.S. and around the world.

The U.S. Nuclear Regulatory Commission (NRC) is developing a "performance-based" rule and regulatory guide related to the integrity of steam generator tubes. Key considerations for such an approach include good inspections of steam generator tubes, sound engineering evaluations of tube condition against performance criteria, and establishment of performance criteria that ensure compliance

---

* Job Code: W6487; NRC Program Manager: Dr. J. Muscara

with the rule. It is expected that as plant age and degradation proceeds, new forms of degradation may appear and new defect-specific management schemes will need to be implemented.

Although the actual implementation of performance-based criteria will be developed primarily by industry, the NRC must be able to evaluate industry-proposed implementations. To support this effort, a new research program on the degradation of steam generator tubing is being sponsored by the NRC at Argonne National Laboratory. The objective of the new program is to provide experimental data and predictive correlations and models that are needed to permit the NRC to independently evaluate the integrity of steam generator tubes. To achieve this objective, the critical areas addressed by the program include evaluation of the process used for the in-service inspection of steam generator tubes, including procedures and equipment, and recommendations for improving the reliability and accuracy of in-service inspection (ISI); validation and improvement of correlations and models for evaluating integrity and leakage of degraded steam generator tubes; and validation and improvement of correlations and models for predicting the generation and progression of degradation in steam generator tubes as a function of aging, including the effects of operational environmental conditions such as temperature, dryout and concentration, stresses, and primary and secondary-side water chemistry.

The new program builds upon the results of NRC steam generator tube integrity and inspection research conducted since 1977. That effort has produced correlations for evaluating the integrity of degraded tubes and quantifying inspection reliability. The results from this past research work have helped to ensure the safe operation of steam generators. However, characterization of degradation in aging steam generator tubes becomes more critical with each passing year as crack initiation times are reached, established degradation proceeds and new forms of degradation appear, inspection technology changes, and regulatory criteria change to reduce excessive conservatism for specific types of degradation. The new program will produce and/or update information, data, and predictive modeling methods for the degradation types and inspection techniques of current interest.

The studies will focus primarily on mill-annealed (MA) Alloy 600 steam generator tubing. Although most steam generators that use Alloy 600 MA will eventually have to be replaced, the behavior of this material will be of concern for many years. However, some testing will also be performed on replacement materials such as thermally treated Alloy 600 or 690. Although these materials are expected to be much less susceptible to degradation than Alloy 600 MA, it is still necessary to predict their behavior.

The technical work in the program is divided into four tasks:

1. Assessment of inspection reliability
2. Research on ISI technology
3. Research on degradation modes and integrity
4. Development of methodology and technical assessments for current and emerging regulatory issues

Brief overviews of the activities in each of these areas are given in the remaining sections of the paper.

Assessment of Inspection Reliability

The objective of this task is to evaluate and quantify the reliability of currently used methods of inspection for current-day flaws. The reliability and accuracy of these techniques must be quantified so that repair criteria and the consequences of degraded tubes remaining in service after inspections can be evaluated. Eddy current and other nondestructive evaluation (NDE) techniques currently used for steam generator tube ISIs will be evaluated with respect to probability of flaw detection and accuracy of sizing to enable evaluation of the consequences of degraded tubes remaining in service after inspections. The methods and test parameters studied will be those currently used for various forms (and locations) of degradation. The results of the NDEs will be validated by inspection and destructive evaluation of the degraded tubing.

The work performed under this task will focus on the performance and evaluation of round-robin (RR) tests by commercial ISI teams on degraded steam generator tubing. The RR tests will include both eddy current and ultrasonic test methods. Teams will report the flaw types, sizes, and locations in addition to other commonly used parameters such as voltage responses from the eddy current tests. The inspection methods used will include those used commercially during this period and in the recent past. The number of tubes inspected by each method and number of teams will be consistent with providing meaningful statistical data on detection probability and characterization accuracy.

Initial testing will utilize a steam generator tube bundle mockup with laboratory-degraded tubes that is being developed at Pacific Northwest Laboratory under the sponsorship of the NRC. Coordination and insights will also be sought from the Performance Demonstration Program at the Electric Power Research Institute (EPRI) NDE Center.

The steam generator tube bundle mockup contains 400 12-foot-long sections consisting of 3600 one-foot-long tube segments and 400 three-foot-long segments. The tubing is Alloy 600 MA with an 0.875 in. o.d. and a wall thickness of 0.050 in. The segments may be rearranged to create a very large variety of defect arrangements, and the arrangement of tubes/specimens is not visible to those conducting the examinations. Simulated conditions include three carbon steel support plates, a tube sheet (simulated by carbon steel sleeves), roll expansion of tubing, and sludge. The mockup is oriented horizontally and does not include U bends. It is 148 in. long, 33 in. wide, and 30 in. high, and contains a variety of flaw types and notches.

It is intended that the studies on the mockup and on other laboratory specimens will be complemented by RR tests performed on actual service-degraded tubes. We will try to work with EPRI and utilities in the U.S. and abroad to determine the feasibility of obtaining access to and conducting in-situ NDE tests on service degraded steam generator tubes and/or build a library of service-degraded tubes removed from generators.

In addition to the RR tests that will be performed by commercial teams, all cracked tubing samples will be nondestructively examined before pressure and leak rate testing. Similarly, cracked tubes from corrosion studies will also be nondestructively characterized. Conventional multifrequency and advanced eddy current tests will be conducted. In addition, alternate eddy current parameters, such as voltage amplitude, and complementary inspection techniques, such as ultrasonic testing, will also be used, and the capability of these parameters and techniques to characterize the structural integrity of degraded tubes will be evaluated.

Research on ISI Technology

The objective of this task is to evaluate advanced NDE and signal analysis techniques for reliable ISI of original and repaired steam generator tubes. In coordination with the task on degradation modes and integrity, improved correlations between eddy current results and flaw morphology, leak rate, and failure pressure will be developed.

The research on improved eddy current inspection of steam generator tubes will focus on four primary areas: (1) analytical predictions of eddy current response as a function of probe type, flaw characteristics, and material properties; (2) evaluation of effective signal analysis procedures through tools such as neural networks; (3) evaluation of flaw imaging and display methods for simple and accurate flaw characterization; and (4) evaluation of improved probes such as the Plus Point and Cecco family of probes. In addition, the use of ultrasonic probes will be pursued. The reliability and effectiveness of improved inspection techniques will be demonstrated through laboratory testing of steam generator tubes that contain various flaws and of the steam generator tube bundle mockup. Final validation will utilize in-service degraded steam generator tubes.

The multiproperty analysis methods developed in NRC-sponsored work at Oak Ridge National Laboratory will be used to examine the effectiveness of multiparameter eddy current correlations for more accurate prediction of failure pressures and leak rates. The goal is to develop robust correlations that will be valid for a wide variety of degradation modes.

In addition to degraded tubing, it is also important to assess the effectiveness of ISI of tubes that have been repaired, e.g., by sleeving. The techniques currently used for the inspection of tubes repaired by various processes, including different sleeving methods, and at different locations in the generator will be identified. Repaired tube specimens to represent actual repairs conducted in the field, concentrating on the various sleeve repairs, will be developed for use in evaluating inspection methods under this task. These specimens will also be used for the measurement of residual stresses associated with various types of repair. This information will be needed for work under other program tasks, such as evaluation of cracking susceptibility.

As degraded tubes become available from the laboratory experimental program, from the mockup, and from service-degraded generators, they will be characterized by a variety of nondestructive tests, and the important test and signal response parameters will be stored for subsequent studies. For example, for eddy current testing with bobbin coil probes, the voltage responses and phase angles from at least four frequencies will be stored. The tests will include standard commercial eddy current and ultrasonic techniques, probes, and procedures as well as advanced and emerging techniques, probes, and procedures. Calibrations will be conducted according to accepted practices and standards. The library of raw data will be available to validate correlations between NDE parameters and flaw size, type, orientation and morphology, and multiparameter correlations between eddy current and failure pressure and leak rate. In addition to this "data library," a collection of laboratory degraded tubes, tubes from the mockup, and tubes from service degraded generators will be kept to help evaluate new and advanced NDE procedures and techniques.

Research on Degradation Modes and Integrity

The objective of this task is to evaluate and experimentally validate models to predict potential degradation modes, progression rates, leak/rupture behavior, failure pressures, and leak rates for steam generator tubes and for repaired tubes under normal operating, accident, and severe-accident conditions.

Deterministic and probabilistic models for predicting failure pressures and leak rates under normal operating and accident conditions from degraded tubes in steam generators have been formulated and used. These models have often been generated from limited data, and/or data and correlations from laboratory work where the flaw morphology and tube conditions do not necessarily represent in-service conditions representative of current-day degradation modes. The work performed under this task will update and validate these models and correlations or, if required, produce new correlations for flaw types that are representative of those that currently affect operating steam generators. For example, outer diameter stress corrosion cracking at tube support plates is typically characterized by groups of relatively short axial cracks with differing depths and lengths, with ligaments of varying size between them, and with varying numbers and distribution around the circumference. Emphasis will be placed on relatively deep defects (80 percent throughwall and greater), because these are the defects that might lead to leakage or ruptures under normal or accident loading conditions. Similarly, additional information is needed to describe the behavior of tubing with circumferential cracks with varying lengths, depths, ligaments, and distributions around the circumference. The primary emphasis again will be on deep cracks. The experimental studies will be coupled with analytical studies of the crack configurations. The analytical studies will be used to determine "critical" configurations; the experimental results then will serve to refine and validate the analytical models.

The tube failure and leak rate test facility has been designed to determine tube failure and leak rates in tubing with complex arrays of axial and circumferential cracks characteristic of those observed in practice and will have sufficient flow capacity so that throughwall cracks can be driven unstable without patches or bladders. Because the circumferential stresses on the tubing due to the pressure loading are twice as large as the axial stresses, even without axial cracks, tubing will fail by radial expansion and rupture unless the circumferential crack encompasses more than a 60° segment of the circumference as shown in Fig. 1. Based on limit load calculations, the failure pressure for the cracked tube also depends markedly on whether the tube is free to bend or is laterally restrained. As shown in Fig. 1, failure pressure for circumferentially cracked tubing is strongly dependent on the degree of constraint imposed upon the tubing. For 0.75-in.-diameter tubing, analysis suggests that as long as the free span of the tubing is <58 in., the tubing will fail at the higher "complete constraint" load. In the test facility, fixtures will be provided so that constraint conditions ranging from the moment-free case to complete constraint can be simulated.

Most studies of tubing failure to date have focused on normal operating conditions and design-basis accidents. Failure pressures and leak rates from degraded tubes that have been subjected to severe-accident conditions are not well understood. Severe-accident analyses suggest that tubes can reach fairly high temperatures. As shown in Fig. 2a, the strength of Alloy 600 decreases rapidly with temperatures. At elevated temperatures, material flow and crack opening will be greater than under normal operating temperatures and the leak rates may be higher, whereas failure pressure will be lower. At temperatures above ≈750°C, even unflawed tubes fails rapidly at the pressures that are predicted to occur in severe accidents [Fig. 2b]. A truly time-dependent critical pressure calculation is complex. Several complicating factors must be considered:

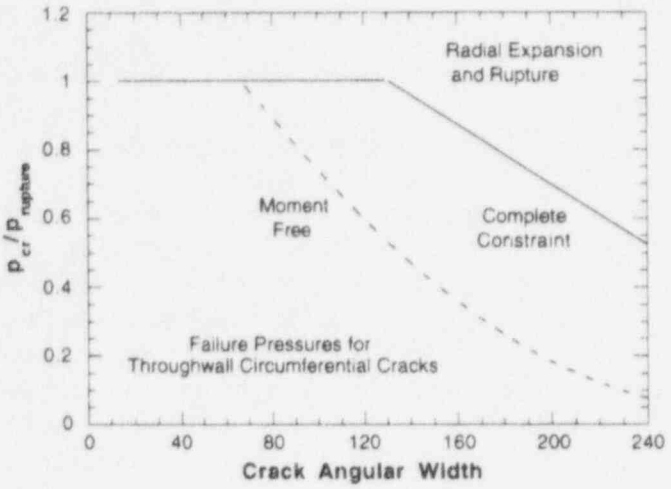

Figure 1
Ratio of failure pressure for tubes containing circumferential throughwall crack (p_{cr}) to failure pressure for an unflawed tube ($p_{rupture}$) as a function of crack angular width. Failure pressures are much lower for the case when there is no lateral restraint on the tubing.

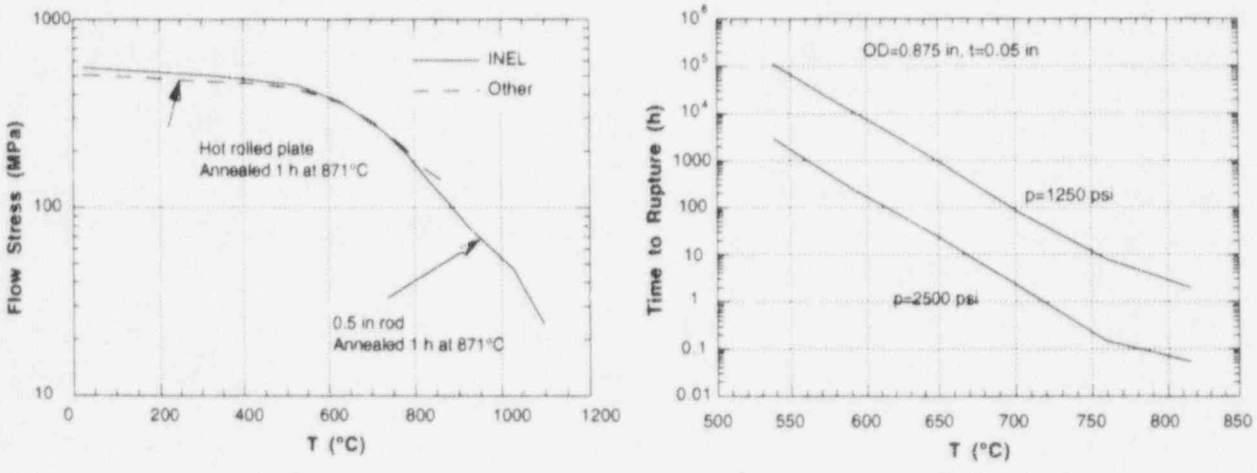

(a) (b)

Figure 2 (a) Flow stress of Alloy 600 as a function of temperature; (b) time to rupture of unflawed tubing subjected to constant internal pressure as a function of temperature.

1) Sub-critical crack growth by creep mechanisms
2) Effects of creep on bulging and stress relaxation around the crack tip
3) Effects of grain growth on mechanical properties.

However, simpler bounding calculations can give significant insight into the behavior of the tubes during accidents. The temperature–dependent flow stress can be used to calculate the "instantaneous" critical pressures of flawed tubes, i.e., the pressure at which a flawed tube will fail "instantaneously" at high temperature. The critical pressure for a 1 in.-long axial throughwall crack in a tube with a 0.875 in. o.d. and a 0.05 in. wall, which is 2.5 ksi at reactor operating temperatures, drops to 1.5 ksi at 500°C and 0.7 ksi at 850°C. For a tube at 500°C, a 0.5 in. throughwall crack would become unstable under a 2500 psi pressure differential; at 850°C virtually any flaw would cause failure under a 2500 psi pressure differential. Even shorter flaws would produce failure at 500°C after some period of time, if creep crack growth and other time–dependent effects are taken into account.

Environmentally assisted crack initiation, crack growth rates, crack arrest and reinitiation can not be predicted or quantified well for "current-day" cracks in operating steam generator tubes. Crack initiation times, crack growth rates, and changes in morphology can be quite variable. Furthermore, the factors that influence the nature of crevices and crevice corrosion cracking are not well understood. To evaluate the continued integrity of currently unaffected as well as degraded steam generator tubes left in service, a better quantitative understanding of the above phenomena and of the variabilities is needed.

Characterization of crevice chemistry will be critical to developing an understanding of crack growth and initiation in secondary side water chemistries. Cooperative efforts are being pursued with EPRI and with staff supported by the Department of Energy Basic Energy Sciences program to characterize crevice chemistries through in situ measurement of electrochemical potential, pH, and chemistry in model crevices. Results from these measurements would be combined with analytical studies that use crevice chemistry codes such as MULTEQ to develop predictive correlations for crevice chemistries as a function of temperature, crevice heat transfer, and primary and secondary-side environments.

Methodology and Technical Assessments for Current and Emerging Regulatory Issues

The objective of this task is to use the data, results, correlations, and modeling assembled in work under the first three objectives to provide technical assessments and evaluation of current and emerging regulatory issues that are related to steam generator tube integrity. These include items such as confirmatory research on existing and new models, evaluation of tube repair methods, and input and assessment for the new rule and regulatory guide on steam generator tube integrity.

For the performance-based rule under development by the NRC, evaluations and assessments are necessary to determine if the proposed criteria provide adequate levels of integrity, if the criteria can be met, and what combinations of inspection requirements (probability of detection, sizing accuracy), sampling plans, and expansion rules will lead to meeting the criteria. This will require a comprehensive, validated model that integrates all important aspects of integrity evaluations, starting from ISI results and ending with a total leak rate at the end of an operating cycle under various assumed conditions. In addition, the probabilities of single and multiple tube ruptures under various reactor coolant conditions must be quantified.

Cracking and failure of tubes repaired by sleeving is an emerging issue. The long term serviceability of tubes repaired by sleeving must be assessed. Key variables that strongly affect serviceability are the material condition, the operating environment, and the level of residual stress remaining in the tube after sleeving. The industry is currently developing various in-situ repair methods for tubes cracked in service as alternatives to sleeving or plugging. The continued serviceability of the repaired tubes must be established and the extent to which the repair may have affected the material properties must be assessed. Criteria for the qualification and acceptance of any tube repair method (sleeving included) are needed.

EMBRITTLEMENT RECOVERY DUE TO ANNEALING OF REACTOR PRESSURE VESSEL STEELS

E. D. Eason, J. E. Wright, and E. E. Nelson
Modeling and Computing Services
6400 Lookout Road, Suite 105
Boulder, Colorado 80301

G. R. Odette and E. V. Mader
Department of Chemical and Nuclear Engineering
University of California, Santa Barbara, California 93106

ABSTRACT

Embrittlement of reactor pressure vessels (RPVs) can be reduced by thermal annealing at temperatures higher than the normal operating conditions. Although such an annealing process has not been applied to any commercial plants in the United States, one US Army reactor, the BR3 plant in Belgium, and several plants in eastern Europe have been successfully annealed. All available Charpy annealing data were collected and analyzed in this project to develop quantitative models for estimating the recovery in 30 ft-lb (41 J) Charpy transition temperature and Charpy upper shelf energy over a range of potential annealing conditions. Pattern recognition, transformation analysis, residual studies, and the current understanding of the mechanisms involved in the annealing process were used to guide the selection of the most sensitive variables and correlating parameters and to determine the optimal functional forms for fitting the data. The resulting models were fitted by nonlinear least squares. The use of advanced tools, the larger data base now available, and insight from surrogate hardness data produced improved models for quantitative evaluation of the effects of annealing. The quality of models fitted in this project was evaluated by considering both the Charpy annealing data used for fitting and the surrogate hardness data base. The standard errors of the resulting recovery models relative to calibration data are comparable to the uncertainty in unirradiated Charpy data. This work also demonstrates that microhardness recovery is a good surrogate for transition temperature shift recovery and that there is a high level of consistency between the observed annealing trends and fundamental models of embrittlement and recovery processes.

INTRODUCTION

The effects of radiation embrittlement can be reduced by thermal annealing at temperatures higher than the normal operating conditions. Although such an annealing process has not been applied to any commercial plants in the United States, one U. S. Army reactor, the BR3 plant in Belgium, and several plants in Eastern Europe have been successfully annealed.[1,2]

A quantitative evaluation of embrittlement recovery due to annealing is required to determine continued operation limits for aging commercial plants. The objective of this work is to analyze the pertinent data on this issue and develop quantitative models for estimating the recovery in 30 ft-lb (41 J) Charpy transition temperature (TT) and Charpy upper shelf energy (USE) due to annealing.

Models for estimating the degree of recovery due to post-irradiation annealing have been developed previously.[3,4,5] All of these preliminary models were calibrated to high flux test reactor data, and their relevance to low flux power reactor situations is limited. They also do not reflect the physical interaction between the temperature of annealing, flux, and the hardening features that are affected by annealing.

In the current work, pattern recognition, transformation analysis, residual studies, and the current understanding of the mechanisms involved in the annealing process were used to guide the selection of the most sensitive variables and correlating parameters and to determine the optimal form for fitting the data. The resulting models were fitted by nonlinear least squares. The use of advanced tools, the larger data base now available, and insight from the surrogate hardness data produced improved models for quantitative evaluation of the effects of annealing. Details on the methodology, mechanistic understanding, and many additional results are given elsewhere.[6,7,8]

DATA BASE DEVELOPMENT

Charpy Data Base

Charpy data were gathered from the TR-EDB[9] and from various annealing reports. Details on the data base development and characterization are given in Reference 6 and an extensive report by Hawthorne.[10] The independent variables in the data base include material chemistries, irradiation time (t_i) and temperature (T_i), annealing time (t_a) and temperature (T_a), fluence (ϕt), flux (ϕ), pre-irradiated transition temperature (TT) and upper shelf energy (USE), and changes in TT and USE due to irradiation. Combinations of variables were also considered, such as the difference T_a-T_i and combinations of chemical components such as Cu*Ni.

Several measures of annealing recovery were investigated as dependent variables, for both transition temperature shift (TTS) and drop in Charpy upper shelf energy (ΔUSE). The final quantities after irradiation and annealing (TT_{ia} and USE_{ia}) were chosen, since they produced better correlations than other candidate dependent variables, such as fraction of the irradiated shift or drop recovered by annealing. The results can be converted algebraically to fraction recovered or other forms of interest.

The entire Charpy annealing data base contains 187 data points. As in most data bases composed from various experiments, there are many cases of missing information. In addition, the data are not uniformly distributed over the ranges of all variables. The data distribution was considered in the analysis and modeling; details are given in Reference 6. The most significant "holes" in the data base are the lack of Charpy data at power reactor flux levels and for medium-to-high Cu, high Ni materials.

Hardness Data Base and Other Surrogate Data

A microhardness data base was assembled from an extensive NRC-sponsored annealing research program at the University of California at Santa Barbara (UCSB) and the literature. The UCSB microhardness data base covers a wide range of T_a (550 to 844°F) and t_a (0 to 600 h) for various irradiation conditions (flux, fluence, and temperature) and alloy compositions (primarily variations in Cu and Ni). In most cases, the results derive from fully controlled experiments: the same heat irradiated over a range of specified conditions and split melt heats irradiated at the same conditions. The measurement technique used led to unusually good accuracy and precision, estimated to be about ±5 DPH. A detailed report of this work is in preparation.[11] A total of 414 primary and 262 secondary hardness observations from this data base were used to help develop and test the correlation functions presented here. Very recent Charpy shift data not used in fitting were also used to test the TTS correlation.

RESULTS

Preliminary correlation models were developed for recovery of TTS and ΔUSE using statistical approaches. In addition, physically-based models were developed. The models derived from pattern recognition and statistical analysis and those derived from mechanistic considerations were compared and iteratively refined. The analyses converged to single models for estimating USE and TTS recovery for engineering purposes, incorporating both statistical and mechanistic considerations. The similar results from these different perspectives, using different fitting techniques, give additional confidence in the fitted models.

Upper Shelf Energy Recovery Model

The following model was developed for the Charpy upper shelf energy after annealing:

$$USE_{ia} = USE_i + \left[1 - 0.586 \exp\left(\frac{-t_a}{15.9}\right)\right] x \left[0.570\,\Delta USE_i + \left(0.120\,T_a - 104\right) Cu + 0.0389\,T_a - 17.6\right] \quad (1)$$

where USE_i and ΔUSE_i are in ft-lb, T_a is in °F, t_a is in hours, and Cu is in wt%. Equation 1 yields a standard error of 5.1 ft-lb. The goodness of fit of Equation 1 is demonstrated graphically in Figure 1, which shows the actual USE_{ia} versus the predicted USE_{ia} with bounds that enclose 90% of the data.

The key trends reflected in the data and represented in Equation 1 are:

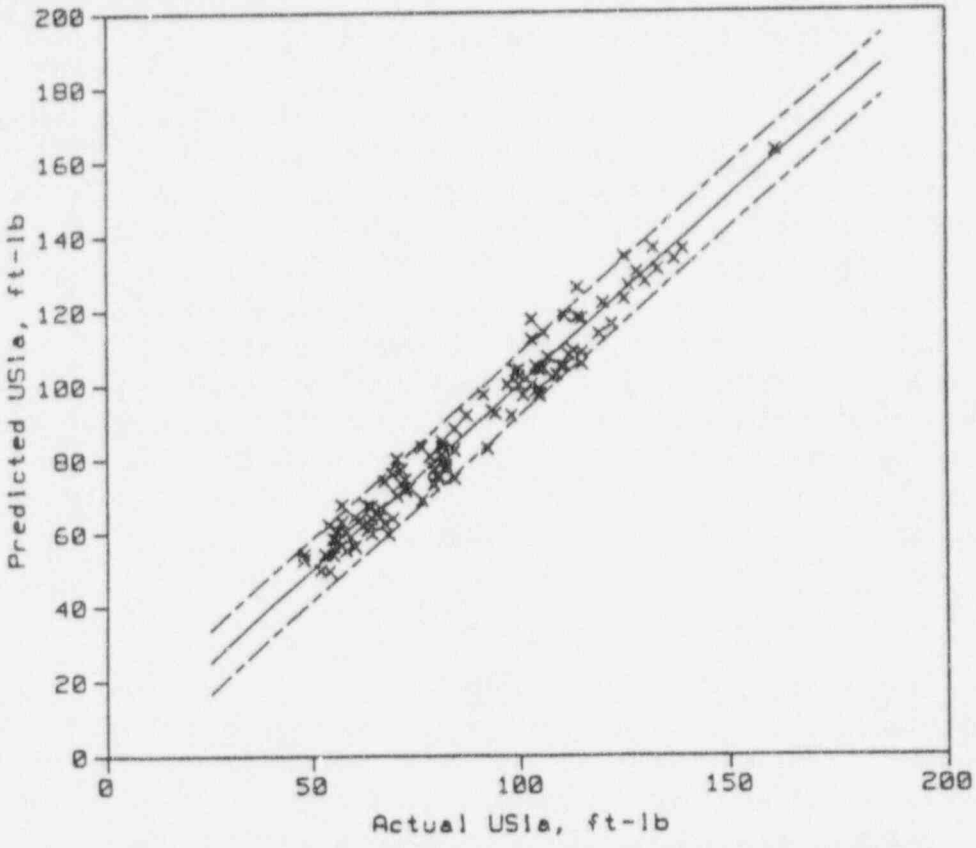

Figure 1. Predicted vs. Measured USE_{ia} for Upper Shelf Model (Eq. 1)

- for long annealing times (t_a > 50 h), the amount of annealing recovery ΔUSE_a = USE_{ia} - USE_i is approximately proportional to the drop in upper shelf energy due to irradiation, ΔUSE_i
- higher Cu makes the irradiation effect more resistant to recovery at low T_a
- recovery increases with increasing T_a, and over-recovery (USE_{ia} > USE_u) is possible.

These trends are expected on a physical basis and are qualitatively similar to the behavior of shift. The two T_a terms (one with a copper interaction) derive from the notion of copper-dependent and copper-independent hardening features recovering over different temperature ranges. That is, even with no copper, some effect of T_a would be expected.

Transition Temperature Shift Recovery Model

The model for annealing recovery of TTS reflects the fact that over-recovery does not occur in the shift data by the use of a *tanh* function. The *tanh* function also captures the nonlinearity in fractional annealing recovery with increasing annealing temperature. The final result of the collaborative analysis is the following model for $T_a \geq 800°F$:

$$TT_{ia} = TT_i - \Delta TT_i \left[0.5 + 0.5 \tanh \left(\frac{a_1 T_a - a_2}{a_3} \right) \right] \qquad (2)$$

where

$$a_1 = 1 + 0.0151 \ln t_a - 0.424 Cu^{(3.28 - 0.00306 T_a)}$$

$$\text{where } Cu = \min \begin{cases} Cu_{\text{measured}} \\ 0.30 \text{ wt \%} \end{cases} \tag{3}$$

$$a_2 = 0.584 \left(T_i + 637 \right) \tag{4}$$

$$a_3 = 95.7 \tag{5}$$

and TT_{ia}, TT_i, ΔTT_i, T_a, and T_i are in °F, t_a is in hours, and Cu is in wt%.

The model has an upper limit on the amount of copper that affects the annealing process. This limit was set by physical considerations, because it is not well defined statistically. Unpublished analytical electron microscopy measurements by Pythian, Odette, and co-workers show matrix copper contents of about 0.3±0.02 wt% following typical stress relief treatments in the range of about 1112 to 1166°F for times up to 80 h. The maximum effective copper concentration may vary from one vessel to another, depending on stress relief heat treatment conditions. The value Cu_{max} = 0.3 wt% was chosen as a good average value for the stress relief temperatures that were commonly used during fabrication of the existing pressure vessels. If a case can be made for lower Cu_{max} for a particular application, Equation 3 should be used with the lower estimate replacing 0.3 wt% (an interpolation). In cases where the maximum effective copper content is believed to be more than 0.3 wt%, the higher estimate of Cu_{max} should be used in Equation 3 (an extrapolation).

An effect of flux is suggested by the Charpy annealing data and the physical considerations, but the lack of low flux data makes calibration difficult. The microhardness data base, covering a broader range of flux, shows that annealing recovery decreases with decreasing flux for annealing temperatures of 750°F or below but not at 800°F or above. Recognizing that the expression in square brackets in Equation 2 is the fractional shift recovered by annealing, fTT_{recov}, it is possible to expand the modeling data base with some low flux hardness data -- specifically, Westinghouse power reactor data[12] -- and calibrate a flux effect. The assumption is made that annealing produces the same fraction recovered for hardness as for Charpy TTS. This assumption is necessary, because Charpy recovery data are not available at power reactor fluxes, but it is also justified by the observed consistency of hardness and shift data, as discussed below.

To account for the flux effect at $T_a \leq 750$°F, a flux-dependent term was added to Equation 4 such that

$$a_2 = 0.584\,T_i - 15.5 \ln\phi + 833 \qquad (6)$$

where ϕ is in units of $n/(cm^2\text{-}s)$. The coefficient on $ln\phi$ and the constant term (+833) in Equation 6 were calibrated to the Westinghouse power reactor hardness data plus Charpy recovery data with $T_a \leq 750°F$, while all other parameters of the model Equations 3 and 5 were calibrated to data at all temperatures. The modeling concept is to use Equations 2 through 5 at high temperature ($T_a \geq 800°F$), where no flux effect is evident, and use Equations 2, 3, 5, and 6 at lower temperatures ($T_a \leq 750°F$), where a flux effect is evident.

Use of the model for annealing treatments between 750°F and 800°F should be avoided pending additional data; there are neither Charpy nor hardness data in that range to help determine the shape of the transition from flux-dependent to flux-independent behavior or the range in temperatures over which such transitions occur. If it is necessary to make estimates of annealing effectiveness for annealing temperatures between 750 and 800°F, interpolation between the results of Equation 4 and Equation 6 or bounding by the use of Equation 6 are the only current options. The treatment of flux given here must be considered preliminary and should be revisited if additional data become available or new fundamental insights into irradiation and annealing mechanisms are discovered. It is probable that the transition range depends on other irradiation, metallurgical, and annealing variables.

The goodness of fit of Equations 2 through 6 is shown by the plot of actual versus predicted TT_{ia} in Figure 2, where the a_2 term is calculated from Equation 4 for $T_a \geq 800°F$ and Equation 6 for $T_a \leq 750°F$. The standard error of the Charpy data is 17.2°F for 151 data points.

DISCUSSION

Upper Shelf Energy Recovery Model

The upper shelf energy model in Equation 1 is remarkably effective, accounting for 96% of the range in the available data ($R^2 = 0.96$). The residuals relative to the model (predicted-measured = p-m) show no trends that have been missed. Flux effects were specifically looked for but not found in the available data. The standard error, at 5.1 ft-lb, is not substantially different from the level of error expected in repeated Charpy tests of the same heat at the same conditions. It is difficult to improve upon a model that can predict the annealed upper shelf energy for a range of irradiation, material, and annealing conditions with no more uncertainty than repeated measurements.

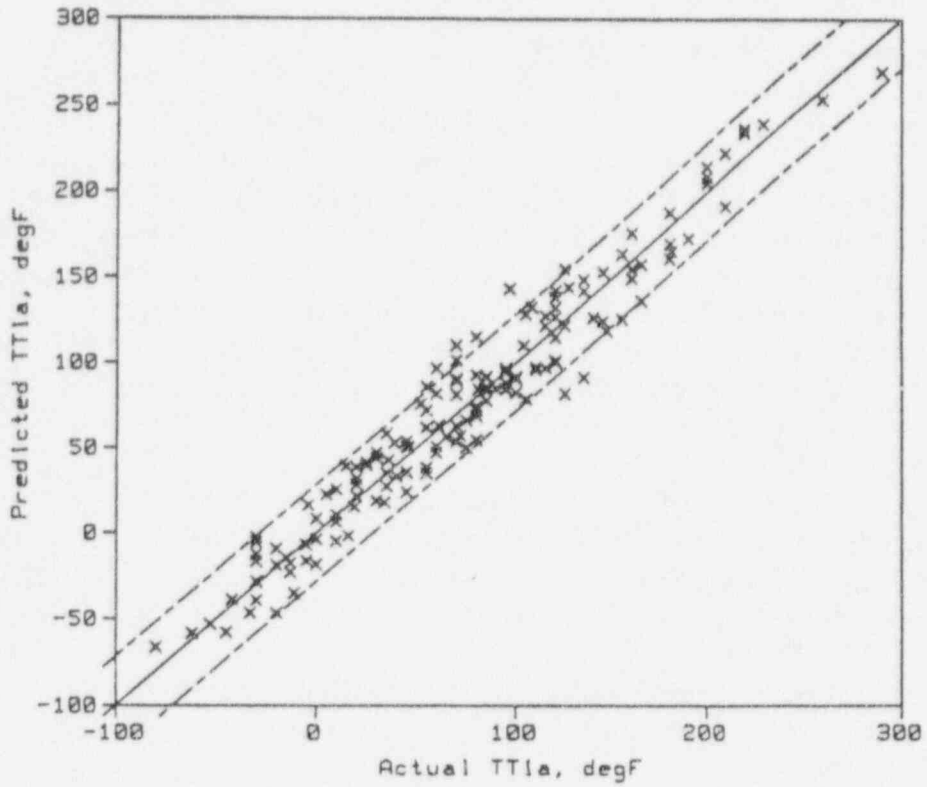

Figure 2. Predicted vs. Measured TT_a for *tanh* Model

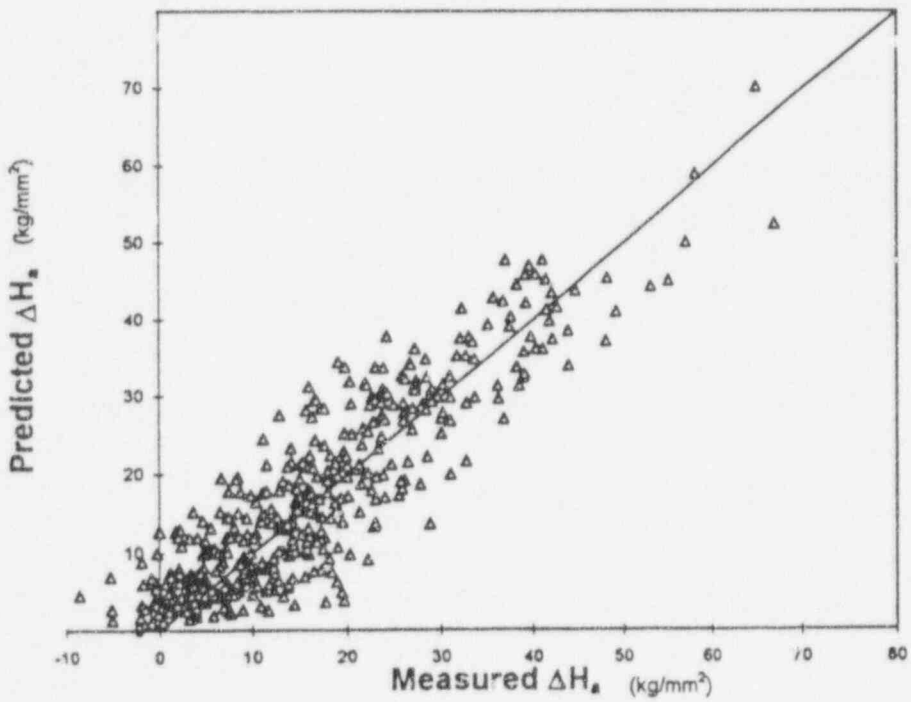

Figure 3. Predicted vs. Measured Hardness Recovered by Annealing, *tanh* Shift Model

Transition Temperature Recovery Model

Transition temperature recovery can be modeled well using the *tanh* model of Equations 2 through 6. The standard error of the model, including the flux term for $T_a \leq 750°F$, is 17.2°F. This is comparable to the standard deviation of TT measurements on a single, well-characterized unirradiated weld (σ = 17°F for twenty locations in a beltline weld[13]). From a practical point of view, this means that the expected error from using the model to estimate TT after irradiation and annealing is not much different from the uncertainty in the original, unirradiated value due to variations within the weld. At R^2 = 0.94, the correlation coefficient is almost as high as for the upper shelf energy model.

Predicted minus measured (p-m) residual plots for the *tanh* model were prepared both for variables included and not included in the model. No significant trends could be detected, suggesting that the model is not missing or incorrectly modeling important effects. The *tanh* model also showed remarkable agreement with a physically-motivated model based on the different annealing behavior of matrix defects and copper-rich precipitates.[10] This good agreement shows that the simple analytic form of Equations 2 through 6 robustly mimics the more complex, physically-motivated model.

Evaluation of single-variable subsets or data groupings that attempt to isolate single-variable trends in the residuals for the *tanh* model did not reveal any significant un-modeled effects of the T_i, T_a, and Cu variables included in the model. A slight trend with Ni was identified in tests that systematically varied Ni, but it was not confirmed in the residuals of the overall data base. Since the data base is deficient in high Ni materials, this is an issue that requires additional experimentation to resolve. No residual effect of P or fluence was found, even in the data from experiments designed to test these effects. This may be because first order effects on annealing are implicitly characterized by the irradiation response (i.e., ΔTT_i).

Good agreement was obtained between very recent shift data from prepublication reports and the literature and the annealing recovery (ΔTT_a) for the *tanh* model. These data were not used in fitting, so they provide independent validation. For the 25 data points the average bias is -1.9°F, and the standard deviation is 16.8°F. These results add further support for the *tanh* model.

Direct application of the *tanh* model to the completely independent and largely controlled hardness data base yielded remarkable agreement, as shown in Figure 3. The mean bias is only -1.0 DPH, and the standard deviation is 5.9 DPH. Using a nominal conversion factor of 3.6, these hardness values are roughly equivalent to shift values of -4 and 21°F, respectively. These results demonstrate that microhardness is an excellent surrogate for evaluating general trends in transition temperature recovery due to annealing.

The effects of flux are a major concern, since the annealing predictions are derived from high flux test reactor irradiations and will be applied to low flux power reactor conditions. Because the trends are consistent, flux can be evaluated by combining the TTS and hardness data bases and extending the latter to include very high flux data

($\sim 5x10^{13}$ n/cm^2-s) from the UCSB data base and much lower data from annealing studies on surveillance specimens.[11] The latter data were used to calibrate the flux term of the *tanh* model; no other hardening data were used in the calibration.

Figure 4 shows the trends in the combined hardness and shift data base as a function of flux for the *tanh* model using the flux term at and below 750°F. The bars represent standard deviations about the average residual shift or hardening fraction for a large number of data points. The "scatter" includes a range of other variables not plotted here. These results reinforce the conclusion that annealing is more sensitive to variables such as ϕ at low T_a. They also support the flux term in Equation 6 for low T_a and the copper term in Equation 3. The agreement between hardness and shift data and the model curve is very good overall. The fact that some very high flux data fall substantially below the flux-dependent *tanh* prediction can be explained by the significant retardation of copper-rich precipitate development at very high damage rates.

Ranges of Validity of Models

Complete mapping of the range of validity in multivariable space, considering interactions and areas of clumping or sparse data, is extremely difficult. The application ranges based on T_a in Table 1 are guided by physical considerations. The limits for Ni and ϕ for $T_a \geq 800$°F have been established based on limited hardness data. These limits must be verified by further experimental research, including developing an extended shift data base. The TTS model should not be applied for conditions with $USE_i > 155$ ft-lb or $USE_i < 36$ ft-lb, the range of the Charpy data base.

Table 1. Model Application Ranges

T_a, °F	Cu, wt%	T_i, °F	t_a, h	Ni, wt%	ϕt, n/cm^2	ϕ, n/(cm^2-s)
≤ 750	> 0.05	500-600	> 50	< 0.8	0.5 - $5x10^{19}$	≥ $5x10^{10}$
≥ 800	> 0.15	500-600	> 50	< 1.2	0.5 - $5x10^{19}$	≥ $5x10^{10}$

The validity range for flux presents a special problem, because low flux Charpy shift data are not available. Based on excellent correspondence between hardness data and TTS data at test reactor flux levels and the trend in hardness data, the TT model with the flux term appears reasonable at power reactor flux levels, nominally as low as $5x10^{10}$ n/(cm^2-s) (E>1MeV). Estimates for even lower flux levels are not precluded but should be viewed as extrapolation. There is no confirmation of the flux trend in Charpy TTS data at power reactor fluxes. There is no data at all to show whether there is a trend in USE data at low flux. Thus the flux term in the shift model and the lack of a flux term in the USE model must be considered best engineering judgement with the present state of knowledge.

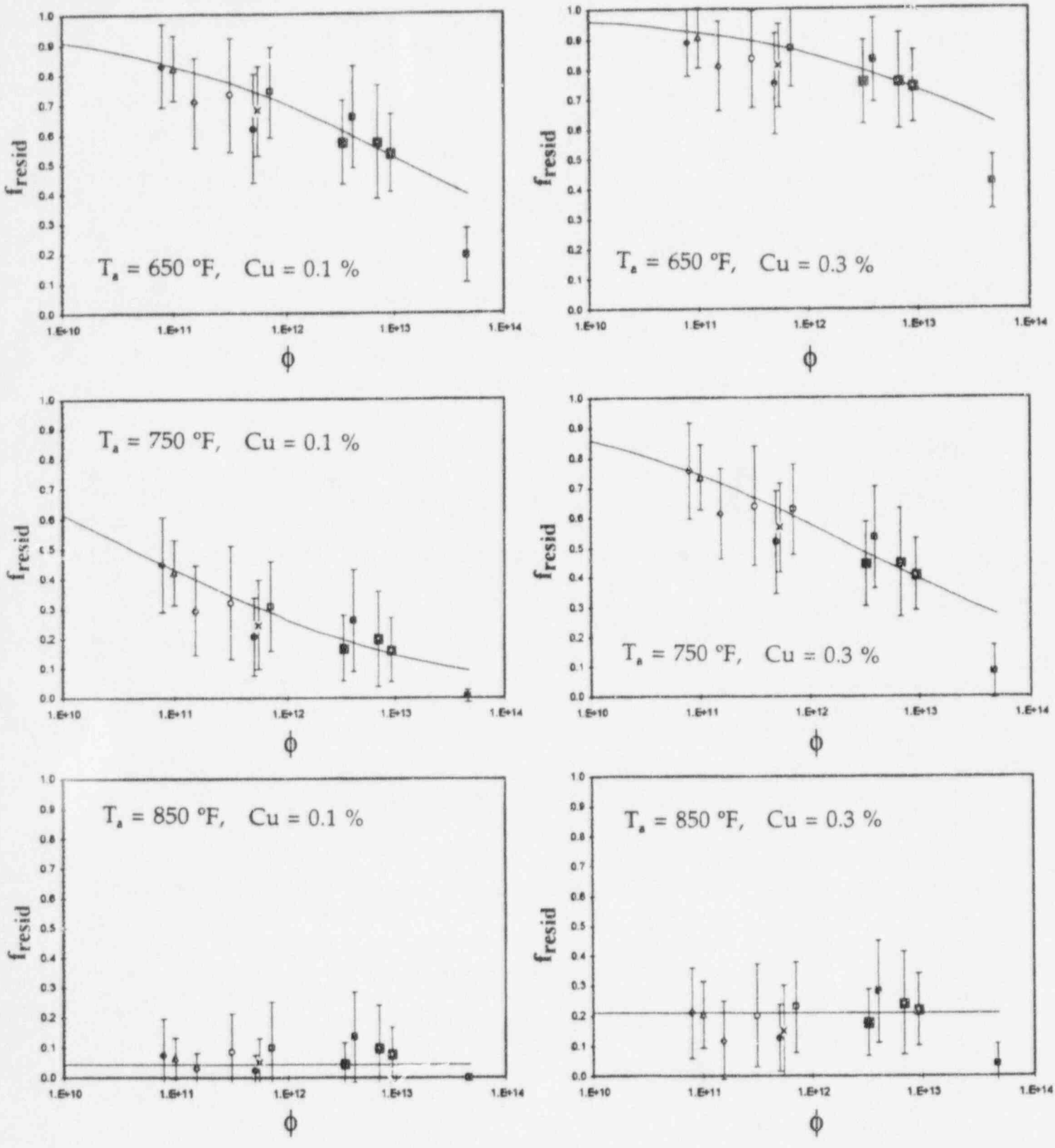

Figure 4. Normalized Residual Fractional Recovery vs. Flux and T_s, *tanh* Model, Westinghouse Surveillance Hardness (△, X, ◊, ◆), UCSB Hardness (■, □, ●, ○), and Shift Data (⊙ , ⊙ , ■)

CONCLUSIONS

Correlation models for predicting both USE and TT embrittlement recovery due to annealing have been developed, with standard errors comparable to the uncertainty in unirradiated Charpy data.

The USE model may predict over-recovery of USE due to annealing, as was evident in the data. The TT model does not allow over-recovery, because no examples of over-recovery were observed in the data.

The TTS model has several physical features built in, including a limit on effective Cu based on solubility considerations and nonlinear effects of annealing temperature. The flux effect is tentative, having been calibrated to a mix of hardness and Charpy data, but it is consistent with the large hardness data base with a range in flux spanning more than two orders of magnitude. The flux effect, like the Cu effect, varies with annealing temperature because of the different responses of the various hardening features.

The *tanh* model for TTS annealing recovery represents a significant improvement over previous model formulations. The model is consistent with an extensive hardness data base, limited shift data not used for fitting, and the current understanding of both embrittlement and annealing mechanisms. The model also provides some important insights lacking in previous treatments, suggesting that flux effects and secondary composition variables can be neglected at high annealing temperatures. While requiring additional confirmation, this is a conclusion of enormous importance. The results can help guide future research studies aimed at refining the predictions and optimizing annealing treatments, considering the effects of both recovery and re-irradiation embrittlement.

Both the upper shelf and transition temperature recovery models should be treated as curve-fits with substantial physical insight built in, rather than as fundamental physical models. Thus, care should be taken to avoid extreme extrapolation beyond the ranges presented in Table 1. The clumping and patterns in the available data, discussed in Reference 6 should be considered during applications. The fact that all the Charpy data are from short-term test reactor irradiations should be considered; the resulting flux effects have been estimated for the shift model using hardness data.

The results suggest a need for additional experimentation with the Cu-Ni compositions most critical to actual plants and at power reactor fluxes.

ACKNOWLEDGMENTS

The authors appreciate advice and encouragement from A. Taboada and A. L. Hiser, current and former project managers, respectively, at the U.S. Nuclear Regulatory Commission (NRC). The advice and support from other NRC and Oak Ridge National Laboratory staff is well appreciated. Special thanks are due to R. Hawthorne for his review and documentation of the annealing data base and recalculation of the older fluences. This work was performed under U.S. NRC contract 04-92-048.

REFERENCES

1. Potapovs, U., G. W. Knighton and A. S. Denton, "Critique of In-Place Annealing of SM-1A Nuclear Reactor Vessel," *American Society of Mechanical Engineers*, Paper 67-WA/ER-3, November 1967; also, *Nuclear Engineering and Design*, Volume 8, 1968, pp. 39-57.

2. Fabry, A., "The BR3 Pressure Vessel Anneal: Lessons and Perspective," *Reactor Pressure Vessel Thermal Annealing Workshop*, Albuquerque, New Mexico, February 17-18, 1994.

3. Powers, A. E., "Post-Irradiation and Co-Irradiation Annealing of Iron and Steel," Knolls Atomic Power Lab Report, KAPL 3440, September 1968.

4. Macdonald, B., "Post-Irradiation Annealing Recovery of Commercial Pressure Vessel Steels," *Effects of Radiation on Materials: Twelfth International Symposium. ASTM STP 870*, F. A. Garner and J. S. Perrin, Eds., American Society for Testing and Materials, Philadelphia, 1985, pp. 972-978.

5. U. S. NRC, "Format and Content of Application for Approval for Thermal Annealing of Reactor Pressure Vessels," Draft Regulatory Guide DG-1027, October 1994.

6. Eason, E. D., J. E. Wright, E. E. Nelson, G. R. Odette, and E. V. Mader, "Models for Embrittlement Recovery Due to Annealing of Reactor Pressure Vessel Steels," NUREG/CR-6327, February 1995.

7. Odette, G. R., "Modeling Radiation Embrittlement in Reactor Pressure Vessel Steels," *Neutron Irradiation Effects in Reactor Pressure Vessel Steels and Weldments*, IAEA TRS, L. M. Davies, Ed. (in press).

8. Odette, G. R., "Radiation Induced Microstructural Evolution In Reactor Pressure Vessel Steels," *Microstructures of Irradiated Materials, MRS Symposium Proceedings 373*, I. Robertson, et al., Eds., MRS, Pittsburgh, 1995, p. 137.

9. Stallman, F. W., J. A. Wang, and F. B. K. Kam, "TR-EDB: Test Reactor Embrittlement Data Base, Version 1," NUREG/CR-6076, January 1994.

10. Hawthorne, J. R., "Compendium of Irradiation-Anneal Data for RPV Steels and Welds from MEA and NRL Weldments," MEA-2541, September 1994.

11. Mader, E. V., "Kinetics of Irradiation Embrittlement and the Post-Irradiation Annealing of Nuclear Reactor Pressure Vessel Steels," PhD Thesis, Materials Department, University of California, Santa Barbara, 1995.

12. Mager, T. R. and R. G. Lott, "Feasibility of a Methodology for Thermal Annealing an Embrittled Reactor Vessel," EPRI Report NP-6113-M, Electric Power Research Institute, February 1989.

13. Nanstad, R. K., D. E. McCabe, R. L. Swain, and M. K. Miller, "Chemical Composition and RT_{NDT} Determinations for Midland Weld WF-70," NUREG/CR-5914, December 1992.

REACTOR PRESSURE VESSEL INTEGRITY RESEARCH AT THE OAK RIDGE NATIONAL LABORATORY*

W. R. Corwin, W. E. Pennell, and J. V. Pace
Oak Ridge National Laboratory
Oak Ridge, Tennessee 37831

ABSTRACT

Maintaining the integrity of the reactor pressure vessel (RPV) in a light-water-cooled nuclear power plant is crucial in preventing and controlling severe accidents that have the potential for major contamination release. The RPV is the only key safety-related component of the plant for which a duplicate or redundant backup system does not exist. It is therefore imperative to understand and be able to predict the integrity inherent in the RPV. For this reason, the U.S. Nuclear Regulatory Commission has established the related research programs at the Oak Ridge National Laboratory described herein to provide for the development and confirmation of the methods used for: (1) establishing the irradiation exposure conditions within the RPV in the Embrittlement Data Base and Dosimetry Evaluation Program, (2) assessing the effects of irradiation on the RPV materials in the Heavy-Section Steel Irradiation Program, and (3) developing overall structural and fracture analyses of RPVs in the Heavy-Section Steel Technology Program.

ORNL EMBRITTLEMENT DATA BASE AND DOSIMETRY EVALUATION PROGRAM

The objective of this program is to develop, maintain, and upgrade computerized data bases, calculational procedures, and standards relating to reactor pressure vessel (RPV) fluence spectra determinations and embrittlement assessments. Uncertainties associated with the predictive methods and data bases are determined. The program is divided into two major tasks: Embrittlement Data Base (EDB) and Dosimetry Evaluation (DE). Under these are several subtasks that assist the U.S. Nuclear Regulatory Commission (NRC) in the area of RPV dosimetry.

The EDB is a compilation of a comprehensive collection of data from surveillance capsules of U.S. commercial nuclear power reactors and from experiments in material test reactors. The EDB work includes verification of the quality of the EDB, provision for user-friendly software to access and process the data, exploration and/or confirmation of embrittlement prediction models, provision for rapid investigation of regulatory issues, and provision for the technical bases for voluntary consensus standards or regulatory guides.

---

*Research sponsored by the Office of Nuclear Regulatory Research, U.S. Nuclear Regulatory Commission, under Interagency Agreements DOE 1886-8109-8L, 1886-8011-9B, and 1886-8616-4W with the U.S. Department of Energy under contract DE-AC05-84OR21400 with Lockheed Martin Energy Systems, Inc.

The EDB is designed for use with a personal computer. It contains a comprehensive collection of data from surveillance capsules of U.S. commercial nuclear power reactors in the Power Reactor Embrittlement Data Base (PR-EDB) and from experiments in material test reactors in the Test Reactor Embrittlement Data Base (TR-EDB). The data are collected (as reported) into "raw data files." Traceability of all data is maintained by including complete references along with the page numbers. External data verification of the PR-EDB is the responsibility of the vendors, who were responsible for the insertion and testing of the materials in the surveillance capsules. Internal verification is accomplished by checking against references and checking for any inconsistencies.

Examples of the information contained in the EDBs are reactor Charpy impact data, tensile test data, reactor type, irradiation environments, chemistry data, and heat-affected zone (HAZ) data, as shown in Figures 1 and 2. The TR-EDB (see Figure 2) additionally has annealing Charpy data.

The EDB-Utility, which is in a menu-driven format with help screens, provides user-friendly software to access, process, and analyze the data. The EDB is in a relational data files format instead of one single-table format, thus saving time and space. The PR-EDB has been recognized as the basis for the industry-wide data base.

The analysis of the data can include tables, model fittings, and graphs. Applications in evaluating radiation embrittlement of reactor vessels include: (1) validation of embrittlement-prediction models; (2) chemistry composition parameter studies; (3) irradiation temperature effects; and (4) investigations of spectrum effects, rate effects, and residual defects modeling.

Several tasks have been completed during this past year or are currently active. Update 6 of the EDB was released in March 1995. It included updated Westinghouse fluence data, new surveillance data, and corrections to previous data. Correlation monitor data were updated for several materials. The International Atomic Energy Agency/Russian data base, which contains seven data files, is being converted to the EDB format.

The DE work supports the NRC through the radiation transport and fluence determination in the area of the RPV. This consists of maintaining and upgrading validated neutron and photon radiation transport procedures, providing calculational support for NRC-sponsored light-water reactor (LWR) dosimetry benchmarks, maintaining cross-section libraries with the latest evaluated nuclear data, and maintaining and updating validated dosimetry procedures and data bases.

With release six of the recommended Evaluated Nuclear Data File (ENDF/B-VI), the cross-section library used in the discrete-ordinates and Monte Carlo multigroup radiation transport codes had to be updated. The new fine-energy-group (199 neutron, 44 photon) library was designated as VITAMIN-B6 (ref. 1), and the broad-energy-group (47 neutron, 20 photon) was designated as BUGLE-93 (ref. 2). This year's effort has concentrated on producing a revised version of VITAMIN-B6, based on ENDF/B-VI, Release 3. To accomplish this effort, the SCAMPI (SCale and AMpx Processing Interface) code system was created from modules of the SCALE[3] and AMPX[4] code systems. In particular, the MALOCS program from AMPX was updated to provide Bondarenko factors in a master library correctly collapsed from a fine-energy-group to a broad-group structure.

Activities in the upcoming year in supporting NRC-sponsored LWR dosimetry benchmarks will include two calculational efforts. The H. B. Robinson reactor and the pool-critical assembly will be calculated using the latest update of the ENDF/B-VI cross sections. Additionally, calculations completed this past year on the H. B. Robinson reactor included determining corrections to the ^{238}U and ^{237}Np fission rates for photofission effects.

One of the key tasks under the DE work is the update and maintenance of the dosimetry cross-section data base for spectrum adjustment codes, such as the LSL-M2 (ref. 5). The LSL-M2 code performs a logarithmic least-squares adjustment procedure to determine the

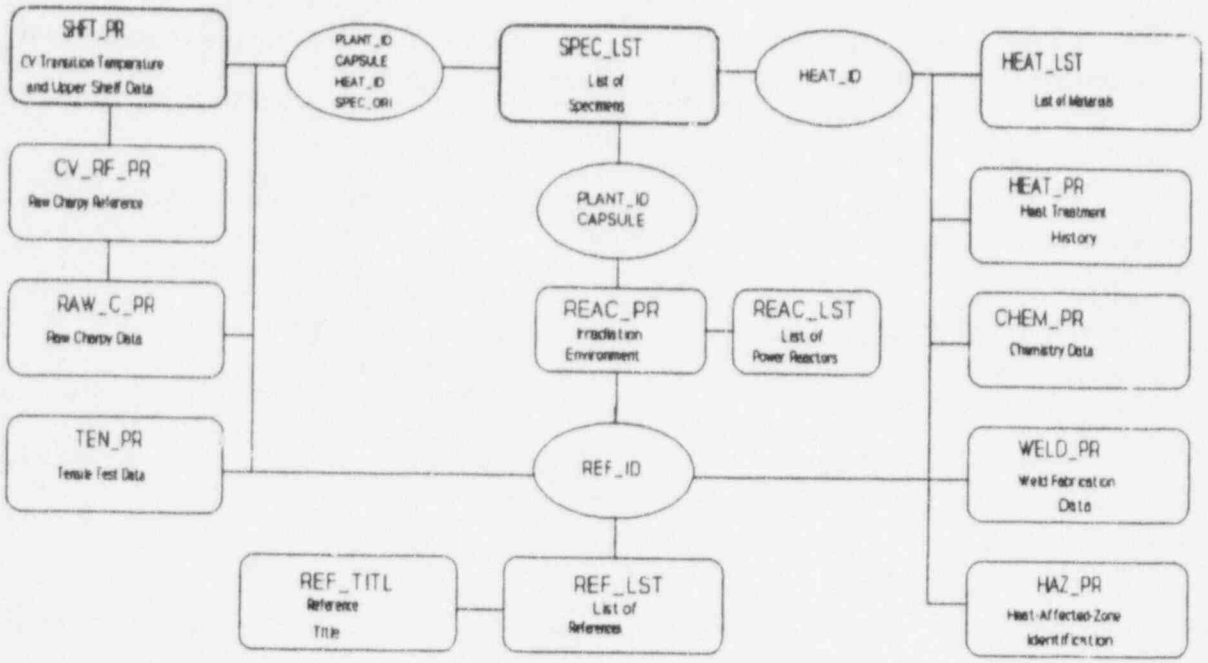

Fig. 1. Architecture of Power Reactor Embrittlement Data Base

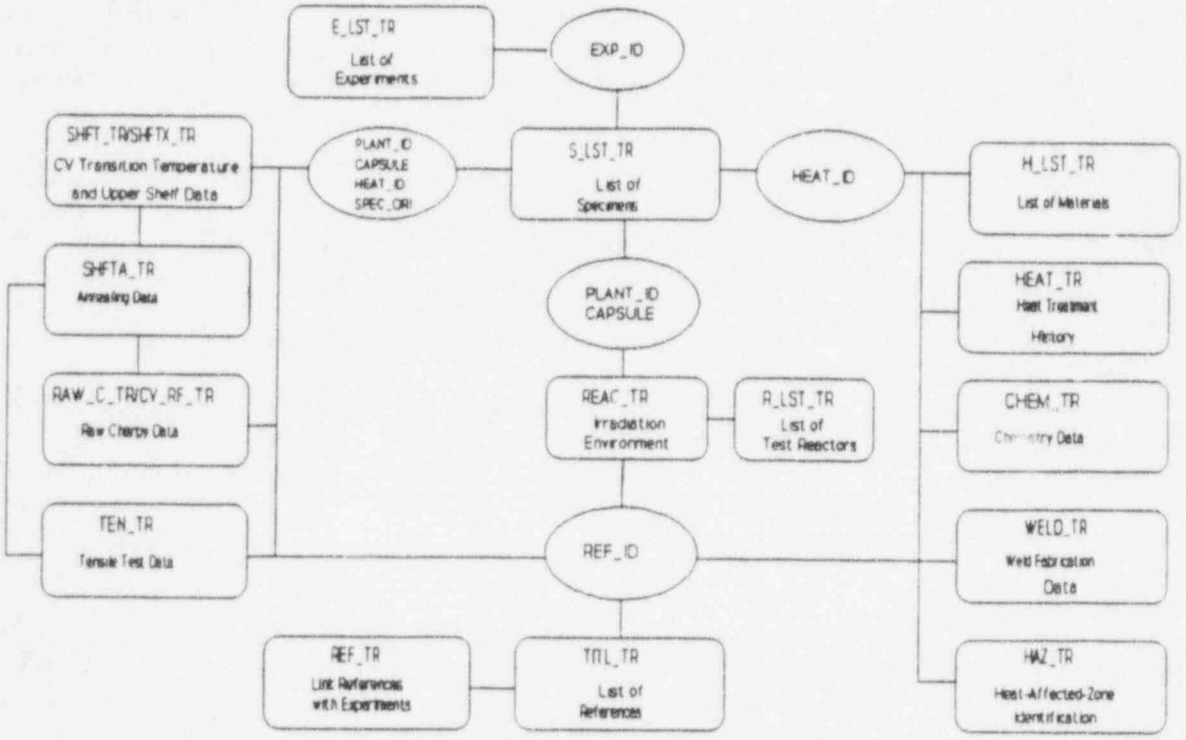

Fig. 2. Architecture of Test Reactor Embrittlement Data Base

neutron spectra from a combination of neutron-physics calculations and foil-activation measurements. It also determines the uncertainties for the output data based on corresponding uncertainties in the input data. Thus, the dosimetry cross-section data base is critical to the correct operation of the LSL-M2 code.

During this past year, the dosimetry cross-section data base[6] was updated based on data from the IRDF 90/G-V2 library,[7] the SNLRML-V1 library,[8] and private information.* The update contains 65 cross sections and covariances, 6 cross sections without covariances, and 6 fission-foil contaminants with no covariances. It contains responses for determining the fluence above 0.1 and 1 MeV; displacements per atom for Fe, Cr, and Ni; Si displacement kerma factors; and the GaAs 1-MeV equivalent damage function. Additionally, it contains the atomic weight, decay constants, and abundance for each reaction.

The information available from this program will provide data for assisting the Office of Nuclear Reactor Regulation, with support from the Office of Nuclear Regulatory Research, to effectively monitor current procedures and data bases used by vendors, utilities, and service laboratories in the pressure vessel irradiation surveillance program.

HEAVY-SECTION STEEL IRRADIATION PROGRAM

The goal of this program is to provide a thorough, quantitative assessment of the effects of neutron irradiation on the material behavior and, in particular, the fracture toughness properties of typical pressure vessel steels as they relate to light-water RPV integrity. Effects of specimen size; material chemistry; product form and microstructure; irradiation fluence, flux, temperature, and spectrum; and postirradiation annealing are being examined on a wide range of fracture properties, and results are being transferred into national and international codes and standards activities. Numerous experimental and analytical investigations of irradiation embrittlement are ongoing within the Heavy-Section Steel Irradiation (HSSI) Program, but in this paper only two will be described. The examples chosen both have important implications and also are illustrative of the type of experimental and analytical investigations conducted within the program.

Thermal Embrittlement Studies

As a result of observations of possible thermal embrittlement from recent studies with welds removed from retired steam generators of the Palisades Nuclear Plant, an assessment was made of thermal aging of RPV steels under nominal reactor operating conditions. Discussions are presented on (1) data from the literature regarding relatively low-temperature thermal embrittlement of RPV steels, (2) relevant data from the U.S. PR-EDB, and (3) potential mechanisms of thermal embrittlement in low-alloy steels.

The literature survey concentrated on effects of long-term aging at temperatures up to 350°C on the ductile-to-brittle transition temperature (DBTT) of RPV steels, for base metal, weld metal, and HAZ. The results of the literature survey are summarized in Figure 3, which includes marks on the aging time scale indicating the approximate time of exposure for the Palisades steam generators [10.8 effective full-power years (EFPY)] and the approximate design life of a commercial RPV (32 EFPY). Unless otherwise stated, the shift in DBTT was determined at an energy level of 30 ft-lb (41 J).

The most commonly used steels for U.S. nuclear RPVs are Mn-Mo-Ni steels. Data are available on A 212 grade B, A 302 grade B, A 533 grade B, and A508 class 2 and 3 steels.

---

*Private communication from T. Seren (VTT Chemical Technology, Finland) to F. W. Stallmann (forwarded to I. Remec, ORNL), May 1994.

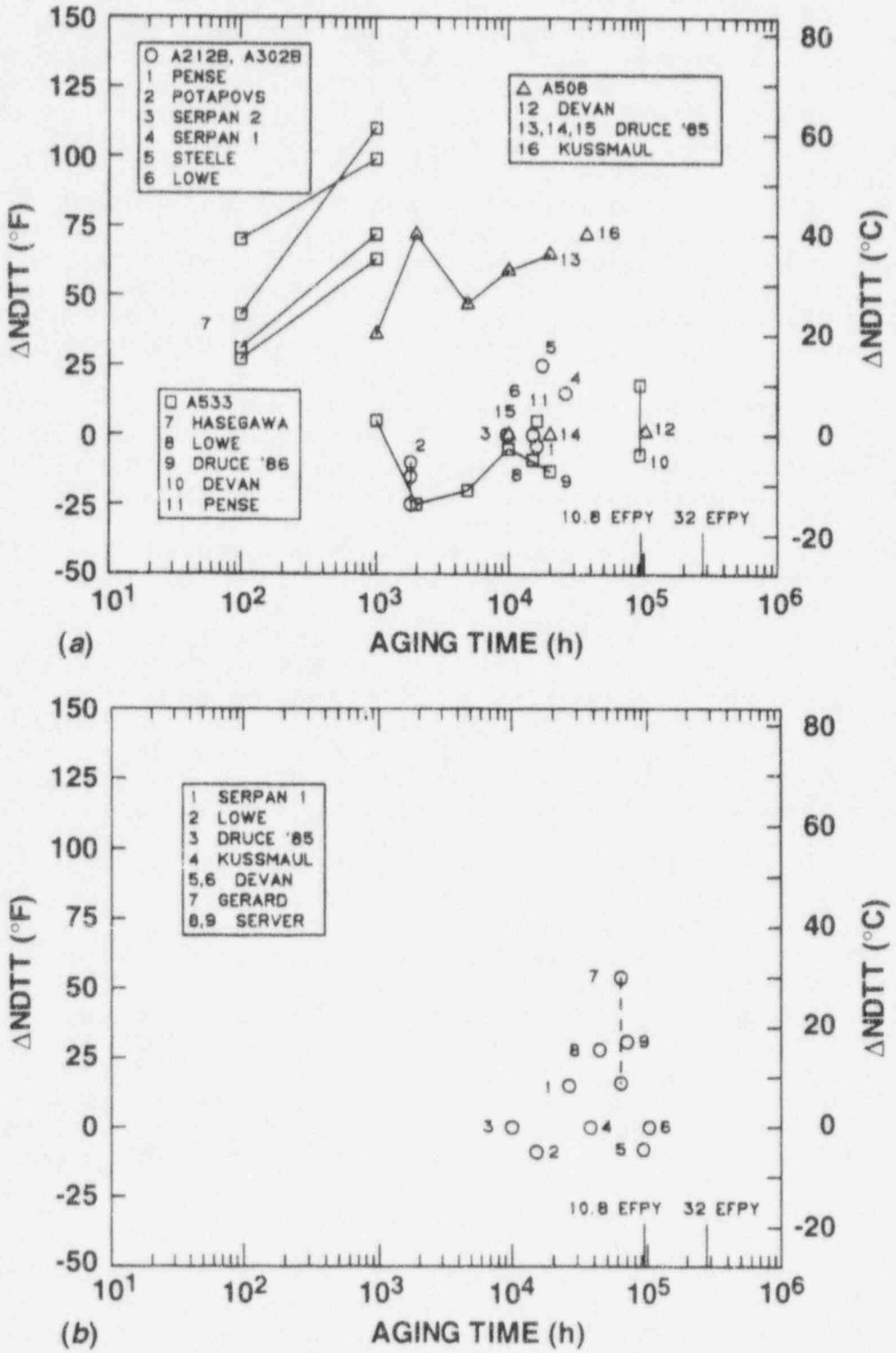

Fig. 3. Shift in ductile-to-brittle transition temperature (ΔNDTT) as a function of aging time for (*a*) base metals and (*b*) weld metals.

Work[9] on A 212 grade B showed that aging at 260°C for 16,000 h decreased the DBTT [calculated at 15 ft-lb (20 J)] by 2°C. Ten heats[10] of A 302 grade B alloys aged at 288°C for 1800 h showed that the DBTT decreased by 5 to 14°C. Tests of unirradiated surveillance A 302 grade B specimens from the Big Rock Point[11,12] and Dresden 1 reactors[13] showed increases in the DBTT of up to 14°C after up to 26,105 h at 301°C, whereas similar aged material from the Oconee 1 reactor[14] showed no effect.

Several studies of A 533 grade B alloy have been performed. Early studies of thermal aging[15] included four heats aged at 300°C for times up to 1000 h. These data are very alarming at first sight, showing increases in the DBTT of as much as 62°C. However, these alloys were not given a postweld heat treatment (PWHT) after the quench-and-temper heat treatment. Therefore, this particular set of data must be viewed with caution, but the results do provide strong evidence of the possible sensitivity of these steels to aging effects. Aging at 300 to 305°C for up to 20,000 h showed either "no change"[16] or a decrease[14] in the DBTT of 5°C. The DBTT of materials from the Arkansas 1 reactor[9] shifted –4 to 10°C after aging at 280°C for 93,000 h.

A 508 class 2 material from the Oconee 3 reactor[17] increased 1°C after exposure at 282°C for 103,000 h. Three A 508 class 3 materials were aged[18] at 300°C for up to 20,000 h. Half-thickness impact specimens taken near the surface showed an increase in the DBTT of 35°C after aging for 2000 h, with no further increase with continued aging to 20,000 h. The unique behavior of the near-surface material from the first alloy was tentatively attributed to a strain-aging effect. Another study with A 508 class 3 material[19] showed that aging at 350°C for up to 10,000 h had "little effect" on the DBTT. Material from the Doel reactor [called Soudotenax 56, apparently similar to A 508 class 3 (ref. 20)], was aged at 287°C for 63,000 h, indicating little effect of aging. Material from the Gundremmingen reactor[21] (alloy 20NiMoCr 2 6) showed an increase in the DBTT of 40°C after exposure for 37,560 h at about 284°C.

There are very few data available for weld metals. Data from the Big Rock Point, Dresden 1, and Oconee 1 reactors[12-14] show small changes, both plus and minus, up to a maximum increase in the DBTT of 8°C after exposure for times ranging up to 26,114 h. Specimens from the Arkansas 1 and Oconee 3 reactors[17] showed changes in the DBTT of –8 to 0°C after exposure up to 103,000 h at about 280°C. Data from the Gundremmingen reactor[21] show no change in the DBTT for weld metal exposed for 37,500 h. Material from the Doel reactor showed an increase in DBTT of 30°C after exposure for 63,000 h at 287°C (ref. 20). However, much of the data was generated with reconstituted specimens, and effects of the reconstitution process must be considered. Data from only unreconstituted specimens yield a much smaller shift of only 9°C. Druce[18] observed no effect of aging at 300°C for up to 10,000 h. Similar work (as reported by Vatter[22]) for aging at 300 or 325°C showed only a "gradual increase" in the DBTT. Data for the Palisades, Indian Point, and H. B. Robinson reactors' surveillance weld metal[23] show increases in the DBTT of 16 to 17°C for aging of up to 70,128 h at 260 to 279°C. However, this comparison is for two different weld wires and locations.

The PR-EDB was examined for indications of thermal aging in the surveillance data. Currently, the PR-EDB contains over 700 data points for transition temperature shift. However, the predictive methodology contained in NRC *Regulatory Guide 1.99*, Rev. 2 (RG 1.99), was based on two sets of data (177 data points in one set and 228 in the other). The current review also compared the data in the current PR-EDB and the previous data set containing 177 data. The number of shift data points versus the time in EFPY for which the tested specimens were exposed under operating conditions in the reactor was examined. For the PR-EDB, the peak in the distribution is at 2 years, but there are over 100 data points available with over 6 years exposure. For the RG 1.99 data, the bulk of the exposures are also for two EFPY with only about 10% of the data beyond 6 years and no data beyond 11 years. Figure 4 provides plots of the residual versus EFPY for base materials and weld materials in the PR-EDB, where residual is defined as measured shift minus RG 1.99 prediction. The data

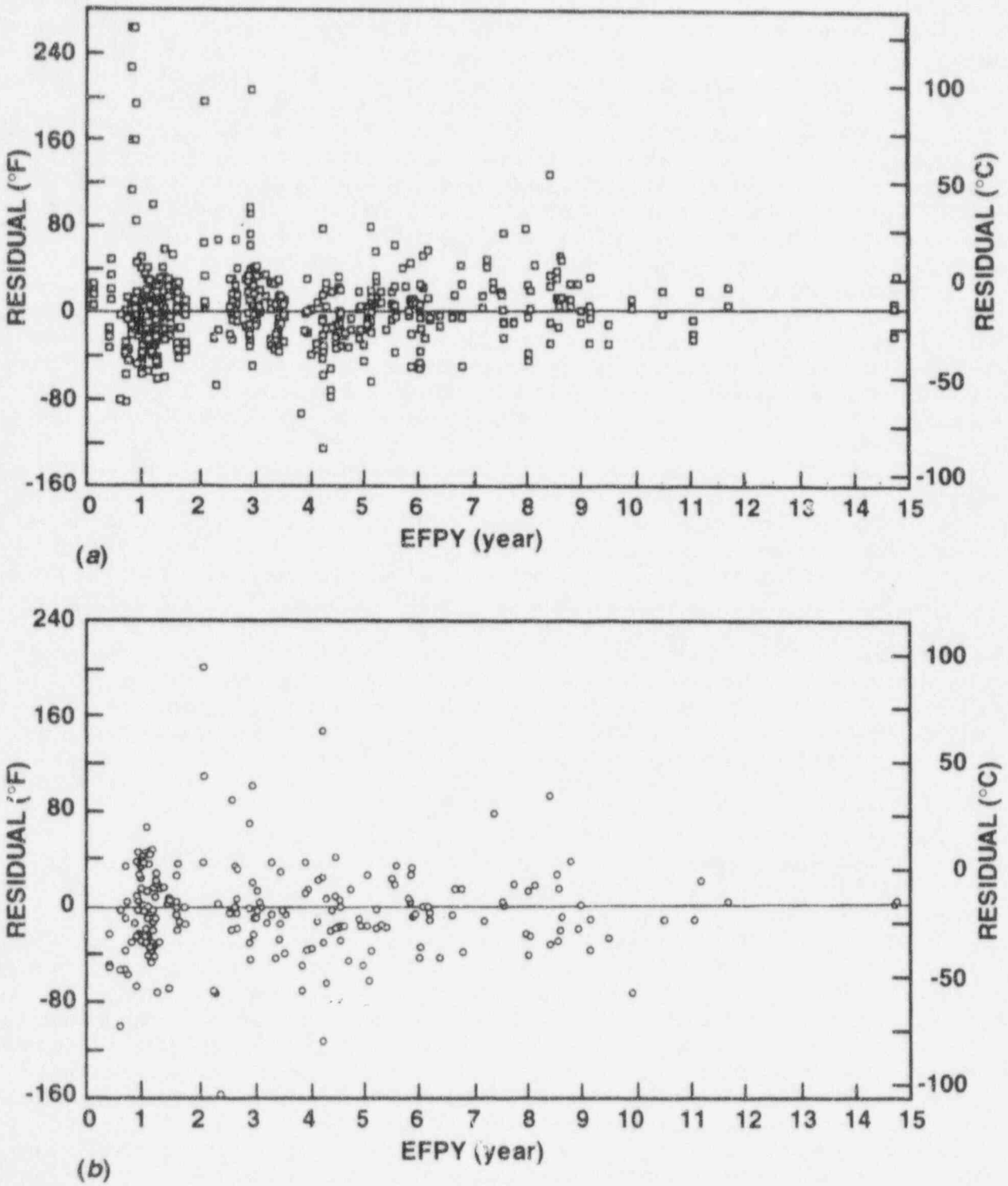

Fig. 4. Plots of residual shift (measured shift – RG 1.99 prediction) versus effective full-power years (EFPY) for (*a*) base materials and (*b*) weld metals from the power reactor embrittlement data base (PR-EDB).

appear to be centered about the residual value of zero. For the PR-EDB, the RG 1.99 predictive equations are clearly valid out to about 9 to 10 years and appear valid out to about 15 EFPY.

The dependence of the 41-J (30-ft-lb) transition temperature shift (ΔT_{41J}) on EFPY and fluence was examined for data sets with fluence less than 1×10^{17} neutrons/cm^2 (E > 1 MeV) where the irradiation-induced shift would likely be very small. Only 4 of the 40 points showed a shift greater than 11°C; one is for an HAZ, while three are for welds, one with 0.35% Cu and 0.73% Ni, and the other two with 0.18% Cu and 0.20% Ni. It is felt that the ΔT_{41J} results from these three capsules do not provide real evidence of large shifts at low fluence due to extremely large data scatter. For 8 thermal capsules, with exposure times ranging from about 10,000 to 43,000 h, the ΔT_{41J} values range from −16 to 11°C with a mean value of about 0°C. The mean and standard deviation for all the low-fluence ΔT_{41J} data shown are 1°C. Thus, the PR-EDB data indicate no trend for a measurable shift for times up to 43,000 h.

It has long been recognized that a number of mechanisms could lead to the embrittlement of RPV steels subject to long-term service at elevated temperatures. These mechanisms include: formation of hardening phases, such as copper-rich precipitates (CRP); segregation of phosphorus to grain boundaries leading to a lower intergranular fracture stress; and segregation of impurities to dislocations leading to strain aging. These phenomena could be accelerated or enhanced under irradiation. Pure thermal aging represents a zero-flux limit of damage-rate dependent effects.

In the late 1970s, Odette et al.[25] proposed that an undefined thermal aging mechanism might be responsible for accelerated low-øt (ø = flux, t = time) embrittlement in surveillance (low-ø) versus test reactor (high-ø) irradiations. In the mid-1980s, Fisher et al. developed a model of embrittlement due to copper precipitation accelerated by irradiation. It was initially applied to C-Mn Magnox steels[26] but later extended to Mn-Mo-Ni RPV steels.[27] Fisher proposed that at very low ø, an independent aging effect due to thermal copper precipitation would become significant, leading to peak hardening in periods of "25 years" at 290°C for copper contents of 0.1%. Odette et al.[28] also carried out an analysis of the peak aging time (t_p) to better quantify the effect of the (nominal) copper content. For nominal copper contents of 0.4% at 288°C, t_p ≈350,000 h or about 40 years, similar to Fisher's results. However, due to a lower assumed effective activation energy, Odette et al. also found that precipitation kinetics at lower copper levels resulted in predicted t_p values that are very large, viz., more than 70,000 years at 0.2% Cu at 290°C. Unfortunately, these predictions represent extreme extrapolations.

The focus of work on aging mechanisms shifted to the potential for embrittlement associated with phosphorus segregation-induced weakening of grain boundaries. The key conclusion of this work[18,22] was that while some phosphorus segregation would occur, end-of-life (EOL) thermal embrittlement would be minimal at temperatures of around 290°C, primarily due to sluggish diffusion kinetics. Work on temper embrittlement has recently shifted to radiation-enhanced or induced segregation. A major motivation was the observation of an increasing incidence of intergranular fracture in fine-grained mild steel welds in United Kingdom Magnox reactors. Jones et al.[29] developed a simple but powerful model, providing a unified treatment of the combined effects of radiation hardening and radiation-enhanced temper (segregation) embrittlement (RETE) mechanisms, accounting for the effects of temperature, flux (or time), and copper content. While there is also a possibility that RETE occurs in Mn-Mo-Ni RPV steels, most data for these alloys do not support this concern.

Thermal aging effects are very sensitive to both composition (e.g., copper on the hardening embrittlement mechanism) and microstructure (e.g., heat treatment on the temper embrittlement mechanism). Therefore, caution must be exercised in making conclusions regarding aging effects outside the existing data base. To evaluate a broader range of compositions and aging mechanisms, a small study was initiated at the University of California, Santa Barbara involving 5 simple model Fe-Cu-Mn-N alloys and 12 commercial split-melt A 533 grade B-type

steels aged at 290 and 350°C for periods up to 7200 h. Preliminary data[24] for the simple model Fe-Cu-X steels show that the alloys without copper experience a small degree of softening, while those with a large copper content of 0.9% show substantial hardening at both 290 and 350°C. The overall effect of manganese and nitrogen appears to be minimal. Based on $t^{1/3}$ kinetics, extrapolation using the t_p hardening in the 0.9% Cu alloys at 290°C is also reasonably consistent with earlier work. Almost all the commercial steel alloys show at least a slight increase in yield strength (s_y)[24] but generally within the overall data scatter of about ±20 MPa. Applying a criteria that there is a minimum of 20-MPa yield stress increase in the s_y at 8000 h and that Δs_y increases systematically with increasing t and temperature, four alloys show a significant effect of aging at 350°C and three out of these four at 290°C. Notably, most hardening is restricted to high-copper (0.4 and 0.8%) and nickel (0.8 and 1.6% at 290°C) alloys and increases with higher concentrations of these elements. While these preliminary short-term results cannot be directly used to address the question of long-term thermal embrittlement, they demonstrate that purely kinetic limits do not preclude thermally induced hardening at temperatures as low as 290°C. There is a significant sensitivity to copper and nickel content and, by implication, to heat treatment, since this affects the effective copper in solution.

Recently, Odette and coworkers have developed a self-consistent assessment of the effect of ø at intermediate to high levels that is able to rationalize complex, and in some cases, seemingly contradictory observations.[30] The primary effect of radiation is to greatly accelerate the formation of CRP as a consequence of radiation-enhanced diffusion (RED) produced by excess vacancies and interstitials, $D^* \approx K(ø)ø$. The RED factor, K, is ø-independent at low rates and varies as $1/ø$ at high rates due to vacancy-interstitial recombination at thermally unstable defect clusters. The predictions of an embrittlement model developed by Stoller[31] led to a similar conclusion. While requiring additional verification, these results suggest that ø effects vanish below a minimum value in the range of about 5×10^{11} neutrons/cm^2-s at 290°C.

Overall, most of the data from the literature suggest that there is no embrittlement in typical RPV steels at these temperatures for times as great as 100,000 h. Only three base and two weld metals show any significant effects of aging. The data from Hasegawa[15] are suspect because these materials did not receive a PWHT. The results from the near-surface material of one forging reported by Druce[18] were not observed with material taken from the middle of the same forging or other similar forgings, suggesting that these results are atypical. The results from the Gundremmingen reactor[21] are difficult to interpret due to the uncertainties associated with the archive material. The data from the Doel reactor[20] are suspect since the results of the reconstituted specimens are significantly different than those from the monolithic specimens. The Palisades data involve comparisons between welds made with different weld wires. The few data available[24] also indicate no evidence for embrittlement of HAZ materials up to 20,000 h. However, none of the data from the literature represents steels with the combination of high copper and high nickel that may increase sensitivity to thermal aging at these temperatures.

Review of the PR-EDB has not revealed convincing evidence of thermal embrittlement. The low-fluence surveillance data show ΔT_{41J} results less than 11°C. For surveillance exposures to about 15 EFPY, the ΔT_{41J} results are in good agreement with the predictions of the current RG 1.99 predictive equations. Although there are a few instances of relatively high ΔT_{41J} values at low fluences, the excessive scatter in the data and level of uncertainty in the ΔT_{41J} measurements render those results inconclusive.

While it is difficult to demonstrate that there are no significant effects of thermal aging, current understanding of both hardening and segregation mechanisms suggests that any thermal embrittlement is naturally incorporated in the effects observed following irradiation. That is, independent thermal aging and irradiation shifts should not be added if ø effects are not important or are properly accounted for. It seems likely that low lead-factor surveillance data provide a reasonable basis for embrittlement predictions. Indeed, theoretical considerations

suggest that by creating alternative trapping and segregation sites, radiation may suppress embrittlement associated with phosphorus segregation.

Thermal Annealing Studies of Irradiated RPV Steels

To assure that RPV failure does not occur during plant operation under both normal and emergency conditions, adequate levels of fracture toughness must be maintained in the RPV throughout its operating lifetime. This assurance is provided by utilizing the fracture toughness (K_{Ic}) curve of the *American Society of Mechanical Engineers (ASME) Boiler and Pressure Vessel Code*[32] that describes the fracture toughness of the RPV material as a function of temperature (T) normalized to the reference nil-ductility temperature (RT_{NDT}), namely, $T - RT_{NDT}$. The shift in the fracture toughness due to neutron irradiation is accounted for by a shift in RT_{NDT} (ΔRT_{NDT}). The upward temperature shift of RT_{NDT} is based on the assumption that it is the same as the Charpy impact curve shift at 41 J. However, the consistent agreement between the Charpy T_{41J} and fracture toughness transition curve shifts due to irradiation has been questioned (refs. 33 through 35).

The most challenging fracture toughness requirements that must be met for vessel materials would typically arise during a pressurized thermal shock (PTS) scenario. These requirements can be categorized by an irradiated RT_{NDT} "screening criterion" called RT_{PTS}. Some early nuclear RPVs may not meet this screening criterion as they near EOL. In particular, it is believed that, in the next decade or so, several vessels may exceed the RT_{PTS}. Thermal annealing may be needed to mitigate the effects of neutron irradiation on fracture toughness. A dozen or so RPVs have already been thermally annealed in Europe.[36,37] Development of an NRC regulatory guide on recovery of properties by annealing is under way. The basis for proposed regression correlations given in the guide is data gathered from the TR-EDB and from various annealing reports.[38] These data deal with recovery of Charpy or hardness properties only. Thus, the proposed regulatory guide is based on the same philosophy as mentioned earlier, namely, the assumption that recovery of the fracture toughness by annealing is the same as the recovery of Charpy T_{41J}.

The objective of this study is to compare the recovery of the fracture toughness and Charpy impact properties by thermal annealing of two irradiated RPV steels.

The materials in this study are American Society for Testing and Materials (ASTM) A 533 grade B class 1 plate, designated Heavy-Section Steel Technology (HSST) Program Plate 02, and the submerged-arc weld from the Midland Unit 1 reactor vessel. This vessel was built for a pressurized-water reactor that was canceled prior to startup. The welds from that vessel have the Babcock and Wilcox designation WF-70. The WF-70 welds were fabricated using copper-coated wire and Linde 80 flux and are known to be low upper-shelf (LUS), high-copper welds. Twenty-four Charpy specimens and 34 compact specimens 12.7 and 25.4 mm thick [0.5T C(T) and 1T C(T), respectively] from a beltline portion of the reactor vessel weld were tested after irradiation at 288°C to a neutron fluence level of about 1.0×10^{19} neutrons/cm^2 (> 1 MeV) at the University of Michigan Ford Nuclear Reactor (FNR).[39] Two hundred and thirty Charpy specimens and 65 compact specimens in sizes ranging from 1/2T to 4T were tested to perform fracture toughness[40] and Charpy impact[41] characterization in the unirradiated condition. In this study, 12 of the Charpy specimens and 6 of the 1T compact specimens that were irradiated to 1.0×10^{19} neutrons/cm^2 (> 1 MeV) were annealed at 454°C for 168 h, and 10 of the Charpy specimens were annealed at 343°C for 168 h.

HSST Plate 02 was produced by Lukens Steel Company. Portions of this plate have been used in many investigations around the world. In the Fourth HSSI Program Irradiation Series, about 70 Charpy and 28 1T compact specimens were tested before and after irradiation at 288°C to neutron fluences from 1.1 to 2.4×10^{19} neutrons/cm^2 (> 1 MeV) in the Oak Ridge Bulk Shielding Reactor.[42] Six irradiated 1T compact specimens left from that program were annealed at 454°C for 168 h, and five irradiated 1T compact specimens were annealed at 343°C

for 1 week. Test specimens in that irradiation series were prepared in the transverse (T-L) orientation. No Charpy specimens were available for an annealing study from that series. Twenty-two Charpy specimens of HSST Plate 02 in the longitudinal (L-T) orientation were irradiated together with the Midland weld to 1.0×10^{19} neutrons/cm^2 (> 1 MeV) at the University of Michigan FNR. Twelve of the specimens were annealed at 454°C for 168 h with ten specimens annealed at 343°C for 168 h. It had been shown previously that values of T_{41J} differ for different specimen orientations, but the irradiation-induced shift of transition temperature is the same for T-L- and L-T-oriented Charpy specimens.[43]

The Charpy V-notch impact data for each material condition were fit with a hyperbolic tangent function to obtain upper-shelf energy (USE) levels and transition temperatures. The elastic-plastic fracture toughness data were analyzed by a procedure based on earlier work by Wallin[44] and developed in an ASTM draft standard by McCabe et al.,[45] applying statistical concepts developed by Weibull.[46] The analysis procedure is based on fitting fracture toughness data to a three-parameter Weibull distribution at the test temperature. Using this procedure only a few replicate tests are needed to obtain the median fracture toughness of pressure vessel steels in the transition temperature regime with predictably good accuracy. Additionally, weakest-link theory is used to explain specimen size effects so that data equivalent to that for a 1T specimen size can be calculated from data measured with specimens of different sizes. This allows the master curve concept for 1T-size specimens to be applied to define the median temperature dependence of K_{JC} in the transition region as follows:

$$K_{JC}(\text{med}) = 30 + \exp\,[0.019(T - T_O)]\ , \qquad (1)$$

where T is temperature in °C, and T_O is the reference temperature at $K_{JC(med)} = 100$ MPa$\sqrt{m}$. The T_O values obtained from data sets at two or more temperatures tend to be the same. In this study, where multiple values of T_O were obtained, they were averaged. Details of this analysis are published elsewhere.[35]

Figures 5 and 6 present Charpy and fracture toughness curves, respectively, of the Midland beltline weld in the unirradiated, irradiated, and irradiated/annealed conditions. The shift of the Charpy transition temperature due to irradiation, ΔT_{41J}, was 103°C compared to a 92°C shift of fracture toughness transition temperature, ΔT_O. Annealing at 343°C for 168 h resulted in full recovery of Charpy USE but in only 49% recovery of ΔT_{41J}. The residual shift (unrecovered after annealing) of the Charpy transition temperature ($\Delta T_{res}CV$) is 53°C. The USE after annealing at 454°C for 168 h increased to 106 J, which is 17 J higher than the USE in the unirradiated condition. The residual shift, $\Delta T_{res}CV$, is 24°C. The fracture toughness specimens were annealed at 454°C for 168 h. The residual shift of the fracture toughness transition temperature ($\Delta T_{res}K$), Figure 6, is 13°C.

Figures 7 and 8 present Charpy and fracture toughness curves, respectively, of HSST Plate 02 in the unirradiated, irradiated, and irradiated/annealed conditions. Charpy specimens available for annealing had the L-T orientation, and no baseline Charpy transition curve was developed for L-T-oriented specimens in the as-irradiated condition. However, the irradiation-induced shift was determined for Plate 02 in the T-L orientation, as reported in ref. 42. Based on those results, and the accepted equivalence of the shift for L-T and T-L orientations,[43] ΔT_{41J} is estimated to be 55°C at 1×10^{19} neutrons/cm^2 (> 1 MeV), as shown in Figure 7. Annealing at 343°C for 168 h resulted in full recovery of the Charpy USE. The residual shift of the Charpy transition temperature after annealing at 343°C is 35°C. Similar to the Midland weld, annealing at 454°C for 168 h resulted in "over-recovery" of the USE; the USE of the irradiated and annealed plate rose 24 J above that of the USE in the unirradiated condition. The ΔT_{41J} recovered almost fully after annealing at 454°C for 168 h since $\Delta T_{res}CV$ was only 6°C. The residual shifts of ΔT_O, however, were 78 and 22°C after annealing for 168 h at 343 or 454°C, respectively.

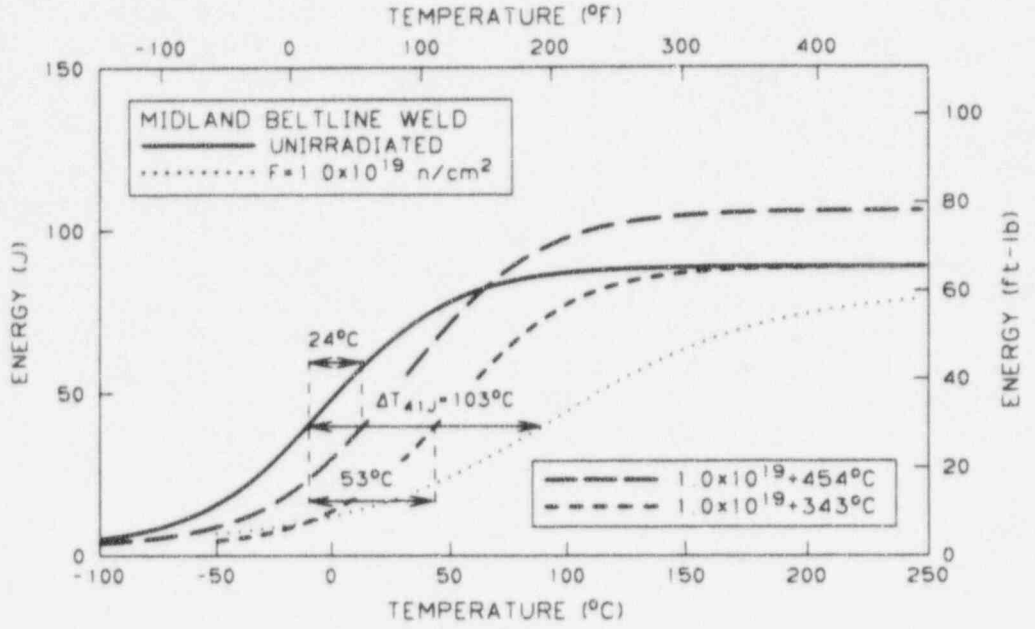

Fig. 5. Charpy impact curves of Midland beltline weld (WF-70) in unirradiated, irradiated, and irradiated/annealed conditions.

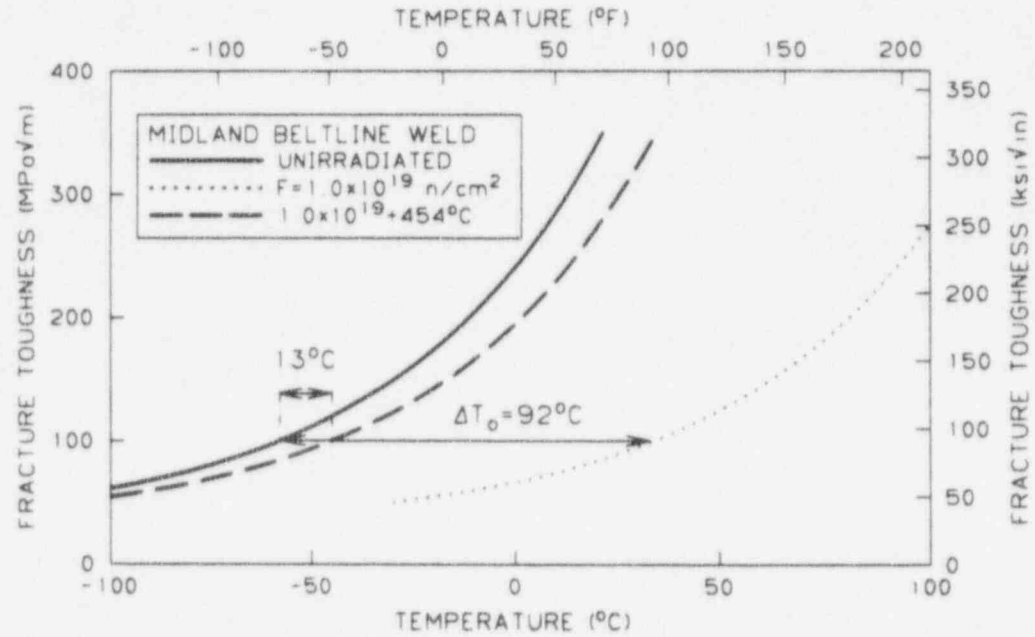

Fig. 6. Fracture toughness master curves of Midland beltline weld in unirradiated, irradiated, and irradiated/annealed conditions.

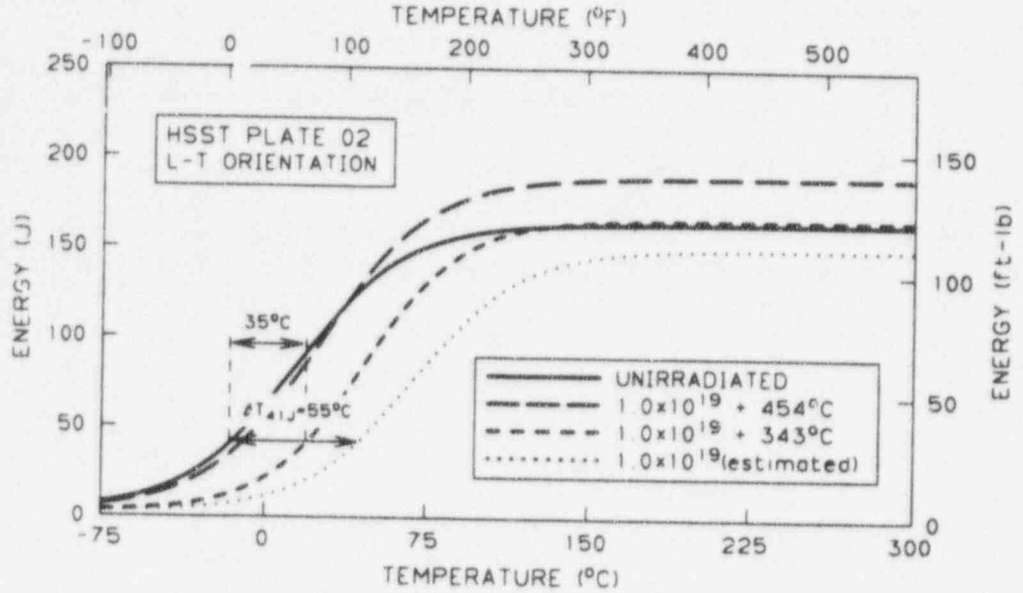

Fig. 7. Charpy impact curves of Heavy-Section Steel Technology Plate 02 (L-T orientation) in unirradiated and irradiated/annealed conditions. Irradiated curve was estimated from T - L data.

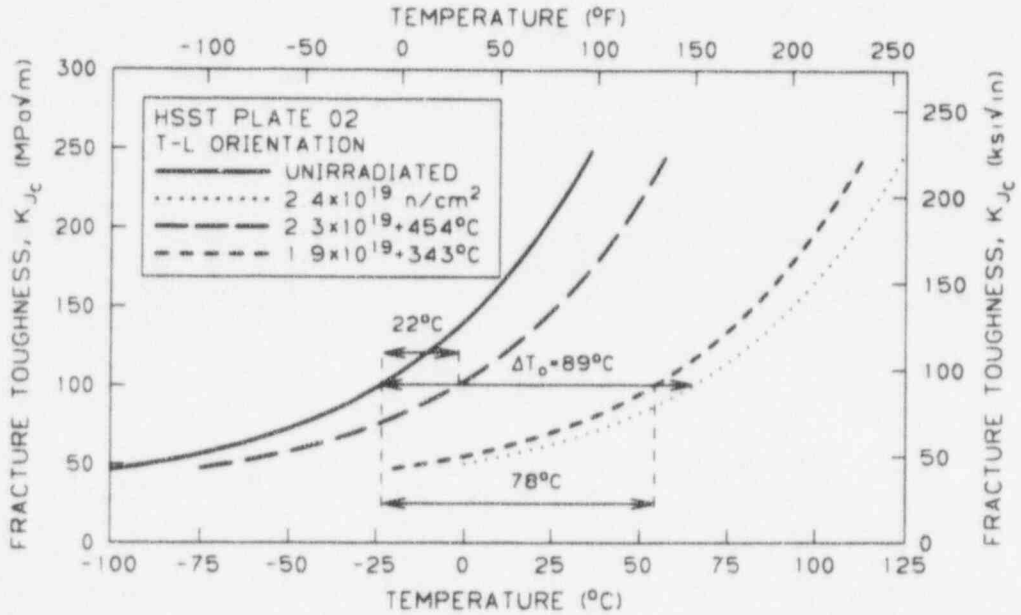

Fig. 8. Fracture toughness master curves of HSST Plate 02 (T-L) in unirradiated, irradiated, and irradiated/annealed conditions.

For both materials, full recovery of the Charpy USE was observed even at the lower annealing temperature, although recovery of the transition temperature was far from complete at 343°C. At the annealing temperature of 454°C, over-recovery of the USE was observed. The definition of over-recovery is that the USE after annealing of irradiated material is greater than that of unirradiated material. In addition to irradiated specimens, unirradiated Charpy specimens of Plate 02 were heat treated at 454°C for 168 h (the same regimen for annealing of irradiated specimens), and there was no change in USE compared with the unirradiated level. Annealing at 454°C for 168 h was also performed on Charpy specimens from the Midland nozzle course weld, irradiated to 1.0×10^{19} neutrons/cm^2 (> 1 MeV), which are identical to the beltline weld metal except for copper content. The USE of irradiated/annealed nozzle course weld was 17 J higher than the unirradiated level, which was also observed for the beltline weld.

Such behavior is consistent with other annealing studies.[47,48] In ref. 47, annealing of irradiated and unirradiated submerged-arc HSSI weld 73W at 454°C for 168 h resulted in the same increase of the USE compared with the unirradiated condition. It might be concluded, therefore, that the observed over-recovery of the USE of weld metal is independent of any irradiation effect since such heat treatment of unirradiated material also resulted in an increase of the USE. Over-recovery of the ductile fracture toughness, as measured by J_{Ic} and tearing modulus, was reported for the irradiated/annealed Linde 80 high-copper, LUS welds.[49,50] It is interesting to note that in ref. 50 welds that over-recovered the ductile fracture toughness did not show full recovery of the fracture toughness in the transition region, which corresponds well with the present Charpy data. The current data on the recovery of the Charpy USE in different materials are generally consistent, but the mechanism responsible for the over-recovery is not clear. The more rapid and more extensive recovery of USE with annealing compared with transition temperature suggests that there are different mechanisms for degradation of these properties upon irradiation. The effect of over-recovery of Charpy USE makes annealing an attractive measure for plant life extension, especially for so-called LUS materials. However, the real value of this advantage can be judged only after an extensive study of the behavior of materials after reirradiation.

The value of ΔT_{41J} of the Midland beltline weld after irradiation to a neutron fluence of 1.0×10^{19} neutrons/cm^2 (> 1 MeV) was about 10°C higher that the ΔT_o. Annealing of the irradiated weld at 454°C for 168 h significantly recovered Charpy and fracture toughness transition temperatures. However, the residual or unrecovered shift of the Charpy 41-J transition temperature was also about 10°C higher than the residual shift of the fracture toughness transition curve.

Sets of compact specimens and Charpy specimens of Plate 02 were irradiated to different neutron fluences, so the comparison of Charpy and fracture toughness recovery cannot be performed as directly as in the case of the Midland weld. To overcome this, the Charpy T_{41J} and fracture toughness T_o shifts from analysis of the Fourth HSSI Irradiation Series[35] were fit to the following equation:

$$\Delta T = A \times F^{1/2} \quad , \tag{2}$$

where ΔT is the shift of fracture toughness T_o and/or Charpy T_{41J}, A is a fitting parameter, and F is neutron fluence ($\times 10^{19}$ neutrons/cm^2); see Figure 9. The first observation is that the fracture toughness shifts due to irradiation are slightly higher than those for Charpy impact toughness. Annealing at 343°C for 168 h resulted in noticeable recovery of ΔT_{41J}, but ΔT_o did not show any recovery. This could be due to different responses of Charpy and fracture toughness properties to low-temperature annealing and/or due to dependence of residual shift on neutron fluence. For a 454°C annealing temperature, the residual fracture toughness shift was 22°C compared with 6°C of the residual Charpy shift. The residual fracture toughness

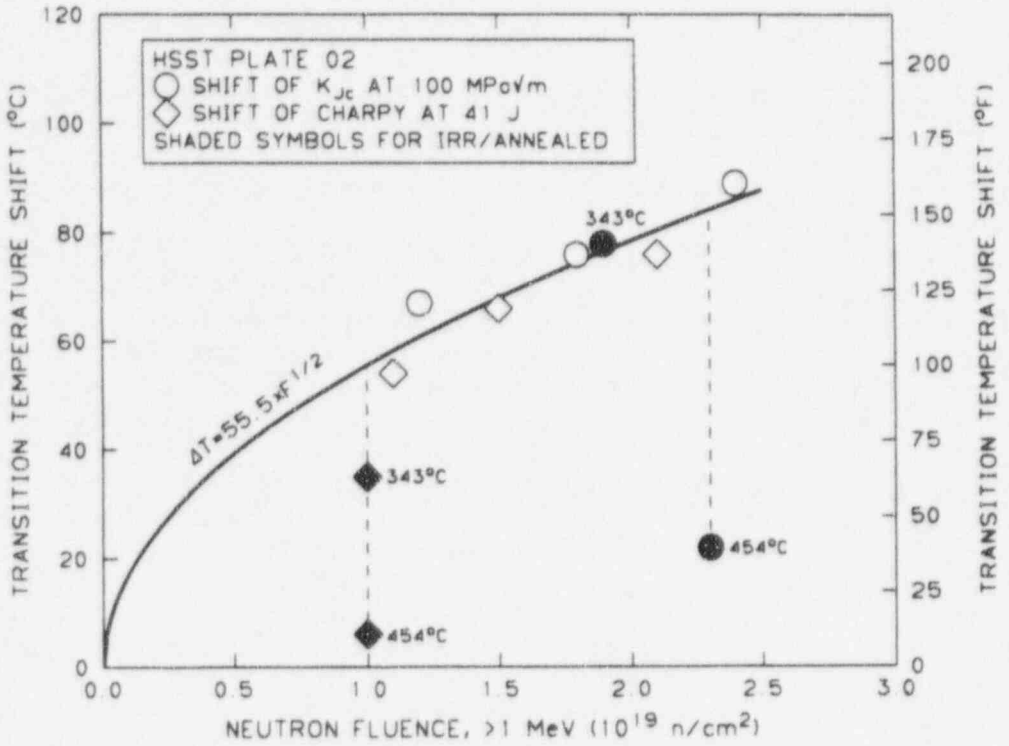

Fig. 9. Comparison of Charpy 41J and fracture toughness 100 MPa√m transition temperature shifts after irradiation and annealing of Heavy-Section Steel Technology Plate 02. Annealing temperature is indicated beside symbol.

shift was higher than $\Delta T_{res}CV$ following annealing by about the same amount as ΔT_o was higher than ΔT_{41J} after the original irradiation.

The data obtained from the annealing investigation of the Midland beltline weld and HSST Plate 02 appear to be consistent. The values of residual shift in fracture toughness are comparable to the residual Charpy transition temperature shifts at 41 J following annealing at 454°C, and the degree of agreement is similar to that observed when the radiation-induced temperature shifts are compared.

To summarize, annealing of irradiated A 533 grade B class 1 steel (HSST Plate 02) and Midland beltline weld (WF-70) at 288°C was performed at 343 or 454°C for 168 h to compare the recovery of the fracture toughness and Charpy impact properties. The Weibull statistic and master curve approach were applied to analyze fracture toughness properties of unirradiated, irradiated, and irradiated/annealed pressure vessel steels. It was concluded that the recovery of the Charpy USE appears to be more rapid and more extensive compared to the Charpy transition temperature, which suggests that there may be different mechanisms for degradation of these properties upon irradiation. At the annealing temperature of 454°C, the Charpy USE rises above the unirradiated level. This effect of over-recovery of Charpy USE makes annealing a very attractive measure for plant life extension, especially for so-called LUS materials. However, the real advantage to be gained can be judged only after an extensive study of the behavior of materials with reirradiation. In addition, shifts of the reference fracture toughness of the materials studied were slightly different from the Charpy 41-J transition temperature shifts. Annealing of A 533 grade B steel (Plate 02) at 343°C for 168 h did not result in any apparent recovery of fracture toughness reference temperature, T_o, compared with noticeable recovery of the Charpy T_{41J}. The values of residual (unrecovered) shift in fracture toughness are comparable to the residual Charpy transition temperature shifts at 41 J following annealing at 454°C for 168 h, and the degree of agreement is similar to that observed between the radiation-induced ΔT_o and ΔT_{41J}.

HEAVY-SECTION STEEL TECHNOLOGY PROGRAM

The goal of the HSST Program is the development, validation, and application of technology for the assessment of fracture prevention margins in commercial RPVs. Its scope includes development and experimental validation of analysis methods, development of testing techniques and generation of materials property data, integration of analysis methods and materials property data, and the transfer of the results to national and international codes and standards bodies. The major focus of the HSST Program is on behavior of shallow flaws, since the initiation probabilities associated with these flaws under PTS loading conditions can strongly influence the predicted failure probabilities for RPVs. Behavior of shallow flaws during a PTS transient would be influenced by the material and fracture properties as well as the mechanical interactions associated with the cladding, heat-affected zone, and the near-surface material. Thus, coordinated experimental and analytical studies are being conducted to provide a quantitative description of effects of the cladding overlay on fracture behavior of shallow surface flaws, including a quantitative description of cladding effects on the fracture behavior of shallow finite-length surface flaws in RPVs under uniaxial and biaxial loading conditions and a basis for improved treatment of surface-flaw geometries in fracture assessment procedures applied to PTS and pressure temperature (P-T) limit transients.

Cladding Issues

One of several issues the HSST Program is investigating is the effect of the clad overlay (henceforth referred to as cladding) on the propensity for cleavage initiation of shallow flaws on the inner surface of c[illegible]Vs. Shallow flaws having depths on the order of the combined thickness of the cladd[illegible] HAZ dominate the frequency distribution of flaws[51] assumed in

probabilistic fracture mechanics assessments of RPVs. Consequently, the initiation probabilities associated with these flaws under PTS loading conditions can strongly influence the predicted failure probabilities for RPVs. Behavior of these shallow flaws during a PTS transient clearly would be influenced by the material/fracture properties and mechanical interactions associated with the elements that comprise the cladding structure, which include the cladding, mixed-alloy region, HAZ, and near-surface base material. Thus, coordinated experimental and analytical studies are being conducted to provide a quantitative description of the effects of the cladding on the fracture behavior of shallow surface flaws.

The principal function of the cladding in an RPV is to minimize the volume of corrosion products entering the primary system coolant. Potential benefits or liabilities of the cladding that relate to the structural integrity of the vessel are not considered in safety assessment procedures applied to RPVs. The fracture mechanics model referred to in the NRC *Regulatory Guide 1.154* (RG 1.154) [ref. 52] for evaluating the integrity of RPVs under PTS loading conditions includes cladding as a discrete region only to the extent that thermal and stress effects are considered in the context of a linear elastic fracture mechanics (LEFM) model. Specifically, consideration of the clad structure is limited to incorporating the relatively lower thermal conductivity and the higher coefficient of thermal expansion (compared to base metal). The cladding and HAZ are assumed to have the same fracture toughness as that of the base metal. Also, all flaws are considered to be surface flaws, i.e., the flaws extend through the cladding to the inner surface of the vessel.

Another important feature of the analysis model in RG 1.154 that may be impacted by cladding issues is the assumption that initial flaws of a depth less than 20% of wall thickness are infinitely long [i.e., two-dimensional (2-D)] for the purpose of calculating stress-intensity factors (K_I). This assumption regarding 2-D initial flaws was based in part on results of analyses and assessments of Oak Ridge National Laboratory (ORNL) unclad thermal-shock experiments (TSEs).[53] These results indicated that, in the absence of cladding, a semicircular surface flaw subjected to sufficiently severe thermal-shock loading will propagate in surface length to become a very long flaw. Furthermore, lateral extension of the surface flaw is predicted to occur before the time in the transient when a 2-D flaw of the same depth would initiate and propagate radially.

Prior Research on Cladding

Much attention has been focused on efforts to better understand the influence of cladding on RPV integrity under postulated accident and operating conditions. At laboratories in the United States and in Europe, numerous experimental and analytical studies have been conducted to examine effects of cladding on fracture behavior when considered as a structural element of an RPV. TSEs performed at ORNL with large test cylinders studied the effects of cladding on behavior of both surface and subclad flaws. Four experiments (TSE-8 through -11) were conducted with cladding and flaws located on the inner surface of the cylinder.[54] The thermal shock was achieved by first heating the cylinder to 93°C and then shocking the inner surface with liquid nitrogen at –196°C. Substantial subsurface and radial propagation of several flaws was observed during two of the clad cylinder experiments (i.e., TSE-8 and -11). In these experiments, there was no breaching of the cladding by subclad flaws or extension of flaws on the surface. The contour of the arrested flaw that extended from an initially semi-elliptical subclad flaw in TSE-8 is depicted in Figure 10. TSE-9 provided a direct comparison of results with the previously performed TSE-7 test,[53] which had essentially the same flaw geometry (i.e., a 26-mm-deep semicircular surface flaw) and loading conditions, but no clad layer. In TSE-7, there were three initiation-arrest events that terminated with a final crack depth of 27.7 mm. By comparison, only a single event occurred in TSE-9, and the extension was only 6.2 mm. The presence of cladding reduced the potential for propagation of both through-clad surface and subclad flaws.

Keeney-Walker et al.[55] analyzed shallow through-clad surface cracks subjected to transient PTS loading conditions (from the Rancho Seco transient) using finite-element techniques and elastic-plastic constitutive models. Because ductile tearing is considered the relevant fracture mode for stainless steel RPV cladding, the J_R methodology was employed to determine the propensity for initiation of tearing in the cladding. Data depicted in Figure 11 for irradiated cladding from an HSSI testing program[56] indicate J_{Ic} of irradiated stainless steel cladding is similar to that of irradiated LUS weld material. Crack-tip stress-intensity factors at the clad-base metal interface (Point 3) on a surface flaw are shown plotted in Figure 12. Results are shown for both elastic and elastic-plastic analyses of the model. The elastic-plastic solution shows that there is a significant reduction in stress-intensity factor at this location, due to substantial plastic deformation in the low-yield stress cladding. Estimated lower-bound tearing toughness curves for cladding, LUS weld metal, and A533 B plate material are superimposed on the applied K_J curves in Figure 12. Comparisons indicate the irradiated cladding toughness is sufficiently high that ductile tearing is unlikely to occur for the conditions assumed in ref. 55.

HSST Cladding-Effects Research

An important part of the HSST program is to provide (1) a quantitative description of cladding effects on the fracture behavior of shallow finite-length surface flaws in RPVs and (2) a basis for improved treatment of surface-flaw geometries in fracture assessment procedures applied to PTS and P-T limit transients. Within this work scope, both analytical studies and validation testing are being performed to resolve important cladding issues and to refine safety assessment procedures.

The HSST Program has defined matrices of uniaxial and biaxial beam tests to investigate and quantify the effects of the clad structure on fracture initiation toughness of 2-D (infinite length) and three-dimensional 3-D (finite length) through-surface shallow flaws. The scope of these tests and the current status are shown in Table 1. A series of full-thickness clad beams[57] have been tested and are currently being analyzed to evaluate the effect of shallow flaw behavior, metallurgical gradients, and residual stresses on cleavage initiation toughness. These beam specimens (Figure 13) were cut from a shell segment of an RPV from a canceled nuclear plant (the plant was not put into service). As such, the material is fully prototypic of A533B RPV materials and fabrication processes. The beam specimens were cut from the full-shell thickness (approximately 230 mm) with the 2-D test flaw machined into the inside clad surface. Normalized flaw depths (a/W ratios) of 0.05 to 0.5 were used. The deep-flaw test provided the baseline for this series, while the shallow flaws were consistent with the actual magnitudes of shallow flaws of interest in RPV PTS assessments. Five of the specimens had the test flaw located in a longitudinal weld joining shell plates, while the remaining three had the test flaw in the base metal. All tests were performed at a normalized temperature near T–NDT = 25°C. A large variation in fracture toughness (i.e., ranging from 225 to 437 MPa$\sqrt{m}$) was observed in tests conducted at T = –25°C (T–NDT = 25°C) on specimens containing through-thickness shallow flaws (approximately 11 mm deep) located near the edge of the cladding HAZ in fabrication weld material. The low-toughness value represents a lower bound to additional shallow-flaw toughness data from A 533 B plate material[58] tested at the same temperature referenced to the nil-ductility temperature (Figure 14).

Measurements of the notch width resulting from wire electrodischarge machining of the clad beam specimens provided input data for residual stress analyses.[59] The peak stress values in the cladding obtained from these analyses were 74 and 87 MPa, respectively. However, residual stress values may be larger in the RPV shell segment from which the clad beam specimens were fabricated. This is a result of removing the beam specimens from the restraining effects of the shell segment, which leads to a partial relaxation of residual stresses.

The biaxial tests[60] shown in Table 1 are being used to investigate the behavior of shallow, finite-length, through-surface flaws where the cladding, temperature, and biaxial load

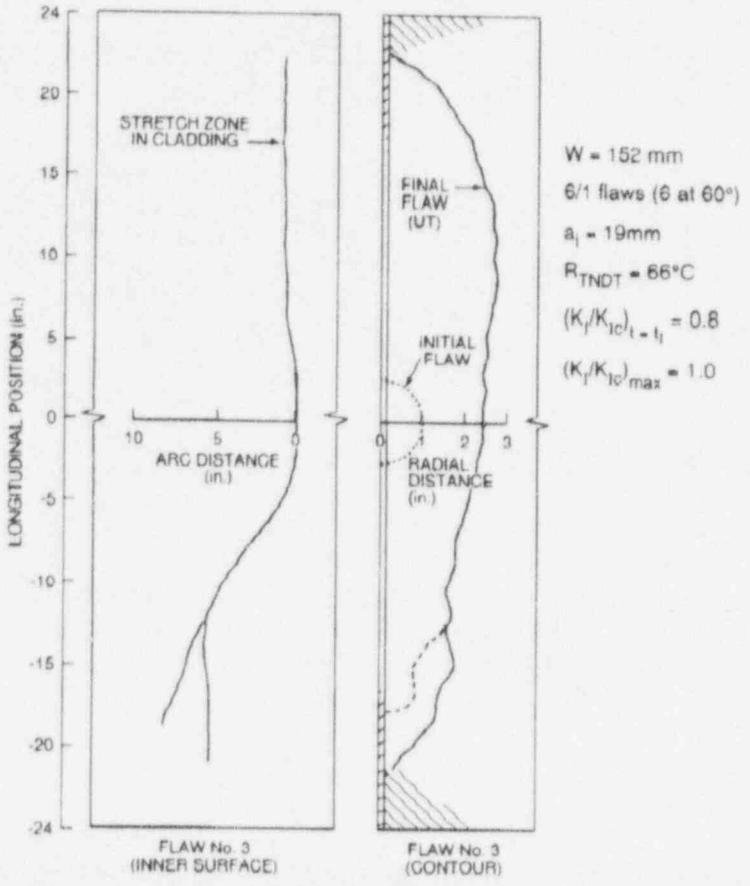

Fig. 10. In TSE-8, one of six 6/1 subclad flaws propagated, extended in length (subclad) and depth, with no penetration of the cladding.

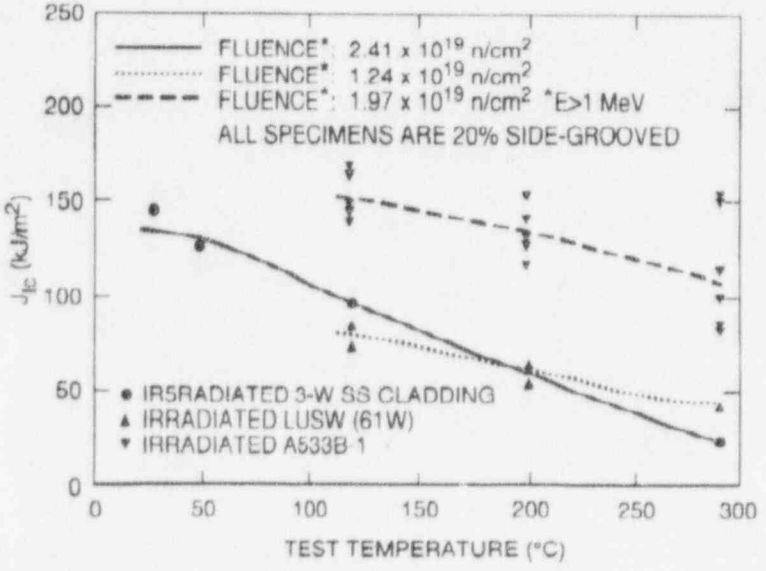

Fig. 11. Ductile tearing initiation toughness of both low–upper–shelf weld material and cladding in the irradiated condition were shown to be approximately half that of irradiated A533B material.

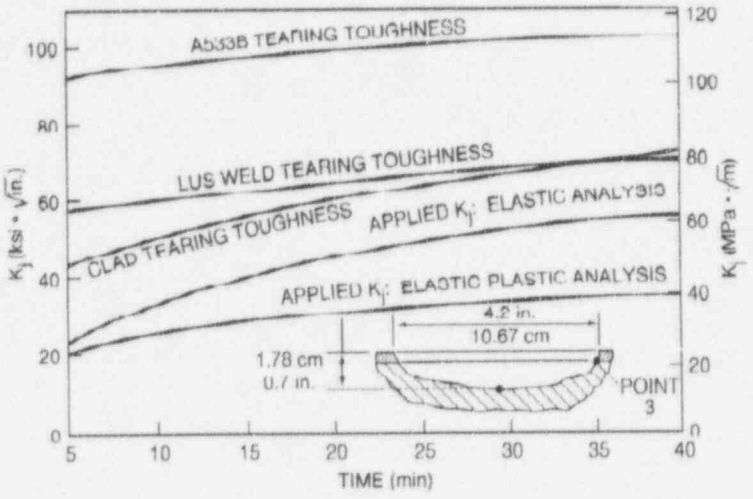

Fig. 12. The applied K_J at the clad-base metal interface remains significantly below the estimated -2σ tearing toughness curve for both cladding and low-upper-shelf weld metal throughout the transient. Plasticity effects significantly reduce the magnitude of the applied K_J at this location (point 3).

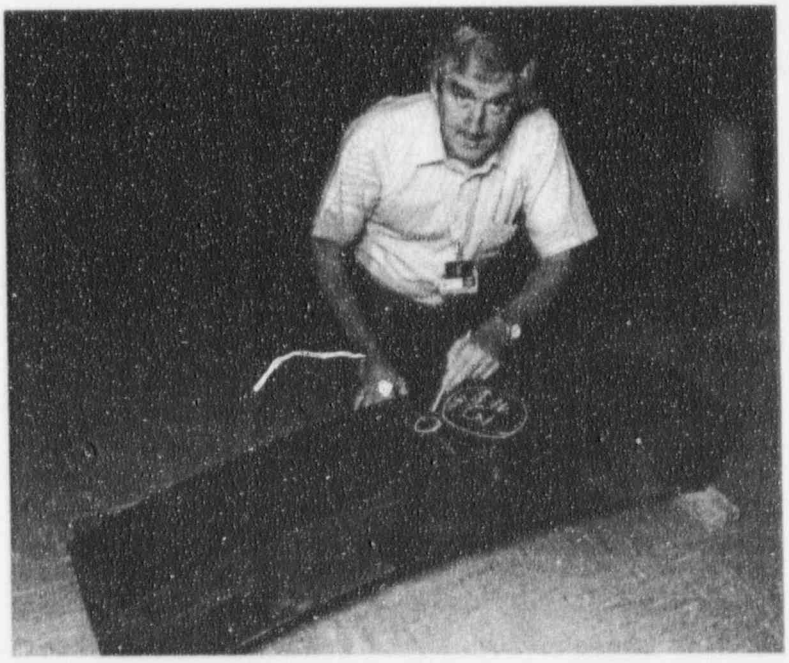

Fig. 13. Prototypical flaw depths, a/W ratios, and metallurgical gradients are present in the full–scale clad beam fracture toughness tests.

ratio are the primary independent variables. The same source material as that used for the full-thickness clad beams specimens is being used here also. Figure 15 shows a schematic diagram of the biaxial specimen. Characterization tests showed that the weld material had a yield strength approximately 38% higher than the surrounding base material (599 versus 440 MPa). This elevated yield stress, which is more prototypic of an irradiated material, combined with a general concern for the fracture behavior of RPV welds, led to a specimen design where the test flaw is located in the welds joining the rolled plates or the shell courses. These tests will help define an envelope of flaw sizes for which cleavage initiation will not be expected under severe PTS-type loading. Such an envelope will allow exclusion of a family of small flaws from probabilistic analyses, potentially contributing to a reduction in the calculated conditional probability of RPV failure. The specimens being tested range from medium (102 × 102 × 102-mm test section) to large-size beams (154 × 154 × 154-mm test section) and will be tested under biaxial load ratios ranging from 0:1 (uniaxial) to 1:1 (full biaxial). Transferability of the data base and methodology developed will be demonstrated through testing of a much smaller number of large-size biaxial beams under 0:1 and 1:1 loading at a single temperature.

Table 1. Matrices of Unclad and Clad Beam Tests Defined to Validate Constraint Methodologies

HSST[a] Task	Specimen configuration	Specimen size	Flaw type	Material	Number of tests planned
H2	Cruciform	Medium[b]	2-D[c], Shallow[d]	Heat- treated[e] A533B Plate	32
H2	Cruciform	Large	2-D[c], Shallow[d]	Heat- Treated[e] A533B Plate	4
H3	Cruciform	Medium[b]	Finite-Length, Shallow[g]	RPV[f] weld with clad layer	24
H3	Cruciform	Large[h]	Finite-Length, Shallow[g]	RPV[f] weld with clad layer	4
H3	Uniaxial	Full Thickness[i]	2-D[c], Shallow	RPV[f] base material with clad layer	3

[a]HSST = Heavy-Section Steel Technology Program.
[b]Normal test section size 4 × 4 × 4 in.
[c]2-D = two-dimensional.
[d]Uniform depth flaw, a/W = 0.1
[e]Heat treated to simulate irradiated material properties.
[f]RPV = reactor pressure vessel.
[g]Semi-elliptic, 0.05 ≤ a/W ≤ 0.25.
[h]Nominal test section size in range of 6 x 6 x 6 in.
[i]Full RPV shell thickness.

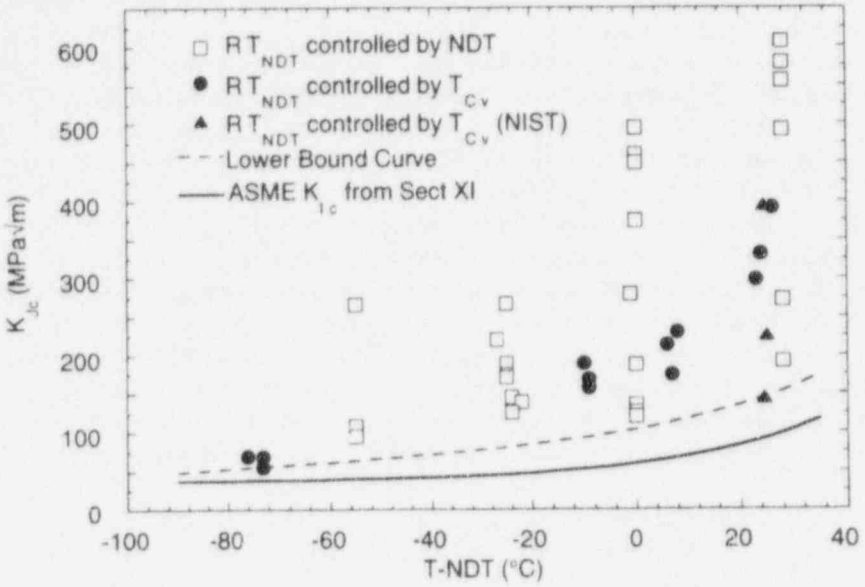

Fig. 14. The shallow-flaw fracture toughness data for A533 plate and weld material has a lower bound similar to that of deep-flaw data, but shows an increase in both mean toughness and data scatter.

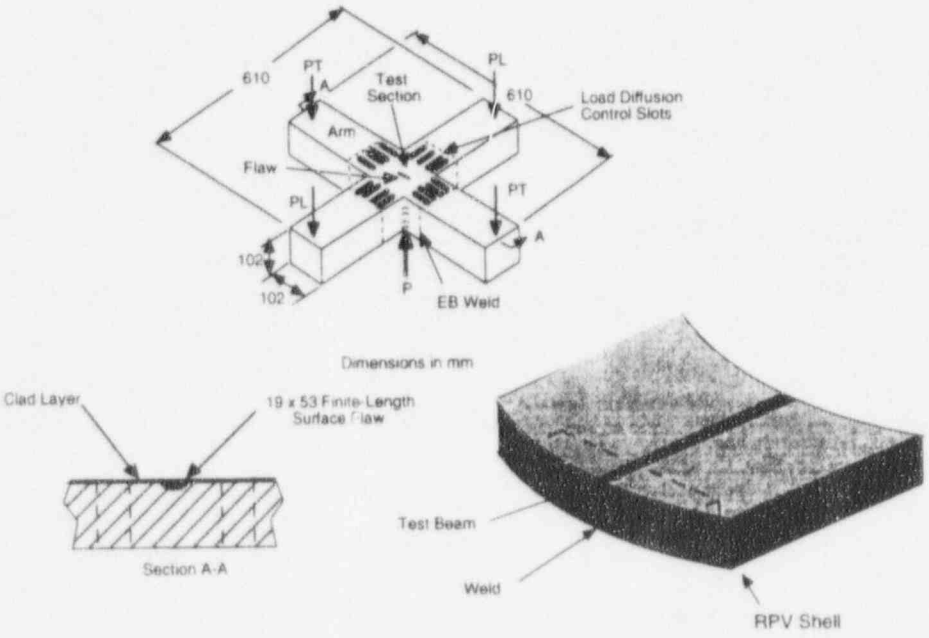

Fig. 15. Finite-length flaw specimens cut from an RPV shell segment are used to investigate the effect of the clad layer and flaw size on initiation behavior of prototypic RPV welds.

Preliminary development tests of the shallow-flaw beam design have been completed. These preliminary tests utilized specimens machined from homogeneous plate material, i.e., no cladding. Figure 16 shows a comparison of typical fracture surfaces from a specimen tested under uniaxial (0:1) loading with one tested under biaxial (1:1) loading. The test flaws are nominally 53 mm long and 20 mm deep. Characteristically, biaxial loading resulted in a shift in the fracture initiation site from near the deepest point to a location near 20° below the free surface. This behavior was substantiated by finite element analyses, the results of which are also shown in Figure 16. The maximum K_I value for the uniaxial case was predicted to be at the deepest point of the flaw. The maximum for the biaxial case was predicted to be near the free surface, although the calculated value at the deepest point was also very near the maximum. While not shown in Figure 16, it was also observed that the mean of the toughness values determined for these tests was approximately 60% above the mean value determined from a group of 1T compact tension specimens, providing further substantiation of the existence of a shallow-flaw effect.

Analytical techniques incorporated into the ORNL-developed FAVOR computer program[61] were used to investigate the effects of selected features of cladding overlay models on fracture assessments of a representative RPV. Specific refinements were introduced into cladding models to take account of a low clad yield stress and a high clad ductility that precludes initiation in the clad layer.[62] Assessments were carried out with the FAVOR code for axially oriented finite-length inner surface flaws with aspect ratios of 2, 6, and 10, as well as for 2-D flaws. Loading of the vessel was provided by stylized thermal transients of varying severity, analogous to the PTS transients utilized in PTS benchmarking exercises cosponsored by the NRC and the Electric Power Research Institute. For a fixed decay (cooldown) constant, the severity of these transients is governed by the final coolant temperature, T_f.

The conditional probability of initiation versus T_f was computed for a reference case defined in terms of an ASME-based fracture toughness correlation, an LEFM model, cladding toughness equal to that of base metal, and a 2-D flaw assumption (curve 1 in Figure 17). Each of the latter elements was changed separately in the model to determine the corresponding change in conditional probability of initiation for PTS transients of varying severity (all modified cases assumed a semicircular flaw). Fracture toughness correlations based on uniaxial (ref. 58 and Figure 14) and biaxial[60] shallow-flaw toughness data sets were considered, in addition to the ASME-based correlations. The combined effects of clad yielding and clad toughness properties provided a decrease in initiation probabilities of one order of magnitude for a semicircular flaw over the range of final coolant temperatures (curve 2 in Figure 17). When a uniaxial shallow-flaw toughness correlation is adjusted for biaxial effects, the resultant correlation provides initiation probabilities that are at least an order of magnitude lower than those obtained from the ASME-based correlation (curve 3 in Figure 17). The combined-effects model that includes both the cladding properties and the biaxial shallow-flaw toughness correlation gave the maximum reduction of approximately two orders of magnitude from the LEFM-ASME-based correlation (curve 4 in Figure. 17).

Interim conclusions based on current cladding-effects research include the following. Shallow surface flaws in the near-HAZ region produced both the minimum fracture toughness and substantial data scatter in tests of full-scale clad single-edge, notched-beam specimens. Analyses of measured data obtained from wire electrodischarge machining notch widths in full-thickness clad beams indicated peak residual stresses in the cladding of 87 MPa. In-process testing of clad-cruciform specimens with finite-length surface flaws will provide data to define a flaw-geometry/transient-severity envelope within which no crack initiation is predicted. Lastly, inclusion of clad mechanical and fracture toughness properties in a PTS analysis has the potential to reduce the conditional probability of crack initiation from finite-length surface flaws by approximately one order of magnitude.

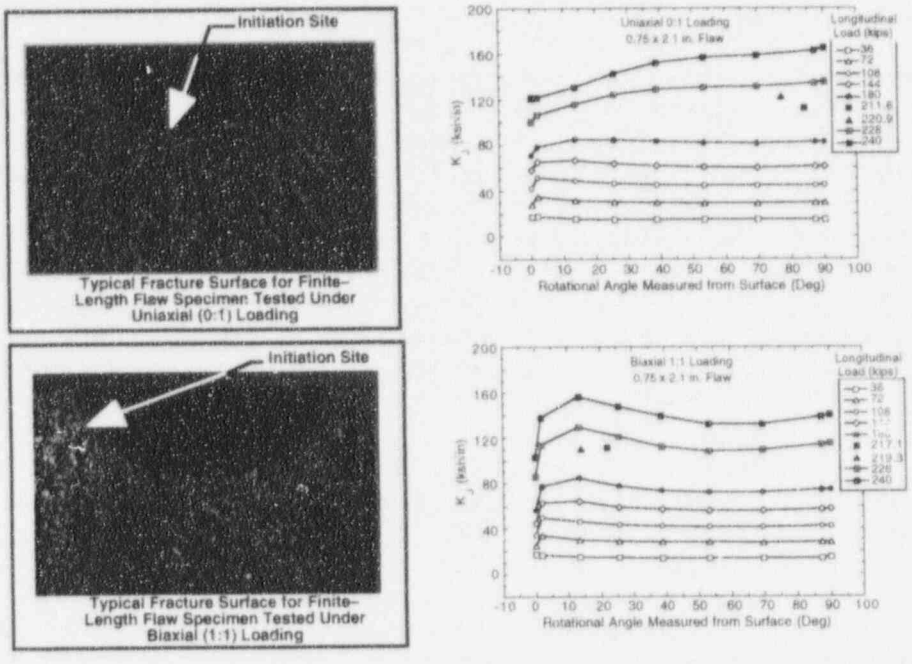

Fig. 16. Examination of fracture surfaces from finite-length flaw specimens verifies pre-test predictions of the effect of biaxial loading on initiation site location.

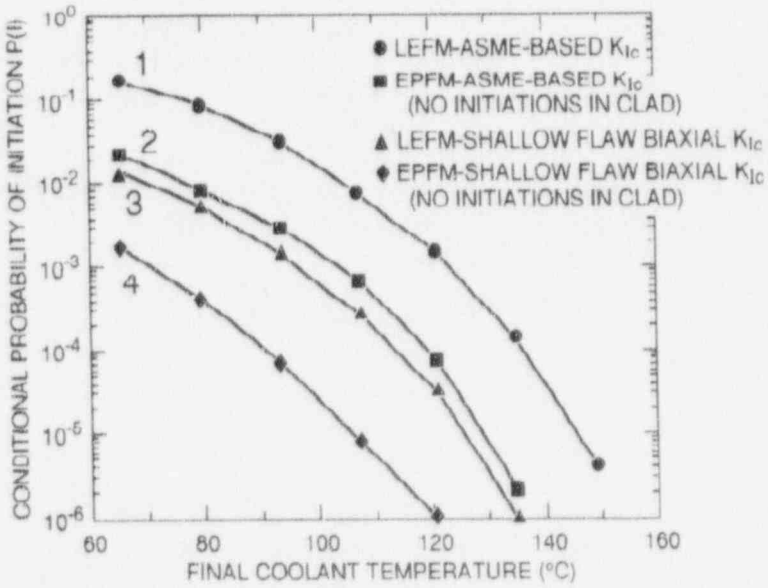

Fig. 17. The conditional probability of crack initiation from semicircular surface flaws decreases by approximately an order of magnitude when clad yield and fracture toughness properties are included in a PTS analysis.

SUMMARY

Results from the ORNL RPV integrity studies provide information needed to aid in resolving major regulatory issues facing the USNRC that involve RPV integrity issues. These issues include PTS, operating P-T limits, low-temperature overpressurization, the specialized problems associated with LUS welds, and the transfer of data from small-scale surveillance specimens to application in RPV structural integrity assessments.

REFERENCES

1. D. T. Ingersoll et al., Martin Marietta Energy Systems, Inc., Oak Ridge Natl. Lab., *Production and Testing of the VITAMIN-B6 Fine Group and the BUGLE-93 Broad-Group Neutron/Photon Cross-Section Libraries Derived from ENDF/B-VI Nuclear Data*, USNRC Report NUREG/CR-6214 (ORNL-6795), January 1995.

2. Ibid.

3. U.S. Nuclear Regulatory Commission, *SCALE: A Modular Code System for Performing Standardized Computer Analyses for Licensing Evaluation*, Vols. 1-3, NUREG/CR-0200, Rev. 4, April 1995. Available from Radiation Shielding Information Center at Oak Ridge National Laboratory as CCC-545/SCALE-4.2.

4. Martin Marietta Energy Systems, Inc., Oak Ridge Natl. Lab., *AMPX-77: A Modular Code System for Generating Coupled Multigroup Neutron-Gamma Cross-Section Libraries from ENDF/B-IV and/or ENDF/B-V*, ORNL/CSD/TM-283, October 1992. Available from Radiation Shielding Information Center at Oak Ridge National Laboratory as PSR-315/AMPX-77.

5. F. W. Stalmann, Martin Marietta Energy Systems, Inc., Oak Ridge Natl. Lab., *LSL-M2: A Computer Program for Least-Squares Logarithmic Adjustment of Neutron Spectra*, USNRC Report NUREG/CR-4349 (ORNL/TM-9933), March 1986.

6. I. Remec and F. B. K. Kam, "An Update of the Dosimetry Cross-Section Data Base for the Adjustment Code LSL-M2," ORNL/NRC/LTR-95120, Lockheed Martin Energy Systems, Oak Ridge Natl. Lab., June 1995.

7. N. P. Kocherov and P. K. McLaughlin, "The International Reactor Dosimetry File," IAEA-NDS-141, Rev. 2, International Atomic Energy Agency, Vienna, Austria, October 1993. Available from the Radiation Shielding Information Center at Oak Ridge National Laboratory as DLC-161.

8. P. J. Griffin et al., "SNLRML Recommended Dosimetry Cross-Section Compendium," SAND92-0094, Sandia National Laboratories, Albuquerque, N.M., 1993. Available from the Radiation Shielding Information Center at Oak Ridge National Laboratory as DLC-178.

9. A. W. Pense and R. D. Stout, "Characterization of heat-treated pressure vessel steels for elevated-temperature service," pp. 8-26 in *Symposium on Heat-Treated Steels for Elevated-Temperature Service*, ed. M. Semchyshen, American Society of Mechanical Engineers, New York, 1966.

10. U. Potapovs and J. R. Hawthorne, "The effect of residual elements on the response of selected pressure vessel steels and weldments to irradiation at 550°F," *Nucl. Appl.* **6**, 27-46 (1969).

11. C. Z. Serpan, Jr., H. E. Watson, and J. R. Hawthorne, "Interaction of neutron and thermal environmental factors in the embrittlement of selected structural alloys for advanced reactor applications," *Nucl. Eng. Des.* **11**, 368-80 (1970).

12. C. Z. Serpan, Jr., and H. E. Watson, "Mechanical property and neutron spectral analyses of the Big Rock Point reactor pressure vessel," *Nucl. Eng. Des.* **11**, 393-415 (1970).

13. L. E. Steele and H. E. Watson, "Interpreting the structural significance of time-dependent embrittlement phenomena to nuclear reactor pressure vessel integrity," *J. Mater.* **7**(2), 178-87 (1972).

14. A. L. Lowe, Jr, "Thermal aging capsule results from Oconee Nuclear Station - Unit 1," pp. 146-54 in *Radiation Embrittlement and Surveillance of Nuclear Reactor Pressure Vessels: An International Study, ASTM STP 819*, American Society for Testing and Materials, Philadelphia, 1983.

15. M. Hasegawa et al., "Effects of copper and phosphorus on temper embrittlement of Mn-Mo-Ni low-alloy steel (ASTM A533-B)," *Trans. JIM* **16**, 641-46 (1975).

16. S. G. Druce, G. Gage, and G. Jordan, "Effect of Ageing on Properties of Pressure Vessel Steels," *Acta Metall.* **34**(4), 641-52 (1986).

17. M. J. DeVan, A. L. Lowe, Jr., and S. Wade, "Evaluation of thermal-aged plates, forgings, and submerged-arc weld metals," pp. 268-82 in *Effects of Radiation on Materials: 16th International Symposium, ASTM STP 1175*, ed. A. S. Kumar, D. S. Gelles, R. K. Nanstad, and E. A. Little, American Society for Testing and Materials, Philadelphia, 1993.

18. S. G. Druce et al., "Effect of thermal ageing on mechanical properties of PWR PV steels and weldments," in *Transactions of the 8th International Conference on Structural Mechanics in Reactor Technology (SMiRT 8)*, Commission of European Communities, Brussels, Belgium, 1985.

19. J. Fukakura et al., "Effect of thermal aging on RPV steel," in *Structural Integrity Approaches - Mechanics and Materials, SMiRT 11 Post Conference Seminar 2, Taipei, Republic of China*, Nucl. Eng and Design, North Holland, Amsterdam, 1991.

20. R. Gerard et al., "In-service embrittlement of the pressure vessel welds at the Doel I and II nuclear power plants," in *Effects of Radiation on Materials: 17th International Symposium, ASTM STP 1270*, ed. D. S. Gelles, R. K. Nanstad, A. S. Kumar, and E. A. Little, American Society for Testing and Materials, Philadelphia, 1995.

21. K. Kussmaul, J. Fohl, and T. Weissenberg, "Investigation of materials from a decommissioned reactor pressure vessel - a contribution to the understanding of irradiation embrittlement," pp. 80-104 in *Effects of Radiation on Materials, 14th International Symposium (Volume II), ASTM STP 1046*, ed. N. H. Packan, R. E. Stoller, and A. S. Kumar, American Society for Testing and Materials, Philadelphia, 1990.

22. I. A. Vatter, C. A. Hippsley, and S. G. Druce, "Review of thermal ageing data and its application to operating reactor pressure vessels," *Int. J. Pressure Vessels Piping* **54**, 31-48 (1993).

23. W. L. Server, ATI Consulting, San Ramon, California, "Credibility of using steam generator welds as surrogates for the Palisades reactor pressure vessel welds" (an independent technical opinion submitted to Consumers Power Company), 1994.

24. R. K. Nanstad et al., "Preliminary review of data regarding chemical composition and thermal embrittlement of reactor vessel steels," ORNL/NRC/LTR-95/1, Lockheed Martin Energy Systems, Oak Ridge Natl. Lab., 1995.

25. K. A. Stahlkopf, G. R. Odette, and T. U. Marston, "Radiation damage saturation in pressure vessel steels: data and a preliminary model," p. 265 in *Proceedings of the Fourth International Conference on Pressure Vessel Technology, I. Mechanical Engineering*, London, 1980.

26. S. B. Fisher and J. T. Buswell, "A model for embrittlement of reactor pressure vessel steels," *Philos. Trans. R. Soc. London* **A315**, 301 (1985).

27. S. B. Fisher and J. T. Buswell, "A model for PWR pressure vessel embrittlement," *Int. J. Pressure Vessels Piping* **27**, 91 (1987).

28. G. E. Lucas and G. R. Odette, "Recent advances in understanding radiation hardening and embrittlement mechanisms in pressure vessel steels," p. 345 in *Proceedings of the Second International Symposium on Environmental Degradation of Materials in Nuclear Reactors -Water Reactors*, ed. J. T. A. Roberts, J. R. Weeks, and G. J. Theus, American Nuclear Society, LaGrange Park, Ill., 1986.

29. C. J. Bolton et al., "The modeling of irradiation embrittlement in submerged-arc welds," in *Effects of Radiation on Materials: 17th International Symposium, ASTM STP 1270*, ed. D. S. Gelles, R. K. Nanstad, A. S. Kumar, American Society for Testing and Materials, Philadelphia, 1995.

30. G. R. Odette et al., "The effect of flux on irradiation hardening of pressure vessel steels," pp. 373-93 in *Effects of Radiation on Materials: 16th International Symposium, ASTM STP 1175*, ed. A. S. Kumar, D. S. Gelles, R. K. Nanstad, and E. A. Little, American Society for Testing and Materials, Philadelphia, 1993.

31. R. E. Stoller, Martin Marietta Energy Systems, Inc., Oak Ridge Natl. Lab., *A comparison of the relative importance of copper precipitates and point defect clusters in reactor pressure vessel embrittlement*, USNRC Report NUREG/CR-6231 (ORNL/TM-6811), 1994.

32. *ASME Boiler and Pressure Vessel Code, An American National Standard*, Sect. XI, Appendix A, American Society of Mechanical Engineers, New York, 1986.

33. A. L. Hiser, Materials Engineering Associates, Lanham, Md., *Correlation of C_v and K_{Ic}/K_{Jc} Transition Temperature Increases Due to Irradiation*, USNRC Report NUREG/CR-4395 (MEA-2086), 1985.

34. K. Wallin, "A Simple Theoretical Charpy-V - K_{Ic} Correlation for Irradiation Embrittlement," pp. 93-100 in *Innovative Approaches to Irradiation Damage and Fracture Analysis*, PVP-Vol. 170, American Society of Mechanical Engineers, New York, 1989.

35. M. A. Sokolov and D. E. McCabe, "Comparison of Irradiation-Induced Shifts of K_{JC} and Charpy Curves: Analysis of Heavy-Section Steel Irradiation Program Data," ORNL/NRC/LTR-95/4, Lockheed Martin Energy Systems, Oak Ridge Natl. Lab., 1995.

36. M. Rogov and S. Morozov, "Annealing Application Experience to Extend Reactor Vessel Life," pp. 13-113 to 13-127 in *Proceedings of the DOE/SNL/EPRI Sponsored Reactor Pressure Vessel Thermal Annealing Workshop*, Vol. 2, SAND94-1515/2, Sandia National Laboratories, Albuquerque, N.M., 1994.

37. A. Fabry, "The BR3 Vessel Anneal: Lessons and Perspective," pp. 5-3 to 5-34 in *Proceedings of the DOE/SNL/EPRI-Sponsored Reactor Pressure Vessel Thermal Annealing Workshop*, Vol. 1, SAND94-1515/1, Sandia National Laboratories, Albuquerque, N.M., 1994.

38. E. D. Eason, J. E. Wright, E. E. Nelson, G. R. Odette, and E. V. Mager, Modeling and Computing Services, Boulder, Colorado, *Models for Embrittlement Recovery Due to Annealing of Reactor Pressure Vessel Steels*, USNRC Report NUREG/CR-6327 (MCS 950302), 1995.

39. D. E. McCabe, M. A. Sokolov, R. K. Nanstad, and R. L. Swain, "Effects of Irradiation to 0.5 and 1×10^{19} neutrons/cm^2 (> 1 MeV) on the Midland Reactor Low Upper-Shelf Weld: Capsules 10.01, 10.02, and 10.05 in the Heavy-Section Steel Irradiation Program Tenth Irradiation Series," ORNL/NRC/LTR-95/18, Lockheed Martin Energy Systems, Oak Ridge Natl. Lab., 1995.

40. D. E. McCabe, R. K. Nanstad, S. K. Iskander, and R. L. Swain, Martin Marietta Energy Systems, Inc., Oak Ridge Natl. Lab., *Unirradiated Material Properties of Midland Weld WF-70*, USNRC Report NUREG/CR-6249 (ORNL/TM-12777), 1994.

41. R. K. Nanstad, D. E. McCabe, R. L. Swain, and M. K. Miller, Martin Marietta Energy Systems, Inc., Oak Ridge Natl. Lab., *Chemical Composition and RT_{NDT} Determinations for Midland Weld WF-70*, USNRC Report NUREG/CR-5914 (ORNL-6740), 1992.

42. J. J. McGowan, R. K. Nanstad, and K. R. Thoms, Martin Marietta Energy Systems, Inc., Oak Ridge Natl. Lab., *Characterization of Irradiated Current-Practice Welds and A 533 Grade B Class 1 Plate for Nuclear Pressure Vessel Service*, USNRC Report NUREG/CR-4880 (ORNL-6484/V1), 1988.

43. G. D. Whitman, pp. 37-41 in *Quarterly Progress Report on Reactor Safety Programs Sponsored by the Division of Reactor Safety Research for July-September 1974. II. Heavy-Section Steel Technology Program*, ORNL/TM-4729, Vol. II, Union Carbide Corp. Nuclear Div., Oak Ridge Natl. Lab., 1974.

44. K. Wallin, "The Scatter in K_{Ic} Results," *Eng. Fract. Mech.* **19**(6), 1085-93 (1984).

45. "Method for Fracture Toughness in the Transition Range," Proposed ASTM Test Practice, Draft 8, ASTM Task Group E08.08.03, American Society for Testing and Materials, Philadelphia, 1995.

46. W. Weibull, "A Statistical Theory of the Strength of Materials," No. 151, in *Proceedings of Royal Swedish Institute for Engineering Research*, Stockholm, Sweden, 1939.

47. S. K. Iskander, M. A. Sokolov, and R. K. Nanstad, "Effects of Annealing Time on the Recovery of Charpy V-Notch Properties of Irradiated High-Copper Weld Metal," in *Effects of Radiation on Materials: 17th International Symposium, ASTM STP 1270*, ed. D. S. Gelles, R. K. Nanstad, A. S. Kumar, and E. A. Little, American Society for Testing and Materials, Philadelphia, 1995.

48. F. W. Stallmann, J. A. Wang, and F. B. K. Kam, Martin Marietta Energy Systems, Inc., Oak Ridge Natl. Lab., *TR-EDB: Test Reactor Embrittlement Data Base, Version 1*, USNRC Report NUREG/CR-6076 (ORNL/TM-12415), January 1994.

49. W. A. Pavinich and A. L. Lowe, "The Effect of Thermal Annealing on the Fracture Properties of a Submerged-Arc Weld Metal," pp. 448-60 in *Influence of Radiation on Material Properties: 13th International Symposium, ASTM STP 956*, ed. F. A. Garner, C. H. Henager, and N. Igata, American Society for Testing and Materials, Philadelphia, 1987.

50. M. A. Sokolov, R. K. Nanstad, and S. K. Iskander, "The Effect of Thermal Annealing on Fracture Toughness of Low Upper-Shelf Welds," in *Effects of Radiation on Materials: 17th International Symposium, ASTM STP 1270*, ed. D. S. Gelles, R. K. Nanstad, A. S. Kumar, and E. A. Little, American Society for Testing and Materials, Philadelphia, 1995.

51. W. Marshall, "An Assessment of the Integrity of PWR Pressure Vessels," Report by a Study Group, United Kingdom Atomic Energy Authority, October 1, 1976.

52. U.S. Nuclear Regulatory Commission, "Format and Content of Plant-Specific Pressurized Thermal Shock Safety Analysis Reports for Pressurized Water Reactors," *Regulatory Guide 1.154*, January 1987.

53. R. D. Cheverton, S. K. Iskander, and D. G. Ball, "Review of Pressurized-Water-Reactor-Related Thermal Shock Studies," pp. 752-66 in *Fracture Mechanics: Nineteenth Symposium, ASTM STP 969*, ed. T. A. Cruse, American Society for Testing and Materials, Philadelphia, 1988.

54. R. D. Cheverton, J. W. Bryson, D. J. Alexander, and T. Slot, "Thermal Shock Experiments with Flawed Clad Cylinders," *Nucl. Eng. Des.* **124**, 109-19 (1990).

55. J. Keeney-Walker, B. R. Bass, and W. E. Pennell, "Evaluation of the Effects of Irradiated Cladding on the Behavior of Shallow Flaws Subject to Pressurized-Thermal-Shock Loading," pp. 15-200 in *Proceedings of the 11th Conference on Structural Mechanics in Reactor Technology (SMiRT 11)*, Vol. G, Atomic Energy Society of Japan,Tokyo, 1991.

56. F. M. Haggag, W. R. Corwin, and R. K. Nanstad, Martin Marietta Energy Systems, Inc., Oak Ridge Natl. Lab., *Irradiation Effects on Strength and Toughness of Three-Wire Series-Arc Stainless Steel Weld Overlay Cladding*, USNRC Report NUREG/CR-5511 (ORNL/TM-11439), 1990.

57. J. A. Keeney, B. R. Bass, W. J. McAfee, and S. K. Iskander, Martin Marietta Energy Systems, Inc., Oak Ridge Natl. Lab., *Preliminary Assessment of the Fracture Behavior of Weld Material in Full-Thickness Clad Beams*, USNRC Report NUREG/CR-6228 (ORNL/TM-12735), October 1994.

58. T. H. Theiss and D. K. M. Shum, Martin Marietta Energy Systems, Inc., Oak Ridge Natl. Lab., *Experimental and Analytical Investigation of the Shallow-Flaw Effect in Reactor Pressure Vessels*, USNRC Report NUREG/CR-5886 (ORNL/TM-12115), July 1992.

59. J. A. Keeney, "Residual Stress Analysis of Full-Thickness Clad Beam Specimens," ORNL/NRC/LTR/-94/37, Lockheed Martin Energy Systems, Oak Ridge Natl. Lab., August 1995.

60. W. J. McAfee, B. R. Bass, J. W. Bryson, and W. E. Pennell, Lockheed Martin Energy Systems, Oak Ridge Natl. Lab., *Biaxial Loading Effects on Fracture Toughness of Reactor Pressure Vessel Steels*, USNRC Report NUREG/CR-6273 (ORNL/TM-12866), 1995.

61. T . L. Dickson, "FAVOR: A Fracture Analysis Code for Nuclear Reactor Pressure Vessels, Release 9401," ORNL/NRC/LTR/94/1, Martin Marietta Energy Systems, Inc., Oak Ridge Natl. Lab., February 1994.

62. B. R. Bass, T. L. Dickson, W. J. McAfee, and J. G. Merkle, "An Assessment of Clad Modeling Effects on Predictions of Cleavage Initiation in Embrittled Reactor Pressure Vessels Subjected to PTS Transients," ORNL/NRC/LTR-95/16, Lockheed Martin Energy Systems, Oak Ridge Natl. Lab., August 1995.

Condition Monitoring and Testing for Operability of Check Valves and Pumps*

D. A. Casada
K. L. McElhaney
Oak Ridge National Laboratory
Oak Ridge, Tennessee

Abstract

A detailed analysis of historical failure data available through the Institute of Nuclear Power Operations' Nuclear Plant Reliability Data System (NPRDS) has been conducted for both check valves and pumps. This analysis, which originated as a part of the Nuclear Regulatory Commission's (NRC) effort to evaluate the effects of age and wear on nuclear systems components, involved the manual review and characterization of several thousand component failure records according to parameters inherent in the NPRDS database and supplemented by those defined by the analyst for each component type. For example, failure information relative to component size, age, system of service, and NSSS vendor was readily available from the NPRDS database and could be compared relatively easily. Determination of parameters such as extent of degradation, affected area, and detection method, however, had to be determined based on manual review and characterization of individual failure narratives.

This paper discusses some of the results of the analyses of historical check valve failure data from 1984 through 1992 and pump failure data from 1990 through 1993. A comparison of the findings of the analyses is made, and emphasis is placed on evaluation of the effectiveness of certain failure detection methods for each component type. Generally speaking, while it was observed that check valve degradation or failure was likely to be detected by code or regulatory required testing, it was discovered that pump degradation or failure was most likely to be discovered by voluntarily implemented plant programs.

Failure rates were found to be strongly influenced by the valve or pump application. The type of plant (BWR or PWR) was also found to significantly influence both the overall failure rate and the method of failure detection.

Check Valve Studies

Background and Methodology

As a result of significant check valve failure events occurring in the mid-1980's, industry and regulatory attention was directed toward identifying and understanding check valve performance issues. One element involved in this process was the review of historical failure data. A collaborative effort among the ASME Operations & Maintenance Committee Working Group on Check Valve Performance (OM-22), NRC, and Oak Ridge National Laboratory (ORNL) involved the review of over 5000 NPRDS failure narratives for check valve failures occurring during the years 1984-1990. The resulting detailed analysis of 1227 of these failures was published in 1993 [1]. A primary goal of this study was to evaluate failure data to identify any significant correlations of failure rates with component age, plant age, or other parameters while considering the effect of the number of valves in service during the analysis period (i.e., component population effects). The study focused on failures involving degradation of valve internal parts. A "failure" was defined as a degradation of one or more valve functions (e.g., failure to open, failure to close, loose/broken parts), not in terms of any resultant system or plant effects.

Desiring to gather additional information and to identify any performance trends, the NRC requested ORNL to update the original check valve analysis for two additional study periods, 1991 and 1992. Supplemental data not available from NPRDS and therefore not included in the 1984-1990 study included data on specific valve type (e.g., swing, lift) as well as information obtained from direct utility surveys sponsored by the Nuclear Industry Check Valve Group (NIC). Results of the 1991 study were published in 1995 [2]; those for 1992 should be available soon.

* Research sponsored by the Office of Nuclear Regulatory Research, U. S. Nuclear Regulatory Commission under Interagency Agreement DOE DE-AC05-840R21400 with the U. S. Department of Energy under contract No. 1886-8632-4W with Lockheed Martin Energy Systems, Inc.

Results

Extent of degradation

One of the parameters characterized and analyzed for the check valve studies was extent of degradation. This parameter is not inherent in raw NPRDS data and therefore has to be characterized by the analyst. It is important to understand that the extent of degradation assigned is based on the loss or degradation of one or more valve functions, and not on real or potential system or plant effects. Accordingly, extent of degradation to the component was characterized as either "moderate" or "significant." Figure 1 shows the trend in check valve failure data from 1984 through 1992 according to extent of degradation. While the data from 1984-1990 indicates that more than 50% of the failures involved significant internals degradation, it is apparent that the trend is toward a decrease in the percentage of significant failures, dropping below 40% in both 1991 and 1992. It is important to note, however, that the screening process employed by ORNL to exclude failure reports from further analysis changed after the 1984-1990 study. While all the studies excluded failure reports involving no internals degradation, nonfailures, and noncheck valves, the 1991 and 1992 studies intentionally included all failures involving internal seat leakage (the 1984-1990 study excluded minor seat leakage events). This change in practice inherently resulted in more moderate type failures in the later studies, but provided a more realistic measure of the kinds of failures being reported. Results from the 1991 and subsequent analyses can therefore be compared on a more consistent basis.

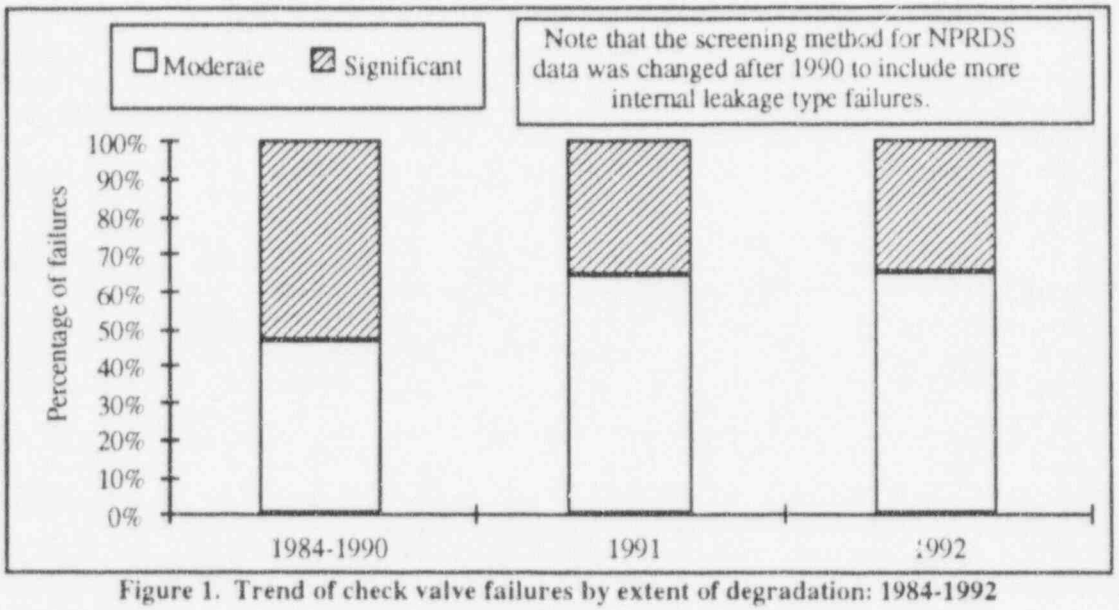

Figure 1. Trend of check valve failures by extent of degradation: 1984-1992

System

One parameter included in the NPRDS database is that of system of service. Figure 2 shows the distribution of significant 1991-1992 failures by relative failure rate for the ten systems with the highest overall failure rates during that period. (Only systems with at least 400 valve-years of service during the time period were considered.) Five systems exhibited failure rates between two and three times the overall relative failure rate. These included RCIC, suppression pool support, diesel starting air, HPCI, and main steam. It is important to recognize that many of the failures in the HPCI and suppression pool support systems involved vacuum breaker valves, and most of the failures occurring in the diesel starting air system involved lift/piston check valves that were either stuck open or stuck closed. Results from the study of 1984-1990 data were consistent with this result, indicating that ESW, feedwater, diesel starting air, and main steam systems, respectively, had the highest relative failure rates for that period.

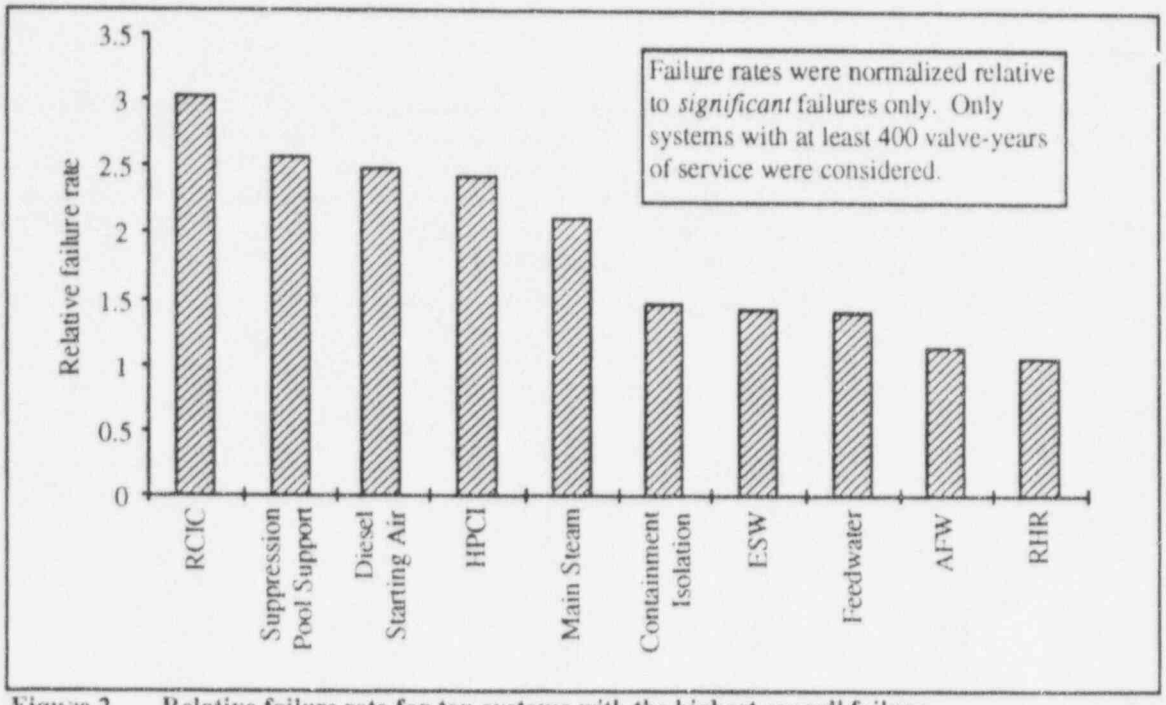

Figure 2. Relative failure rate for ten systems with the highest overall failure rates for significant 1991-1992 check valve failures

Valve size

Figure 3 shows the relative failure rate and fraction of valve population for all 1991-1992 failures by size group. Valves in the smallest group (less than or equal to 2 in.) failed at a rate about equal to the overall relative failure rate, while those in the largest group (greater than 10 in.) failed at a rate about 1.3 times that of the overall average. Those between 2 and 10 in. failed at rates below the overall average. The 1991-1992 data shows a slight increase in the relative failure rate of valves in the smallest size group compared to 1984-1990 data (not shown).

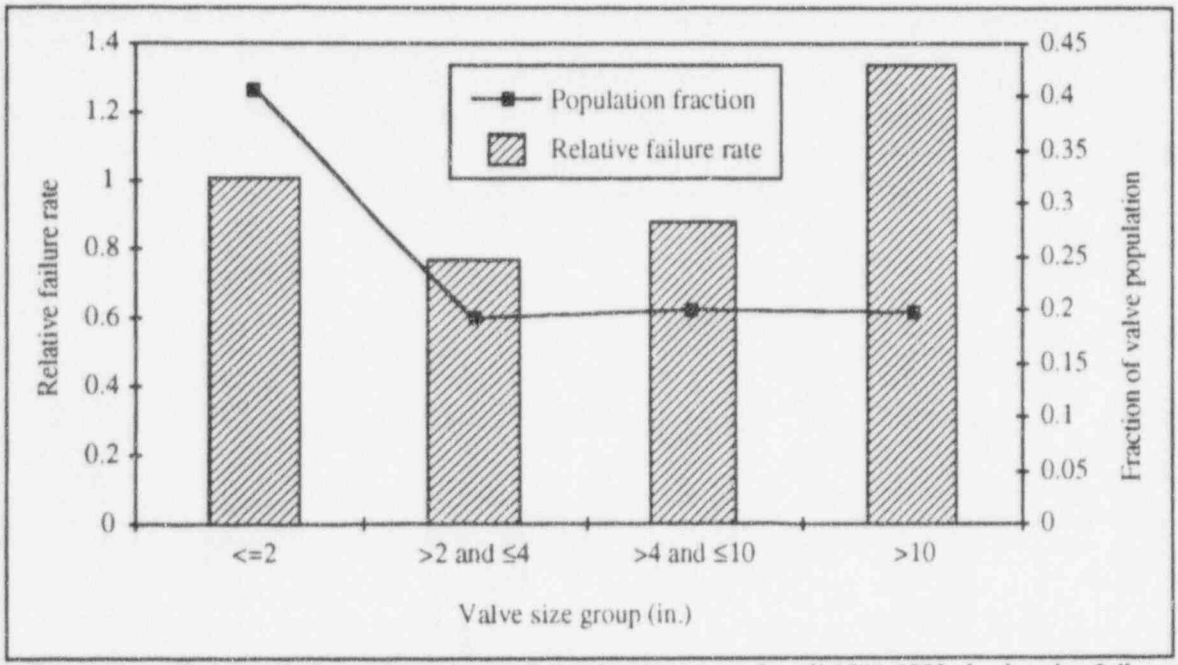

Figure 3. Relative failure rate and population by size group for all 1991-1992 check valve failures

Valve age group

In general, data from 1984 through 1992 has not shown a significant relationship between failure rate and either valve or plant age. Relative failure rate by valve age group for 1991-1992 failures is shown in Fig. 4. As can be seen, no appreciable differences in relative failure rates according to component age are apparent; however, a slight increase is noted from less than 5 years of age to 15 years of age. These results are consistent with those of the 1984-1990 analysis. The greater than 20 year age group shows the highest relative failure rate, at just over 1.2. Data for this age group was not available for the 1984-1990 study, due to the younger age of many plants.

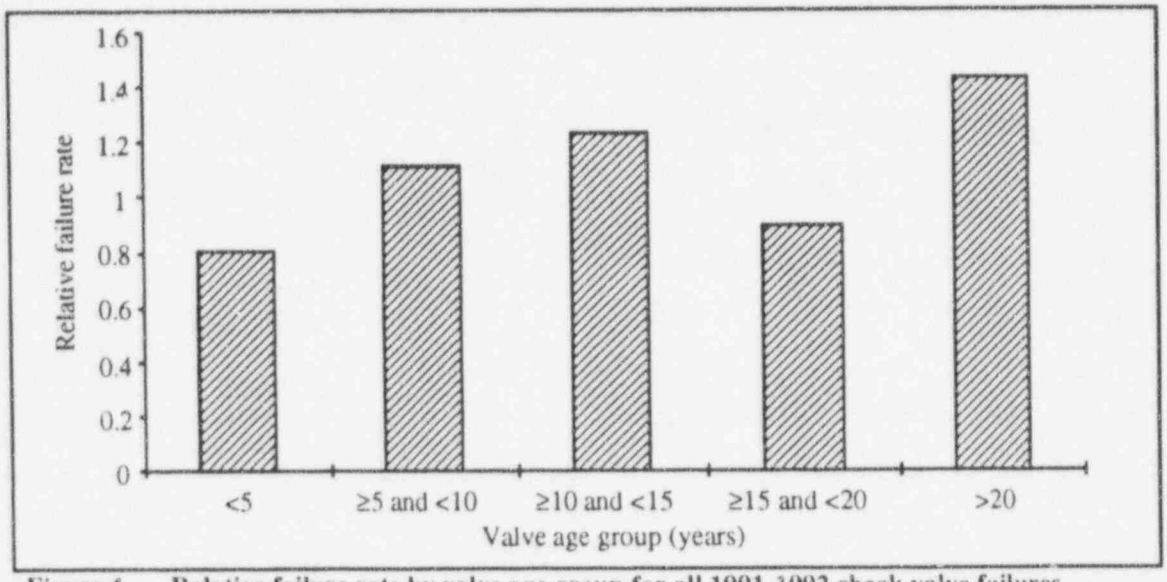

Figure 4. Relative failure rate by valve age group for all 1991-1992 check valve failures

NSSS and plant type

For 1991-1992 failures, Fig. 5 shows the relative failure rate and population by NSSS, while Fig. 6 shows relative failure rate by plant type. From both figures, it is apparent that the higher relative failure rates occur in BWR plants. This finding is consistent with 1984-1990 data. Although it is not certain why this trend continues, it has been theorized that more failures may have been discovered in BWRs than in PWRs due to the BWR plants' practice of leak testing more valves and including more valves in inservice testing programs. Further cross-correlation of the data has shown that BWR plants have a much higher fraction of failures detected programmatically than do PWRs, a result which may substantiate the theory.

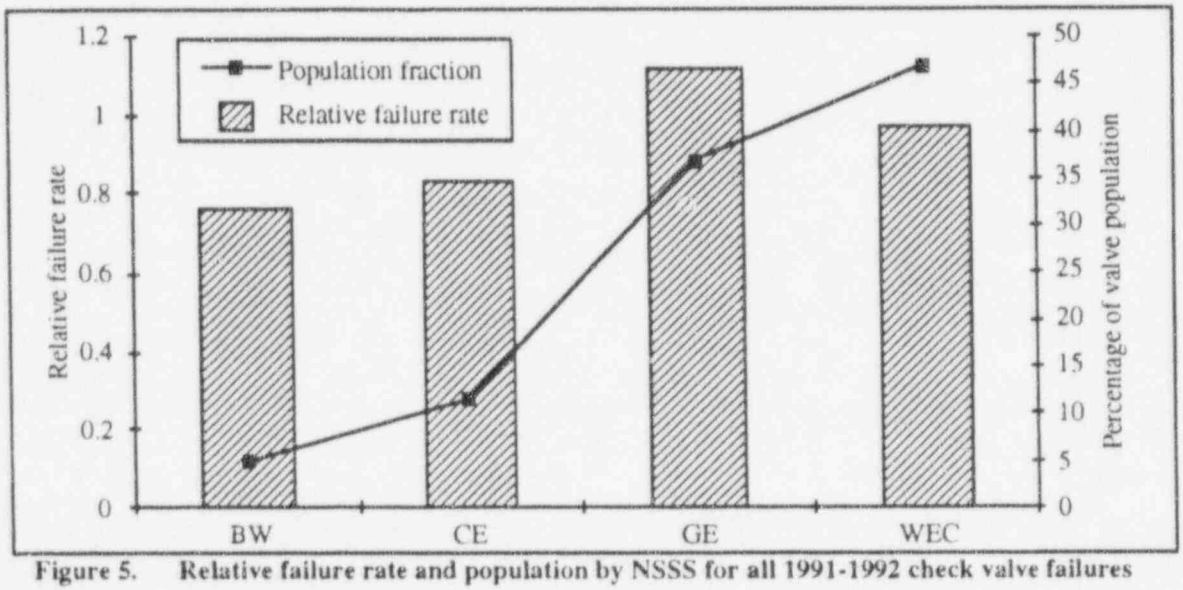

Figure 5. Relative failure rate and population by NSSS for all 1991-1992 check valve failures

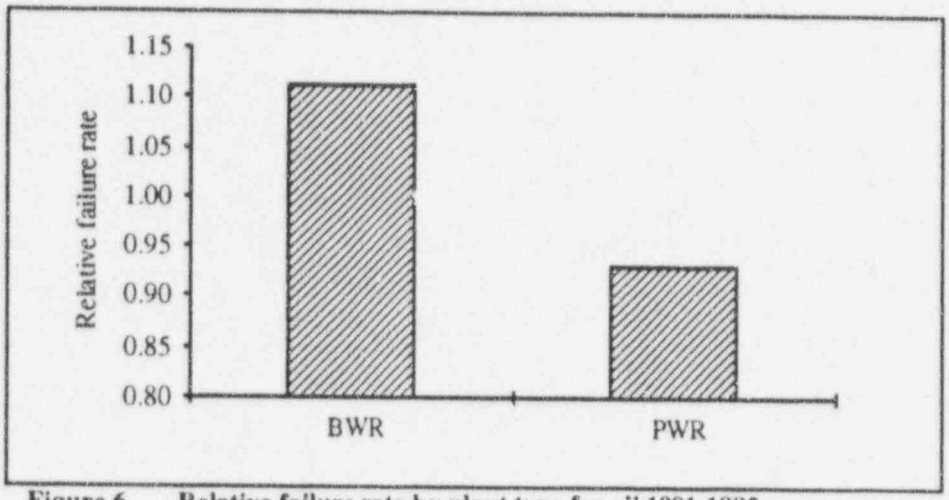

Figure 6. Relative failure rate by plant type for all 1991-1992 check valve failures

Method of detection

Figures 7, 8, and 9 show, in absolute number of failures, the distribution of failures by method of detection. Figure 7 plots the significant failures occurring from 1984 through 1992 by method of detection, Fig. 8 plots the same data for 1991-1992 only, and Fig. 9 shows all 1991-1992 failures. The method of detection for the check valve analyses was defined as either "programmatic" or "nonprogrammatic." Check valve failures detected "programmatically" included those observed during the conduct of some code or regulatory required function, such as a surveillance test, inservice inspection or test, leak test, or periodic preventive maintenance. Those detected "nonprogrammatically" were those detected during routine or incidental observation, by abnormal equipment operation, during special inspection, or where the detection method was unclear from the failure narrative.

While the number of significant failures detected programmatically from 1984 through 1992 was only slightly greater than those detected by nonprogrammatic means (522 to 427), it is encouraging that in the later years, the programmatically detected failures dominated. For significant 1991-1992 failures, 221 failures were detected programmatically vs only 74 by nonprogrammatic means. And as shown in Fig. 9 for all (i.e., including both significant and moderate categories) 1991-1992 failures, the ratio is even greater: 654 failures detected programmatically to just 184 detected by other means. The data suggest that in the more recent years the increased attention given to ensure check valve operability has resulted in significant improvements in failure detection by programmatic means.

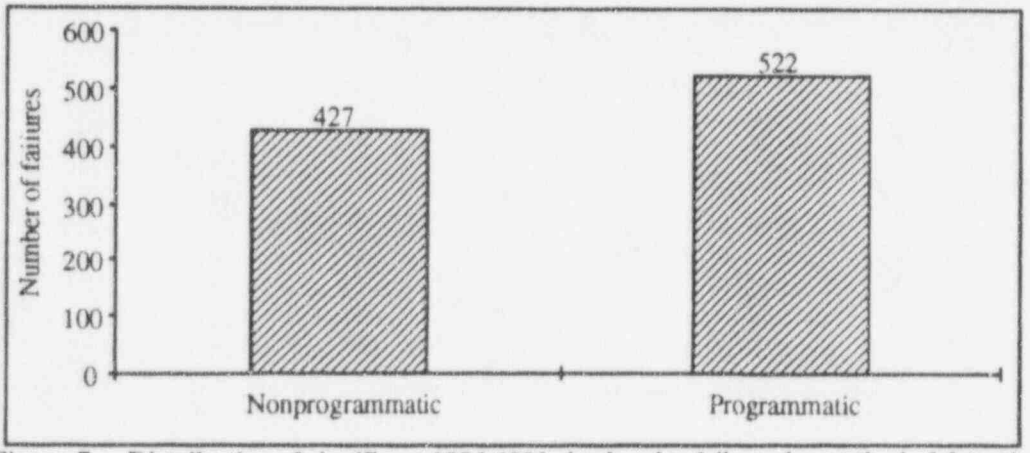

Figure 7. Distribution of significant 1984-1992 check valve failures by method of detection

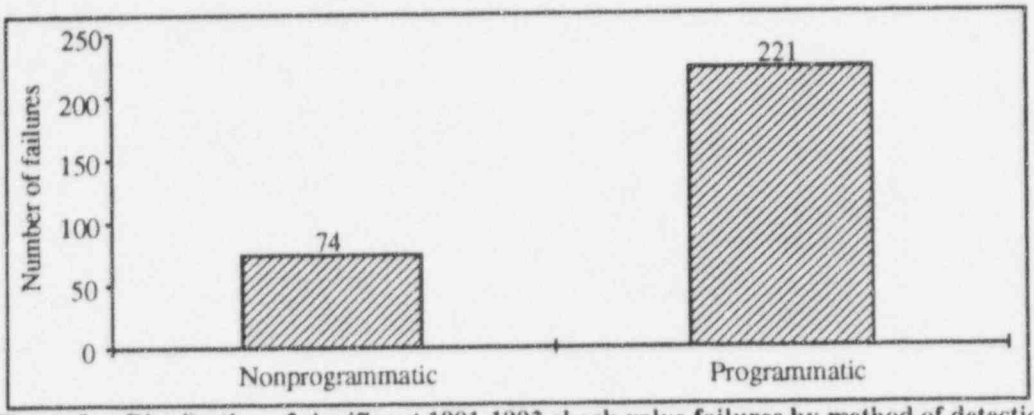

Figure 8. Distribution of significant 1991-1992 check valve failures by method of detection

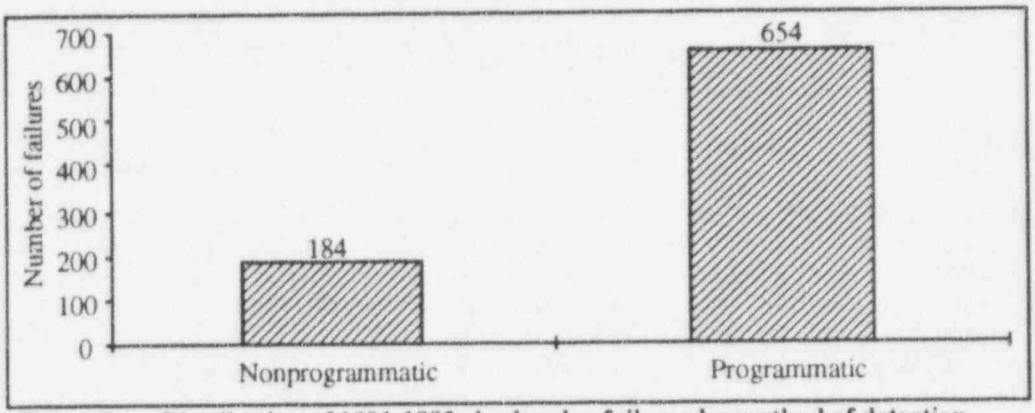

Figure 9. Distribution of 1991-1992 check valve failures by method of detection

Affected area

Another cross-correlation of interest is that of discovery process and affected area. Figure 10 plots 1991-1992 check valve failures by affected area and general discovery process. From this chart it is apparent that the dominant method of detection, irrespective of affected area, has been programmatic. Figure 11 replots the same information without programmatically detected failures so that the relationship between other general detection methods versus failure area is clarified. It is interesting to note that a large fraction of failures involving all areas (except those where general wear is cited) were detected by routine observation. Except for programmatically detected failures, the highest fraction of failures involving the hinge pin area were detected by abnormal equipment operation.

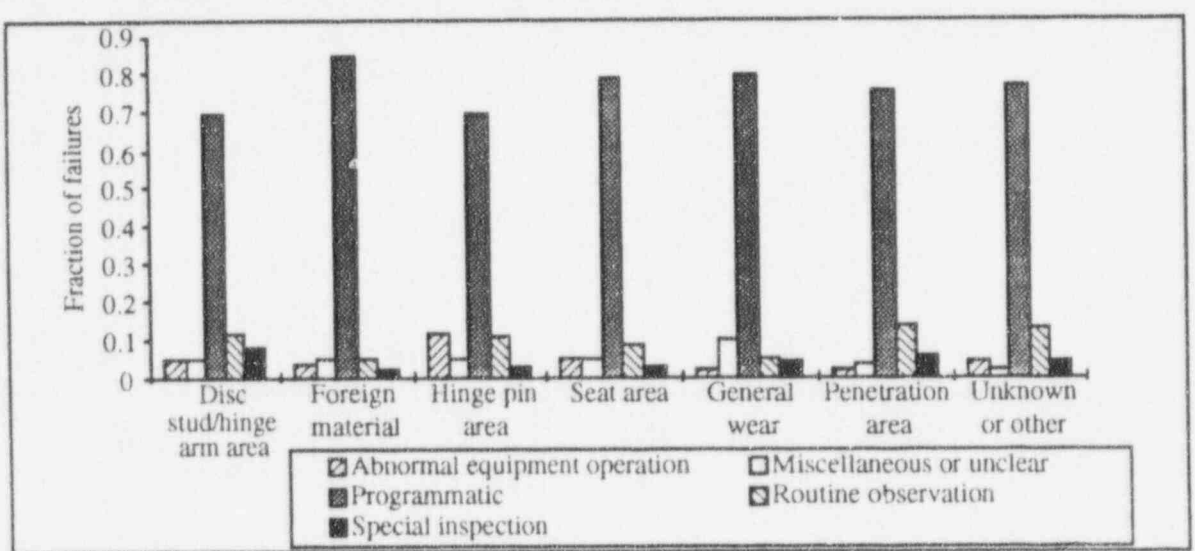

Figure 10. Distribution of 1991-1992 check valve failures by affected area and general discovery process

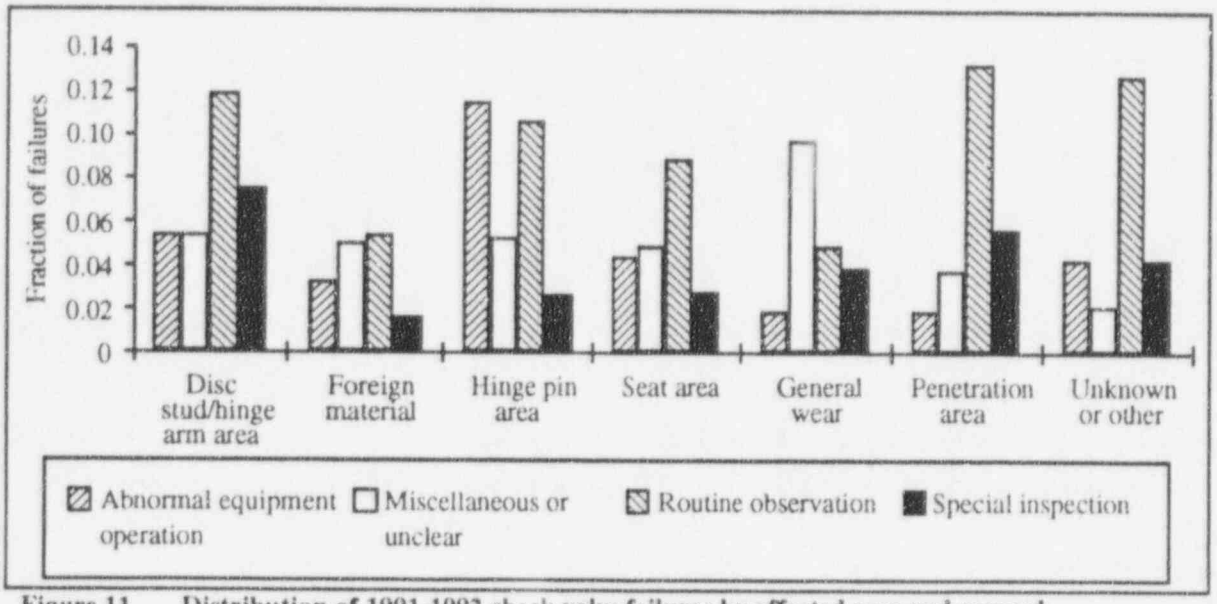

Figure 11. Distribution of 1991-1992 check valve failures by affected area and general discovery process (without programmatically detected failures)

Figure 12 again plots 1991-1992 failures by affected area and general discovery process, but this time only failures that were judged to be significant in terms of extent of degradation are included. Again, the dominant method of detection for all areas was programmatic. Figure 13 replots the same data without programmatically detected failures for clarification. It is interesting to note that for the disc stud/hinge arm, foreign material, hinge pin, and seat areas, many of the failures not detected programmatically were found by abnormal equipment operation.

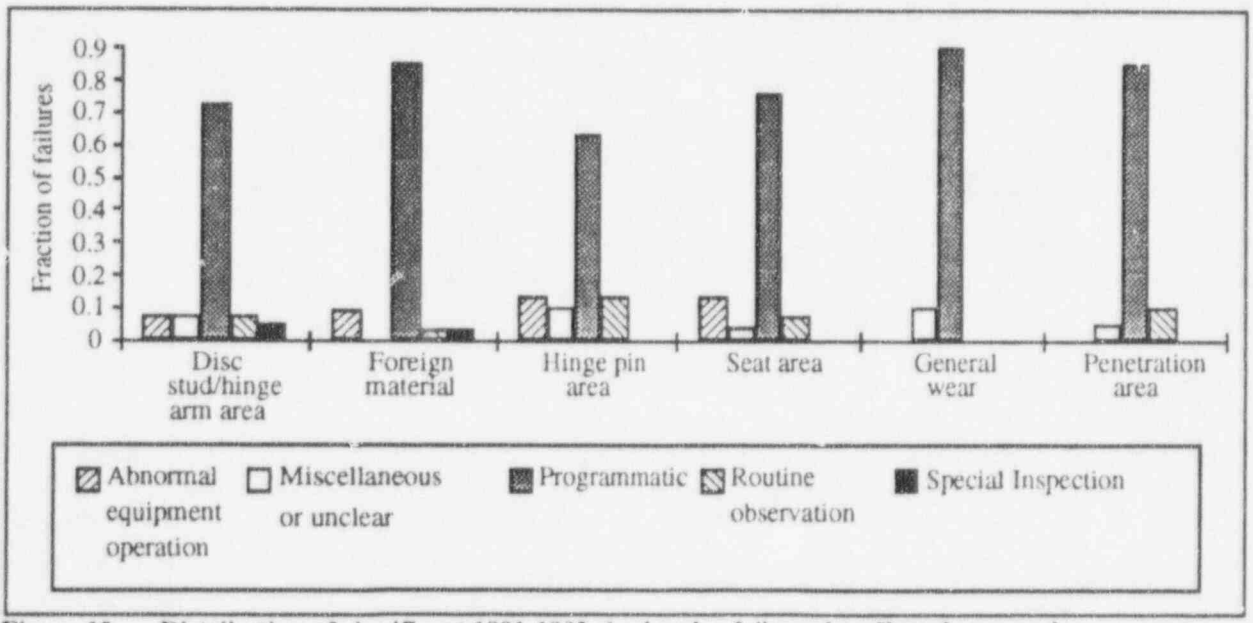

Figure 12. Distribution of significant 1991-1992 check valve failures by affected area and general discovery process

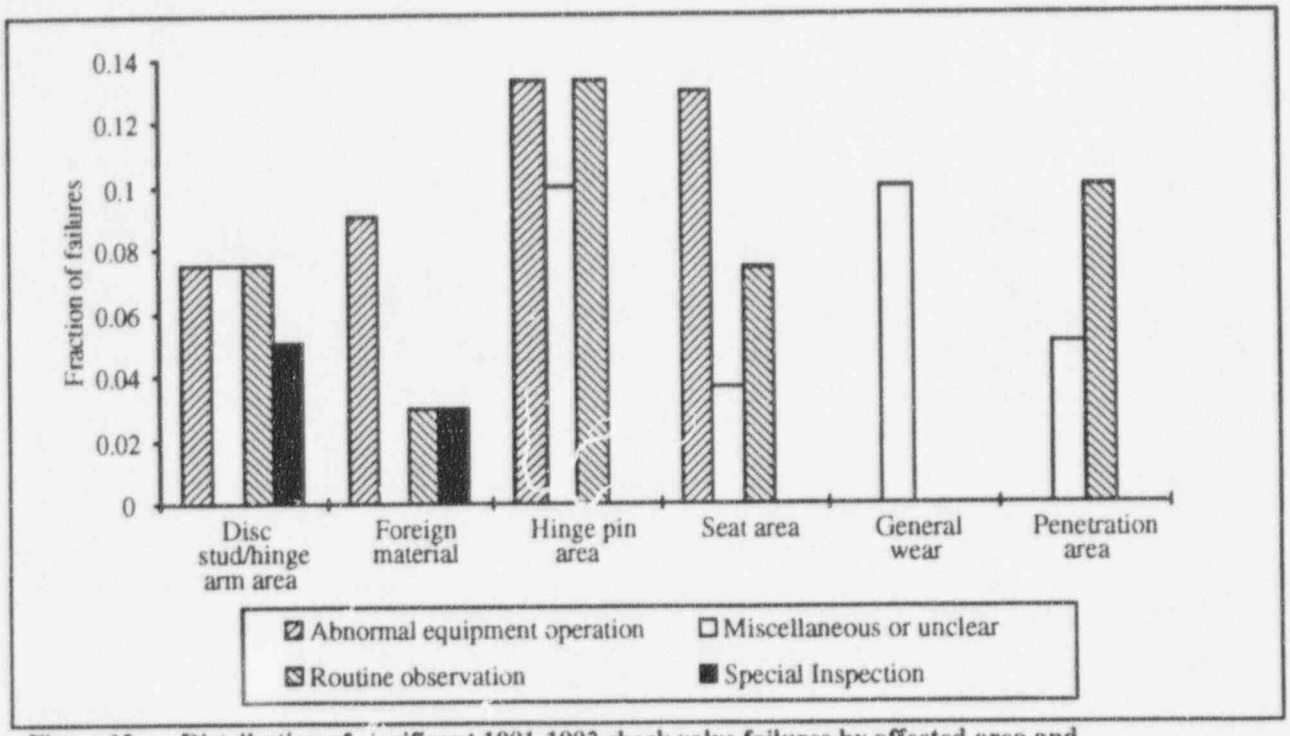

Figure 13. Distribution of significant 1991-1992 check valve failures by affected area and general discovery process (without programmatically detected failures)

Pump Study

Background and Methodology

Although the design and normal operating functions of fluid systems used at current generation reactors are diverse, almost all normally operating and standby fluid systems share the common feature of depending upon pumps to provide motive power for the process fluid. Malfunctions of other components, such as valves, instrumentation, controls, motors, and power supplies can often be minimized or overcome by human intervention. In the case of pumps and their drivers, however, many failures cannot be dealt with by manual interaction.

Recognizing the importance of reliable pump operation in these systems, ORNL undertook a study of pump failure data available from NPRDS. The pump study used, as closely as possible, the same methodology applied to evaluate check valve failures. The differences in methodology that should be noted are:

(1) The check valve studies evaluated all check valve failures. The pump study was limited to specific pump and pump motor applications.

(2) Due to fundamental differences in failure modes and their significance, the extent of degradation categories for pumps were different than those applied to check valves. (For purposes of this paper, however, pump failures are divided into "significant" failures and all failures.)

(3) The study periods for the two types of components were different.

Results

The pump failure data review [3] studied and characterized failures occurring in the years 1990-1993 of centrifugal pumps and used in safety-related service in several critical systems at BWR and PWR plants. The systems included are identified in Table 1.

Table 1. Systems included in the pump failure study

PWR plants	BWR plants
• Auxiliary feedwater (AFW)	• Component cooling water (CCW)
• Component cooling water (CCW)	• High pressure coolant injection (HPCI)
• Containment spray (Cont. spray)	• Emergency service water (ESW)
• Charging/high pressure safety injection (CVCS/HPSI)	• Low pressure core spray (LPCS)
• Emergency service water (ESW)	• Reactor core isolation cooling (RCIC)
• Low pressure safety injection/residual heat removal (RHR)	• Low pressure coolant injection/residual heat removal (RHR)

In addition to studying the failures of the pumps themselves, the failures of motor drives used for these pump applications were studied. Non-motor drives (turbines used on AFW, RCIC, and HPCI pumps) were not included because of previous studies of the experience with turbine drives [3, 4, 5].

A total of 7210 pump-years of experience was accumulated by the studied pumps during the 1990-1993 period (2405 at BWRs and 4805 at PWRs). There were 797 failures of the studied pumps and 143 failures of the associated motors reported to the NPRDS database during the period.

Extent of Degradation

Although the fundamental characterization of failures by extent of degradation for pumps was done at a slightly greater level of resolution than for check valves, the failures are segregated here into two categories -- all failures and significant failures only. Those failures that are classed as significant are those for which the pump either would not operate at all, would not operate to the level required to perform its safety function, or was operating at a degraded level with near-term continued operation in jeopardy.

The reported failure rates and the distribution of all pump and motor failures by extent of degradation for BWR and PWR plants is shown in Figure 14. It should be emphasized that although the rates are shown in absolute terms, the authors strongly discourage blindly using these failure rate values for other purposes without considering other factors such as reporting practices and recovery time.

There were clearly more pump than motor failures (more than 5 times as many, considering all failures). However, there were only 3 times as many pump failures compared to motor failures for those failures classed as significant. This is an important finding, since the existing ASME Code test requirements for pumps [7] do not explicitly address motor monitoring. ASME Working Group OM-6 (charged with responsibility for pump test requirements) is beginning to consider the merits of specifically incorporating motor testing into the Code. While there are other factors to be considered, such as the practicality of periodic motor testing and whether periodic inservice testing or monitoring would be effective at detecting motor degradation prior to failure, the failure data clearly indicate that motors are an important factor in overall pump drive train reliability.

Another finding of particular interest is that although motor failure rates for BWR and PWR units are similar, the pump failure rate for PWRs is approximately double that of BWR units. This was found to be true for all failures and significant failures only.

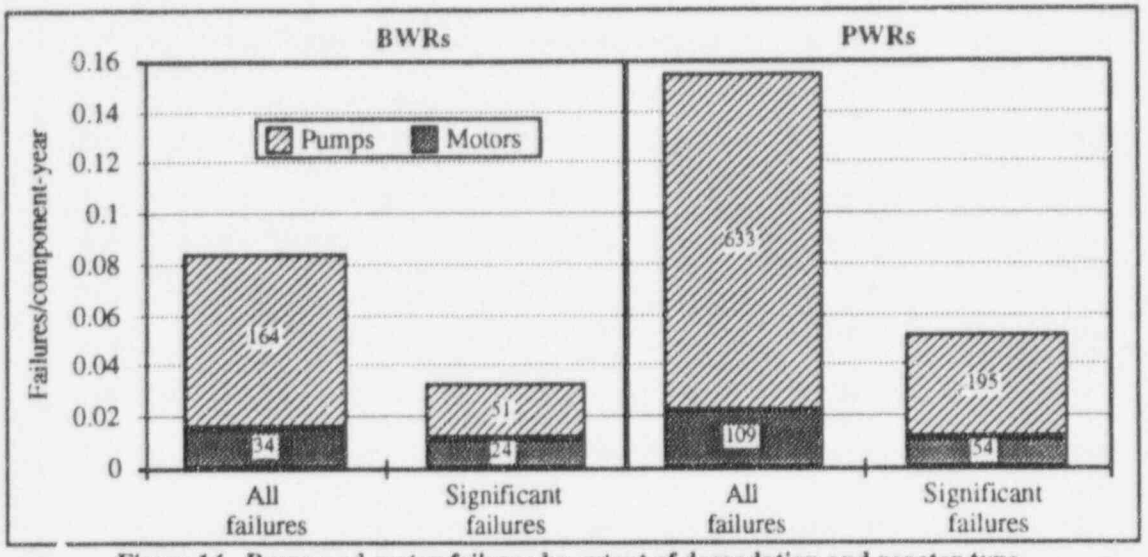

Figure 14. Pump and motor failures by extent of degradation and reactor type.

System

The system in which pumps are used was found to be an important factor in regards to both failure rate and mode. Figure 15 shows the absolute failure rates for pumps and motors by system for BWR and PWR plants. Some features of particular note are:

- ESW pumps and motors at both plant types have substantially higher overall failure rates. The failure rates for significant failures in ESW are almost three times those of the next closest system (CCW) at BWRs, almost twice that of the next highest system at PWRs (AFW).
- The failure rate for BWR system pumps is strongly related to the system usage. For example, normally operating systems (such as ESW and CCW) have higher failure rates than do systems that are occasionally used (such as RHR and RCIC), which in turn have higher failure rates than systems whose primary usage is for testing (HPCI and LPCS).
- In general, the same system usage effect appears in the PWR data. The primary exception is AFW, which has both an overall and significant failure rate that is comparable to those of CCW and CVCS/HPSI. Note that the CVCS/HPSI data represents a mixture—at some plants, the HPSI pumps are used solely for testing or emergency response, while at others, they serve the dual function of charging. Thus, the actual usage of CVCS/HPSI pumps can be at either extreme.

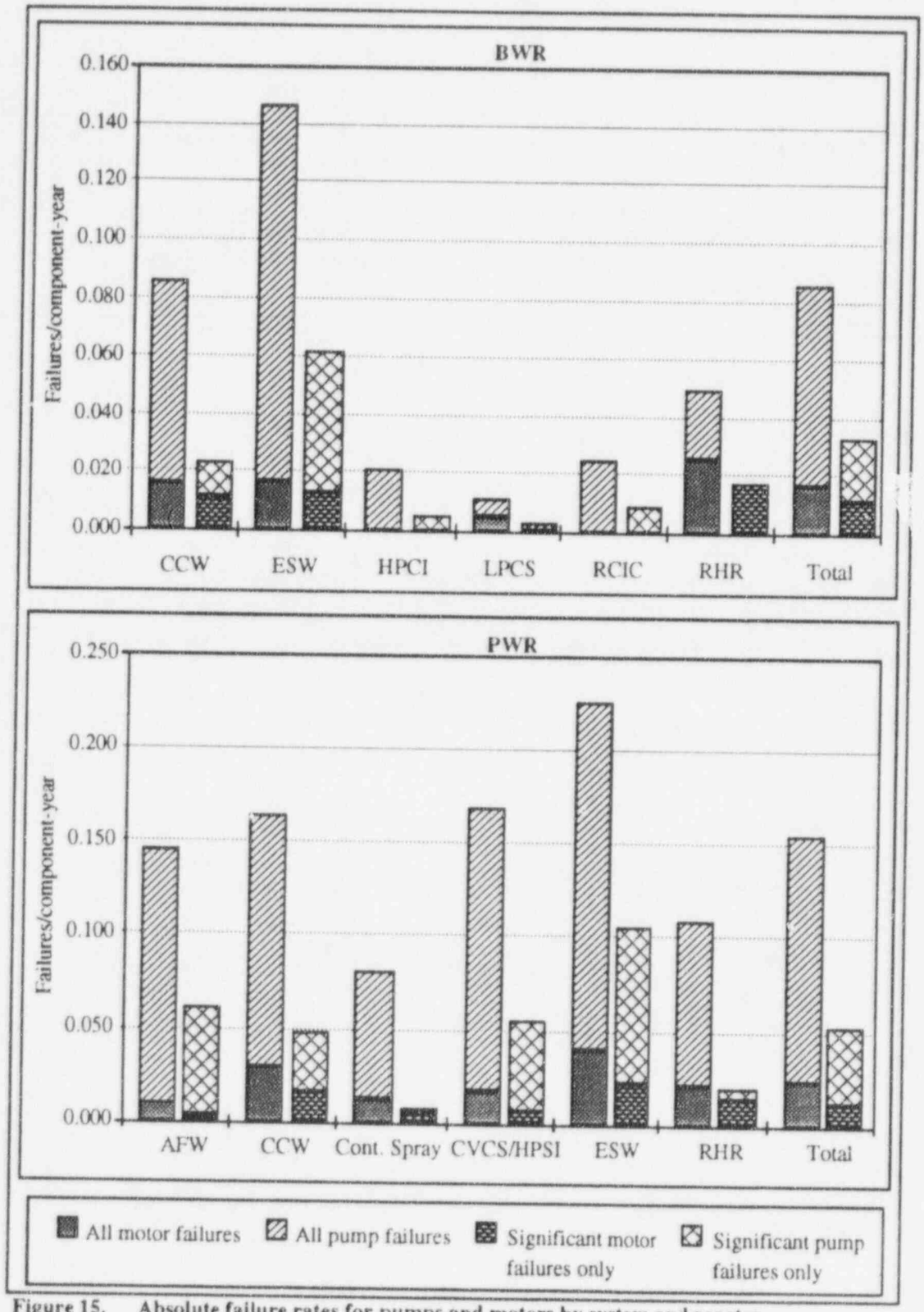

Figure 15. **Absolute failure rates for pumps and motors by system and reactor type. Note that the y-axis scaling is different for the two graphs.**

Age Group

The relative failure rate as a function of component age for all pumps (motors not included) at BWR and PWR plants is shown is Figure 16. For the BWR plants, there is a clear age-related trend in that the failure rate drops significantly after a period of infant mortality. The same trend appears to occur, to a lesser extent, for the PWR plants in the transition from <5 to ≥5 and <10 year group, but then reverses in subsequent age groups. For the significant failures only, the PWR plant failure rate trend as a function of age group resembles the classical "bath tub" shape.

The fact that BWR plants have had better experience than PWR plants is clearly illustrated in this Figure 17, where the ratio of PWR to BWR failure rates as a function of age group for significant failures is shown. During the early years of operation, the performance of pumps at BWR and PWR units is similar. But over time, the failure rate relationship changes dramatically.

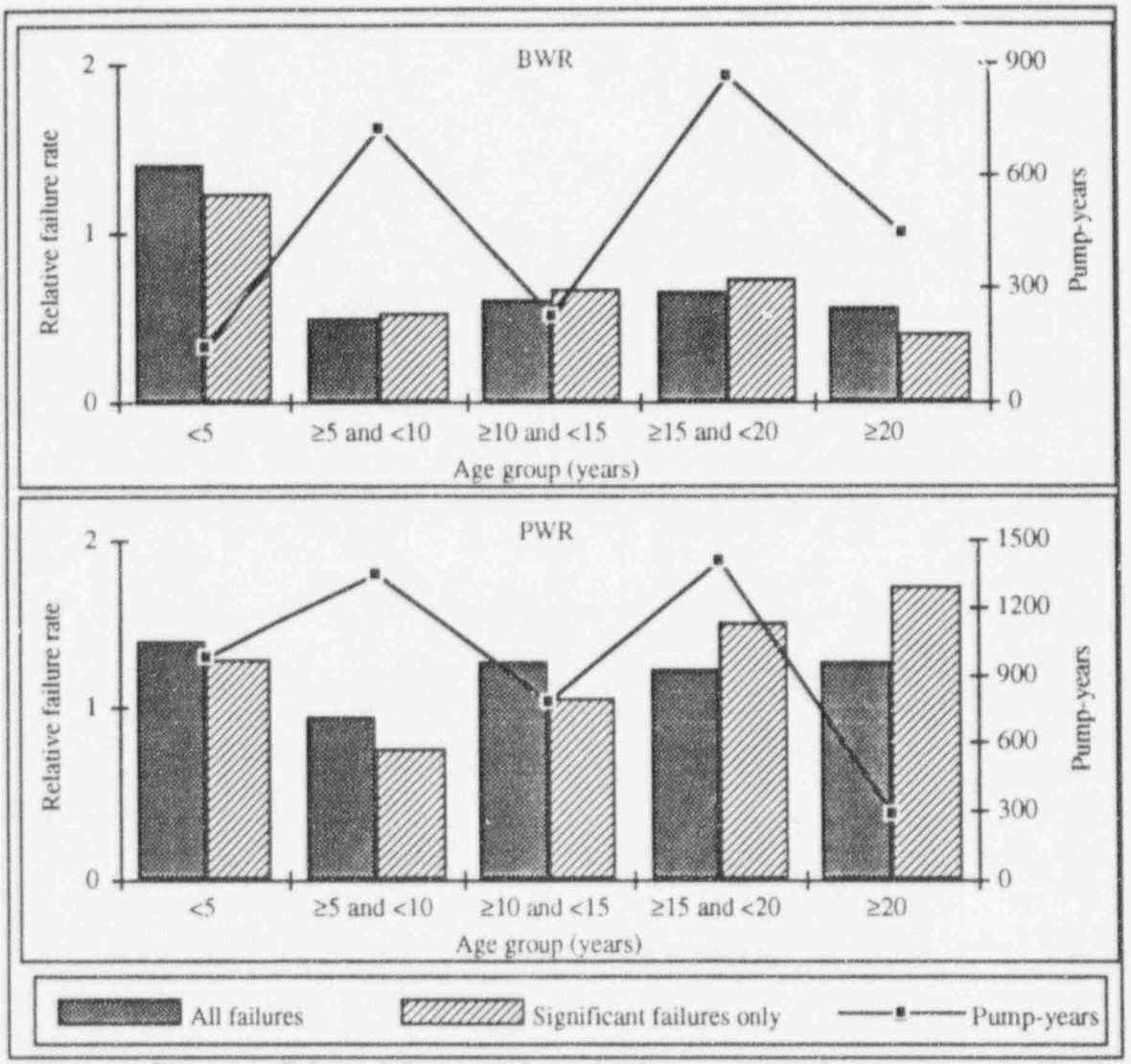

Figure 16. Relative failure rates for pumps by age group and reactor type.

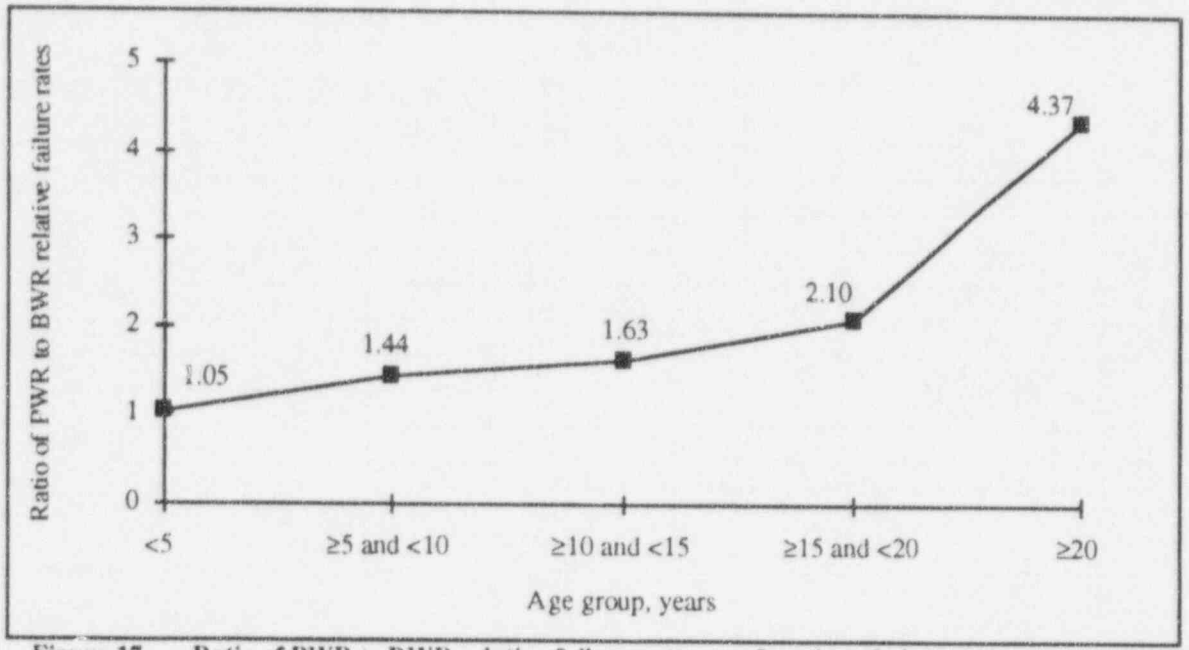

Figure 17. Ratio of PWR to BWR relative failure rates as a function of plant age for significant failures

Affected area

All failures were characterized by the affected area. Table 2 presents the numbers of failures by extent of degradation and reactor type and a comparison of the normalized failure rates at BWR and PWR plants. It is notable that PWR pumps had higher failure rates in all areas than BWR pumps (excluding the "Unknown" category).

Table 2. Pump failures by affected area and reactor type

Affected area	All failures		Significant failures only		PWR to BWR failure rate (significant failures)
	BWR	PWR	BWR	PWR	
Alignment/balance	2	5	1	3	1.50
Bearing	23	133	18	74	2.06
Shaft, coupling, keys	8	19	6	18	1.50
Internals	26	77	22	69	1.57
Oil leak	13	11	0	0	N/A
Other	14	133	4	14	1.75
Seal/packing	87	280	5	40	4.00
Unknown	2	2	2	2	0.50
Total	633	164	54	195	1.91

Tables 3 and 4 tabulate the numbers of significant failures by affected area and system for PWR and BWR plants. Of 69 significant failures involving internals, 49 were in ESW pumps; 12 of 18 shaft/coupling/key failures occurred in ESW pumps. However, only 12 of 74 significant failures in which a bearing was affected involved ESW pumps.

Table 3. Number of PWR pump failures by affected area and system (significant failures only)

Affected area code	AFW	CCW	Cont. Spray	CVCS/ HPSI	ESW	RHR	Total
Alignment/balance	2	0	0	1	0	0	3
Bearing	14	22	2	22	12	2	74
Shaft, coupling, keys	0	2	0	4	12	0	18
Internals	6	5	0	9	49	0	69
Oil leak	0	0	0	0	0	0	0
Other	7	0	0	6	1	0	14
Seal/packing	15	7	1	7	8	2	40
Unknown	0	0	0	0	2	0	2
Total	42	26	2	44	77	4	195

Table 4. Number of BWR pump failures by affected area and system (significant failures only)

Affected area code	CCW	ESW	HPCI	LPCS	RCIC	RHR	Total
Alignment/balance	0	1	0	0	0	0	1
Bearing	3	13	1	0	1	0	18
Shaft, coupling, keys	0	6	0	0	0	0	6
Internals	0	22	0	0	0	0	22
Oil leak	0	0	0	0	0	0	0
Other	0	4	0	0	0	0	4
Seal/packing	0	5	0	0	0	0	5
Unknown	0	2	0	0	0	0	2
Total	3	46	1	0	1	0	51

Method of detection

While the check valve failure studies classified failures by two general detection method classifications, three general methods of detection were used for pumps – regulatory/code, plant programmatic, and nonprogrammatic. Failures included under the regulatory/code category were those that were detected during regulatory/code required testing by means prescribed by the ASME Code. The failures detected by plant programmatic means are those that were detected by plant programs that are routinely implemented, but not mandated by regulation. Failures detected by the third category, nonprogrammatic, are those that were detected by neither of the other two methods.

This deviation from the classification used in the check valve studies (i.e., adding the plant programmatic category) came in part from the observation that a significant number of failures were detected by plant programmatic means not implemented as a part of a regulatorily mandated surveillance test. But more significantly, the change in classification was prompted by the simple recognition that many pump failures manifest themselves by means that allow detection by human senses - sight, smell, sound, and touch. Check valve failures, other than those involving external leakage (which were explicitly excluded from the studies) do not lend themselves to such detection means. Some of the plant programmatically detected failures were found during the process of preparing for or conducting regulatorily required testing, but were noted not because of the regulation or code criteria, but because of good practices and observation patterns of utility employees.

Figures 18-20 show the numbers of failures by detection means for all failures (Fig. 18), all failures except those involving only seal or packing leakage (Fig. 19), and significant failures only (Fig. 20). Although many of the failures detected by plant programmatic means involved seal or packing leakage only where visual observation was the specific means of detection, Figures 19 and 20 indicate that plant programmatic means were also the leading means for detecting other failures.

Figure 21 illustrates the distribution of significant failures by detection means and affected area for three critical areas. The number of failures for each category is shown at the top of each chart column. Over five times as many bearing problems

at PWR plants were detected by plant programmatic means than by regulatory/code testing. Further review of these bearing failures detected by plant programmatic means indicated that the principal ways of detecting the problems were routine oil monitoring (either sampling or simple visual observation) and operators noticing hot or noisy/excessively vibrating bearings. Of the 10 failures involving bearings at PWRs in which regulatory/code monitoring was employed, 5 were detected by elevated temperature (for which monitoring is not required in the more recent versions of the Code), 1 by failure to start, and only 4 by vibration.

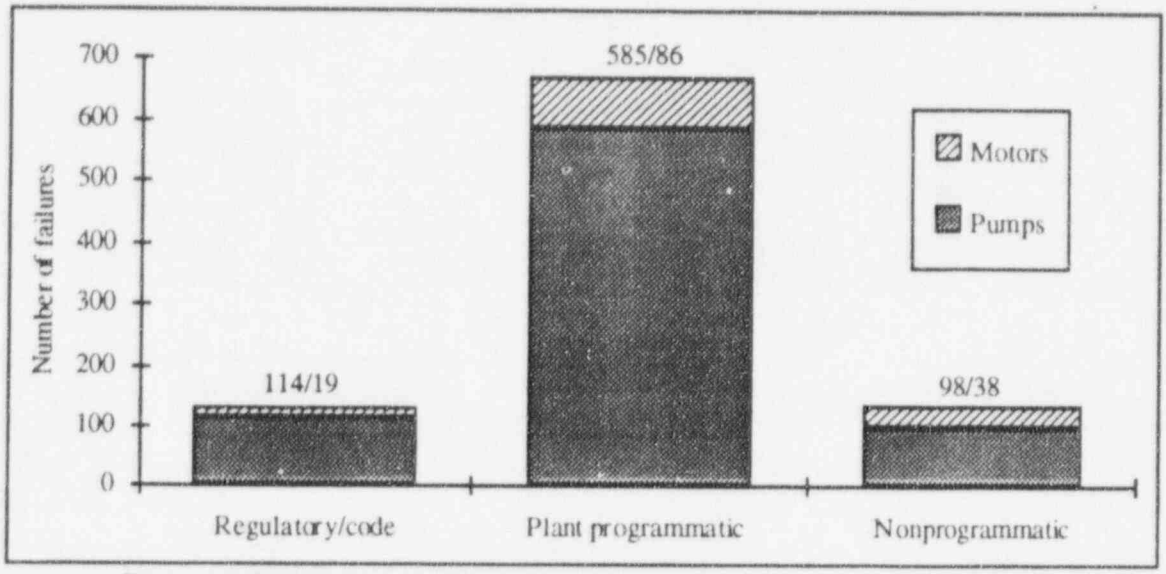

Figure 18. Distribution of failures by general method of detection (all failures).

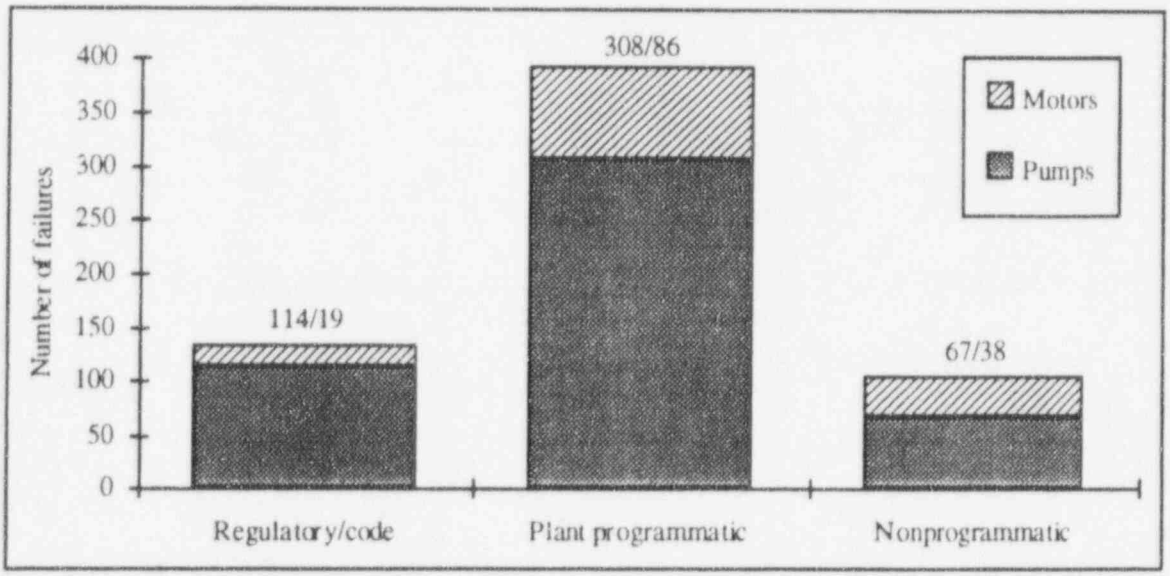

Figure 19. Distribution of failures by general method of detection (seal failures excluded).

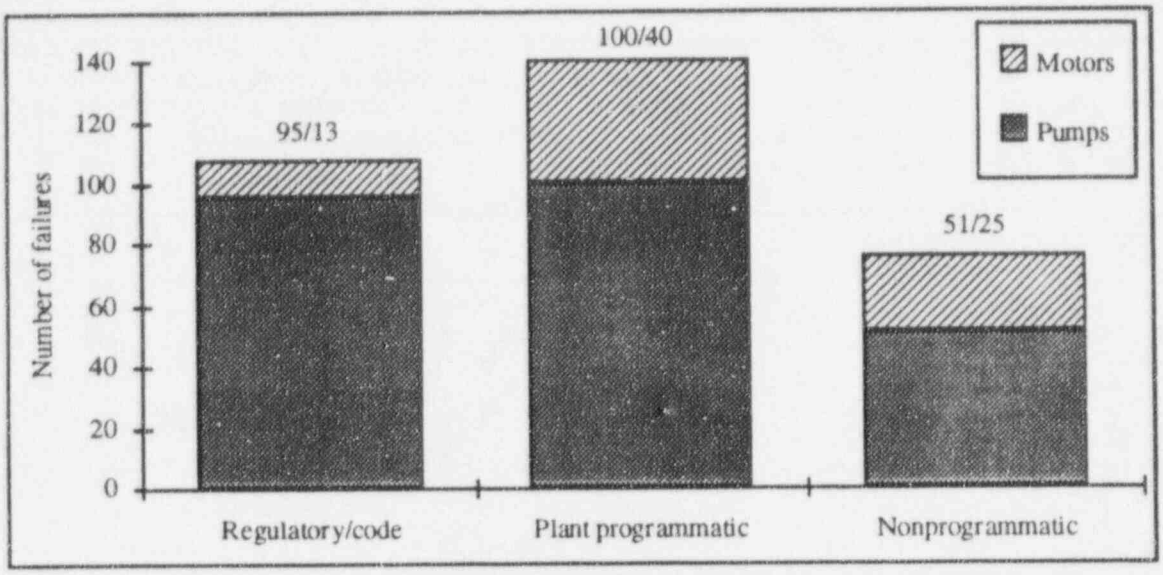

Figure 20. Distribution of failures by general method of detection (significant failures only).

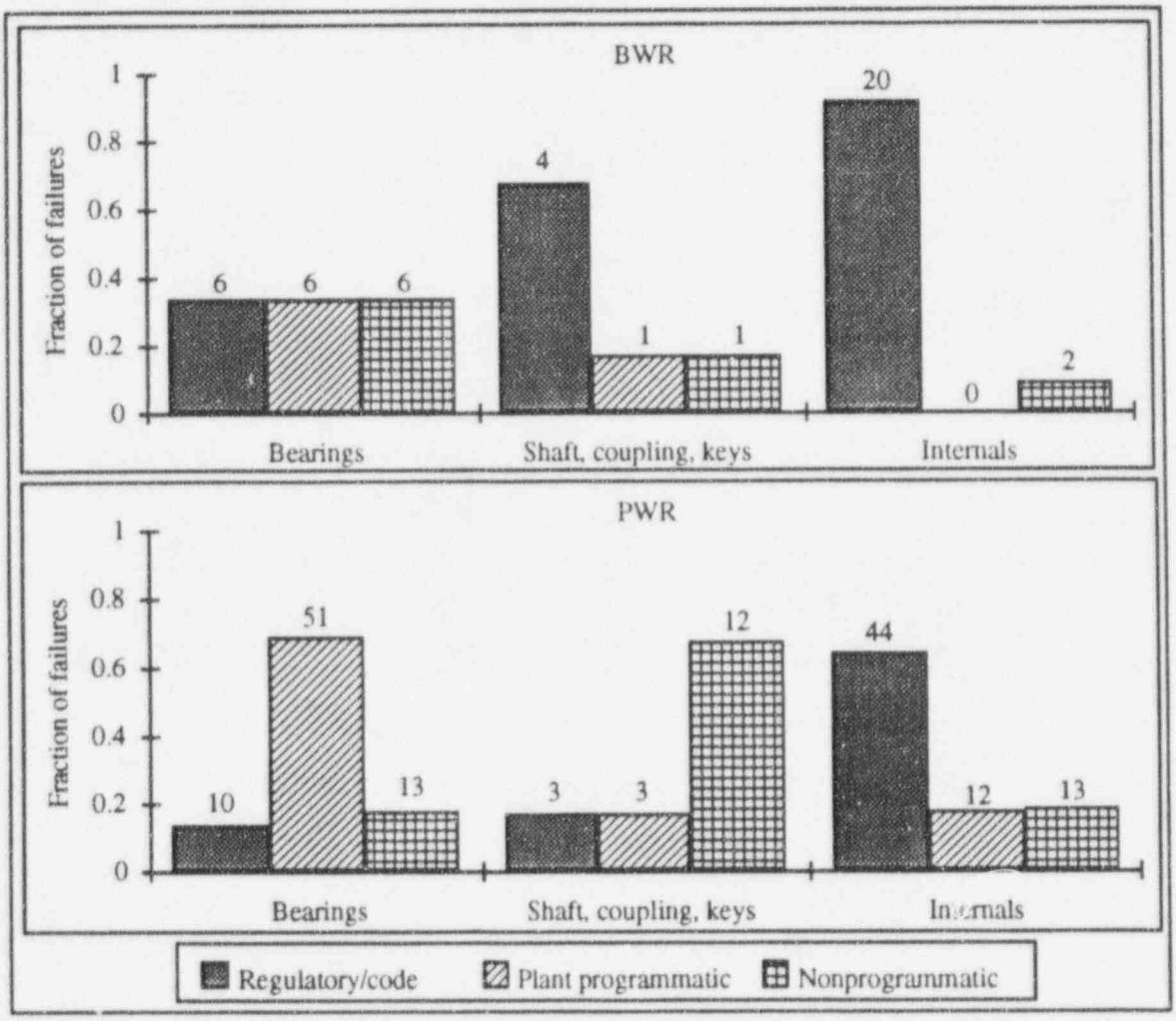

Figure 21. Distribution of significant pump failures by affected area and method of detection.

Tables 5 and 6 show the distribution of significant pump failures by system and detection process. Systems that are not included in these tables had no significant level failures.

Table 5. Distribution of significant PWR pump failures by system and detection process

General detection process	AFW	CCW	Cont. Spray	CVCS/ HPSI	ESW	RHR	Total
Regulatory/code	11	2	1	4	45	0	63
Plant programmatic	27	21	1	25	12	3	89
Nonprogrammatic	4	3	0	15	20	1	43
Total	42	26	2	44	77	4	195

Table 6. Distribution of significant BWR pump failures by system and detection process

General detection process	CCW	ESW	HPCI	RCIC	Total
Regulatory/code	0	30	1	1	32
Plant programmatic	2	9	0	0	11
Nonprogrammatic	1	7	0	0	8
Total	3	46	1	1	51

From the information shown in these tables and further review of the data, several particularly useful insights into the effectiveness of monitoring practices were gained:

- As was shown previously, ESW pumps had the highest failure rates of any of the systems studied. ESW pumps were an even more important contributor for those failures detected by regulatory/code mandated means. There were 95 significant level pump failures detected by regulatory/code mandated testing; 75 were in the ESW system. Of these 75 ESW pump failures, 61 involved internals wear; thus, almost two-thirds of all regulatory/code detected pump failures (for significant level failures) were associated with degradation of ESW pump internals.
- Of the 95 regulatory/code detected failures, 32 occurred at BWR plants. Of the 32 BWR failures, 30 were in the ESW system; 20 of the 30 ESW failures involved internals degradation.
- Of the 63 pump failures detected by regulatory/code required monitoring at PWR plants, 45 occurred in the ESW system. Of these 45 ESW pump failures at PWR plants, 41 involved internals degradation.
- Summarizing the last two bullet items, almost two-thirds (61 of 95) of the failures detected by regulatory/code required monitoring involved internals degradation of ESW pumps.
- Further review of these failures showed that 39 of the 95 regulatory/code detected pump failures were in ESW pumps at only five units. Thus, over 40% of all significant pump failures detected by regulatory/code required testing were found in one system at five units. The primary factor in the higher failure rates at these units was the quality of water being pumped (either high silt levels or foreign material presence).
- The distribution of failures detected by plant programmatic means at PWR units was decidedly more evenly distributed, with approximately equal fractions coming from four systems: AFW, CCW, ESW, and CVCS/HPSI.
- A total of 51 significant pump failures occurred at BWR units. Of these 51 failures, 46 (90%) involved ESW pumps. In contrast, 77 of the 195 significant PWR pump failures (40%) involved ESW pumps.
- Of the pump failures detected by regulatory/code testing, 83% (5 out of every 6) were classified as significant (i.e., level 4 or 5). This is not unexpected, since most failures thus reported fall into the required action range. Those failures that were not classified as significant either involved some increased vibration level (which was not deemed excessive by conventional criteria) or were nuisance type reports (for example, a pump delivered 24 gpm instead of the required 25 gpm under recirculation conditions).
- Only 17% of the significant bearing failures were detected by regulatory/code testing; almost 2/3 of the significant bearing failures were detected by plant programmatic means.

Summary

Although the check valve and pump studies differed somewhat in their approaches, some general comparisons can be made with regard to certain of their common parameters:

Extent of degradation

Although there were over five times the number of pump failures than motor failures, only three times as many pump failures as motor failures were classified as significant. In absolute terms, the percentage of significant component failures is about equal for pumps/motors from 1990-1993 (considering all plants) and for check valves during 1991 and 1992 - about 35%. Also, the percentage of significant component failures during this period was slightly higher for BWRs than for PWRs; about 38% versus 34% for both pumps/motors and check valves. It is important to note here that the system effects of significant check valve failures and significant pump/motor failures are normally dramatically different. For example, when a significant pump or motor failure occurs, one train of a system is typically lost until repairs can be made. On the other hand, even when a check valve sticks open (the most common significant failure mode), the system effect is negligible in many cases and can be dealt with by human intervention in most others.

System

Failure rates for both types of components were found to depend highly upon system of service. (For this paper, failure rates were plotted in absolute terms for pumps and motors, and were also segregated by plant type. Overall relative failure rates only were calculated for check valves; they were not further subdivided according to plant type.) Both check valves and pumps/motors in the ESW system exhibited relatively high failure rates as compared to other systems. Other factors influencing failure rates by system were found to include system usage, process fluid, specific pump or check valve type (e.g., swing check versus lift/piston check) and plant type.

Component age group

Results of the analyses by age group differed for pumps and check valves. For 1991-1992 check valve failures, no significant differences in relative failure rates according to component age were apparent. For pump failures occurring during 1990-1993, however, other patterns were evident. For BWRs, the failure rate (all failures and significant failures only) drops after a period of infant mortality. This occurs also in PWRs, but the failure rate again rises after about ten years of age. For significant PWR pump failures only, the trend resembles the classic bath tub shape. The oldest age group for both check valves (all failures) and PWR pumps exhibits the highest overall failure rate.

Plant type

It was discovered that check valves in BWR plants have exhibited higher relative failure rates than those in PWR applications. This finding taken by itself may be misleading, however, since the data suggests that there are simply more check valve failures being detected at BWRs due to their inservice and leak testing programs. Pumps in BWRs have had much less failure experience than their PWR counterparts. Plotted as a function of age, it is clear that during the early years of operation, pump performance is similar, regardless of plant type. Over time, however, the superior performance of pumps in BWR applications becomes apparent; in the $ 20 years age group the relative failure rate of PWR pumps is over four times that of BWR pumps.

Affected area/method of detection

While the check valve studies used only two general detection method classifications (programmatic and nonprogrammatic), the pump study added a third category. For pumps, then, the three general detection method classifications as assigned by ORNL were regulatory/code (corresponding to "programmatic" detection for check valves), plant programmatic, and nonprogrammatic. The plant programmatic category was added for pumps because of the recognition that many pump failures are detected by plant personnel by observation of some anomaly rather than by implementation of some code or regulatory criteria.

For check valves, the most common method of detection was programmatic. This holds true regardless of analysis period or level of degradation. When 1991-1992 failures were broken down further by general discovery process, the fraction of failures detected by programmatic means was far greater than the other detection processes (e.g., routine observation,

abnormal equipment operation), independent of affected area. The trend in failure detection method from 1984 through 1992 also shows an increase in the percentage of failures detected programmatically. Analysis of the data for check valves indicates that testing requirements mandated by codes and regulations are effectively detecting most check valve problems.

The same does not hold true for pumps. Voluntarily implemented plant programmatic controls were responsible for the detection of 73% of all pump failures and 41% of the significant pump failures. Regulatory/code required testing was responsible for only 14% of all failures and 39% of significant failures. The data also revealed that of the 95 significant failures detected by regulatory/code required testing, 75 failures involved ESW pumps. Of these 75 ESW pump failures, 61 involved internals wear; 56 of the 61 failures were indicated by failure to meet required flow or head. In summary, almost two-thirds of all pump failures detected by regulatory/code methods involved internals degradation of ESW pumps.

About 60% of all significant ESW pump failures were detected by regulatory/code required monitoring. In contrast, only 15% of the significant failures of pumps used in PWR plants in systems other than ESW were detected by regulatory/code required monitoring. More than four times as many significant pump failures in non-ESW systems at PWR plants were detected by nonmandated plant programs as by regulatory/code required methods.

Observations and Conclusions

When compared on the basis of certain specific parameters, some similarities between the historical performance data of check valves and pumps can be noted. For example, both component types exhibited similar percentages of failures classified as significant in terms of extent of component degradation. For both pumps and check valves, the system of service was found to play an important part in determining the rate at which the components fail. When investigated even farther, it has also become apparent that other factors play an important role in failure rate determination, including system usage, process fluid, and specific component type. Some results relative to component age group were also comparable, such as the increase in relative failure rate for both PWR pumps and check valves in the >20 years age group.

Analysis of component behavior according to other parameters, however, reveals some differences in their performance history. Some differences were noted in terms of performance according to age group. In general, check valve performance has shown no definitive pattern based on age group, except that older valves have consistently shown a somewhat higher relative failure rate. Some pump failure patterns, however, have shown an age-related correlation. Differences according to plant type have appeared also. Check valve failure rates have been shown to be higher for BWR plants than for PWRs; pump failure experience has been better at BWRs. The two findings may not be in conflict, however. It has been theorized that the higher check valve failure rate at BWRs may simply be the result of better inservice testing and monitoring practices at BWRs that tend to identify more failures than do the PWR practices.

Probably the most significant difference in the performance history of check valves and pumps as revealed by analysis of their NPRDS failure records is that of their method of detection. For check valves, the data clearly shows that most failures have been detected by (code or regulatory required) programmatic methods. This finding holds true regardless of affected area of the component. For pumps, however, the greatest fraction of failures have been found not by code or regulatory required testing or monitoring programs, but rather by the good practices of plant personnel. In the case of check valves, since the occurrence in the mid-1980's of potentially serious events (involving components in which their severely degraded condition went undetected), much industry and regulatory attention was devoted to the development and implementation of plant monitoring and testing programs. Review of NPRDS failure trend data from 1984 through 1992 has shown that these programs have been effective; the percentage of failures detected programmatically has increased, and overall extent of degradation has declined. Failure rates for most parameters showed a decline, and NPRDS reporting practices showed improvement.

For pumps and their motors, voluntarily implemented plant programs have been more successful at finding degraded operation than have regulatory/code mandated methods. There appear to be several reasons why this has been the case:

(1) The ASME Code has historically allowed pumps to be tested at any reference point, including minimum flow. Hydraulic and vibration data collected at minimum flow conditions may be of minimal value. Also, operation at these conditions may contribute to accelerated pump wear and degradation.

(2) One of the leading causes of both pump and motor degradation has been bearing wear. The Code requirements for vibration testing have not been effective in identifying bearing-related problems.

(3) Voluntarily implemented plant programs tend to focus on effective activities. Tasks that provide no value are usually discontinued. Regulatorily mandated tasks which provide minimal return on the resource investment cannot be dismissed.

(4) Human observations are a valuable diagnostic tool. More bearing failures were detected by operator observation than by implementation of regulatory/code mandated testing.

The observations that bearing degradation was both a leading source of pump and motor failures and was primarily detected through nonprogrammatic means suggests that alternative bearing health monitoring techniques, for example spectral analysis, high frequency demodulation, or shock pulse methods, would be likely to significantly improve programmatic detection experience.

References

1. "A Characterization of Check Valve Degradation and Failure in the Nuclear Power Industry, 1984-1990," NUREG/CR-5944, Vol. 1, ORNL-6734, Vol. 1, D. A. Casada and M. D. Todd, September 1993.

2. "A Characterization of Check Valve Degradation and Failure in the Nuclear Power Industry, 1991 Failures," NUREG/CR-5944, Vol. 2, ORNL-6734, Vol. 2, K. L. McElhaney, July 1995.

3. D. A. Casada, "A Characterization of Pump and Pump Motor Degradation and Failure Experience in the Nuclear Power Industry," Oak Ridge National Laboratory Technical Letter Report to the USNRC, ORNL/NRC/LTR/95-24 (draft).

4. D. A. Casada, "Auxiliary Feedwater System Aging Study," USNRC Report NUREG/CR-5404, Vol. 1, Oak Ridge National Laboratory.

5. D. F. Cox, "Aging of Turbine Drives for Safety-Related Pumps in Nuclear Power Plants," NUREG/CR-5857, Oak Ridge National Laboratory.

6. J. R. Boardman, "Operating Experience Feedback Report - Reliability Of Safety-Related Steam Turbine-Driven Standby Pumps," NUREG-1275, U. S. Nuclear Regulatory Commission.

7. ASME/ANSI OMa-1988 Addenda to ASME/ANSI OM-1987, Operation and Maintenance of Nuclear Power Plants, Part 6, Inservice Testing of Pumps in Light-Water Reactor Power Plants.

CORRODION EFFECTS ON FRICTION FACTORS[a]

H. L. Magleby, Idaho National Engineering Laboratory
Dr. S. J. Shaffer, Battelle

Abstract

This paper presents the results of NRC-sponsored material specimen tests that were performed to determine if corrosion increases the friction factors of sliding surfaces of motor-operated gate valves, which could require higher forces to close and open safety-related valves when subjected to their design basis differential pressures. Friction tests were performed with uncorroded specimens and specimens subjected to accelerated corrosion. Preliminary tests at ambient conditions showed that corrosion increased the friction factors, indicating the need for additional tests duplicating valve operating parameters at hot conditions. The additional tests showed friction factors of corroded specimens were 0.1 to 0.2 higher than for uncorroded specimens, and that the friction factors of the corroded specimens were not very dependent on contact stress or corrosion film thickness. The measured values of friction factors for the three corrosion films tested (simulating three operating times) were in the range of 0.3 to 0.4. The friction factor for even the shortest simulated operating time was essentially the same as the others, indicating that the friction factors appear to reach a plateau and that the plateau is reached quickly.

Background

The ability of valves to perform their safety functions is an ongoing issue for nuclear power plants. The U.S. Nuclear Regulatory Commission (NRC) and the Electric Power Research Institute (EPRI) have sponsored considerable testing to provide bases for predicting the forces to close and open these safety-related valves when subjected to their design basis differential pressures. These tests, however, used new or refurbished valves. A question to be answered is "will aging as a result of some period of operation cause the forces to increase?" Also, in-plant tests are sometimes used to establish the required operating forces and the torque switch settings for motor-operated valves. The question to be answered for these tests is "should a margin be added to the torque switch setting to account for a possible increase in operating forces resulting from aging?" The objective of this NRC-sponsored project is to begin answering these questions.

---

a. Work supported by the U.S. Nuclear Regulatory Commission, Office of Nuclear Regulatory Research, under DOE Idaho Operations Contract DE-AC07-94ID13223; Dr. G. H. Weidenhamer, Technical Monitor.

Many of the safety-related valves are gate valves. A sketch of a flexible-wedge motor-operated gate valve is shown in Figure 1. The forces that need to be overcome to operate these valves are shown in Figure 2 and are:

$$F_{stem} = F_{packing} \pm F_{stem\ rejection} \pm F_{net\ vertical\ pressure\ on\ disc} + F_{friction\ vertical\ component}$$

Although not exact, a simplified equation is helpful in identifying these forces. The equation is:

$$F_{stem} = F_{packing} \pm A_{stem}P + \mu A_{disc}\Delta P \qquad \text{where}$$

A_{stem} = Area of the stem
P = Valve pressure
μ = Disc friction factor
A_{disc} = Pressure area of the disc
ΔP = Differential pressure across the disc.

The packing friction force is usually not a large part of the total force, and changes in this friction, unless very large, are not usually important. The area of the stem, pressure, area of the disc, and differential pressure do not change with age. The remaining term, μ, the disc friction factor, can change with age and is the focus of this study.

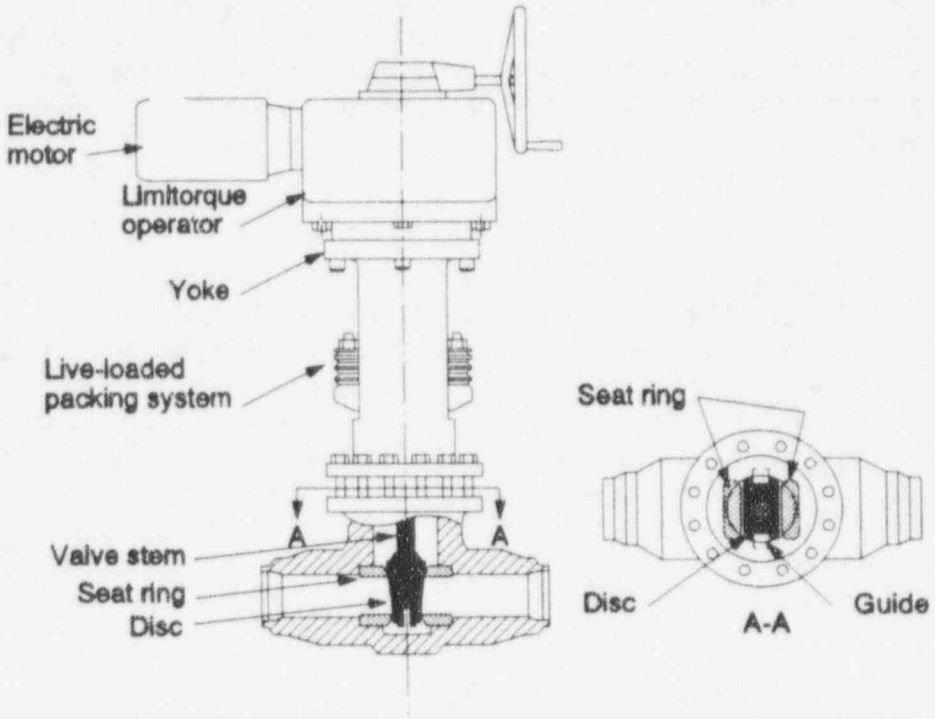

Figure 1. Flexible-wedge motor-operated gate valve.

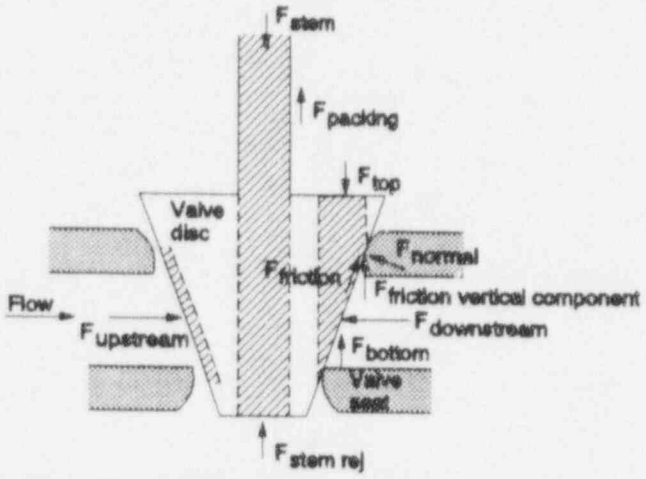

Figure 2. Forces to overcome to operate a gate valve.

For most valves, the friction vertical component is the largest of these forces. The friction occurs between the sliding surfaces, which are the disc and the guides (shown in Section A-A of Figure 1) when the valves are mostly open and the disc and body seats as the valve nears closure (see Figure 2). Changes in the characteristics of these surfaces with age could increase μ and result in increased forces required to operate the valves. Corrosion, which occurs to some degree even in the high-purity water of nuclear power plants, is a likely mechanism that could change the characteristics of these surfaces. Therefore, our initial investigations are focusing on the effect of corrosion on friction factors.

The largest force usually occurs when the disc is fully in the flow stream just prior to seating (As shown in Figure 2). In this case, the friction is between the disc and body seats. However, if the friction factor between the disc and the guides were to increase sufficiently because of corrosion, the largest force could occur when the disc is still riding on the guides. For some valves, even without an increase in the friction factor between the disc and the guides, the largest force can occur when the disc is still riding on the guides. These are valves with relatively large clearances that allow the disc to tip (as shown in Figure 3). The tipping, if excessive, can lead to interference as the disc enters the body seat, which may cause considerable metal deformation and result in high closing forces. The interference is not related to aging and is not included in this study. Tipping can also cause a relatively large net vertical force from changing pressure distribution around the disc. This increased vertical force can occur when the disc is still riding on the guides. In this case, tipping reduces the contact area, thereby raising the contact stress which, if sufficient, can lead to damage of the sliding surfaces. The damage could accentuate the increase in stem force required to operate the valve. For most valves both the body and disc seats are Stellite 6 and the contact surfaces between the body and disc guides are either carbon steel or Stellite 6. Therefore, our project investigates the effect of corrosion on the friction factors of these materials and the contact stresses that would damage them. Most of our tests at this time have been for Stellite 6 on Stellite 6. We have only preliminary results for carbon steel and most of the work remains to be completed.

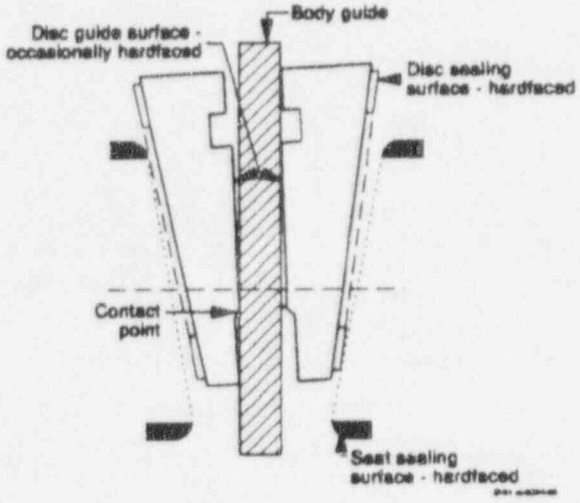

Figure 3. A guide-restrained tipped disc.

Preliminary tests

To begin the project, we searched nuclear plant operational databases, reviewed literature, and contacted experts for information relevant to the effect of corrosion on friction. The information we obtained (Gemant 1950; Yust 1985; Miyoshi 1985; Baranov 1986; Buckley 1982; Guruswamy 1981, and Scherchenko 1980) was insufficient to resolve the issue of the effect of corrosion on friction factors. Therefore, the NRC and the Idaho National Engineering Laboratory (INEL) concluded that testing would be necessary.

Our first approach was to conduct relatively simple tests with available equipment to determine if corrosion could affect friction. We tested corroded and uncorroded specimens of the materials used for the sliding surfaces in the valves at ambient conditions. Some samples were tested while exposed to air. Others were tested with a stream of demineralized water directed at the sliding interface of the specimens. This approach avoided the need to design and build special friction test equipment capable of testing in high temperature water.

We included carbon steel plate, forgings, and castings to represent the valve and disc guide materials. We used weld deposits of Stellite 6 on carbon steel plate for the seat material.

Half of the samples were corroded by installing them in an autoclave with water chemistry simulating the chemistry of a Boiling Water Reactor (BWR) reactor water cleanup (RWCU) line (See Table 1). The temperature was raised to 550°F and the corrosion accelerated by imposing a small electrical current. A sketch of the autoclave is shown in Figure 4. The thickness of the resulting corrosion films were from 1.5 to 3.0 micrometers (μm). The other half of the samples were not corroded so that comparisons between the two conditions could be made.

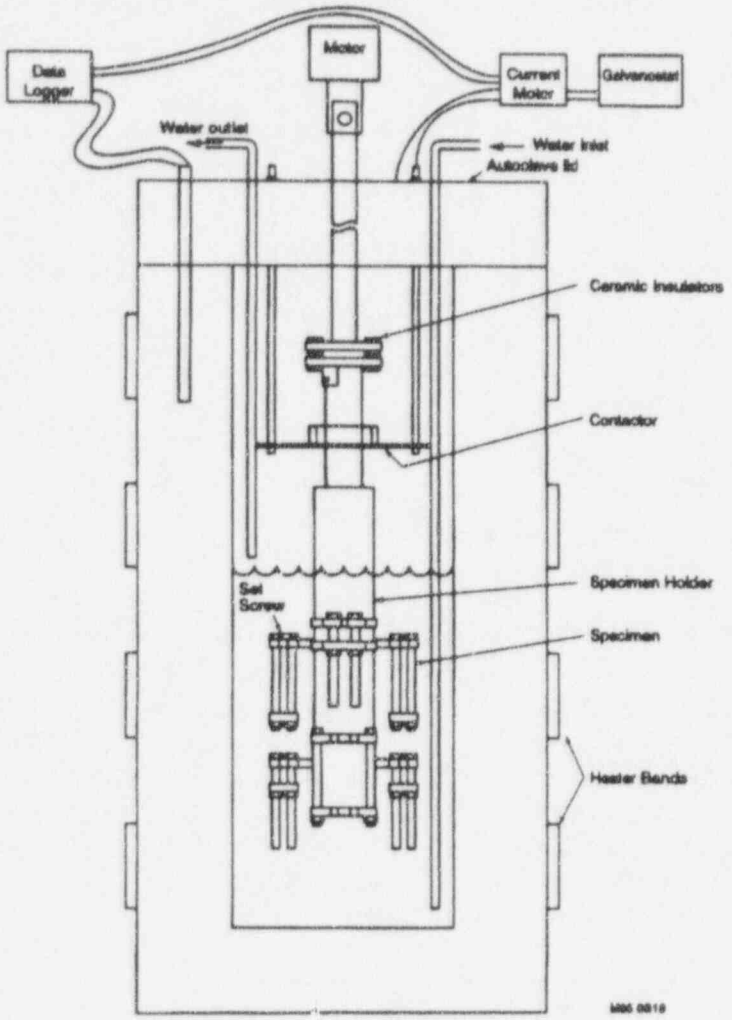

Figure 4. Autoclave for developing accelerated corrosion films.

Table 1. Water chemistry for BWR reactor water cleanup system inlet line.

Characteristics	Value
Temperature (°C)	288
pH (room temperature)	6.5 to 7
Oxygen (ppb)	100 to 200
Conductivity (μS/cm)	< 1.0
Fluid velocity (ft/sec)	2.2 to 2.8

A test fixture was designed and built for use with a Tinius-Olson Universal Testing Machine to perform the friction tests. A sketch of the test fixture is shown in Figure 5.

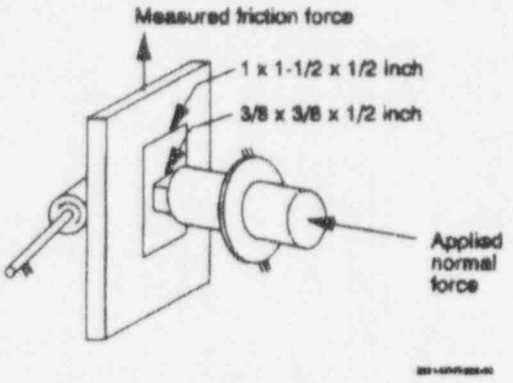

Figure 5. Fixture for preliminary friction tests.

The results of the friction tests on the corroded and the uncorroded specimens at ambient conditions dry and with a spray of deionized water are shown in Table 2. The results show an increase in friction factors for the corroded specimens. The increases for Stellite 6 were from 0.18 to 0.33 with high contact stress dry, and 0.20 to 0.47 with low contact stress wet. The increase for carbon steel wet was from 0.23 to 0.48. These tests are single stroke tests. Experience has shown that the initial strokes for cold friction tests of uncorroded Stellite 6 specimens are usually low and increase to a higher plateau for multiple strokes (Harrison 1994). Our friction factors in the range of 0.2 would be expected to increase with multiple strokes. Also, our preliminary tests showed that the corroded carbon steel surfaces were more susceptible to galling.

Table 2. Friction factors from preliminary tests.

Material	Condition	Nominal contact stress (ksi)	Post-test surface condition	Friction factor
A36/A105	Dry uncorroded	20.3	galling	0.38 to 0.68
A36/A105	Dry corroded	20.5	galling	> 1.0
A36/A105	Wet uncorroded	10.5	no galling	0.23
A36/A105	Wet corroded	3.5	no galling	0.48
A216/A216	Wet uncorroded	10.5	no galling	0.18
A216/A216	Wet corroded	3.5	galling	0.63 to > 1.0
Stellite	Dry uncorroded	20.0	no galling	0.18
Stellite	Dry corroded	17.5	no galling	0.33
Stellite	Wet uncorroded	3.5	no galling	0.20
Stellite	Wet corroded	3.5	no galling	0.47

These preliminary tests showed that corrosion is likely to affect the friction factors. However, the preliminary tests raised questions about the validity of the results because the friction test rig may have accentuated galling due to edge effects from the overturning moment, and because the friction tests did not duplicate in-plant valve parameters of (a) being submerged in high-purity water at 550°F and 1,050 psi, (b) contact stress of about 10 ksi, and (c) a relative velocity between the sliding surfaces of 12 to 18 in./min. To resolve the questions would require that the specimens be tested while submerged in high temperature pure water, have typical contact stress, and typical relative velocity between the sliding surfaces. We concluded that to answer the question "would corrosion have a similar effect on the friction factors of in-plant valves" would require additional tests.

Second-phase tests

Second-phase tests are currently underway that better duplicate the parameters for in-plant valves. Results for Stellite 6 surfaces are described in this paper. The corrosion films were established as before. A photograph of the autoclave used for the accelerated corrosion is shown in Figure 6. Accelerated corrosion runs were performed to obtain three corrosion film thicknesses. The thickness was measured directly from mounted and metallographically polished cross sections using a scanning electron microscope (SEM) at magnifications of 1,000 to 10,000 as required. The accelerated corrosion runs and the corresponding corrosion film thicknesses are shown in Table 3.

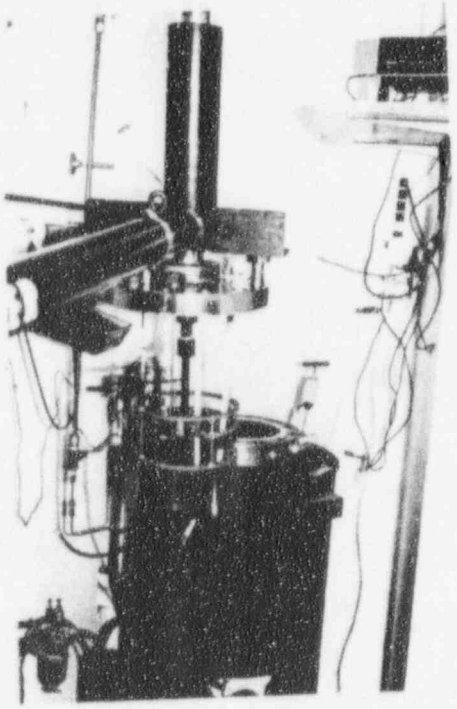

Figure 6. Photo of autoclave used for accelerated corrosion of the test specimens.

Table 3. Summary of accelerated corrosion runs and friction test loads.

Corrosion run no.	Current density (mA/cm^2)	Duration	Oxide thickness (μm)	Friction test stress (ksi)
—	—	—	Native < 2,000 Å	10
1	0.13-0.17	11 days	0.5-1.0	10
1	0.13-0.17	11 days	0.5-1.0	10
1	0.13-0.17	11 days	0.5-1.0	40
1A	0.19	+ 2-1/2 days	3-5	10
2	0.29-0.42	14 days	3-9	10
2	0.29-0.42	14 days	3-9	40

We had limited success in relating the corrosion film thicknesses of Stellite 6 to operating times in BWR RWCU lines. The most pertinent literature we were able to find was the work of Hocking and Lister (Hocking 1988 and Hocking 1985) and the work of the Atomic Energy of Canada (Lister 1989). While the primary purpose of their work was to determine the cobalt release rates into the primary coolant, we used their data to estimate the corrosion film growth rate. The work of Hocking and Lister suggested a parabolic growth model, while the AEC work suggested a linear growth model. The two models were used to bound the growth rate. These bounds are shown in Figure 7 and give a range of 2.5 to 15 μm for 18 months exposure to BWR chemistry.

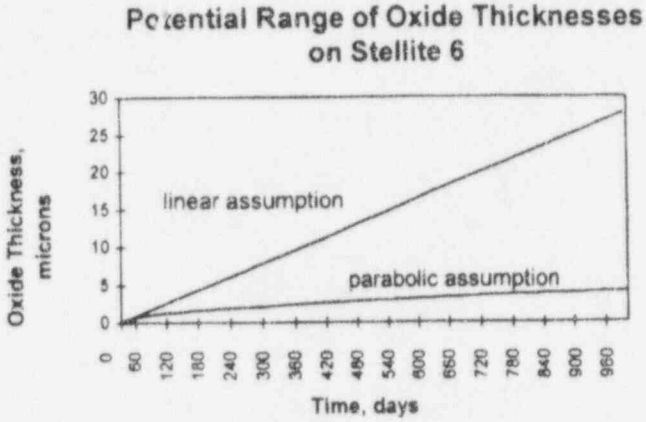

Figure 7. Models to bound the corrosion film growth rate for Stellite 6 in BWR RWCU system chemistry.

To simulate actual operating conditions, the friction tests were conducted in an autoclave simulating BWR primary coolant temperature, pressure, and water chemistry. Seat contact stresses, assuming uniform load distribution, for typical 4 and 6 in. valves with 1,050 psi differential pressure were calculated as 7.8 and 12.6 ksi, respectively. An additional load due to wedging of the disc can be of the order of the contact stress. Normal stress levels of 10 and 40 ksi were applied for the friction

tests to bound the range of stresses found in typical RWCU system valves and to provide some extended applicability. The contact stresses used for each of the test specimens are shown in Table 3. Also, the friction tests were conducted simulating the closing speed of actual valves. Typical 6-in. motor-operated valves close in 20 to 30 seconds, corresponding to 18 to 12 in. per minute. The tests for this project were performed at 16 in. per minute. Also, the friction test apparatus used for the project (See Figure 8) had a symmetrical design and sample configuration that minimizes edge loading and avoids accentuating galling.

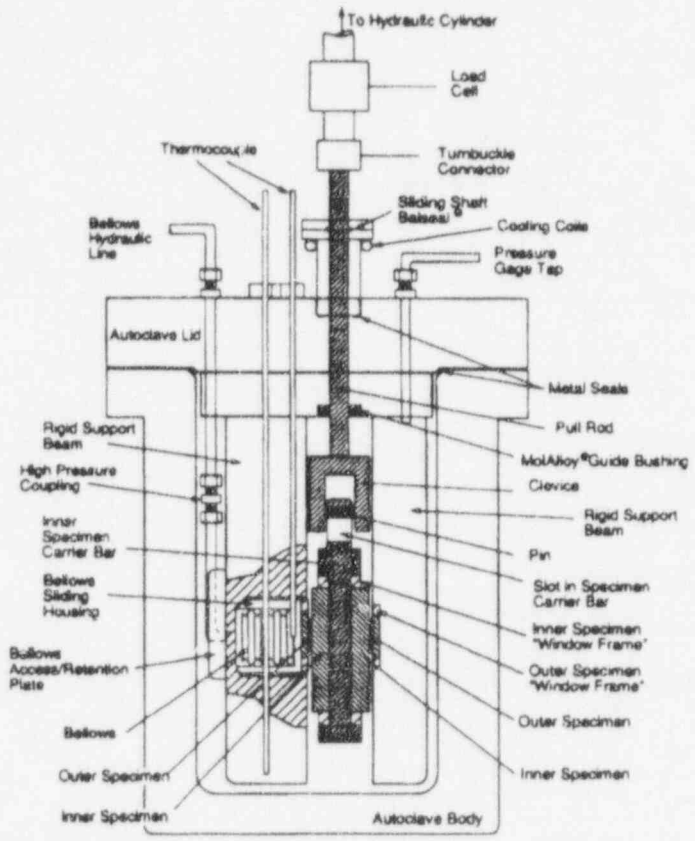

Figure 8. Autoclave apparatus for friction tests.

Some second-phase friction testing at actual operating conditions using the more representative apparatus has been completed for Stellite 6. Tests for carbon steel will follow. Preliminary results for Stellite 6 tests, shown in Figure 9, confirm the findings from the earlier tests. Friction factors increased from approximately 0.2–0.3 for uncorroded specimens to approximately 0.3–0.4 for corroded specimens. Corroded specimen tests at contact stress of 10 ksi and 40 ksi had similar results. However, in the 40 ksi test, the friction factor decreased after a few strokes. Experience has shown that for Stellite 6, the friction factors are lower for high contact stress (Harrison 1994). However, in the case for the corroded specimens, the initial strokes for the high contact stress had friction factors essentially the same as for the lower contact stress, indicating that friction factors for corroded surfaces may be less dependent on the contact stress. The friction factors for the high contact stress decreased only after several strokes, which may indicate that the higher contact stress is

more effective in removing the corrosion film. Tests were conducted with oxide film thickness of 0.5 to 1, 3 to 5, and 3 to 9 μm. The tests at the three corrosion film thicknesses were performed to investigate the effects of operating time. Although we have had only limited success in correlating corrosion film thickness to operating time, the three thicknesses nominally span the range of expected operating time. The results were similar for the three thicknesses, indicating that the friction factors may be independent of corrosion film thickness.

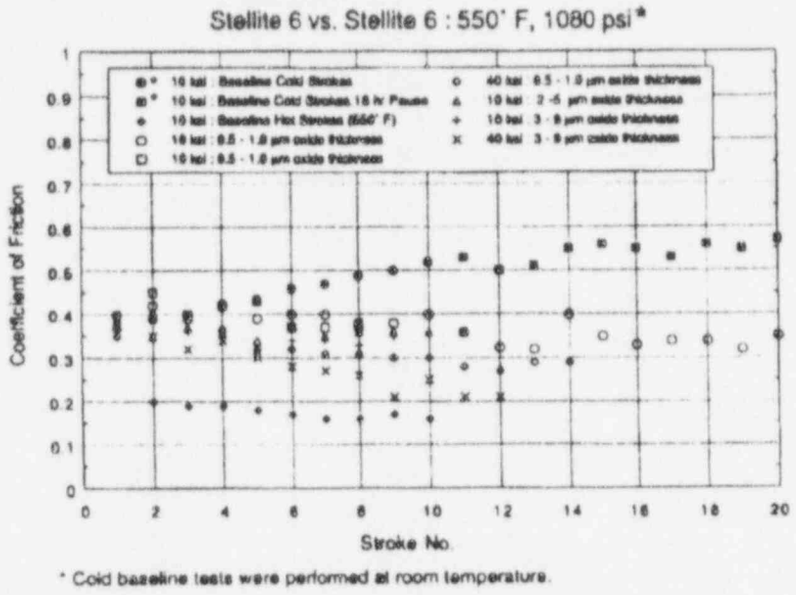

* Cold baseline tests were performed at room temperature.

Figure 9. Friction test results for Stellite 6 at 550°F and 1,080 psi.

Results and Conclusions

The tests of Stellite 6 specimens at hot conditions showed that friction factors for the corroded specimens were 0.1 to 0.2 higher than for the uncorroded specimens. Measured values of the friction factors of the corroded specimens were not very dependent on contact stress or corrosion film thickness. The measured values for the corroded specimens at hot conditions were in the range of 0.3 to 0.4.

The friction factors measured for the three corrosion film thicknesses were essentially the same, indicating that the increase in friction factor with operating time may have reached a plateau. The friction factor had reached a plateau even for the shortest simulated operating time, indicating that the plateau is reached quickly.

References

Baranov, N. G. and L. M. Fedorchenko, 1986, "Physicochemical Processes of Formation of Surface Films in Friction," *Poroshkovaya Mettalurgiya (Kiev), 25,* 1, pp. 78-82.

Buckley, D. H., 1982, "Surface Films and Metallurgy Related to Lubrication and Wear," *Progress in Surface Science, 12,* 1, pp. 1-154.

Gemant, A., 1950, *Frictional Phenomena*, Brooklyn, New York: Chemical Publishing Co.

Guruswamy, V. and J. O'm.Bockris (eds.), 1981, *Comprehensive Treatise of Electrochemistry, 4,* New York: Plenum Press, pp. 463-471.

Harrison, D. H., P. S. Damerell, J. K. Wang, and M. S. Kalsi, 1994, *Gate Valve Performance Prediction, Proceedings of the Third NRC/ASME Symposium on Valve and Pump Testing,* July.

Hocking, W. H. and D. H. Lister, 1988, "Corrosion of Stellite 6 in Lithiated and Borated High-Temperature Water," *Surface and Interface Analysis, 11,* pp. 45-59.

Hocking, W. H., F. W. Stanchell, E. McAlpine, and D. H. Lister, 1985, "Mechanisms of corrosion of Stellite 6 in Lithiated High Temperature Water," *Corrosion Science, 25,* 7, pp. 531-557.

Lister, D. H. and R. D. Davidson, 1989, *Corrosion-Product Release in Light Water Reactors,* Electric Power Research Institute, EPRI NP-6512, September.

Miyoshi, K., D. H. Buckley, G. W. P. Rengstorff, and H. Ishigaki, 1985, "Surface Effects of Corrosive Media on Harness, Friction, and Wear of Materials," *Wear of Materials,* pp. 302-312.

Scherchenko, A. S., 1980, "Study of Friction Properties of Natural Oxide Films," Mekh. i Fiz. Kontaktn Vazimodeistviya, Kalinin, *Chemical Abstracts, 96,* Issue 96:23414j, pp. 81-86.

Yust, C. S., 1985, "Tribology and Wear," *International Metals Review, 30,* 3, pp. 141-145.

Results of a Literature Review on the Environmental Qualification of Low-Voltage Electric Cables[1]

R. Lofaro, B. Lee, and M. Villaran
Brookhaven National Laboratory
J. Gleason
GLS Enterprises, Inc.
S. Aggarwal
U.S. Nuclear Regulatory Commission

INTRODUCTION

In the design of nuclear power plants in the U.S., safety-related electric equipment must be qualified to provide reasonable assurance it can withstand the effects of a design basis event (DBE) and still be able to perform its prescribed safety function, even if the accident were to occur at the end of its service life. The requirement for environmental qualification (EQ) originates from the General Design Criteria in the Code of Federal Regulations, Title 10, Part 50 (10 CFR 50). The acceptable method of performing the qualification of this equipment has evolved over the years, starting with the NRC Division of Operating Reactors (DOR) Guidelines, which were issued in Bulletin 79-01B [1], and NUREG-0588 [2] requirements and ending with the current EQ Rule, 10 CFR 50.49 [3]. While the EQ methods described in these documents have the same overall objective, there are some notable differences for which a clear technical basis has not been established. One difference is the preaging requirement for equipment prior to LOCA testing.

In addition, specific issues related to current EQ practices have been raised by the U.S. NRC which need to be addressed. These issues, which are discussed in detail later in this paper, are related to the sources of conservatism and uncertainty in IEEE Standard 323-1974 [4], which is the qualification standard currently endorsed by the NRC. To address these issues, the NRC Office of Nuclear Reactor Regulation (NRR) implemented a Task Action Plan (TAP) [5], and the Office of Nuclear Reactor Research (RES) initiated a complementary research program. The current focus of this program is on the qualification of low-voltage instrumentation and control cables. These cables were selected since they are not typically replaced on a routine basis, and their degradation could impact plant safety.

As the first step in developing a research approach, NRC/RES sponsored a public workshop on EQ in November 1993. Panels of experts from across the country attended and participated in individual meetings to provide input in four major areas related to EQ; 1) preaging techniques, 2) operating experience, 3) condition monitoring (CM), and 4) LOCA testing. One of the main conclusions drawn from the workshop is that a great deal of work has already been performed in the area of EQ, and it should be reviewed before any new work is initiated. The information gathered at these meetings was published in NUREG/CP-0135 [6], and subsequently used by NRC/RES to define specific details of a Research Program Plan [7]. In response to the workshop, the RES Research Program Plan includes a literature review and analysis as the first objective.

---

[1]Work performed under the auspices of the U.S. Nuclear Regulatory Commission.

Brookhaven National Laboratory (BNL) is the lead laboratory assisting NRC/RES in the EQ Research Program. BNL performed a literature review to consolidate and assess the vast body of research work that has been completed related to the qualification of electric cables, operating experience and other relevant information. The objective of this review was to determine which of the EQ related issues identified could be fully or partially resolved by past or ongoing work, and which required additional study. The results of the review are being used as input to optimize the scope of future EQ research.

EQ ISSUES

To properly focus the review, the issues to be addressed in this research program were first clearly identified and documented using input from the 1993 EQ Public Workshop [6], as well as from discussions with NRC staff and EQ experts. The issues identified are consistent with both the NRR TAP [5] and the RES Research Program Plan [7].

The EQ issues identified are important for the current licensed plants and for extended life consideration. The issues identified can be categorized into seven major issues, which are presented as broad questions in the first column of Table 1.

The first issue is related to the preaging techniques used in the qualification process. As part of current EQ requirements (10CFR50.49, Regulatory Guide 1.89), prior to LOCA testing, the equipment to be qualified must first be preaged to simulate its expected condition at the end of its qualified life. The issue of preaging was identified for evaluation due to the many questions raised related to the accelerated aging practices used on the cable specimens. The questions focus on the methods used to calculate the exposure times and temperatures for accelerated thermal aging (Arrhenius), the dose rates used for accelerated radiation aging, and the synergistic effects of thermal and radiation aging. Also, there are other environmental and service conditions, in addition to heat and radiation, which can degrade the functional capability of safety-related equipment and which are not always simulated accurately in the preaging process. Uncertainties in preaging can affect the overall result of the qualification process.

Conservatism in the qualification process is the subject of the second issue. The large number of variables that influence cable degradation make it impossible for the qualification process to exactly duplicate actual in-service conditions for a specific cable. In addition, since only one sample of new cable is required to be tested, no statistical base for the qualification test results is established. Therefore, to provide an acceptable level of confidence that installed cables will perform their intended safety function under a DBE, a number of conservatisms are included in the qualification process. An example is the addition of a second temperature/pressure transient to the LOCA profile the cable is tested to, even though an actual DBE may include just one. Also, the peak temperature and pressure expected during the DBE are increased for the qualification test. Based on the many years of qualification experience obtained since these requirements were developed, it is felt that these conservatisms should now be reviewed to determine if they are acceptable, or if they need to be modified.

Issue 3 relates to the variations in cable manufacture that are found in the industry. In the manufacturing process, variations occur in the different additives and the vulcanization system used in the cables. Differences may also occur over the years due to changes in resin and additive suppliers. Variations also exist in the construction of the cable itself; for example, multiple conductors versus single conductor, or bonded jacket versus un-bonded jacket. These variations can potentially affect the aging characteristics of the cable, however, details are incomplete as to methods used to account for cable variations in the

qualification process. Typically, one sample of a particular cable type is qualified, and similarity criteria are used to qualify other "similar" cables, therefore, not all cable constructions are tested. Since the implications of this are unknown, this was included as the third issue to be addressed.

When cables are installed, there are many localized field conditions that can arise which may affect the degradation rate of the cable. An example is areas of unusually high temperature or radiation, commonly called "hot spots." Another example is areas where the cable is mechanically stressed, such as at bends and support locations, or where installation or maintenance damage has occurred. These are commonly referred to as "weak-links". Some of the stresses imposed by these field conditions are accounted for by simulated mounting configurations, and others are not specifically addressed. To address the questions related to installed field conditions, this fourth issue was identified for evaluation in the program.

One of the most important issues to be addressed in this research effort is related to the evaluation of cable condition monitoring (CM) methods. If the condition of the cables can be accurately determined in the plant, this would provide an increased level of confidence that plant safety is not compromised by cable degradation. Currently, elongation-at-break is the best laboratory indicator to assess embrittlement and cable degradation. However, this method has limitations since it is destructive, it requires relatively large samples, and its effectiveness at predicting accident survivability is unknown. The fifth issue was identified to include the evaluation of other potentially more versatile CM methods in this program.

As part of the current EQ requirements, a qualified life is assigned to the equipment being qualified. This qualified life is a time-based value which typically has a maximum value equal to the current licensed life of the plant (40 years), but can be less. As plants approach the end of their license and anticipate extended life operation, an important question which must be addressed is whether it is possible to extend the qualified life of the electrical equipment. The sixth issue identified for evaluation in this program addresses that question by considering the technical basis for maintaining and extending the existing qualification requirements.

The seventh issue addresses the graded approach to EQ that currently exists. Since different vintages of plants used different qualification requirements, depending on when they were licensed, questions have been raised as to the technical basis for considering these different approaches to qualification acceptable. This issue addresses those questions by examining the various differences in the qualification requirements and their impact on plant safety.

For each of the seven major issues, a number of specific sub-issues were identified, and individual analyses, hereafter called dossiers, were prepared for each sub-issue. The dossiers are the means used to document the results of the literature review and analysis. They provide background information on the sub-issue, a listing of the specific questions to be answered for the sub-issue, and the results of the literature review related to that sub-issue. The dossiers developed are identified in the second column of Table 1. For each sub-issue, specific topics that need to be addressed were identified. There are a total of 43 topics identified. These are shown in the third column of Table 1. The dossiers will be discussed in more detail later in this paper.

LITERATURE REVIEW APPROACH

In conducting the literature review, BNL searched a variety of library sources. In addition, NRC placed a request for information in the Federal Register. To date, over 400 reports have been obtained and

reviewed by BNL. This includes technical reports and papers related to cable qualification and polymer research performed by Sandia National Laboratories (SNL), Electric Power Research Institute (EPRI), and others. Also, actual cable manufacturer qualification test reports were obtained and reviewed. EQ experts were consulted and their input was obtained. In addition, the Nuclear Utility Services (NUS) EQ database and the Idaho National Engineering Laboratory (INEL) EQ database were reviewed to identify the information in them and evaluate their usefulness. Research from other countries was also reviewed, including France, Japan, Canada, Germany, and the United Kingdom.

The literature reviewed was grouped into three basic areas; aging characterization, design basis accident testing, and condition monitoring methods. The first two areas are directly related to the EQ process for cables in nuclear applications. The third involves methods for assessing the level of degradation of cable insulation and jacket materials with respect to expected service life.

In reviewing the documents obtained, a number of them were not relevant to the seven major issues, and were not considered further. The documents that were relevant were reviewed in detail and summarized in an interim report. The interim report provides a technical basis for resolving several of the sub-issue topics identified, and for recommending additional research for others. As the program progresses and new documents are obtained, they are reviewed and added to the interim report, if they are relevant and provide new information. Current plans are to publish the final results of the literature review in NUREG/CR-6384 [8].

ANALYSIS OF THE LITERATURE

The information and data collected during BNL's literature search and review were categorized according to the seven major EQ issues to facilitate their analysis. The primary source of information for the review and categorization process was the literature identified and described in BNL's interim literature review report [8]. Other sources of information reviewed include the results of the 1993 EQ Public Workshop [6], along with some additional literature and documentation obtained and reviewed subsequent to the interim literature review report.

Drawing upon the information gleaned from the entire body of research and literature reviewed, an analysis of each sub-issue and its related topics was conducted. The approach taken was to assign an individual reviewer to study each sub-issue in detail, review the applicable literature, and determine the status of the research with respect to resolution of the topics related to that sub-issue. Upon completing the analysis, the individual reviewer prepared a draft dossier describing the review, analysis, and recommendations for resolution. A total of thirteen dossiers, designated as A through M, were developed to cover the seven major issues, as described in Table 1.

The draft dossiers were initially reviewed and commented upon by all members of the BNL EQ Research Team, and then by an outside panel of EQ experts. Finally, the NRC provided their review comments and guidance on the draft dossiers. By following this approach to the analysis of the EQ issues, BNL was able to systematically apply the information and research results identified in the literature review to the resolution of several sub-issue topics. The recommendations in these dossiers represent a consensus between BNL staff, and a panel of EQ experts, and were submitted to the NRC program manager for review.

The final dossiers document the analysis results, and the direction to be taken in the present research work toward resolution of outstanding issues. The dossiers provide the background and evolution of each topic, describe the significant problem areas associated with the topics, and summarize the outstanding issues and questions that must be resolved.

Based on the literature analysis, each sub-issue topic was grouped into one of three resolution categories: 1) resolved by past work, 2) unresolved but further research under this program is not warranted, and 3) unresolved, warrants further research at this time. It should be noted that these recommendations apply only to the performance of this EQ research program and do not imply that no further research should be conducted in any specific area. The recommendations simply reflect the priority of the sub-issue topics as they relate to the objectives of this program.

Unresolved topics were prioritized to avoid duplication of previous efforts and to address the most significant issues, particularly those areas that have not yet been studied extensively. The review process described above provided confidence that the most pressing issues had been properly identified and prioritized.

RESULTS

As previously mentioned, each of the seven major issues was broken down into specific sub-issues and related topics which need to be addressed to completely resolve the major issue. From the literature analysis, each topic was categorized according to its resolution based on past work. Figure 1 shows the resolution categories for the 43 sub-issue topics, which are listed in Table 1. As shown in this figure, 18 topics are categorized as Category 1, resolved by past work; 6 topics as Category 2, unresolved but does not warrant further research in this program; and 19 topics as Category 3, unresolved and warrants further research in this program. As shown by these numbers, a total of 24 issues out of 43 were eliminated from this program based on past research identified in the literature review.

Of the 18 topics in Category 1 (resolved), three are in the area of preaging techniques, eight are related to issues on LOCA testing, two are in the area of cable manufacturing, one is in the area of condition monitoring, and four are related to the graded approach to EQ. For these topics, sufficient information was available from past work to answer the questions of concern, and no additional effort is needed in this program to pursue these issues.

Six topics are categorized as Category 2, unresolved but do not warrant further research. Many of these topics have had prior research or have been addressed in methods common to qualification. Additionally, prior research and procedures have suggested that these topics may have minimal impact on the cable qualification process and, although research to fully understand the topic is incomplete, they are judged to not warrant further research at this time. The topics listed below are assigned to this category:

- Oxygen diffusion limitations during thermal aging
- Dose rate effects for radiation preaging
- The effects of electrical surges on aging
- Preaging synergistic/sequence effects
- The effects of oxygen in LOCA simulation
- The effects of manufacturing processes on aging

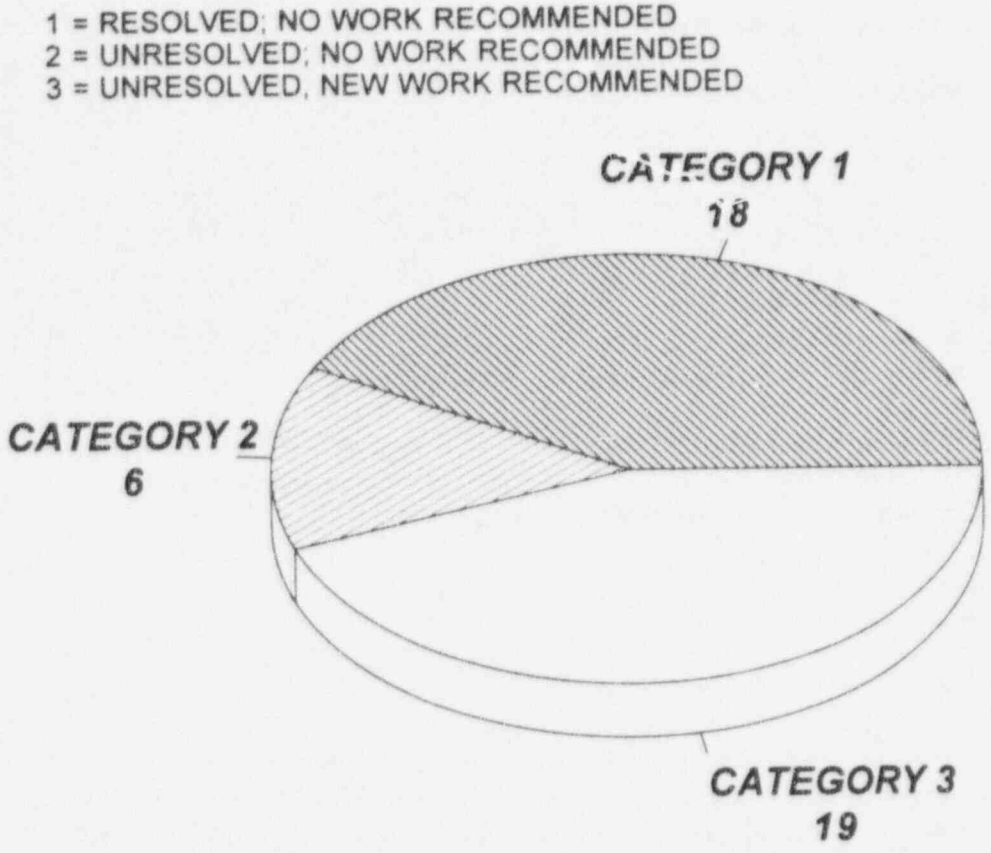

Figure 1 Distribution of EQ topic resolution categories

A total of 19 topics are categorized as unresolved, and further research on them is recommended in this program. As indicated in Table 1, three of the Category 3 topics are related to the issue of preaging methods and two are related to cable manufacturing processes. Eight of the Category 3 topics are related to the effects of installed conditions on the cable aging processes. Two topics are identified under the issue of condition monitoring for further research. Four topics, related to the overall EQ philosophy and how it applies to current and extended life operation, are recommended for further evaluation in this program. Each of the topics for which additional study is recommended is discussed in more detail in the following paragraphs.

Thermal Aging (Dossier A)

Of primary interest in the area of thermal aging is a comparison of the condition of cables naturally aged in a plant environment with the condition of cables artificially aged to the same service life using Arrhenius methods. This comparison would provide a measure of how well artificial aging simulates actual aging conditions, and what degree of conservatism is built into the process. The literature analysis shows that work related to this type of comparison is limited, and has not been able to completely resolve this issue. Since a direct comparison is the most effective way to determine the acceptability of current artificial aging methods, it is recommended that this be included in the program. These tests will involve

measurement of material properties using the CM techniques recommended for study (see discussion on CM research). These tests will also be useful for evaluating the phenomenon of decreased degradation at elevated aging temperatures for some cable materials, which was reported in the literature.

Another unresolved issue related to thermal aging is the subject of activation energies, which still has some uncertainties. Concern has been raised with respect to the accuracy of activation energies used in the past since they have a significant effect on the qualified life of a component. Determination of these values requires a great deal of effort, and it is not recommended that this be done for any significant number of materials. However, it is recommended that activation energies for the four cable materials (XLPE, EPR, Hypalon, Neoprene) to be studied in this program be verified. This will provide a basis for determining the validity of this issue, and can be done in support of the previously discussed comparison of naturally aged and artificially aged cables.

Effects of Humidity on Aging (Dossier C)

The literature analysis shows that the effects of humidity have not been adequately addressed in past work. Humidity can be a problem if present on cable degraded by other mechanisms, such as heat, radiation, mechanical stress, or inadvertent damage. Additional tests evaluating the synergistic effects of humidity, radiation and thermal stresses are recommended as a first approach, to see if the most common insulation and jacket materials are susceptible. Comparison with samples exposed to combined radiation and thermal stresses in a dry environment will be performed to help address this issue.

Effect of Cable Construction on Aging (Dossier H)

In past work [9], some multiconductor cables with EPR insulation were found to have a higher propensity for failure during a LOCA compared to a single conductor cable insulated with the same EPR compound. Even though several hypotheses have been suggested to explain this result, sufficient information was not available to draw a definitive conclusion. Therefore, it is recommended that LOCA tests be performed on multiconductor and single conductor cable samples to study this phenomenon.

In addition, past work raised questions on the behavior of bonded jacket cables. Cables with EPR insulation and bonded CSPE jackets developed cracks much earlier compared with unbonded jacket cables. Since the reasons for this difference are not clearly understood, this issue remains unresolved and it is recommended that additional research be performed. The research should use the same cable materials, and the degradation should be monitored during the preaging process so that the failure mechanism may be determined.

Effects of Installed Environment and Installed Configuration on Aging (Dossiers I and J)

Past work and experience show that some of the environments and configurations in which cables are installed expose them to higher levels of stress. The environmental "hot-spots" are areas of elevated temperature and/or radiation above levels that are normally expected. In addition, bends, vertical runs, and other installation configurations can produce "weak links" in the cable. While these hot-spots and weak-links are known to exist in the plants, the degree to which they accelerate the degradation and failure rate of cables is very plant specific and cannot be generically quantified. Testing has not, and can not completely resolve this issue. Therefore, it is not recommended that any specific new research be performed in an attempt to resolve this issue since no generic answer is feasible. Rather, this is best

addressed at individual plants by surveying suspected areas to identify and characterize hot-spots and weak links. Once these have been identified, condition monitoring methods can be used to evaluate cable condition and predict residual life. It is believed that the research on CM will provide useful information for addressing this issue and should be a major focus of this program. BNL is currently in the process of obtaining naturally aged cable samples from various types of hot spots and high-stress configurations, and it is recommended that they be tested to characterize the degradation due to these conditions. This could provide some insights into understanding how these unique installation conditions affect cable degradation.

Condition Monitoring (Dossier K)

From a review of the literature and discussions with experts in the field, it was determined that one of the most promising areas of research for this program could be in the area of condition monitoring. If cable condition can be measured in situ in the plant, and its accident survivability established, many of the concerns regarding the qualification process would be resolved. While a great deal of work has been performed on CM in the past, the effectiveness of the various CM techniques has not been completely determined, and acceptance criteria have not been established. Therefore, a primary focus of this research program will be to evaluate various CM techniques. These will include techniques that show promise for in situ use, as well as several inexpensive, simple to perform techniques. It is recommended that the following CM methods be evaluated for their effectiveness in monitoring cable condition and predicting LOCA survivability. These methods were identified from the literature analysis, as well as discussion with NRC and EQ experts:

1. Chemical Property Measurements
   - Fourier Transform Infra-Red (FTIR) Spectroscopy
   - Oxidation Induction Time

2. Physical Property Measurements
   - Indenter Modulus
   - Elongation at break

3. Electrical Property Measurements
   - AC Impedance
   - Time Domain Reflectometry

4. Simple/Inexpensive to Perform Measurements
   - Current Signature
   - EMF Measurement
   - Hardness
   - Insulation Resistance
   - Thermography
   - Visual Examination

Elongation-at-break will be performed as a baseline method for correlation of results. Also, functional testing, voltage withstand, and leakage current measurements will be performed for those samples undergoing LOCA testing.

It is recommended that the CM research include an evaluation of the various CM methods for determining current cable condition, as well as predicting accident survivability. The data required for this research include preaging and LOCA testing on both naturally and artificially aged cable samples. CM measurements will be taken periodically throughout the preaging process, and both before and after exposure to accident conditions.

EQ for Present and Extended Life (Dossier L)

One significant issue which will have to be addressed as plants consider extended life operation is how to address continued qualification of electric equipment. Currently, a time-based qualified life is assigned to the equipment based on the preaging performed. Once the qualified life has expired, the component must be replaced or requalified. Typically, the qualified life does not extend beyond the licensed life of the plant. An alternative is to consider modifying the EQ philosophy to incorporate a condition-based qualified life, for which the qualified life is determined solely by the condition of the equipment and not its age. This would allow equipment to continue operating as long as its condition is above a predetermined acceptable level. As a parallel effort to the aforementioned research discussed, it is recommended that insights gained from this project be used to evaluate the feasibility of the change in philosophy.

CONCLUSIONS

This literature review has shown that a great deal of work has been performed in the area of EQ of electric cables. The related subject areas are varied and range from polymer research to actual qualification test reports. Much of this work is directly applicable to the resolution of issues raised recently by the NRC. Of the 43 specific topics identified for resolution, 18 have been resolved by the analysis of past work. This will result in a significant savings in time and effort for this research program.

In addition, the literature review also helped to focus recommendations for future work to areas that can immediately benefit from additional research. It was determined that six specific areas would not immediately benefit from additional research in this program since an extensive amount of work had already been done and its impact appears to be minimal. The areas for which additional research is recommended in this program are those in which the issue is important enough to merit further research and resolution is promising.

Table 1 Recommendations from the EQ Literature Review

EQ MAJOR ISSUES	SUB-ISSUES/ DOSSIER TITLE	TOPICS FOR SPECIFIC QUESTIONS TO BE ADDRESSED IN DOSSIER	RESOLUTION CATEGORY*	RECOMMENDED WORK			COMMENTS
				CM	LOCA	OTHER	
Q1: Are existing preaging techniques, based upon the accelerated thermal and radiation aging methodology, adequate to account conservatively for natural age-related degradation?	A. Thermal Aging	A.1 Arrhenius application	3	X			Compare natural with accelerated aged cables.
		A.2 Oxygen diffusion limitations	2				
		A.3 High accelerated aging temperatures	1				
		A.4 Activation energy estimates	3	X			Verify activation energy for cables to be studied.
	B. Radiation Aging	B.1 Dose rate effects	2				
		B.2 Types of radiation used	1				
	C. Other Aging Factors	C.1 Humidity effects	3	X	X		Compare samples aged in a dry environment to those aged in a humid one.
		C.2 Electrical surges	2				
		C.3 Preaging synergistic/sequence effects	2				
		C.4 Use of slab samples for preaging research	1				

Table 1 (Cont'd)

EQ MAJOR ISSUES	SUB-ISSUES/ DOSSIER TITLE	TOPICS FOR SPECIFIC QUESTIONS TO BE ADDRESSED IN DOSSIER	RESOLUTION CATEGORY*	RECOMMENDED WORK			COMMENTS
				CM	LOCA	OTHER	
Q2: What is the overall level of conservatism in EQ LOCA testing, and post-LOCA testing?	D: LOCA Profiles	D.1 Temperature/pressure margins	1				
		D.2 Single versus double peak	1				
		D.3 Superheated versus saturated steam	1				
	E: LOCA Simulation Methods	E.1 Presence of oxygen	2				
		E.2 Effect of chemical sprays	1				
		E.3 LOCA synergistic/sequence effects	1				
		E.4 Accident total radiation dose (source term)	1				
	F: Cable Monitoring During LOCA	F.1 Functional test performance (actual loads, leakage current) & LOCA acceptance criteria	1				
		F.2 Mandrel bend (voltage withstand/submergence)	1				
Q3: What is the effect of variations in cable manufacture on the aging process and how should they be handled?	G: Manufacturing Processes	G.1 Fire retardant additives effect on aging, coloring agents, antioxidants and fillers, variations in base polymer materials, variations in curing	2				
	H: Cable Construction	H.1 Multiple versus single conductor designs	3		X		Multiconductor cable to be LOCA tested to study past results
		H.2 Bonded jacket cables	3		X		Bonded jacket cable to be LOCA tested to study past results
		H.3 Specialty cables (e.g., Kapton)	1				
		H.4 Similarity criteria	1				

Table 1 (Cont'd)

EQ MAJOR ISSUES	SUB-ISSUES/ DOSSIER TITLE	TOPICS FOR SPECIFIC QUESTIONS TO BE ADDRESSED IN DOSSIER	RESOLUTION CATEGORY*	RECOMMENDED WORK			COMMENTS
				CM	LOCA	OTHER	
Q4 Degradation from typically encountered field conditions is not usually accounted for in the aging simulation process. Does this impact the qualification of cable?	I. Installed Environment	I.1 Hot spots (temperature, radiation, humidity)	3	X	X		CM and LOCA tests will be performed on representative naturally aged samples, if available.
		I.2 Excessive vibration	3	X	X		(Same as I.1)
		I.3 Water/steam/liquid impingement	3	X	X		(Same as I.1)
		I.4 Maintenance activity damage	3	X	X		(Same as I.1)
	J. Installed Configuration	J.1 Bends, vertical runs, overhangs	3	X	X		(Same as I.1)
		J.2 Cable trays, conduits	3	X	X		(Same as I.1)
		J.3 Fire protection coatings	3	X	X		(Same as I.1)
		J.4 Installation damage	3	X	X		(Same as I.1)
Q5 What in situ inspections and condition monitoring techniques or methods are effective in determining (non-destructively) the state of installed cables, and what are the relevant indicators of cable degradation?	K. Condition Monitoring	K.1 Identification of existing and promising methods	1				
		K.2 Link to LOCA survivability	3	X	X		Cables will be preaged and LOCA tested with CM performed periodically.
		K.3 Measure of effectiveness	3	X	X		(Same as K.2)

Table 1 (Cont'd)

EQ MAJOR ISSUES	SUB-ISSUES/ DOSSIER TITLE	TOPICS FOR SPECIFIC QUESTIONS TO BE ADDRESSED IN DOSSIER	RESOLUTION CATEGORY*	RECOMMENDED WORK			COMMENTS
				CM	LOCA	OTHER	
Q6: Based on current knowledge, what technical basis can be developed to demonstrate continued validity of EQ?	L: Maintaining and Extending EQ	L.1 Re-qualification options	3			X	As a parallel effort, insights gained will be used to evaluate the feasibility of a condition-based qualified life
		L.2 Definition of qualified life	3			X	(Same as L.1)
		L.3 Use of operating experience	3			X	(Same as L.1)
		L.4 Extension of qualified life	3			X	(Same as L.1)
Q7: What is the technical basis for considering the graded approach to EQ (DOR vs. NUREG Cat. I&II) acceptable?	M: EQ Graded Approach	M.1 Effect of preaging variations	1				
		M.2 Effect of test parameter margins	1				
		M.3 Effect of test sequence variations	1				
		M.4 Effect of accident profile variations	1				

* Categories: 1. Resolved by past work
2. Unresolved; does not warrant further research
3. Unresolved; warrants further research

REFERENCES

1. U.S. NRC IE Bulletin 79-01B, "Environmental Qualification of Class 1E Equipment," including Attachments and Supplements 1 to 3, 1979.

2. Szukiewicz, A. J., "Interim Staff Position on Environmental Qualification of Safety-Related Electrical Equipment," NUREG-0588, Revision 1, 1979.

3. Code of Federal Regulations, Title 10, Part 50.49, "Environmental Qualification of Electric Equipment Important to Safety for Nuclear Power Plants."

4. IEEE Standard 323-1974, "Standard for Qualifying Class 1E Equipment for Nuclear Power Generating Stations," 1974.

5. U.S. NRC, Office of Nuclear Reactor Regulation, Task Action Plan, "Environmental Qualification (EQ), 10 CFR 50.49," October 1994.

6. Lofaro, R., et. al., "Workshop on Environmental Qualification of Electric Equipment," NUREG/CP-0135, BNL NUREG-52409, May 1994.

7. U.S. NRC, Office of Nuclear Regulatory Research, Research Program Plan, "Reactor Aging and Renewal, Electrical & Mechanical Components: Environmental Qualification of Electric Equipment," July 1994.

8. Subudhi, M., and Lofaro, R. "Literature Review of Environmental Qualification of Class 1E Electric Cables," Brookhaven National Laboratory NUREG/CR-6384, to be published.

9. Bustard, L.D., "The Effect of LOCA Simulation Procedures on Ethylene Propylene Rubber's Mechanical and Electrical Properties," NUREG/CR-3538, SAND83-1258, 1983.

DOE-SPONSORED CABLE AGING RESEARCH AT SANDIA NATIONAL LABORATORIES

K. T. GILLEN, R. L. CLOUGH, M. CELINA, J. WISE AND G. M. MALONE
SANDIA NATIONAL LABORATORIES, ALBUQUERQUE, NM 87185, USA

ABSTRACT

Cables have been identified as critical components requiring detailed technical evaluation for extending the lifetime of Light Water Reactors beyond 40 years. This paper highlights some of the DOE-sponsored cable aging studies currently underway at Sandia. These studies are focused on two important issues: the validity of the often-used Arrhenius thermal aging prediction method, and methods for predicting lifetimes in combined thermal-radiation environments. Accelerated thermal aging results are presented for three cable jacket and insulation materials, which indicate that hardening of the outside surface has an Arrhenius temperature dependence and correlates well with reductions in ultimate tensile elongation. This suggests that the indentor approach is a promising NDE technique for cable jacket and unjacketed insulation materials installed in thermally-dominated regions of nuclear power plants.

INTRODUCTION

In the task of extending the lifetime of Light Water Reactors beyond 40 years, cables have been identified as important components requiring detailed technical evaluation. Polymeric components (e.g., insulation and jacketing materials) represent some of the most critical and potentially susceptible cable materials. In particular, NRC comments on the Low-Voltage, Environmentally-Qualified Cable Industry Report [1] focused on the uncertainties and possible insufficiency of data regarding (1) synergistic and dose-rate effects and (2) the Arrhenius thermal aging methodology. Our aging research program is attempting to develop unique experimental techniques and aging models that will help resolve both of these issues. We have derived an aging approach to handle synergistic and dose-rate effects [2-6]. This methodology, which we refer to as time-temperature-dose rate superposition, has been successfully applied to several important nuclear power plant cable materials. We are also developing a detailed understanding of the Arrhenius methodology and methods for testing its validity [7-8]. This paper highlights our recent investigations of nuclear cable materials and describes some counterintuitive combined environment studies on crosslinked polyolefin (CLPO) cable insulation materials in which mechanical degradation slows as the aging temperature is raised.

RESULTS AND DISCUSSION

Thermal Aging Studies

Predictions and/or simulations of the lifetimes of nuclear power plant cable materials exposed to aging environments dominated by thermal effects are typically based on the Arrhenius methodology. This approach was derived from the knowledge that the rate of a chemical reaction is usually proportional to $\exp(-E_a/RT)$, where E_a is the Arrhenius activation energy, R is the gas constant and T is the absolute temperature. Although the polymers comprising cable materials degrade by a complex series of chemical reactions, steady state kinetic analysis of these reactions typically yields a rate expression with an approximately Arrhenius temperature dependence, where E_a represents an effective activation energy for the underlying mix of reactions. If the overall degradation mechanism remains unchanged throughout the experimental temperature range, the logarithm of the time to a given amount of degradation (property change) should be linearly related to the inverse absolute temperature, yielding Arrhenius behavior.

Figure 1 shows ultimate tensile elongation data versus aging time at five aging temperatures for a nitrile rubber material [7,8]. As shown in Fig. 2, these data display excellent Arrhenius behavior when analyzed at $e/e_0 = 0.75$, 0.5 and 0.25 [7]. A more rigorous analysis uses the time-temperature superposition principle to shift all of the data of Fig. 1 to a common reference temperature, T_{ref} [2,5]. This is accomplished by multiplying the times appropriate to experiments conducted at each temperature T by a shift factor, a_T, given by

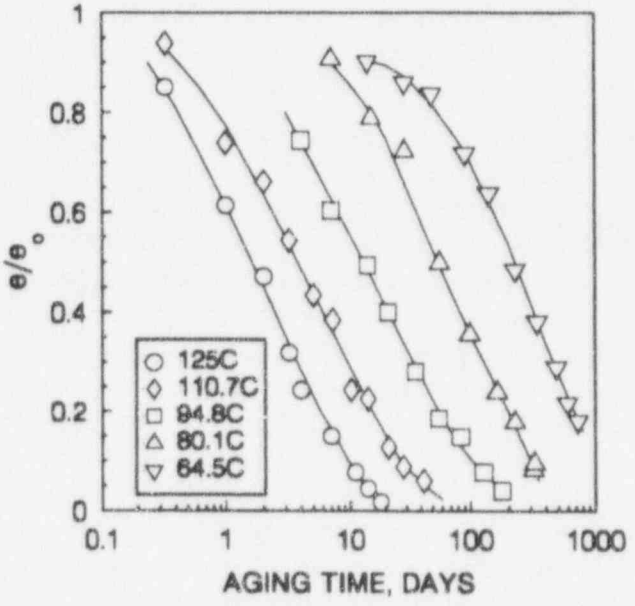

Fig. 1. Ultimate tensile elongation (e) of the nitrile rubber normalized to its unaged value (e_0) versus air-oven aging time and temperature.

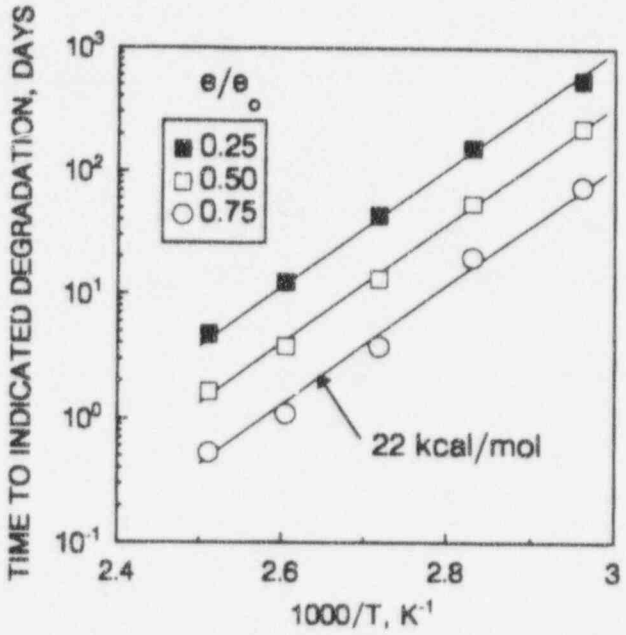

Fig. 2. Conventional Arrhenius plots of elongation results for the nitrile rubber.

$$a_T = \exp\{(E_a/R)\,[(T_{ref})^{-1} - (T)^{-1}]\}$$

Figure 3 shows time-temperature superposed results at a reference temperature of 50°C for the data of Fig. 1 using an E_a of 22 kcal/mol. Excellent superposition occurs, which is not surprising given both the linearity of the Arrhenius plots in Fig. 2 and the independence of the slopes to the amount of damage. In comparing the normal Arrhenius analysis approach with time-temperature superposition, it should be noted that the former uses a processed, truncated data set (typically a single degradation level such as $e/e_0 = 0.5$). The time-temperature superposition approach is superior because the entire data set is used to determine the activation energy (E_a) and to confirm Arrhenius behavior.

Although the Arrhenius model appears to work for many materials, closer scrutiny raises some significant concerns. For example, Arrhenius behavior is often observed for ultimate tensile elongation results, whereas the (typically unreported) ultimate tensile strength data from the same mechanical property tests are non-Arrhenius. This non-Arrhenius behavior is seen for the nitrile material in Fig. 4, when its tensile strength data are time-temperature superposed using the same 22 kcal/mol E_a found to apply to the elongation data. In fact, it is clear from this figure that the tensile strength data could never be superposed, since it drops in the latter stages at some temperatures and increases at others.

The apparent contradiction between the elongation and tensile strength results was resolved [7,8] through the use of our unique modulus profiling apparatus [9,10]. This technique allows us to quantitatively map the modulus of a material with ~50μm resolution. After aging, samples were cut and modulus measurements were taken across the sample cross-section. Figure 5 shows

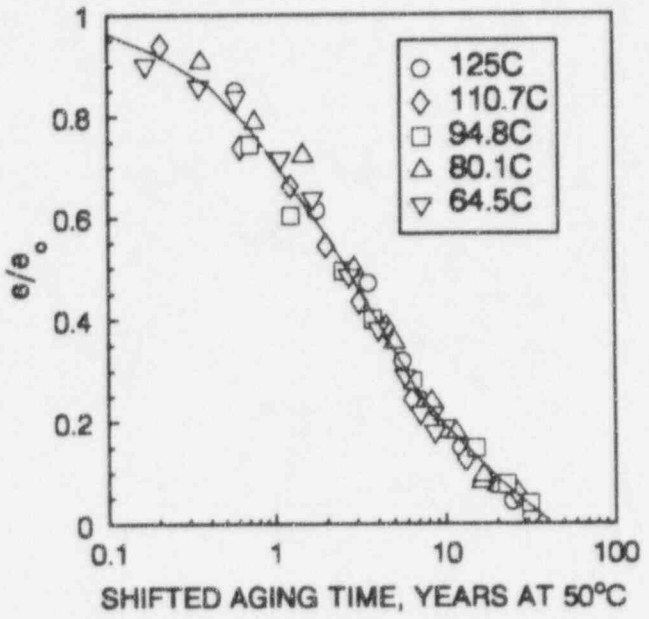

Fig. 3. Time-temperature superposition of the data from Fig. 1 using E_a = 22 kcal/mol.

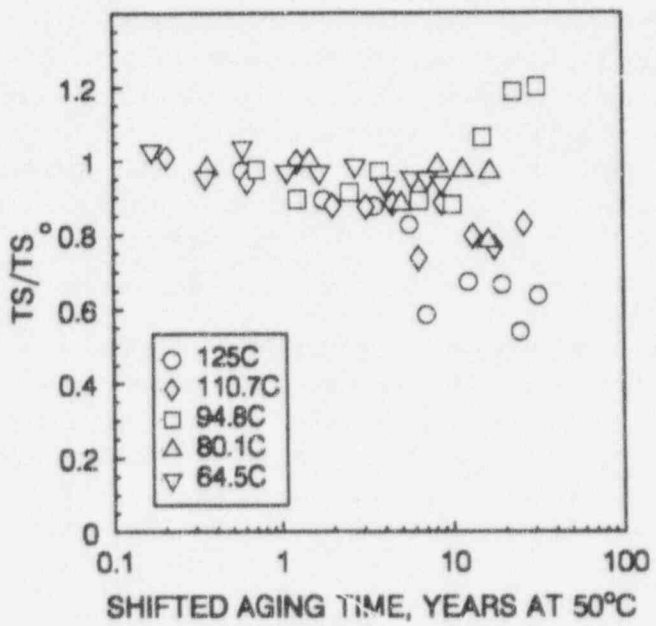

Fig. 4. Time-temperature superposition of the normalized nitrile ultimate tensile strength data using E_a = 22 kcal/mol.

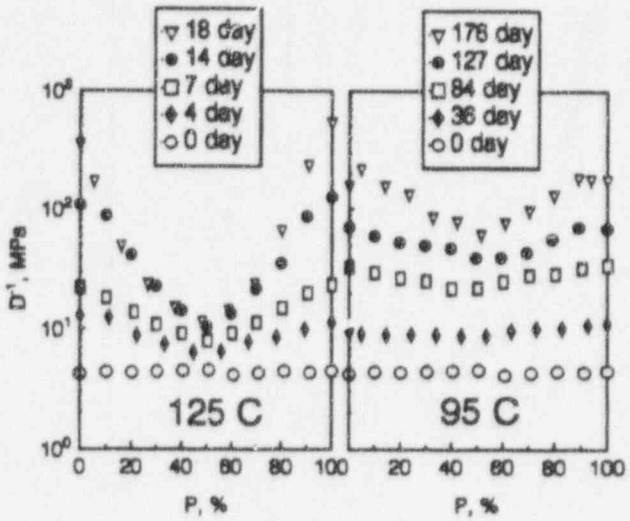

Fig. 5. Modulus profiles for 2.0-mm thick nitrile rubber samples after aging for various times at the indicated temperatures. The abscissa, P, refers to the percentage of the total distance from one air-exposed sample surface to the opposite air-exposed surface.

representative results at the highest temperature (125°C) and an intermediate temperature (95°C), where P refers to the percentage of the distance from one air-exposed surface of the sample to the opposite air-exposed surface. The heterogeneous behavior observed is very common under typical air-oven aging conditions and is due to diffusion-limited oxidation (DLO). This phenomenon leads to equilibrium oxidation at the air-exposed sample surfaces and reduced or non-existent oxidation towards the sample interior [7-11]. The importance of DLO depends upon sample thickness and the competition between oxygen consumption in the material and the diffusion rate of oxygen into the material [12,13]. Since the E_a for oxygen consumption is typically much larger than that for oxygen diffusion, the importance of DLO normally drops as the temperature is lowered, as seen in Fig. 5.

Since the tensile strength of a material is dependent upon the integrated force across a material at tensile failure, the presence of temperature-dependent DLO effects (Fig. 5) can be used to explain the failure of the Arrhenius model for this property. For the elongation, modulus values (related to hardness) are maximum at the surface, where equilibrium oxidation occurs. During tensile testing, cracks can be expected to initiate in the most embrittled portion of the material, which, due to DLO, will be the surface. If these cracks, once initiated, propagate quickly through the material, then the equilibrium surface oxidation will determine (and have the same E_a as) the tensile elongation. This turns out to be the case [7,8], as demonstrated in Fig. 6, which shows that the surface modulus values have an excellent correlation with the normalized elongation results.

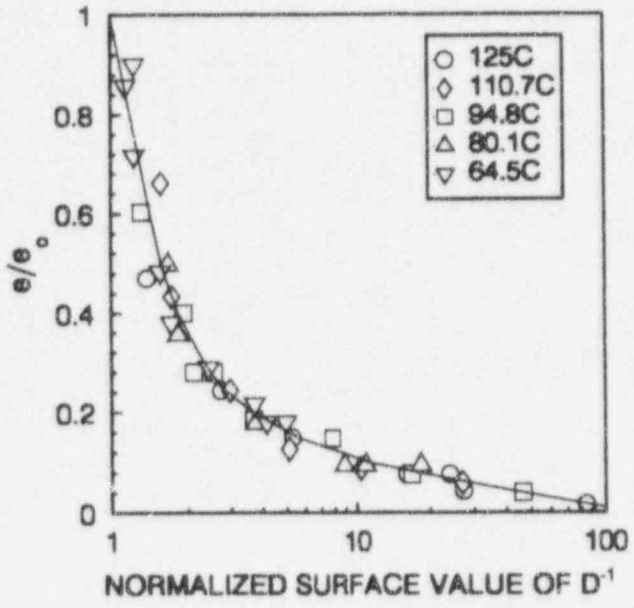

Fig. 6. Normalized elongation (e/e_o) plotted versus the normalized surface modulus for the nitrile rubber.

Many of the behaviors noted above for the nitrile material are commonly observed for other elastomeric materials. For instance, we have documented surface modulus increases (oxidative hardening), important DLO effects and immediate propagation of surface-initiated cracks for neoprene and styrene butadiene rubber materials [7]. Theoretical modeling of typical accelerated air-oven aging conditions indicates that DLO effects should be quite common for ~1 mm thick polymeric materials [14]. But these behaviors cannot be assumed to be universal, as we will now show for three nuclear cable materials.

One cable material studied was a 15 mil individual hypalon jacket wrapped over the EPR insulation from a three conductor Anaconda Flame-Guard FR-EP cable. The three hypalon individual jackets were all black but two had "painted" white and red surfaces to distinguish conductors. To minimize DLO effects material was separated from the overall jacket and insulation and then oven-aged at temperatures ranging from 100°C to 150°C. Modulus profiles were obtained on the material with the white outer surface; results for aging at 150°C are shown in Fig. 7. Except for a small increase at the outer surface presumably caused by the presence of the harder white "paint", the profiles are flat for both unaged and aged materials. Since similarly shaped profiles occur at lower temperatures, DLO effects are insignificant over the entire temperature range, not unexpected given the small sample cross-section.

The best time-temperature superposition of the tensile elongation results for this hypalon material occurs using an E_a of 25.5 kcal/mol; this is shown in Fig. 8 at a T_{ref} of 50°C. The same value of E_a also leads to excellent superposition of the tensile strength data (not shown), which is not surprising given the absence of any important DLO effects. Based on our earlier discussion, we expect the decrease in tensile properties to be based on the modulus increases resulting from

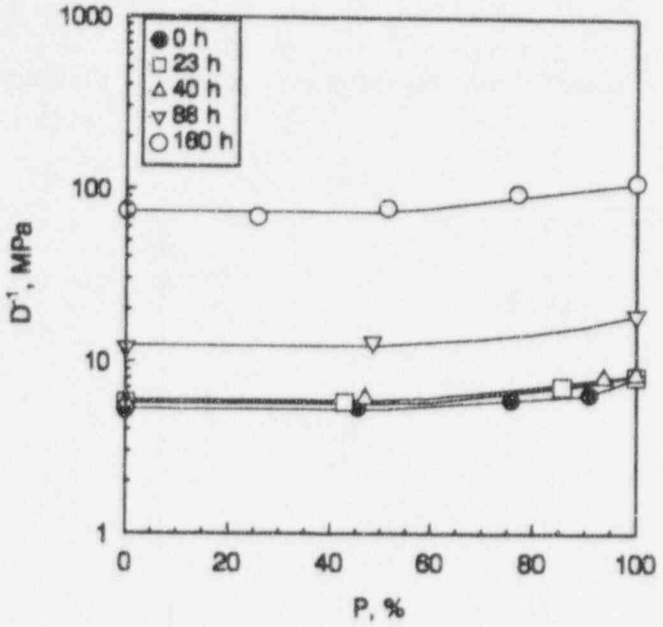

Fig. 7. Modulus profiles for 0.4 mm thick Anaconda hypalon samples after aging for the indicated times at 150°C.

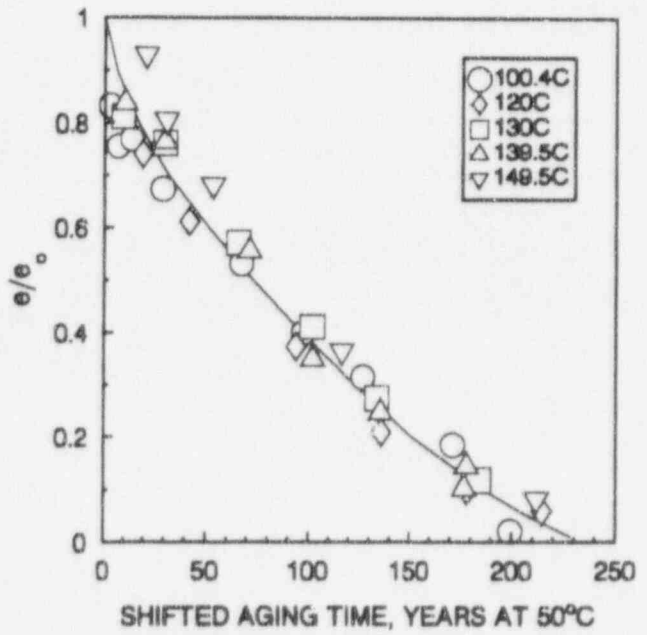

Fig. 8. Time-temperature superposition of the normalized elongation data for the Anaconda hypalon using E_a = 25.5 kcal/mol.

oxidative crosslinking. These modulus increases versus time and temperature are plotted in Fig. 9. As expected, excellent time-temperature superposition of these data occurs for E_a = 25.5 kcal/mol (Fig. 10). Finally, Fig. 11 shows the excellent correlation between modulus and tensile elongation.

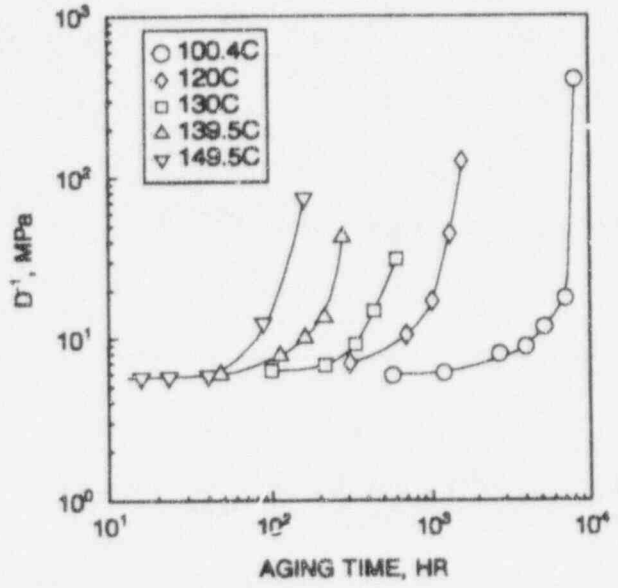

Fig. 9. Modulus values of the Anaconda hypalon versus aging time at the indicated air-oven aging temperatures.

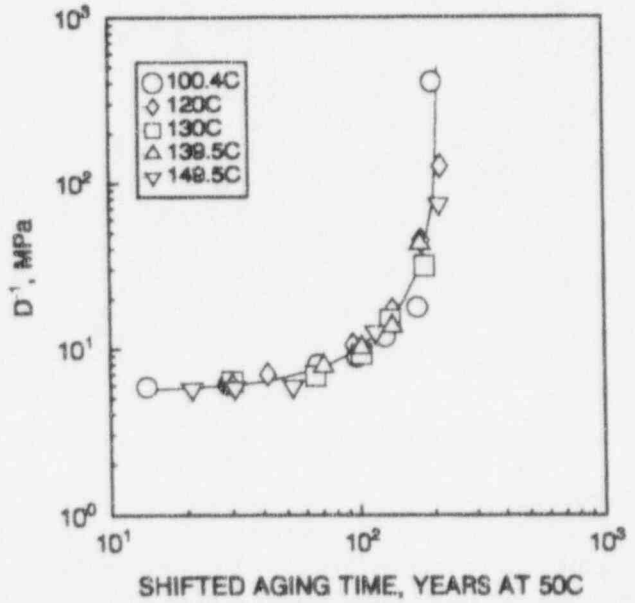

Fig. 10. Time-temperature superposition of the modulus results from Fig. 9 using E_a = 25.5 kcal/mol.

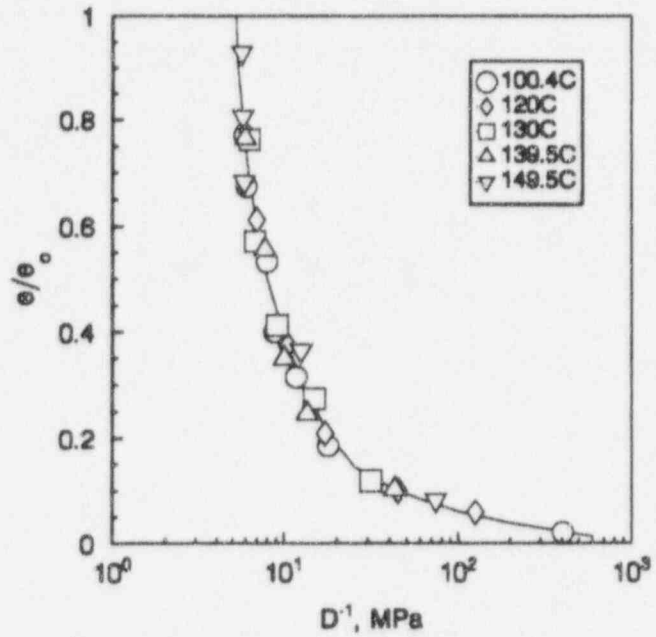

Fig. 11. Normalized elongation (e/e_o) plotted versus the normalized surface modulus for the Anaconda hypalon.

From this figure, we conclude that substantial material degradation occurs when the material modulus increases to ~30 MPa.

The second cable material is another hypalon, the FR jacket of a single conductor Kerite FR cable. Although this material had a number of unusual behaviors, it will be apparent that its overall behavior is generically similar to that of the Anaconda hypalon. Mechanical property data were taken versus time at approximately 10°C intervals from 160°C to 90°C. Figure 12 shows a conventional Arrhenius plot for four levels of change in ultimate tensile elongation value. For the five lowest temperatures, parallel lines corresponding to an Arrhenius activation energy of 26 kcal/mol accurately describe the data, but slight deviations are apparent at the three highest temperatures of 140°C, 150°C and 160°C. It turns out that modulus profile results and theoretical calculations [13,14] indicate the presence of important DLO effects above approximately 130°C, implying that the observed deviation from Arrhenius behavior is due to DLO anomalies. Experimental evidence for these DLO effects is seen in Fig. 13, which shows modulus profile results at 160°C, where P = 0 and P = 100 correspond to the outer and inner surfaces, respectively. Because the Arrhenius model fails above 130°C due to DLO effects, we restrict time-temperature superposition analysis to the data from 130°C to 90°C. The result, shown in Fig. 14, indicates that excellent superposition of the data from this temperature range is possible with an E_a of 26 kcal/mol. The E_a value and the resulting predictions at 50°C for this hypalon material are quite similar to those for the earlier Anaconda hypalon material (25.5 kcal/mol and the predictions shown in Fig. 8).

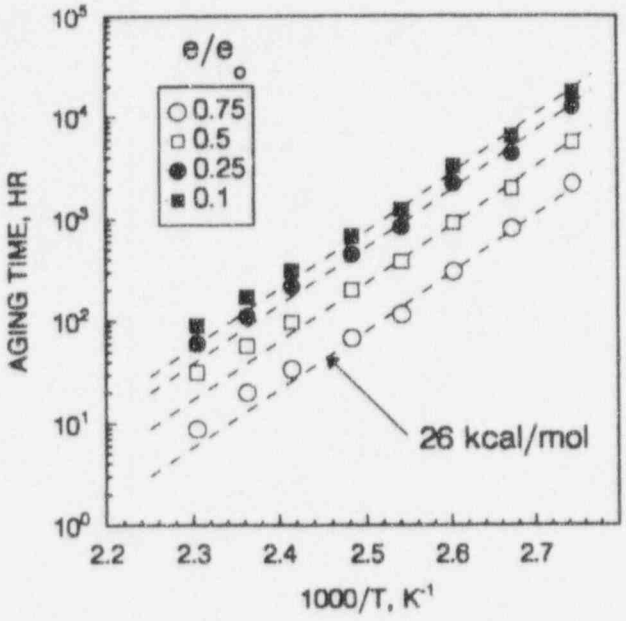

Fig. 12. Conventional Arrhenius plot of elongation results for the Kerite hypalon jacket.

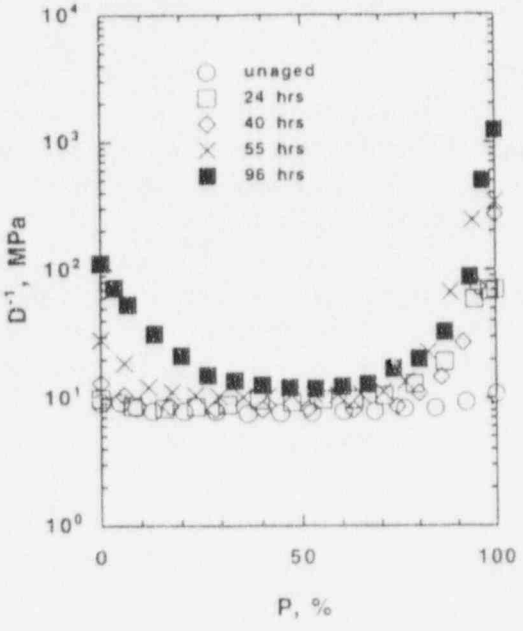

Fig. 13. Modulus profiles for 1.5 mm thick Kerite hypalon jacket materials after aging at 160.7°C for the indicated times. The outside surface of the jacket corresponds to P = 0.

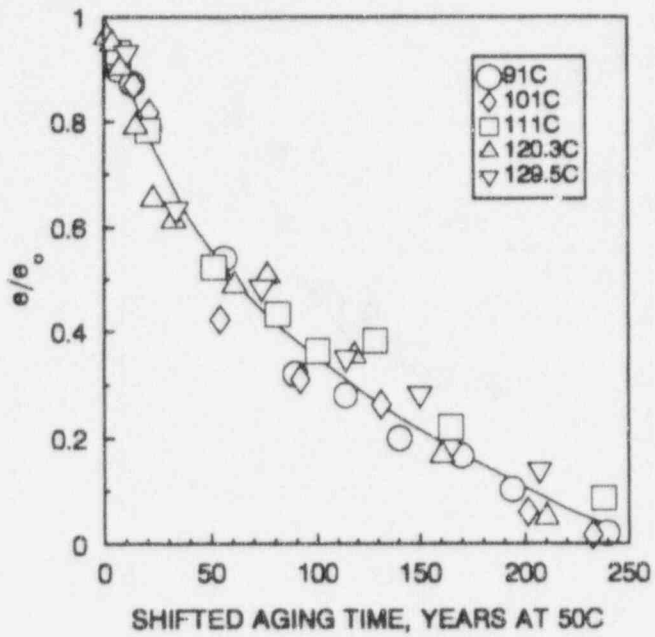

Fig. 14. Time-temperature superposition of the normalized elongation data for the Kerite hypalon jacket using E_a = 26 kcal/mol. Data above 130°C were not used in this plot.

Besides showing strong evidence of DLO effects, the modulus profile results of Fig. 13 show that an enhanced oxidation mechanism occurs near the inside surface of the material (P = 100). It turns out, however, that the enhanced inside oxidation is not correlated to mechanical failure (manuscript in preparation). We therefore examine the Arrhenius behavior of the modulus at the outside surface of the material, since this will be correlated to the equilibrium oxidation in the absence of DLO effects. Following the procedure used in Figs. 9 and 10 for the Anaconda hypalon, we carry out time-temperature superposition on the outside modulus results for the Kerite jacket, and find that 26 kcal/mol gives excellent superposition, as seen in Fig. 15. This is the same E_a determined for the elongation data at temperatures ranging from 90°C to 130°C, which adds confidence to the predicted extrapolations of Fig. 13 and confirms that the outside surface modulus is an ideal parameter for determining the Arrhenius E_a and is an excellent predictor of jacket condition. The slight deviations from Arrhenius behavior for elongation data above 130°C indicates that cracks do not immediately propagate at the higher temperatures where DLO effects are present.

The third cable material studied was the FR insulation of the Kerite FR single conductor cable, a proprietary compound. Oven aging was run at temperatures ranging from approximately 160°C to 120°C and the tensile elongation results gave excellent time-temperature superposition with an E_a of 23 kcal/mol, as seen in Fig. 16. The same value of E_a led to superposition of the outside surface modulus values from modulus profiling results. Therefore we again find a reasonable correlation between the modulus changes and tensile elongation results (Fig. 17).

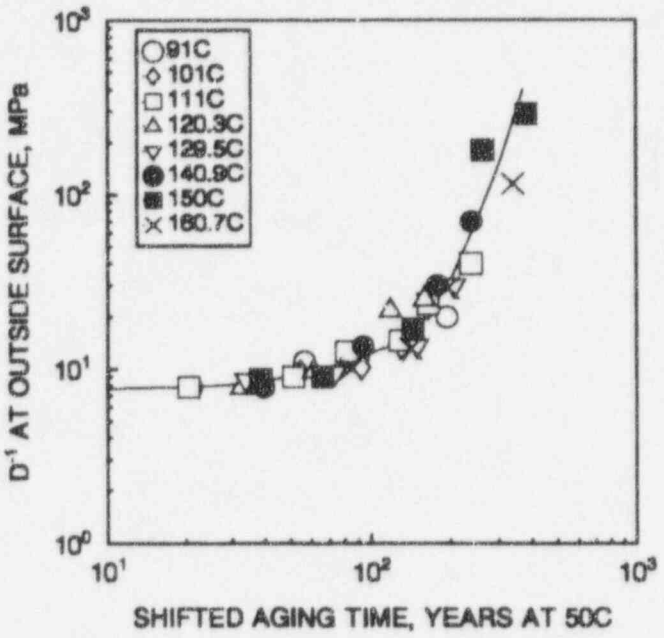

Fig. 15. Time-temperature superposition of the outside surface modulus values for the Kerite hypalon jacket material using E_a = 26 kcal/mol.

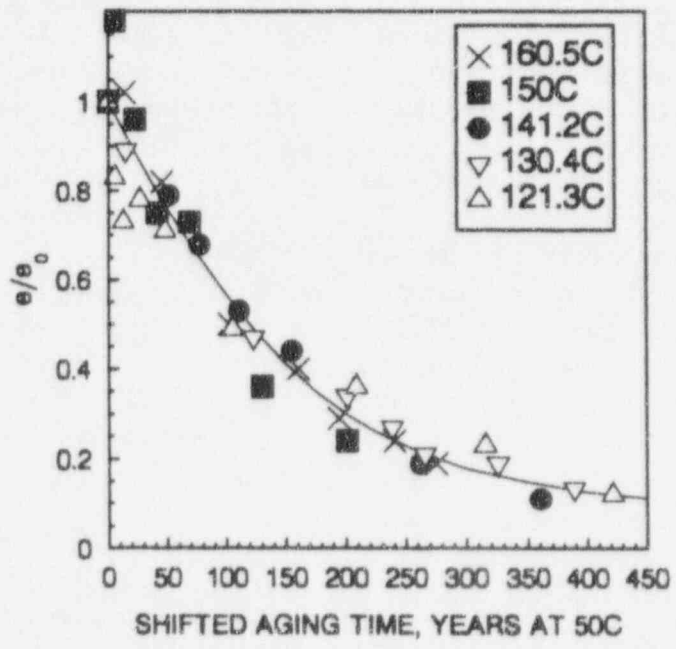

Fig. 16. Time-temperature superposition of the normalized elongation data for the Kerite FR insulation using E_a = 23 kcal/mol.

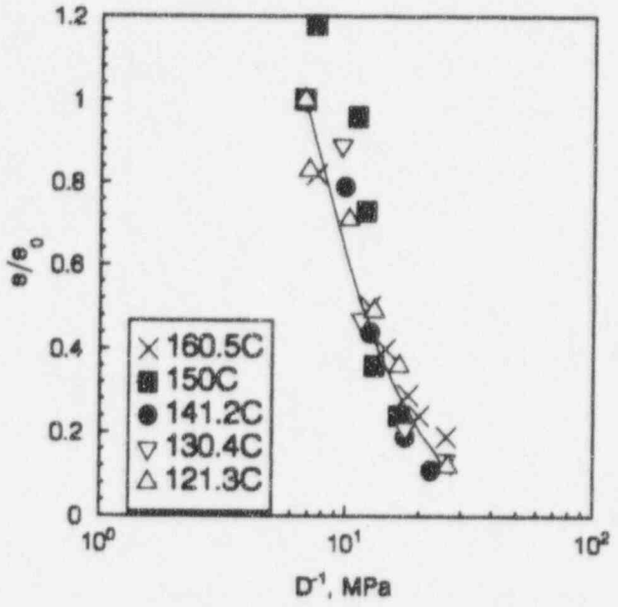

Fig. 17. Normalized elongation (e/e_0) plotted versus the normalized surface modulus for the Kerite FR insulation.

Superposition is not achieved, however, when the same E_a is used to shift the tensile strength data, as seen in Fig. 18. Unlike earlier materials where DLO effects caused non-superposition of the tensile strength data, modulus profile results indicate that DLO effects are unimportant for the Kerite insulation material, except for slight effects at 160°C. Therefore the tensile strength results implicate changes in the chemical mechanism. They, in fact, suggest that the relative mix between scission and crosslinking events (the former tending to decrease tensile strength, the latter tending to raise it) favors a relative decrease in scission as the temperature is lowered. This evidence of a change in the mix of reactions as the temperature is lowered raises concerns over the extrapolation of the high temperature results (160°C to 120°C) to the temperatures of relevance to nuclear power plant aging (e.g., 50°C). For this reason, we are currently using ultrasensitive techniques to obtain oxygen consumption data for this material from 160°C down to temperatures approaching 50°C. These data should allow us to determine whether there is evidence of a change in E_a for oxygen consumption over the extrapolation region. If no evidence is found, it would suggest that the E_a for elongation and modulus should not change significantly.

The above results make it clear that perhaps the two best parameters for measuring degradation and making lifetime predictions are the ultimate tensile elongation and the surface modulus of the material. When DLO effects are important, tensile strength data are often meaningless, but elongation and surface modulus results can still be correlated if cracks that initiate at the hardened surfaces of materials quickly propagate through the material. When surface-initiated cracks do not propagate, elongation data can become non-Arrhenius and only the surface modulus data remain predictive of the true E_a for the degradation mechanism. This

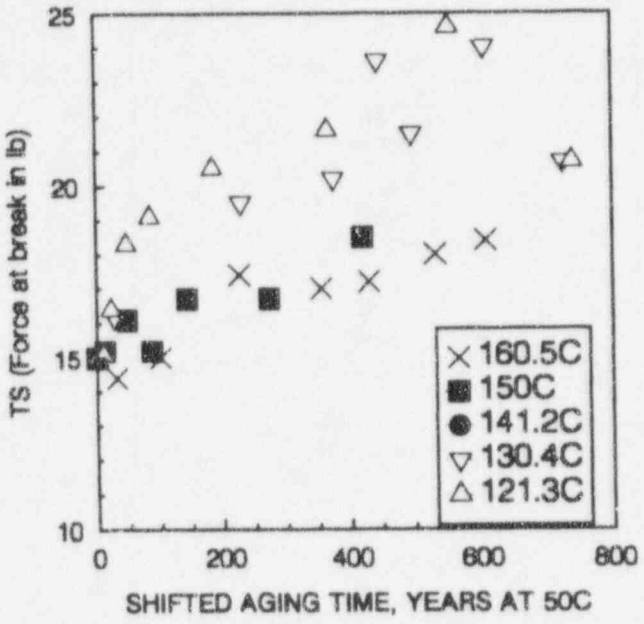

Fig. 18. Time-temperature superposition of the tensile strength data for the Kerite FR insulation using the same activation energy (23 kcal/mol) found to superpose the elongation results in Fig. 16.

discussion offers compelling evidence that the indentor approach is a promising non-destructive evaluation technique for thermal-dominated regions of nuclear power plants [15-17]. This specially designed portable test apparatus measures the penetration force of a blunt, conical probe as a function of penetration depth into the jacket of a cable. A slope (units of force per length) is extracted from the force versus penetration curve. This leads to the so-called "indenter modulus", which, though not a true modulus (units of force per area), is closely related to modulus. Although the indenter modulus is sensitive to more than just the surface modulus value, the relative importance of subsurface values diminishes with depth, implying that it is dominated by near surface modulus values. In addition, under the long-term, low-temperature aging occurring under ambient nuclear power plant conditions, DLO effects will be minimal, implying that relatively homogeneous modulus values might be expected. If correlations like those shown in Figs. 6, 11 and 17 can be made for important cable materials and if the resulting surface modulus values can be correlated with indenter modulus results, the indenter approach may prove to be the most viable NDE technique for assessing the condition of thermally-dominated, in-plant cable jackets.

Combined Radiation Plus Temperature Studies- Yankee Rowe cables

In earlier reports [2-6], we introduced and tested a time-temperature-dose rate superposition methodology which can be used for making predictions under combined radiation plus temperature environments, even in the presence of dose-rate and synergistic effects. When applicable, the methodology allows predictions to be made at the low dose rates existing under ambient nuclear power plant aging conditions. The methodology was successfully applied to many

nuclear cable materials, and extrapolated predictions from the model were verified by comparisons with intermediate-term (7 to 12 year) results for similar or identical materials aged in nuclear environments. The methodology failed for several EPR and CLPO materials in which it was found that, at a constant dose rate, a decrease in aging temperature surprisingly increased the rate of mechanical degradation.

We are currently receiving naturally aged cables from Yankee Rowe, some of which were installed around 1960 (silicone, polyethylene, PVC and butyl materials), others in the late 70's and early 80's (CLPE, CLPO, neoprene, hypalon materials). We are attempting to obtain materials that came from high radiation aging areas of the plant (dose rates greater than 1 R/hr) and high temperature regions (greater than 45°C) either singly or in combination. Yankee Rowe will provide best estimates of the average environments seen for each section of cable. If available, Yankee Rowe will also supply us with "unaged" warehouse cables corresponding to the plant-aged cables, and sections of the plant-aged cables from benign aging environments. These materials will be used to estimate baseline properties and as sources of "unaged" materials for accelerated simulations.

We will use various techniques (e.g., tensile properties, infrared analyses, swelling, solubility, density, modulus profiling) to determine the levels of degradation in the materials. For materials removed from higher radiation environments, we will generate combined environment data at our radiation-aging facility to test the time-temperature-dose rate superposition methodology. If the material is from a generic class of previously studied materials [2-4], we will compare the generic model predictions with the ambient-aged cable material results. Yankee Rowe materials dominated by thermal aging will be used to test the Arrhenius thermal aging methodology.

Combined Radiation Plus Temperature Studies- Anomalous Materials

We find unusual behaviors for several CLPO and EPR materials, where the combined environment degradation rate under constant dose-rate conditions can *increase* as the temperature is lowered. As one example, combined environment experiments were run on a Brandrex CLPO insulation material using dose rates ranging from 17 Gy/h to 5200 Gy/h (1 Gy = 100 rad) at temperatures from 22°C to 120°C. Tensile tests versus aging time at each combined environment were used to estimate the dose required for the ultimate tensile elongation to decrease to 100% absolute (initial value was ~310%). The resulting values of dose to equivalent damage (DED) are plotted in Fig. 19 versus dose rate and temperature. DED plots are useful for discussing and analyzing combined environment data, since a dose-rate effect at a selected temperature can be immediately recognized if the DED values depend on dose rate. For the Brandrex CLPO, the higher temperature results (60°C and higher) shown in Fig. 19 are consistent with expectations. That is, under constant dose-rate conditions, the degradation rates increase as the temperature increases. But the results at 41°C and 22°C (solid symbols) are counterintuitive, since they show that the degradation rate at these temperatures are approximately 2.5 to 3 times faster than at 60°C. Gel content data, shown in Fig. 20, give further evidence for a fundamental difference in degradation mechanism at these lower temperatures. The gel content is sensitive to the polymer network properties and intrinsically related to the competition between chain scission and crosslinking events, which are the molecular level basis of the degradation (the former tends to

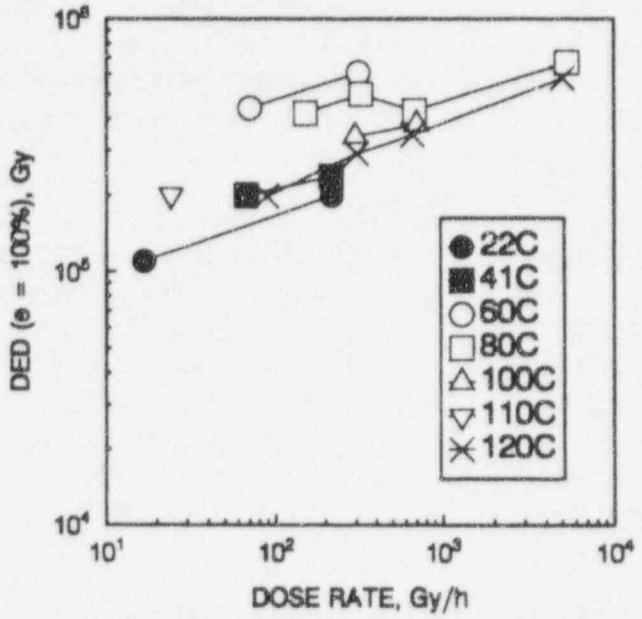

Fig. 19. Dose required for the ultimate tensile elongation of the Brandrex CLPO to decrease to 100% (initial value of 310%) versus dose-rate and temperature.

decrease gel content, while the latter tends to increase it). The results shown in Fig. 20 indicate that high temperature dominance by crosslinking switches abruptly to low temperature dominance by chain scission.

Similar behaviors exist for other CLPO materials. As an example, selected results from our studies and from a long-term, low dose-rate program [18] are plotted in Fig. 21 for a Rockbestos CLPO. Degradation rates are again faster at 22°C and 40°C than at higher temperatures, but for this material, the rates continue to decrease until the temperature reaches approximately 100°C.

Since ambient nuclear power plant aging temperatures are often in the range of approximately 20°C to 50°C, these counterintuitive effects must be understood before confident lifetime predictions for such materials can be generated. These CLPO materials are semi-crystalline, and melting plus reforming of crystallites (equivalent to molecular rearrangements) occurs over most of the temperature ranges investigated in Figs. 19 and 21. In fact, the dangers of extrapolating accelerated aging results across a transition of a material or modeling results through a transition region, such as the crystalline melting point region, are well recognized [2-6]. The relative changes in the amorphous fraction and the relative molecular mobility at different temperatures will clearly be one contribution to the observed behavior. We have also determined that reactivities of hydroperoxide species, which are important intermediates in the chemistry, appear to influence these anomalous effects. We are currently using a variety of techniques, including annealing experiments, oxygen consumption measurements, differential scanning

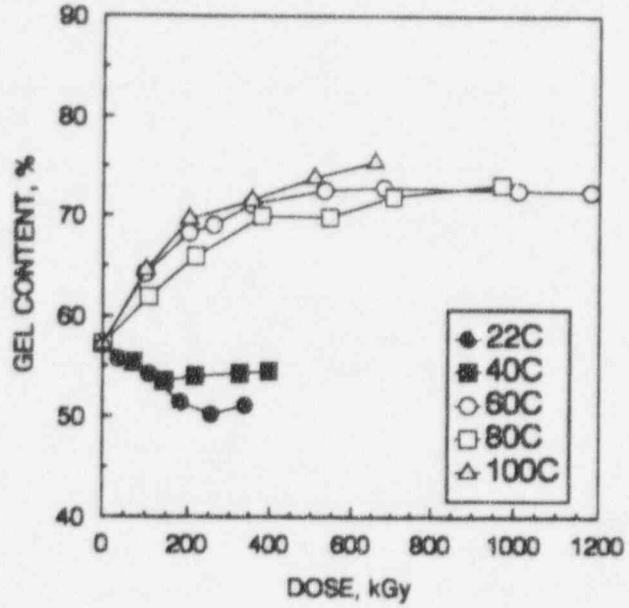

Fig. 20. Gel content results versus temperature for combined environment aging of Brandrex CLPO at dose rates of ~250 Gy/h.

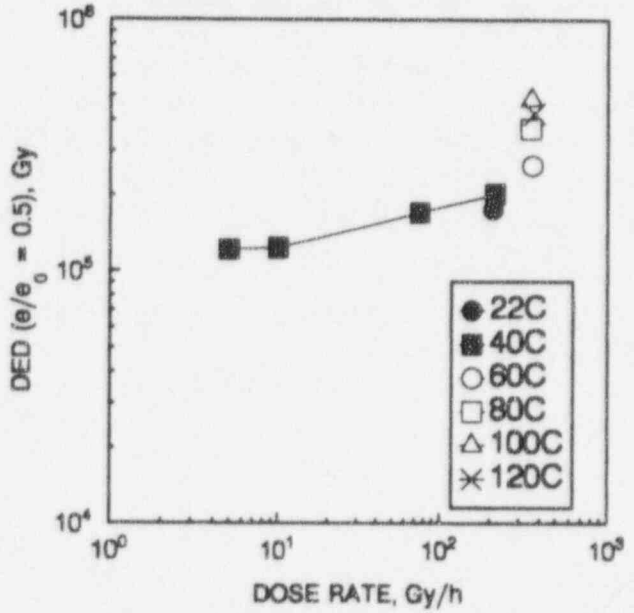

Fig. 21. Dose required for the normalized ultimate tensile elongation (ϵ/ϵ_0) to reach 0.5 versus dose-rate and temperature.

calorimetry, infrared analyses, density, solubility and swelling, to further understand the basis and extent of these complex effects.

ACKNOWLEDGMENT

This work was supported by the United States Department of Energy under Contract DE-AC04-94AL85000.

REFERENCES

1. Bustard, L. and Holtzman, P., "Low-Voltage Environmentally-Qualified Cable License Renewal Industry Report; Revision 1", TR-103841 (July, 1994).
2. K. T. Gillen and R. L. Clough, "Time-Temperature-Dose Rate Superposition: A Methodology for Predicting Cable Degradation Under Nuclear Power Plant Aging Conditions", Sandia Labs Report, SAND88-0754 (August, 1988).
3. K. T. Gillen and R. L. Clough, "Predictive Aging Results for Cable Materials in Nuclear Power Plants", Sandia Labs Report, SAND90-2009 (November, 1990).
4. K. T. Gillen and R. L. Clough, "Aging Predictions in Nuclear Power Plants- Crosslinked Polyolefin and EPR Cable Insulation Materials" Sandia Labs Report SAND91-0822 (June, 1991).
5. K. T. Gillen and R. L. Clough, "Accelerated Aging Methods for Predicting Long-Term Mechanical Performance of Polymers", in **Irradiation Effects on Polymers,** D. W. Clegg and A. A. Collyer, Eds., Elsevier Applied Science, London, 1991., Ch. 4.
6. K. T. Gillen and R. L. Clough, "Predictive Aging Results in Radiation Environments", Rad. Phys. and Chem., 41, No. 6, 803 (1993).
7. K. T. Gillen, R. L. Clough and J. Wise, "Predicting Elastomer Lifetimes from Accelerated Thermal Aging Experiments", in **Advances in Chemistry Series No. 249, Lifetime, Degradation and Stability of Macromolecular Materials**, R. L. Clough, K. T. Gillen and N. Billingham, Eds., ACS Books, Washington, D. C., in press.
8. J. Wise, K. T. Gillen and R. L. Clough, "An Ultrasensitive Technique for Testing the Arrhenius Extrapolation Assumption for Thermally-Aged Elastomers", Polym. Degrad. & Stabil., in press.
9. K. T. Gillen, R. L. Clough and C. A. Quintana, "Modulus Profiling of Polymers", Polym. Degrad. & Stabil., 17, 31 (1987).
10. K. T. Gillen and R. L. Clough. "Polymer Insights Available from Modulus Profiling Data.", Polym. Eng. and Sci., 29, 29 (1989).
11. R. L. Clough and K. T. Gillen, "Oxygen Diffusion Effects in Thermally Aged Elastomers", Polym. Degrad. & Stabil., 38, 47 (1992).
12. A. Cunliffe and A. Davis, Polym. Degrad. & Stabil., 4, 17 (1982).
13. K. T. Gillen and R. L. Clough, "Rigorous Experimental Confirmation of a Theoretical Model for Diffusion-Limited Oxidation", Polymer, 33, 4358 (1992).
14. J. Wise, K. T. Gillen and R. L. Clough, "Quantitative Model for the Time Development of Diffusion-Limited Oxidation Profiles", submitted for publication.
15. G. J. Toman, and G. Sliter, "Development of a Nondestructive Mechanical Condition Evaluation Test for Cable Insulation", Proceedings: Operability of Nuclear Power Systems in Normal and Adverse Environments, Albuquerque, New Mexico, September 29- October 3, 1986.

16. J. B. Gardner and T. A Shook, "Status and Perspective Application of Methodologies from an EPRI Sponsored Indenter Test Project", Proceedings: Workshop on Power Plant Cable Condition Monitoring, EPRI EL/NP/CS-5914-SR, July, 1988.
17. G. J. Toman, S. Hunsader and D. Peters, "In-Plant Indenter Use at Commonwealth Edison Plants", Proceedings of the EPRI Power Plant Cable Condition Monitoring Workshop, February 9-11, 1993, San Francisco.
18. Atal, F. Carlin, J. Chenion, G. Gaussens and P. Le Tutour, "Aging Program Generated by Long-Term Irradiation of Electrical Links (VEILLE)", Progress Report No. 11, CIS International, Saclay, August 18, 1993.

DOE-SPONSORED AGING MANAGEMENT GUIDELINE FOR ELECTRICAL CABLE AND TERMINATIONS

R.F. Gazdzinski
Ogden Environmental and Energy Services, Inc.
1777 Sentry Parkway West, Suite 300
Blue Bell, PA 19422

I. Abstract

The DOE-sponsored Aging Management Guideline (AMG) for Electrical Cable and Terminations provides an analysis of the potential age-related degradation mechanisms and effects for low-voltage and medium-voltage extruded cables and associated terminations used in commercial nuclear power plants. The AMG examined historical industry failure data and correlated this with postulated aging mechanisms and effects. Existing and developmental testing and condition monitoring techniques were evaluated, as well as current industry practices, in order to assess whether all significant aging mechanisms/effects are being effectively managed. Results of the study indicate that some aging mechanisms and effects are not directly addressed by current industry maintenance and surveillance practices; however, empirical evidence indicates that low- and medium-voltage cable and terminations are in general very reliable. A limited number of nondestructive (or essentially nondestructive) techniques currently available are potentially useful for evaluating low-voltage cable condition; however, such techniques do not currently exist for monitoring medium-voltage cable. Troubleshooting or diagnostic techniques are available to identify certain types of degradation.

II. Purpose and Objective

To operate a nuclear plant beyond the original licensing period, utilities must show that the aging of components within the scope of the license renewal rule is managed such that these components will not degrade to the extent that they are incapable of performing their intended function(s). The purpose of the AMG is to provide guidance for the effective management of aging of low- and medium-voltage electrical cable and associated terminations used in nuclear power plants[1] which will provide assurance of continued functionality during both the current and license renewal term. The AMG provides an analysis of the potential age-related degradation mechanisms and effects for low- and medium-voltage electrical cable and terminations, and acceptable guidelines for developing aging management programs for controlling significant degradation mechanisms/effects. Use of these guidelines can provide utilities with a basis for verifying that effective means for managing age-related degradation of cable systems have

[1] High-voltage systems were not included within the scope of this document because they generally constitute an extremely small fraction of the total cable population at any given plant, and are often highly specialized in construction (i.e., oil filled) with little commonality to the more prevalent low- and medium-voltage systems.

been established, or structuring such programs if not currently in existence. A suggested methodology for performing an aging management review pursuant to 10CFR54 is also provided.

III. Methodology

The study evaluates the main subsystems within cable, including the conductors, insulation, shielding, tape wraps, jacketing, drain wires, as well as all subcomponents associated with each type of termination. The principal aging mechanisms[2] and effects resulting from environmental and operating stresses on these systems were identified, evaluated, and correlated with actual plant experience (including NPRDS, LER, and host utility data) to determine if they are actually being experienced. Those postulated mechanisms/effects which were also observed in the empirical data were termed "significant and observed." Installation stressors were also examined. Then, the maintenance procedures and condition monitoring/testing methodologies used by plant operators were evaluated to determine if the effects of these significant and observed aging mechanisms and effects are being detected and managed. Other available and developmental testing and condition monitoring techniques are also identified and discussed. Where an aging mechanism or effect appeared not to be fully managed or not considered, additional plant-specific activities to manage the aging mechanism/effect were identified and recommended.

IV. Scope

The equipment covered by the guideline includes all low- and medium-voltage cables and their terminations. Cable trays, penetrations, conduit, conduit seals, and other ancillary equipment are not directly addressed; however, potential interactions between these components and cables and terminations are examined.

The group of cables and terminations described in 10CFR54 as being within the scope of the license renewal rule includes (1) safety-related; (2) non-safety-related whose failure could prevent satisfactory accomplishment of a safety-related function; and (3) those relied on in safety analyses or plant evaluations to perform a function that demonstrates compliance with the NRC regulations for environmental qualification (10CFR50.49), pressurized thermal shock (10CFR50.61), etc. Additionally, those cables not included in one of the above categories yet important to continuity of power production or some other aspect of plant operation may be considered.

Classification of cable systems was conducted in terms of their voltage rating; low-voltage (600 Vac and below/250 Vdc and below) and medium-voltage (2 kVac through 15 kVac) systems were considered. The great majority of plant circuits fall within the low-voltage category. Cable systems were also further grouped according to use or function. Categories of plant cable based on use include power, control, and instrumentation cable, local and panel wire, telephone/security cable, thermocouple extension wire, specialty cable[3], lighting cable, and grounding cable.

---

[2] Aging mechanisms were evaluated since they are considered essential to the understanding of aging effects as set forth in the license renewal rule (LRR).

[3] Used for specialized applications requiring specific cable attributes, properties, or configuration; examples include cable for neutron detectors, area radiation monitors, and control rod position indication circuits.

Included within the scope of "terminations" in the AMG are plug-in/multi-pin/single-pin type connectors, compression fittings, fusion fittings, splice insulations (tape and heat-shrinkable tubing), and terminal blocks.

The component boundaries for the cable systems covered in the study included all components of the electrical cable and wire, as well as any terminations. Cable raceways (including trays, conduits, and duct banks), support or restraint systems, or other ancillary cable system components were not within scope. Electrical wire (e.g., panel or local wire) was addressed only at the major electrical equipment level. Bulk wire installed in MCCs or control boards was covered; however, wiring internal to (or part of) individual devices, modules, or subcomponents was not within scope because it may have special applications or conditions within the devices.

Cables and connectors associated with neutron/radiation monitoring and control rod drive position indication were also within scope. Cable and connectors which are internal to or originate in discrete electrical devices (such as ribbon cable used in amplifier drawers, plotters, etc., and circuit card connectors), as well as containment electrical penetration assembly leads, were not within scope. Motor leads (pigtails) were not within scope except for connected splices and/or terminations.

V. Characterization of Installed Equipment

EPRI NUS Cable Database for EQ Cable

The EPRI NUS Cable Database is a computer-based li[illegible] of EQ cables (and terminations) installed in EPRI-member nuclear power plants. The database used for this task was dated April 1993, and identified 67 plants, comprising 101 units. Each database entry wa[illegible] then categorized as being either a cable, splice and/or termination, or "other" devices.[4] The electrical [illegible]able listing consisted of 1,660 entries representing 53 cable manufacturers, along with several cable types of unknown manufacture. The analyses of the EPRI NUS Database are considered generally applicable to both EQ and non-EQ circuits, based on the assumption that the same types and configurations of cable are used in both types of applications at most plants.[5] Table 1 lists the ten most significant cable manufacturers contained in the database (based on number of entries). Table 2 shows the various material categories identified in the database. Note that per Table 2, EPR and XLPE insulations are most common, being used in slightly over one-third of all EQ circuits each. The next most common insulations (silicone rubber and "Kerite" proprietary) are each used in about 5% of the circuits installed.

The only termination-related entries described splices and seals. The only splice-producing manufacturer currently listed in the EPRI NUS Database was Raychem. There were six Conax seals listed and these are all at one plant; however, these types of devices were not within the scope of the guideline. The remaining splice-related entries (which number more than 100) all described Raychem

---

[4] "Other" devices included area radiation monitors, transmitters, thermocouples, and nuclear instruments which are not considered to be within the scope of this AMG.

[5] The most significant exception to this observation is the use of PVC-insulated cable and wire. Although PVC-insulated cables were rarely used by the industry in EQ applications, PVC-insulated cable is used widely in non-EQ circuits in many plants.

splice insulation. None of the other common nuclear plant splice manufacturers (such as Okonite, Scotch, and Kerite) were noted and/or included in the database by the contributing plant(s).

Table 1. Manufacturers in EPRI NUS EQ Cable Database

Manufacturer	No. of Database Entries	Rank
Okonite	359	1
Rockbestos	316	2
Boston Insulated Wire & Cable Co.	150	3
Anaconda Wire & Cable	128	4
Kerite Co.	109	5
Brand-Rex	98	6
Samuel Moore	77	7
General Electric	69	8
Cerro Wire & Cable Co.	47	9
Raychem	46	10

Table 2. Insulation Materials; EPRI NUS EQ Cable Database

Insulation	No. of Database Entries	% of Total
Butyl Rubber	20	1.6
CSPE	28	2.3
ETFE	39	3.2
EPR	434	35.5
FR	36	2.9
Industrite	2	< 1
Kerite	61	5.0
Mineral	12	1.0
Neoprene	2	< 1
Polyethylene	52	4.3
Polyimide	8	< 1
Polypropylene	3	< 1
PVC	12	1.0
Silicone Rubber	63	5.2
Styrene	1	< 1
XLN	3	< 1
XLPE	439	35.9
Total	1222	

VI. Historical Performance

Five sources of information were used in the AMG to characterize historical performance:

- NPRDS data
- LER data
- NRC Notices, Bulletins, Circulars, and Generic Letters
- Industry analyses and reports relating to cables
- Host utilities and plant surveys

These sources each provide a somewhat different perspective on cable and termination component aging. Several limitations are inherent in any comparison of these results, stemming primarily from the variations in equipment types within the population, differing scope of equipment included, reporting criteria, classification of failures, and criteria used in the analysis. Accordingly, no statistical inferences (such as mean-time-between-failure) were drawn concerning component failure probability.

The results obtained from the analyses of the NPRDS and LER data are summarized below. Information obtained from the remaining sources is discussed in detail in the AMG, and was also used in the formulation of the specific conclusions regarding historical performance listed at the end of this section.

A. Nuclear Plant Reliability Data System (NPRDS)

The NPRDS database was searched based on various keywords contained in the narratives. This method was chosen because no separate classification or descriptive category for "cable" or "terminations" was included in the NPRDS system, and many cable or termination failures are reflected in reports regarding the end device or load center (such as motors or electrical switchgear) rather than the circuit component itself. This search generated 5260 potentially applicable reports, whose event dates ranged from November 1975 through mid-1994. Based on analysis of the NPRDS data, a total of 1458 reports applicable to low- and medium-voltage cable and termination failure were identified. Table 3 summarizes the findings of this analysis.

B. Licensee Event Reports (LERs)

The LERs used in this analysis covered the period from early 1980 through April 1994. The abstracts of 2536 LERs were identified via keyword search of the LER database maintained by Oak Ridge National Laboratory. Of the 2536 reports reviewed, 624 (25%) were ultimately retained as being applicable to electrical cable and terminations of the type considered by this AMG. These reports were then categorized by voltage range (low, medium, or neutron detecting, to be consistent with the NPRDS data), component, subcomponent, failure mode, failure cause, and method of detection. Categorization by manufacturer was not practical due to the near complete lack of component manufacturer information. Table 4 summarizes the findings of the LER analysis. For all components and voltage ranges, the great majority of failures noted were detected during operation of the component, and affected its functionality. This result is somewhat expected, in that the criteria specified in 10CFR50.73 are primarily oriented toward reporting of operational failures and those which potentially impact plant safety.

C. Overall Conclusions Regarding Equipment Historical Performance

Several generic observations were made regarding the empirical information described above:

1. The number of cable and termination failures (all voltage classes) that have occurred throughout the industry is extremely low in proportion to the size of the population.

2. Thermal aging and embrittlement of insulation appears to be the most significant aging mechanism for low-voltage cable. This aging mechanism is predominantly from localized hotspots and occurs near end-devices; aging due to ambient environment or ohmic heating may also be present to a lesser degree

3. Localized radiolytic degradation affects low-voltage cables to a much lesser degree. Degradation resulting from exposure to external chemical substances occurs infrequently.

4. Localized thermal, radiolytic, and incidental mechanical damage appear to be the most significant aging mechanisms for neutron monitoring circuit cables located in proximity to the reactor vessel.

5. Failures of connectors constitute a large percentage of all failures noted for low-voltage (30% for NPRDS, 58% for LERs) and neutron monitoring systems (83% for NPRDS, 24% for LERs). A large percentage of these connector failures can be attributed to oxidized, corroded, or dirty contact surfaces.

6. Failures of hookup or panel wire constitute a substantial percentage (36% for NPRDS, and 14% for LERs) of the total number of low-voltage circuit component failures noted. A large fraction of these failures are not the result of aging influences, but rather stem from design, installation, maintenance, modification, or testing activities.

7. Wetting coupled with operating voltage stress appears to produce significant aging effects on medium-voltage power cable.

8. Splice insulation systems, compression and fusion fittings, and terminal blocks all appear to be relatively failure-free components. Loosening or breakage of lugs are the most significant compression/fusion fitting failures.

9. Damage to cable insulation during or prior to installation may be crucial to the cable's longevity, particularly for medium-voltage systems.

VII. Aging Mechanisms and Effects

As previously stated, aging mechanisms and effects were initially postulated for each cable and termination component based on known stressors (including heat, radiation, mechanical stress, voltage stress, humidity, contaminants, oxygen/ozone, and internal and external chemical influences). Those mechanisms and effects which could potentially affect the intended function of the component were termed "significant." This list was then compared to the empirical data discussed in the preceding section to identify those which were being experienced in the field at frequencies substantially greater than other mechanisms. In this manner, purely "hypothetical" aging mechanisms were eliminated. Aging mechanisms and effects included in this reduced list were termed "significant and observed." These mechanisms/effects are summarized in Table 5.

Table 3. Summary of NPRDS Failure Data

Voltage Range	Component	No. of Failures/%[1]	Failed Subcomponent[2]	Significant Failure Modes[2]	Significant Failure Causes[2]
Low (Max. 1000 Vac)	Cable	150/14.5	Insulation (65%); conductors (19%); unidentified (12%)	Short to ground (54%); open circuit/ high resistance (23%); unidentified (11%).	Heat (18%); mechanical stress (15%); unidentified (49%).
	Connector	314/30.3	Contacts/pins (19%); misc. hardware (8%); Unidentified (66%).	High resistance/open (48%); bent/ deformed components (24%); shorts to ground (12%).	Oxidation/corrosion/dirt(44%); normal aging (5%); unidentified (39%).
	Compression/ Fusion Fitting	132/12.8	Lug (83%); associated hardware (15%).	Loosening or breakage (71%); high electrical resistance (17%).	Mechanical stress (16%); oxidation/corros./dirt (17%); unidentified (61%).
	Hookup and Panel Wire	377/36.4	Insulation (56%); conductors (39%).	Short circuit to ground (45%); high resistance/open circuit (44%).	Mechanical stresses (17%); heat damage (11%); unidentified (59%).
	Terminal Block	36/3.5	Terminal posts/hardware (54%); insulating blocks (29%).	Broken or loose components (67%); short circuit to ground (21%).	Mechanical stresses (13%); unidentified (67%).
	Splice/ Insulation	26/2.5	Insulation (18%); conductors (18%); unidentified (53%).	Short circuit to ground (29%); High resistance/open (29%); unidentified (24%).	Mechanical stress (24%); unidentified (47%).
	Total	1035/100			
Medium (Max. 15 kVac)	Cable	24/68.6	Insulation (92%).	Short circuit or grounding (62%); insulation cutting, breaking, or cracking (21%).	Various; 54% unidentified.
	Connector	4/11.4	Various	Broken/loose components (75%)	None identified
	Splice/ Insulation	6/17.1	Insulation (100%)	Shorting to ground (100%)	Various
	Compression/ Fusion Fitting	1/2.8	Fitting	Broken	Mechanical stress
	Total	35/100			
Neutron Monitor (1 to 5 kV)	Connectors	321/82.7	Contacts/pins (19%); other hardware (8%); unidentified (66%).	High resistance/open circuit (47%); bent/ deformed components (17%); shorting to ground (15%); unidentified (10%).	Oxidation/corrosion/dirt(34%); nearby work (15%); moisture intrusion (13%); unidentified (24%).
	Cable	67/17.3	Insulation (83%); conductors (10%).	Shorting to ground (61%); damaged/over-heated insulation (18%); unidentified (9%).	High temperature (18%); unidentified (55%).
	Total	388/100			

Notes: 1. Number of failures does not include those attributed to maintenance or other personnel error.
2. Level of significance for table equals 10%.

Table 4. Summary of LER Failure Data

Voltage Range	Component	No. of Failures/%[1]	Failed Subcomponent[2]	Significant Failure Modes[2]	Significant Failure Causes[2]
Low (Max. 1000 Vac)	Cable	101/18.3	Insulation (20%); unidentified (66%).	Short to ground (16%); loose or broken components (10%); unidentified (55%).	Moisture intrusion (10%); unidentified (62%).
	Connector	319/57.7	Unidentified (86%).	Loose or broken subcomponents (59%); unidentified (30%).	Oxidation/corrosion/dirt (13%); unidentified (75%).
	Compression/Fusion Fitting	22/4.0	Fitting/Lug (89%)	Loosening or breakage (68%); unidentified (10%).	None (74% unidentified).
	Hookup/Panel Wire	80/14.5	Insulation (34%); conductors (41%); unidentified (18%).	Breakage (42%); short circuit (40%); unidentified (18%).	None (90% unidentified).
	Terminal Block	21/3.8	Insulating blocks (38%); posts/hardware (24%).	Broken or loose components (24%)	None (50% unidentified).
	Splice/Insulation	10/1.8	Conductors (50%)	None identified.	None identified.
	Total	553/100			
Medium (Max. 15 kVac)	Cable	26/52.0	insulation (27%); conductors (19%); unidentified (54%).	Short to ground (27%)	None (54% unidentified)
	Connector	20/40.0	Associated hardware (70%); contacts/pins (30%).	Broken or loose subcomponents (55%) of the failures.	None (95% unidentified)
	Splice/Insulation	1/2.0	Insulation	Short to ground	Moisture intrusion
	Compr./Fusion Fitting	3/6.0	Fitting/lug (100%)	Loosening/breakage (100%)	Mechanical stress (100%)
	Total	50/100			
Neutron monitor (1 to 5 kV)	Connectors	5/23.8	None identified.	None identified.	None identified.
	Cable	16/76.2	None identified.	None identified.	None identified.
	Total	21/100			

Notes:

1. Number of failures does not include those attributed to maintenance or other personnel error.
2. Level of significance for table equals 10%.

Table 5. Summary of Cable and Termination Stressors, Significant and Observed Aging Mechanisms, Degradations, and Potential Effects

Voltage Category	Component	Subcomponent(s)	Applicable Stressors	Aging Mechanisms	Degradation	Potential Effects	Remarks
Low	Cable	Insulation and Jacketing	Heat, oxygen	Thermal/thermoxidative degradation of organics (environmental and ohmic/induced currents)	Embrittlement, cracking, melting, discoloration	Reduced insulation resistance (IR); electrical failure	
			Radiation, oxygen	Radiolysis and photolysis of organics; radiation-initiated oxidation	Embrittlement, cracking, discoloration, swelling	Reduced IR; electrical failure	Photolysis only applicable to exposed UV sensitive materials
			External mechanical stresses	Wear or manipulation	Cutting, chafing, abrasion, splitting	Reduced IR; electrical failure	Work in area; personnel traffic; poor support practices
	Connector	Contact Surfaces	Electrochemical stresses (moisture, oxygen, etc.)	Corrosion and oxidation of metals	Corrosion and oxidation of external surfaces of contacts	Increased resistance and heating; loss of circuit continuity	
	Compression Fitting	Lug	Vibration, tensile stress	Deformation and fatigue of metals	Loosening of lug on conductor; breakage of lug	Loss of circuit continuity; high resistance	
Medium	Cable	Insulation	Moisture; voltage stress	Moisture intrusion; water treeing; electrical treeing	Formation of water trees; localized damage	Electrical failure (breakdown of insulation)	
Neutron Detecting	Cable	Insulation	Heat	Thermal degradation of organics (environmental)	Embrittlement, cracking, melting, discoloration	Reduced IR; electrical failure	Typically occurs near heat source such as reactor vessel
			Radiation	Radiolysis of organics	Embrittlement, cracking, discoloration, swelling	Reduced IR; electrical failure	Typically occurs near or under reactor vessel
			External mechanical stresses	Wear or manipulation	Cutting, cracking, chafing, abrasion	Reduced IR; electrical failure	Incidental contact, work in area
	Connectors	Contact Surfaces	Electrochemical stresses (moisture, oxygen, etc.)	Corrosion and oxidation of metals	Corrosion and oxidation of external surfaces of contacts	Increased resistance and heating; loss of circuit continuity	

Non-significant Aging Mechanisms and Effects

The following aging mechanisms and effects identified during this study are considered non-significant:

- Aging of cable filler material
- Electrical fault-induced mechanical and thermal stress on cable and termination components
- Aging of cable tape wrap (other than shielding or semi-conducting layer in medium-voltage cable)

VIII. Aging Management Techniques

The following generic aging management activities were identified as potentially being performed during the operation, maintenance, surveillance, and condition monitoring of cable systems:

- Measurement of component or circuit properties
- Visual or physical inspection
- Operability testing
- Cleaning
- Component repair or replacement
- Thermographic inspection
- Monitoring of temperature or other environmental conditions
- Analysis of circuit loading and operating time
- Arrhenius analysis and use of accelerated aging data

A large number of currently available and developmental condition monitoring technologies were reviewed as part of the study to determine which were potentially effective at measuring or monitoring component aging. These techniques are summarized in Table 6.

A. Commonly Used Techniques

Vendor and utility maintenance procedures from a number of different sources were reviewed to identify those maintenance and surveillance techniques listed in the preceding section which are commonly used to maintain electrical cable and terminations. In addition, personnel from appropriate maintenance organizations at several nuclear plants were contacted for further insight on maintenance practices employed for each class of equipment. Industry sources and reports were also reviewed for applicable data and information. Based on this review, the following maintenance and troubleshooting techniques were identified as being in relatively common use:

- Measurement of insulation resistance (IR)
- AC and DC high potential testing (hipot)
- Measurement of capacitance, inductance, and polarization index
- Visual/physical inspection of cable and terminations
- Cleaning of connector contacts at time of associated equipment maintenance.

Additionally, environmental monitoring coupled with Arrhenius analysis is employed by many plants, especially with respect to environmentally qualified systems. Thermographic inspection was found to be only occasionally used at a limited number of plants. Table 7 summarizes the significant and observed aging mechanisms/effects for cable systems, current preventive and corrective maintenance activities, other potentially useful techniques.

Table 6. Condition Monitoring (CM) Techniques

Type	Technique	Degradation Addressed	Test Type	Field/Lab Test[6]	Troubleshooting (TS) or CM
Destructive	Elongation at Break	Localized[7]	Mechanical	Lab	CM
	Tensile Strength	Localized[7]	Mechanical	Lab	CM
Non-Destructive	Compressive Modulus	Localized[7]	Mechanical	Field	CM
	High Potential (Hipot)	Bulk	Electrical	Field	TS
	Insulation Resistance (IR)	Bulk	Electrical	Field	CM, TS
	Insulation Power Factor	Bulk	Electrical	Field	CM
	Polarization Index (PI)	Bulk	Electrical	Field	CM
	Capacitance	Bulk	Electrical	Field	TS
	Partial Discharge	Fairly Localized	Electrical	Lab	CM, TS
	Time Domain Reflectometry	Bulk	Electrical	Field	TS
	Tan Delta/Low Freq. Tan Delta	Bulk	Electrical	Field	CM
	Density (CT)	Localized[7]	Chemical	Lab	CM
Essentially Non-Destructive	Density (columns)	Localized[7]	Mechanical	Lab	CM
	Oxidation Induction Time (OIT)	Localized[7]	Chemical	Lab	CM
	Oxidation Induction Temperature	Localized[7]	Chemical	Lab	CM
	Fourier Transform IR (FTIR)	Localized[7]	Chemical	Lab	CM
	UV Spectroscopy	Localized[7]	Chemical	Lab	CM
	Gel Content	Localized[7]	Chemical	Lab	CM
	Plasticizer Content	Localized[7]	Chemical	Lab	CM
	Electron Spin Resonance (ESR)/Nuclear Magnetic Resonance (NMR)	Localized[7]	Chemical	Lab	CM

[6] Note: Field techniques may also generally be used in the lab.

[7] Test is performed on localized sample of material; properties of bulk of material can be inferred.

Table 7. Summary of Stressors, Aging Mechanisms, Effects, and Maintenance, Surveillance, and Condition Monitoring Techniques

Voltage Category	Component	Sub-component	Applicable Stressors	Aging Mechanisms	Aging Effects	Common Maintenance, Surveillance, or CM Techniques	Periodicity	Common Corrective Maintenance Techniques	Other Potentially Useful Maintenance or CM Techniques
Low	Cable	Insulation and Jacketing	Heat	Thermo-oxidative degradation of organics (ohmic and environmental)	Embrittlement, cracking	Visual inspection	Inspection of accessible portions during routine operations or equipment maintenance only	Visual inspection, insulation resistance (IR), polarization index, capacitance; repair or replacement	Compressive modulus, OIT, thermography, temperature profiling, circuit analysis
			Radiation	Radiolysis and photolysis of organics	Hardening, cracking, crazing, swelling	Visual inspection	Inspection of accessible portions during routine operations or equipment maintenance only	Visual inspection, IR, polarization index, capacitance; repair or replacement	Compressive modulus, OIT, radiation profiling
			External mechanical stresses	Wear or manipulation	Cuts, abrasion, tearing	Visual inspection	Inspection of accessible portions during routine operations or equipment maintenance only	Visual inspection, IR, polarization index, capacitance; repair or replacement	
	Connector	Contact Surfaces	Electro-chemical stresses	Corrosion and oxidation of metals	High resistance	Visual inspection, cleaning	Inspection/cleaning generally only during maintenance	Visual inspection, Time Domain Reflectometry (TDR), capacitance; repair or replacement	
	Compression Fitting	Lug	Vibration, tensile stress	Deformation and fatigue of metals	High resistance, breakage	Visual inspection	Inspection generally only during maintenance	Visual inspection, TDR; repair or replacement	Thermography for power circuits
Medium	Cable	Insulation	Moisture and voltage stress	Moisture intrusion, water treeing	Dielectric breakdown and fault to ground	Visual inspection for moisture intrusion, DC hipot (few)	Inspection generally only during maintenance	Visual inspection, IR/PI, capacitance, TDR, AC and DC hipot, AC power factor; repair or replacement	
Neutron Monitoring	Cable	Insulation	Heat	Thermoxidative degradation of organics (environmental)	Embrittlement, cracking	Visual inspection	Inspection of accessible portions during routine operations or equipment maintenance only	Visual inspection, IR, polarization index, capacitance; repair or replacement	Compressive modulus, OIT, temperature profiling
			Radiation	Radiolysis of organics	Hardening, cracking, crazing, swelling	Visual inspection	Inspection of accessible portions during routine operations or equipment maintenance only	Visual inspection, IR/PI, capacitance, TDR; repair or replacement as required	Compressive modulus, OIT, radiation profiling
			External mechanical stresses	Wear or manipulation	Cuts, abrasion, tearing	Visual inspection	Inspection of accessible portions during routine operations or equipment maintenance only	Visual inspection, IR, polarization index, capacitance, TDR; repair or replacement	
	Connectors	Contact Surfaces	Electro-chemical stresses	Corrosion and oxidation of metals	High resistance	Visual inspection, cleaning	Inspection/cleaning normally only performed during system maintenance	Visual inspection, TDR, capacitance; repair or replacement	

VIII. Significant Component/Aging Mechanism Combinations Not Addressed By Current Programs

Comparison of the currently employed aging management techniques and the significant and observed aging mechanisms/effects demonstrates the following:

1. Not all of the aging effects resulting from significant and observed aging mechanisms are being detected by methods currently employed by plant operators or fully managed by existing programs;

2. Not all of these aging mechanisms are fully detectable via currently existing techniques.

Specifically, the following combinations may require additional plant-specific aging management activities:

- Localized thermal, radiation-induced, or mechanical degradation of low- or medium-voltage cable insulation and jacketing

- Thermal degradation of low- and medium-voltage power cable insulation for circuits resulting from continuous or near-continuous loading at a significant percentage of their ampacity limits

- Degradation of medium-voltage power cable insulation routinely exposed to wetting or submergence

- Degradation of connector contact surfaces associated with neutron monitoring circuits (and similar low-current/impedance-sensitive applications) resulting from oxidation or corrosion.

The following aging considerations were also identified:

- Damage to medium-voltage cable insulation, jacketing, and shielding prior to or during installation

- Damage to low-voltage panel and local wire resulting from maintenance activities.

- Damage to aged low-voltage field cable resulting from movement or other maintenance activities.

In effect, Table 7 shows that the aging of cable systems components is sometimes left essentially unmitigated until some sort of problem or failure is detected. However, these observations must be considered in light of the overall significance of this aging in terms of cable system performance. Figure 1 shows failures for low-voltage cable, panel/hookup wire, and terminations for the years 1974 through 1993. The total number of failures for each category was divided by the number of nuclear plants in operation[8] during each individual year to estimate the number of failures per plant per year. As shown in the figure, the peak failure rates recorded were approximately 0.7 failures per plant per year for low-voltage terminations (all), 0.7 for panel/hookup wire, and 0.3 for cable. Average cable failure rates are also substantially lower than those for the other low-voltage components. Note that those failures not

[8] This data was obtained from the American Nuclear Society's annual listing of world nuclear power plants.

affecting functionality are also included in this number, such that the actual number of failures affecting function would likely be somewhat less.

Figure 2 shows failures for medium-voltage cable and terminations for the years 1974 through 1993. The peak failure rates recorded were 0.12 termination failures per plant per year (1975), and roughly 0.04 cable failures per plant per year (1983). Based on extrapolation of this data, each plant would experience a medium-voltage termination failure roughly every 8 years on average, and a medium-voltage cable failure every 25 years. Figure 3 illustrates similar data for neutron monitoring systems, which shows that the peak and average failure rates for terminations are greater than those for the associated cables, yet both are still quite low (less than 0.6 failures per plant per year).

It should be noted that the failure rates determined above may underestimate actual failure rates somewhat based on the fact that (1) not all plants in operation in a given year report their failures to NPRDS, and (2) plants which do report to NPRDS may not report all of their failures. However, even if the number of failures for any voltage category is quadrupled (e.g., assuming only half of the operating plants report, and only half of the actual failures experienced by these plants are reported), the total number of failures per plant per year are still extremely low in light of the large number of circuits in the typical plant[9]. The cause(s) of the apparent rise in failure rate for both low-voltage and neutron monitoring circuits beginning in about 1980 is unknown; numerous possible explanations (including an increase in the percentage of operating plants reporting to NPRDS, increased plant management sensitivity resulting from events at TMI-2, or an actual increase in the component failure rate) exist. Note also that analysis of the component age at failure yielded no clear trend or distribution for any of the equipment categories.

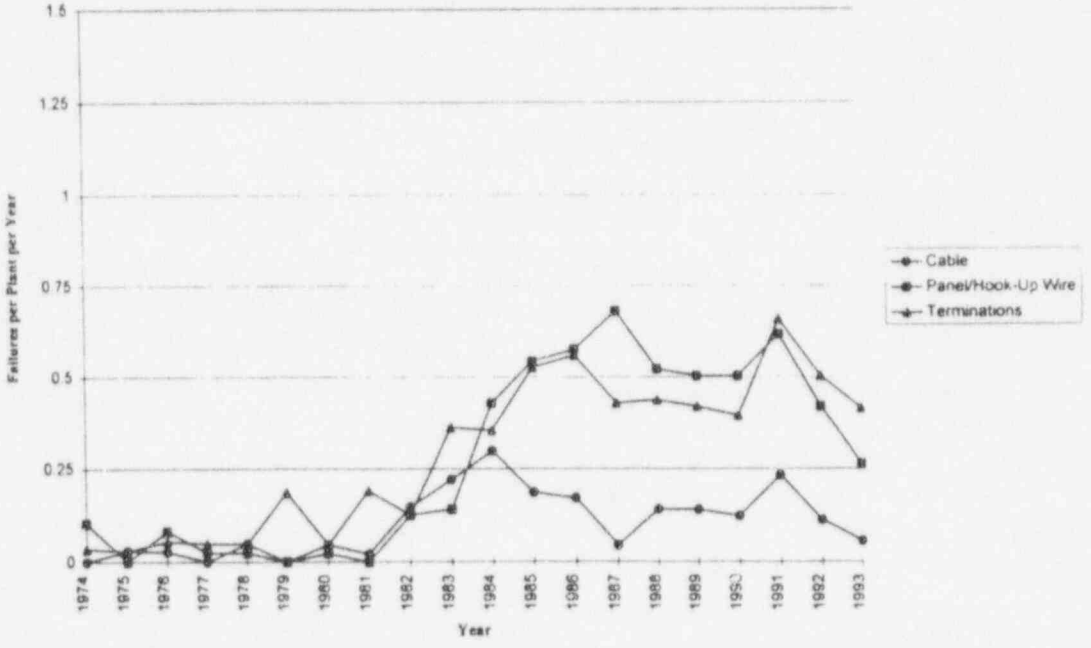

Figure 1. Low-Voltage Cable and Termination Failures versus Time (NPRDS)

[9] One plant (PWR) contacted as part of the study indicated in excess of 50,000 individual circuits installed in two units.

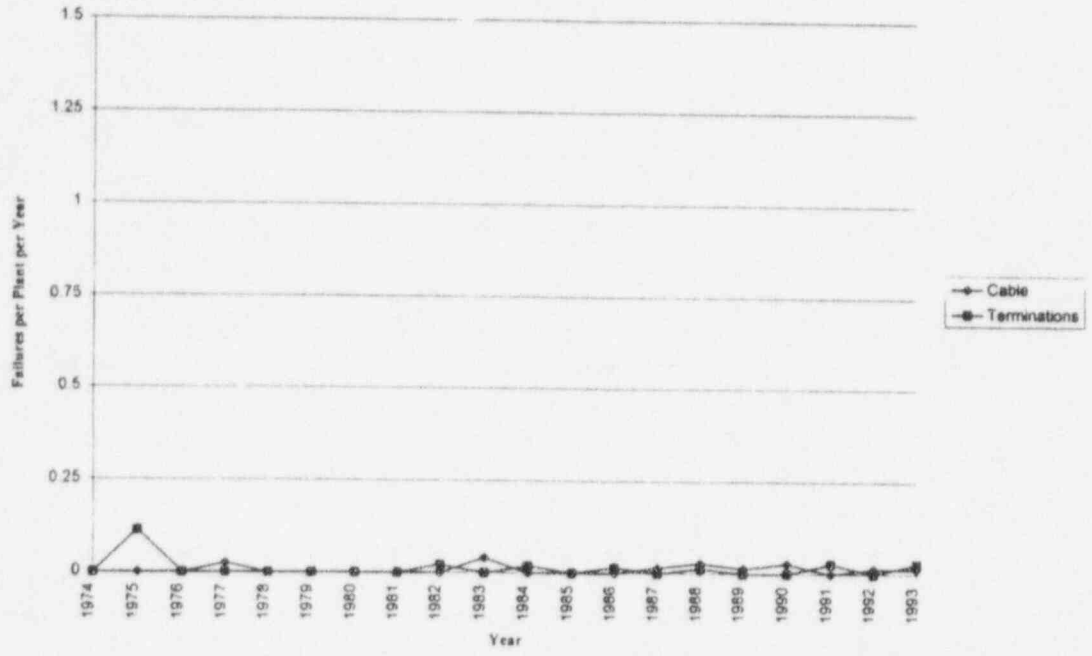

Figure 2. Medium-Voltage Cable and Termination Failures versus Time (NPRDS)

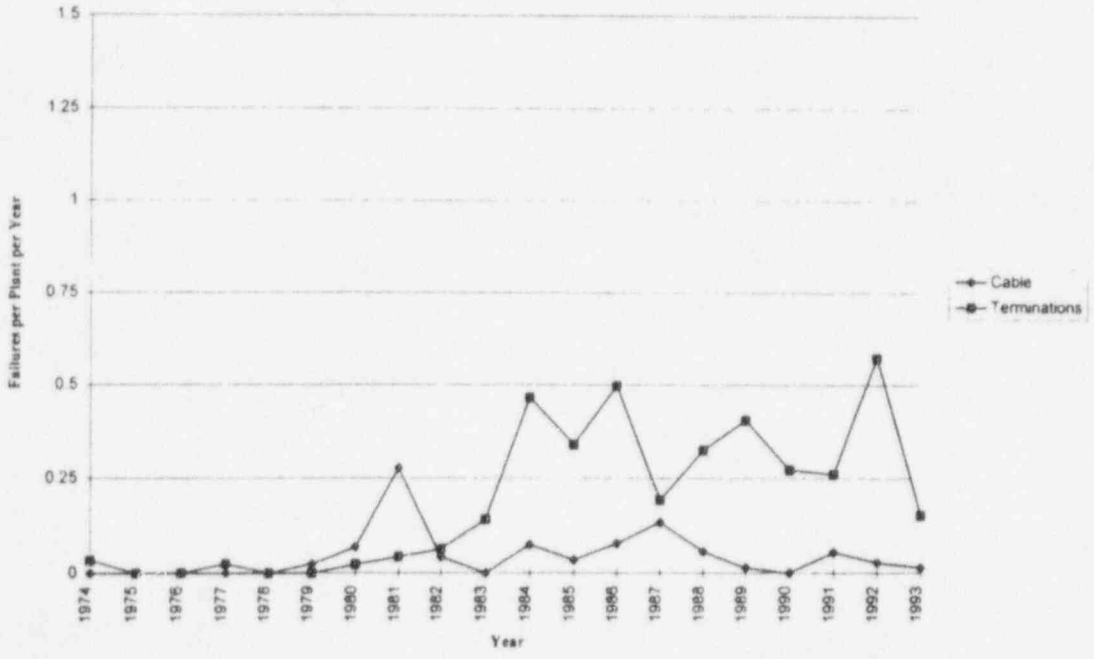

Figure 3. Neutron Monitoring Cable and Termination Failures versus Time (NPRDS)

IX. Conclusions and Recommendations

A. Conclusions

The following general conclusions are applicable to electrical cable and termination aging:

1. Nearly all cables and terminations that are included within the scope of this AMG have been highly reliable (see conclusion 3 below). They are expected to perform their safety function and meet all regulatory requirements during the current licensing term.

2. The great majority of cables and terminations currently installed in operating plants can be expected to continue to perform their safety function and meet all regulatory requirements during an extended period of operation after the expiration of the current licensing period.

3. Based on analysis of historical failure data, the number of cable and termination failures that have occurred throughout the industry is extremely low in proportion to the overall population.

4. The stressors and aging mechanisms affecting cables and terminations are generally well understood and characterized; however, knowledge of some areas (including combined and natural aging environments) is more limited.

5. Cable and termination aging can be evaluated on an on-going basis, using theoretical techniques, measurement of physical properties, and periodic inspection.

In addition to the general conclusions cited above, the following specific conclusions were identified:

1. Additional aging management will be required only for a relatively small fraction of the total plant cable and termination population. Specifically, cables and terminations may warrant more careful consideration if they are:

   - located near high heat and/or radiation sources,
   - subject to continuous or near-continuous loading at a significant percentage of their ampacity limits,
   - exposed to submergence/wetting (medium-voltage) or adverse chemical environments,
   - subject to repeated or continuous damaging mechanical stress, or
   - used in impedance-sensitive applications (such as neutron monitoring equipment).

2. The mechanical properties of low-voltage cable insulation must generally degrade significantly (such as embrittlement and cracking, or cut-through damage) before any effect is seen in the electrical properties. This condition is not generally true, however, for medium-voltage cable.

3. Most degradation of installed cable (and terminations) appears to occur at or near the end-devices/connected loads, as opposed to affecting the bulk runs.

4. Current maintenance, surveillance, or testing activities may be partially or wholly ineffective at identifying certain types of incipient cable or termination aging degradation. Simple periodic visual/physical inspection is a highly effective means for assessing the condition of low-voltage cable insulation and jacketing as well as some organic termination components.

5. Installation practices can be a significant determinant in the aging and longevity of medium-voltage power cable systems.

6. Existing environmental qualification practices coupled with design/application conservatisms provide assurance that aging mechanisms and effects will not preclude EQ cable from performing its required function during its qualified life. Note that non-EQ components are frequently identical or similar to their EQ counterparts, thereby allowing effective application of conclusions and information related to the EQ components to the non-EQ equipment.

7. The potential for failure under accident conditions exists for certain bonded cable systems due interaction between the conductor insulation and jacket when aged under certain conditions. The aging conditions under which these failures were observed are not typically experienced in nuclear plant applications; however, the response of these cable systems to accident exposure following aging under natural conditions is not well understood at present. Therefore, additional evaluation for suitability during the license renewal period may be warranted.

8. Substantial progress has been made in the last few years to develop methods for evaluating the aging of low-voltage cable. Of these, tests which measure physical properties of the cable insulation/jacket appear most promising at present. Such techniques (and others subsequently developed) may be a viable approach to managing the aging of cable system components not otherwise managed by existing practices.

9. No currently available technique was identified as being effective at monitoring the electrical aging of medium-voltage power cable. Some methods may be effective at detecting severe electrical degradation or monitoring certain types of degradation (such as thermal aging); however, correlation of these measurements with the expended or remaining life of these cables has not been demonstrated.

B. Recommendations

The following recommendations regarding cable and termination aging management are presented:

1. Aging management activities should consider specific cable types used in certain installations/applications, and address the degradation mechanisms of most significance. For low-voltage systems, instances of older or more aging-susceptible materials used on cables (such as PVC, butyl, or neoprene rubber) that are connected to heavy continuous loads or routed through "hotspot" areas should be considered. Particular attention should be payed to components or cable segments located in proximity to the end-device. Similarly, medium-voltage power cables routinely subject to wetting or submersion, and oxidation of connectors used in neutron monitoring circuits should be affirmatively addressed.

2. Accurate characterization of plant environments (especially those of the more severe areas such as primary containment) is important to effectively managing the aging of certain cable systems. Such characterization should be conducted to assist in establishing representative qualified lives for environmentally qualified components, and help identify circuits/components which may undergo accelerated aging with respect to the rest of the population.

3. Based on the similarity between many EQ and non-EQ cables and terminations, existing information and analyses related to the aging of EQ components should be considered for use with non-EQ components where applicable to assist in management of their aging.

4. Condition monitoring is not currently warranted for all applications of medium-voltage cable. Because no technique is currently developed to a sufficient degree to permit effective monitoring of dielectric aging without the threat of inducing further degradation, preventive measures should be considered as means of extending medium-voltage cable longevity.

5. In cases where condition monitoring is deemed appropriate (such as where aging effects can not otherwise be adequately managed by existing practices), a program to determine baseline aging condition of affected components using a non-destructive test or evaluation method should be considered.

6. If cables are to be replaced for any reason, then plant cable installation practices and procedures should be reviewed to ensure their adequacy with regard to preventing cable damage during installation.

7. Information derived from natural or low-acceleration factor aging programs currently underway may yield a better understanding of degradation resulting from combined environments and natural aging conditions, and should be used to supplement present knowledge regarding the aging of cable and termination materials. Additionally, input from ongoing qualification activities (such as follow-on analyses, testing, condition monitoring, and maintenance) should be incorporated into existing programs as appropriate.

8. Applications of environmentally qualified cable potentially susceptible to bonded jacket/insulation failure should be further evaluated for adequacy during the license renewal period. Recent experimental data suggests that the probability of post-accident failure may substantially increase for such cables exposed to aging temperatures above about 55°C over 40 years (or about 52°C over 60 years)[10] and simultaneous radiation aging. Accordingly, circuits subject to such aging environments should be considered.

C. Proposed Methodology for Conducting Aging Management Review

An aging management review of long-lived and passive SSCs is performed to demonstrate that the effects of aging are adequately managed such that the intended equipment function is maintained for the extended period of plant operation, consistent with the current licensing basis (CLB). No specific methodology is set forth in 10CFR54 for accomplishing an aging management review for equipment

[10] Based on Arrhenius extrapolation using activation energy of 1.10 eV.

within the scope of the LRR. The basic methodology described in Reference 1. includes (1) identifying SSCs within the scope of the rule, (2) identifying applicable aging effects and their impact on SSC intended function, and (3) determining the ability of applicable plant programs to identify and mitigate these effects. Where aging effects are not completely managed for the period of extended operation by existing programs, appropriate actions must be taken to address these effects. A generic methodology for performing an aging management review for electrical cable and terminations is proposed below; by implementing this methodology, a reasonable assurance of continued operations in accordance with the CLB can be maintained for the equipment within the scope of this guideline.

Step 1: Identification of Equipment Potentially Requiring Additional Aging Management Activities

The first step of the proposed methodology seeks to identify those circuits for which adequate aging management can be readily demonstrated. One of the grouping approaches described below is used to eliminate those circuits not exposed to significant aging stressors from further consideration. Depending on the specific approach employed in this step, the fraction of circuits potentially requiring additional aging management activities can be substantially reduced with comparatively little effort.

One variant of the group method is to treat cable systems as a "commodity;" the initial disposition of circuits is performed (based on the primary stressor(s) of concern) without regard to circuit location or whether the circuit is within the scope of the license renewal rule. For example, a service-limiting temperature for cable insulation/jacketing material could be calculated and used as the primary screening tool. Another approach is to demonstrate aging management for groups of components through analysis or evaluation of the "worst-case" environment or installation. That is, groups of circuits can be dispositioned based on their physical similarity to the worst-case application, and a showing that the aging stressors of concern are enveloped.

A third alternative involves use of what is called a "plant spaces" approach. Under the plant spaces approach, structures which utilize or house no circuits potentially includable within the scope of license renewal may be eliminated from further consideration. After any such structures are eliminated, a space-by-space evaluation of the environments in the remaining structures is performed considering factors such as ambient temperature and localized heat sources, radiation, and moisture. Specifically, the effects of aging for all low-voltage instrument and control cables/terminations and all medium-voltage cables/terminations that are installed in areas having all of the following characteristics can be demonstrated to be adequately managed:

- The room ambient temperature never exceeds the 60-year service limiting temperature applicable to the material(s) of concern.[11]

---

[11] The 60-year service limiting temperature is chosen based on an analysis of the relevant materials of construction for the plant circuit components of interest (i.e., those components whose thermal degradation will adversely affect functionality, such as cable insulation). An appropriate material property (such as elongation-at-break) and endpoint are identified, and the temperature at which this endpoint is reached (over 60 years) is considered the service limiting temperature. In lieu of such a plant specific analysis, 95°F (35°C) may be used as a conservative 60-year service limiting temperature for all materials.

- The threshold radiation dose for the material(s) of concern is greater than the 60-year normal TID for all areas in the room.[12]
- There are no cables or connections that must be moved or manipulated frequently (more than once or twice per refueling cycle).
- The area is free from significant wetting/submergence, and cables are located above flood levels.
- There is no salt or other corrosive or chemical environments.
- There are no hot process lines or end-devices.

The only type of circuit within such "benign" spaces that must be analyzed further is any low-voltage power circuit that is energized for long periods and loaded with currents that are a significant percentage of the conductor ampacity. In the case of circuits which run through several plant spaces (and environments), the most conservative environment is used as the basis for decision.

Step 2: Identify Circuits Potentially Subject to Accelerated Aging or Degradation

After using one of the "group" approaches to identify the subset of circuits for which aging management can be initially demonstrated, examination of the operating and environmental conditions applicable to the remaining circuits is performed. By selecting only those circuits or groups of circuits which are exposed to *significant* environmental, operational, or installation stressors, the number potentially requiring additional aging management activities may be further reduced. Specific guidelines for this selection process by voltage category/function are provided (based on the previous conclusions).

Step 3: Examination of Plant-Specific Historical Data

By examining maintenance records, operating history, plant-specific failure data, and canvassing plant electrical and maintenance personnel for input, circuits routinely experiencing degradation of the types described above may be readily identified. In this fashion, a plant's experience derived from operating and maintaining the equipment can be incorporated to identify high-stress environments and applications which may not always be readily apparent. Additionally, the aging and degradation of many circuits selected for inclusion under these steps can be validated; some circuits or groups of circuits previously selected for further evaluation may even be eliminated based on a showing of no historical degradation in spite of the presence of significant aging stressors. Another component of the historical review should include evaluation of root-cause analyses.

Step 4: Identification of Existing Aging Management Programs

Next, existing plant aging management programs are identified; this information will be used in Step 5 below to support the ultimate determination of aging management effectiveness for the subset of the cable/termination population selected in Step 3 above. A generic list of activities or programs which potentially detect and/or mitigate the effects of aging is compiled for each separate classification of component based on voltage category and the specific application under consideration; this list is then compared to individual circuits or groups of circuits as required.

---

[12] A 60-year TID value of 10^3 Gy (10^5 rads) can be used as a conservative value of limiting radiation threshold in lieu of plant-specific analysis.

Step 5: Evaluation of Aging Management Effectiveness

After a list of potentially applicable activities is generated, these activities are evaluated against the aging stressors and effects previously identified for a specific circuit or group of circuits. This evaluation is performed based on the stressors and effects which were used to initially select the circuit/group for further consideration. Criteria which can be used in determining whether aging effects are managed by such programs include:

(1) detection and mitigation of aging effects before loss of function (i.e., the failure of the component is progressive, and monitoring frequency is such that detection occurs before loss of function),

(2) the ability to monitor parameters of the component which can be correlated to aging effects,

(3) the existence of specific acceptance criteria, alert, or action values for determining the need for corrective action,

(4) specific inclusion of the equipment under evaluation within the program(s),

(5) the presence of administrative program controls and formal reviews, and

Step 6: Identification of Additional Aging Management Activities

After the completion of Step 5, a list of required additional aging management activities required to demonstrate adequate management per the LRR is generated. These activities may take the form of enhancements to existing programs (such as expanding the scope of testing/inspection, trending of data, or changing the frequency of performance) or creation of new programs or initiatives (such as establishment of a condition monitoring program, or design changes to equipment). Factors to be considered in determining appropriate additional activities include (1) the relative risk significance of the circuit(s) under consideration, (2) the nature of the aging effect and current technology (i.e., can it be monitored/detected by currently available means?), (3) periodic repair/replacement versus monitoring, (4) the cost of implementation.

X. Acknowledgements

The assistance and sponsorship of the Department of Energy's Light Water Reactor Technology Center at Sandia National Laboratories during preparation of this document is acknowledged. The Electrical Cable and Terminations AMG is scheduled for publication in December, 1995; for additional information, contact Mr. Duli Agarwal, DOE Headquarters (NE-50).

XI. References

1. NEI Report 95-10, "Industry Guideline for Implementing the Requirements of 10 CFR Part 54 - The License Renewal Rule," Draft Revision C, August 18, 1995.

AN OVERVIEW OF THE BWR ECCS STRAINER BLOCKAGE ISSUES

Aleck W. Serkiz
Michael L. Marshall, Jr.
Robert Elliott

United States Nuclear Regulatory Commission
Washington, D.C.

This paper provides a brief overview of actions taken in the mid 1980s to resolve Unresolved Safety Issue (USI) A-43, "Containment Emergency Sump Performance," and their relationship to the BWR strainer blockage issue; the importance of insights gained from the Barsebäck-2 (a Swedish BWR) incident in 1992 and from ECCS strainer testing and inspections at the Perry nuclear power plant in 1992 and 1993; an analysis of an US BWR/4 with a Mark I containment; an international community sharing of knowledge relevant to ECCS strainer blockage, additional experimental programs; and identification of actions needed to resolve the strainer blockage issue and the status of such efforts.

Nuclear power reactor licensees in the United States of America (US) are required to ensure long-term cooling to the reactor core in accordance with the Code of Federal Regulations (CFR), specifically 10 CFR 50.46, "Acceptance Criteria for Emergency Core Cooling Systems for Light Water Nuclear Power Reactors." Following a postulated loss-of-coolant accident (LOCA), LOCA generated debris (e.g., thermal insulation), operational debris (e.g., corrosion products), and foreign materials may migrate to the emergency core cooling system (ECCS) suction strainer in boiling water reactors (BWRs) and block (clog) the suction strainer. If the resistance across the strainer is great enough, the performance of the ECCS pumps may be degraded because of a decrease in net positive suction head (NPSH) and result in a reduction or elimination of flow available for core cooling and decay heat removal. Debris blockage of ECCS suction strainers is a safety concern.

The United States Nuclear Regulatory Commission (NRC) first addressed this concern as part of the resolution of Unresolved Safety Issue (USI) A-43, "Containment Emergency Sump Performance" in the mid 1980s. The technical findings and regulatory analysis were published as References 1 and 2. The resolution of USI A-43, as the title implies, focused primarily on pressurized water reactors (PWRs). A limited plant survey at that time indicated that US BWRs were insulated primarily with reflective metallic insulation (RMI) rather than fibrous insulation; therefore, concerns related to LOCA generated fibrous debris were not judged to be of major concern for BWRs (an insulation condition which has changed). In 1985, the NRC issued Regulatory Guide 1.82, Rev. 1,"Water Sources for

Long-Term Recirculation Cooling Following a Loss-of-Coolant Accident" (Ref. 3) and Generic Letter (GL) 85-22,"Potential for Loss of post-LOCA Recirculation Capability Due to Insulation Debris Blockage" (Ref. 4). The cost benefit analysis performed as part of USI A-43 did not support a backfit of operating reactors, but the guidance contained in Regulatory Guide (RG) 1.82, Rev. 1 was forwardfitted to all future construction applicants. Although no backfit action was required, GL 85-22 clearly noted that: (1) "....a single generic solution is not possible....," (2) "the 50% screen blockage assumption....should be replaced with a more comprehensive requirement to assess debris effects on a plant-specific basis," and (3) "....that RG 1.82, Rev. 1 be used as guidance for the conduct of 10 CFR 50.59 reviews dealing with the changeout and/or modification of thermal insulation installed on primary system piping and components." Events at two operating reactors in 1992 and 1993 compelled the NRC to re-evaluate the debris blockage aspects of USI A-43 for BWRs and its resolution of the issue.

On July 28, 1992, a safety relief valve (SRV) inadvertently opened in the Barsebäck-2 nuclear power plant , a Swedish BWR, and discharged into the drywell. The steam jet stripped fibrous insulation from adjacent pipes and part of that insulation debris was transported to the wetwell pool and accumulated on two strainers. After about one hour, the resultant increase in head loss from debris blockage across the strainers caused the plant operators to stop pump operations to prevent damage to the pumps. The plant operators backflushed both strainers, then reinitiated containment spray. The Swedish Nuclear Power Inspectorate (SKI) required that immediate measures be taken to prevent strainer clogging for the five oldest Swedish BWRs, before they were allowed to startup. Similar reviews and actions were quickly undertaken by regulators in Finland and Switzerland.

On January 16 and April 14, 1993, two events involving the clogging of ECCS strainers occurred at the Perry nuclear power plant, a US BWR. The first Perry event involved clogging of residual heat removal (RHR) pump suction strainers by debris in the suppression pool. The second Perry event involved deposition of fibers from temporary drywell cooling filter materials inadvertently (i.e., foreign material) dropped into the pool on these strainers coupled with the filtration of suppression pool particulates (i.e., corrosion products or "sludge"). These Perry events also demonstrated that small amounts of fibrous materials and corrosion products in the suppression pool could result in unacceptable suction strainer pressure losses. Corrosion products (e.g., iron oxide) have since been identified to be present in large quantities in US BWR suppression pools which have not been cleaned regularly. The Perry incidents raised further concerns regarding prior conclusions reached for BWRs and resulted in the NRC's issuance of Bulletin 93-02 (Ref. 5), which requested licensees to remove fibrous air filters and any other temporary sources of fibrous material, that were not designed to withstand a LOCA from the containment. In addition, licensees were requested to take any immediate compensatory measures necessary to ensure the functional capability of the ECCS.

In January 1994, SKI sponsored a workshop on the Barsebäck strainer event, under the auspices of the OECD/NEA (Ref. 6). During the workshop SKI shared with the to provide feedback to the nuclear reactor community information regarding the Barsebäck event, post-Barsebäck findings, post-Barsebäck experimental findings, and corrective

actions taken or planned. At the meeting the NRC staff learned about the 'robust' solution imposed upon the Swedish utilities. The 'robust' solution involved:

1. Changeout of thermal insulations to insulations that are less likely to block the strainer or induces less severe head losses across the strainer,

2. Very large increases in suction strainer surface area, and

3. Installation of alternate suction strainer designs.

Most Swedish reactors had the capability to backflush the suction strainers prior to the Barsebäck event, but backflushing is generally considered part of the 'robust' solution. Because of differences in plant and containment design, operations, and regulatory environment, the NRC staff did not considered the 'robust' solution a practical solution for US BWRs. It should be noted that the NRC staff was not convinced at that time (i.e., January 1994) that strainer blockage was a safety concern for US BWRs.

10 CFR 50.46 and General Design Criteria (GDC) 35 provide the regulatory basis for addressing this concern. 10 CFR 50.46 requires that each boiling and pressurized light-water reactor be provided with an ECCS designed so that its calculated cooling performance conforms to five criteria. The fifth criterion cited in the regulation specifically addresses the long term cooling capability of the ECCS. It states that "after any calculated successful initial operation of the ECCS, the calculated core temperature shall be maintained at an acceptably low value and decay heat shall be removed for the extended period of time required by the long-lived radioactivity remaining in the core." An underlying assumption that goes with the requirement to remove decay heat for the extended period of time required by the long-lived radioactivity is that the ECCS shall continue to operate for the entire time that it is needed to remove decay heat. GDC 35 requires licensees to have a system to provide abundant emergency core cooling. In addition, the ECCS shall be provided with suitable redundancy in components and features to assure that the safety function can be accomplished, assuming a single failure. The lessons of Barsebäck and Perry have demonstrated that the ECCS is susceptible to a potential common-cause failure due to clogging of the suction strainers that could prevent them from being able to perform their safety function of decay heat removal over the long term. This lesson was reinforced by a recent strainer clogging event that occurred at Limerick, Unit 1 on September 11, 1995.

A stuck open safety relief valve at Limerick led to the initiation of both loops of suppression pool cooling. The "A" loop subsequently experienced flow and current oscillations, an indication of a clogged strainer. Limerick operators shutdown and restarted the pump with no further complications, and the rest of the event was mitigated without any additional problems. Post-event strainer inspection revealed that the suction strainer had been clogged by a combination of polyethylene fibers and corrosion products (sludge). The sludge is generally present in US BWRs; however, the fibrous material that was present in the suppression pool was due to a failure at some time to prevent the introduction of foreign material into the suppression pool. The Limerick event is described

in more detail in References 7 and 8.

Because of the 1992 Barsebäck event, the 1993 Perry events, and the actions and research of Swedish and Finnish regulatory authorities, the NRC began to evaluate the effects of debris blockage of suction strainers on the long-term cooling function of the ECCS system. The purpose of the evaluation was to determine if strainer blockage was a safety concern for US BWRs and to judge the adequacy of the resolution of USI A-43 as it pertains to BWRs. The initial thrust of this study was both probabilistic and deterministic, with emphasis on estimating the probability of losing NPSH margin. During the course of the study the probalistic aspects were de-emphasized and the deterministic aspects were elevated, because the staff's analysis and research indicated that debris blockage for BWRs was a greater safety concern than early analysis had concluded. The initial and subsequent results of the study revealed that only a small quantity of fibrous insulation debris and corrosion products was needed to induce large head losses. Also, most of the breaks modeled in the study lead to the loss of ECCS pumps because of strainer blockage. The initial results of the study were reported in a draft report (Ref. 9), in August 1994. There are several major differences between the current BWR analysis and the PWR analysis conducted under USI A-43. The major differences are:

1. A BWR specific LOCA scenario was analyzed,

2. Non-fibrous debris, primarily corrosion products, was considered in the current analysis,

3. Smaller insulation debris fragments, considered more representative of LOCA generated debris, were used in experiments, and

4. RMI was not considered benign with regards to strainer blockage, because of the results of Finnish experiments (Ref. 10).

In addition to the above differences, the NUREG/CR-6224 study provides a more comprehensive assessment of the accident scenario, which is summarized in Figure 1. During the course of the study, it became apparent that the modeling considerations and their relationship to the LOCA progression as shown in Figure 1 were needed to develop an engineering resolution of the BWR suction strainer blockage issue. A pictorial representation of the four major aspects, debris generation, debris transport in the drywell, debris transport in the wetwell, and head losses due to debris blockage, is shown in Figure 2.

During the course of the study it became apparent that the knowledge base for analyzing this safety concern was limited. The NRC funded the following experiments in support of the NUREG/CR-6224 analysis and the resolution of the BWR Strainer Blockage Issue:

1. Head loss experiments with two different fiberglass insulations and combinations of fiberglass insulation debris and corrosion products,

2. Head loss experiments with RMI; combination of RMI and fiberglass: and combination of RMI, fiberglass, and corrosion products,

3. Filtration experiments of corrosion products through a fiberglass medium,

4. Debris settling tests with fiberglass, corrosion products, and RMI debris, and

5. A singular RMI debris generation experiment.

The results of the fiberglass and corrosion products experiments were used to develop and refine the models in the NUREG/CR-6224 study and the models embodied in the Blockage 2.x code. The Blockage 2.x code is a calculation tool that was developed to estimate the head loss caused by debris blockage. The results of the RMI experiments will be used to make a determination on the severity RMI debris accumulation on suction strainers. Extensive use was made of experiments performed by Swedish and Finnish utilities and organizations. The NRC staff's participation in the International Working Group (IWG) on ECCS Recirculation Reliability (Ref. 11), which was formed under the auspices of the OECD/NEA CSNI/PWG-1, gave the staff access to these foreign reports. Also the staff reviewed numerous analytical and experimental reports provided by licensees and industry organizations such as the Boiling Water Reactor Owners Group (BWROG), Performance Contracting, Inc. (PCI), and Transco Products, Inc. In addition, numerous discussions were held with the BWROG ECCS Suction Strainer Committee to facilitate the development of potential fixes.

The current state of knowledge regarding the US BWR ECCS strainer blockage issue leads to the following observations and conclusions:

1. A singular (or generic) solution is not possible in the US because of the variations in BWR containment designs, installed passive strainers, ECCS long term cooling requirements, variability of installed insulation materials, and foreign materials present. In retrospect, GL 85-22 (Ref. 4) correctly stated: "It was concluded that a single generic solution is not possible, but rather that debris blockage effects are governed by plant specific design features and post-LOCA recirculation flow requirement."

2. Calculational models to accurately predict amounts of debris generated and the physical characteristics of such debris are lacking. Insights on levels of destruction have been extracted from HDR tests and are reported in NUREG-0897, Rev. 1, (Ref. 1). Steam and air blast tests have been used to generate fibrous insulation debris (Refs. 12 and 13) to gain insights into insulation debris characteristics, which were then used to formulate fibrous debris for head loss experiments. Recent re-considerations related to replacing fibrous insulations with RMI prompted the NRC to fund a steam blast test

(Ref. 14) which simulated a steam line LOCA to gain insights on the types and characteristics of such materials (see Figures 3 and 4). These pictures clearly illustrate the variability of debris sizes and characteristics generated resulting from this steam blast experiment. A Swedish consortium has conducted a more extensive series of blast tests on RMI (Ref. 15) representative of those used in European plants but that detailed information has not been placed into the public domain.

In the meantime, considerable discussion and debate continues regarding the use of jet expansion/impingement models (Ref. 16) to calculate debris generated, use of cone models rather that spherical models, for estimating zones of destruction, etc. It is unfortunate that engineering judgments and simplifications from Reference 1 (see Figure 5) were adopted as defacto debris generation standards for many years without heeding the cautions noted at that time. Ten years later, the calculational ability to accurately calculate quantities and the physical characteristics of debris generated by a pipe break is not much further ahead and still relies heavily on engineering judgment coupled with selective degrees of conservatism. More recent experiments still support the judgment that a very severe level of destruction will occur within a 3 to 5 L/D break zone boundary and that precise debris generational calculational models do not exist. The IWG (Ref. 11) did not support use of use of jet expansion/impingement models for debris calculation.

3. Drywell transport of LOCA generated debris is the second area of continuing technical debate. Some small scale atypical experiments (Ref. 17) suggest that drywell transport is less that 10%, but even those experimenters did not support using a less than 10% transport factor for nuclear plant applications. Barsebäck-2 post-event analyses (Ref. 11, Appendix D) suggest that a transport factor closer to 50% occurred due to a combination of blowdown by the steam jet and washdown by the containment sprays. The NRC has selected a 100% transport factor for conservatism and modeling limitations for this phase was used in the proposed RG 1.82, Rev. 2.

4. Suppression pool debris transport models which include settling and materials dependence (to a varying degree) have been developed from separate effects experiments conducted at the Alden Research Laboratory and have been used to develop the models reported in NUREG/CR-6224 (Ref. 18). There appears to be consensus that suppression pool debris transport modeling as described in Reference 8, is acceptable and reasonably well understood.

5. Experiments over the past 3 - 4 years have produced considerable data to estimate pressure drop associated with debris materials which

can be transported to the suction strainers. Chapter 4 and Appendix A of Reference 11 are recommended reading for an overview of available information. However, this database clearly illustrates the variability associated with various insulation materials and the necessity for supporting experimental data if detailed calculations are required (i.e., determining the adequacy of NPSH margins at values of 1 to 2 feet of water).

In addition, these strainer head loss experiments have clearly demonstrated the strong influence of filtration and capture of corrosion or other particulates by fibers transported to suction strainers (Ref. 18, Appendices B and E). Corrosion products are present in US BWR suppression pools, and small amounts of fibrous materials can be easily entrained onto suction strainers followed by entrapment particulates. The recent Limerick-1 event (Ref. 7) is an illustration of the ease of transport and accumulation of such materials onto a suction strainer under suppression pool cooling mode conditions. It therefore appears that periodic (i.e., at refueling outages) suppression pool cleaning is a prudent measure and should be adopted.

In retrospect, it is clear that prior USI A-43 evaluations and findings developed in the mid 1980s, when compared to the current knowledge base and recent plant incidents, will under-estimate the potential for loss of long term cooling capability during the post-LOCA period for US BWRs. Based on the current knowledge base and available plant information the conclusion was reached that passive suction strainers currently installed in US BWRs are probably undersized and susceptible to the detrimental effects of debris blockage. The NRC staff considers larger strainer surface areas the best solution to the BWR Suction Strainer Blockage Issue. Increased strainer surface area offers several benefits such as (1) larger area for debris accumulation, thus thinner debris layers and (2) lower head losses for a given debris layer thickness because of a lower approach velocity. This can be illustrated with equations[1] developed to estimate head loss across a blocked strainer.

equation 1 $$\Delta H = a V^{b} t_e^{c}$$

equation 2 $$\Delta H = (\alpha(\varepsilon)\mu V + \beta(\varepsilon)\rho_w V^2)\, t_e$$

equation 3 $$\Delta H = dv + eV^2$$

---

[1]These equations were developed for fiberglass insulation debris or a combination of fiberglass insulation debris and corrosion product, and they may not be applicable to other types of debris such as RMI debris.

where,

ΔH	is the head loss
V	is the approach velocity
t_e	is the effective debris bed thickness
t_a	is the actual debris bed thickness
a, b, c	are empirical constants
$\alpha(\varepsilon)$, $\beta(\varepsilon)$	are functions of bed porosity
μ	is the fluid dynamic viscosity
ρ_w	is the fluid density

and

$$d = 17.7 (M_L^{0.85}) (1 + 0.23 (\frac{M_C}{M_L}))^{1.37}$$

$$e = 17.7 (M_L^{0.93}) (1 + 0.27 (\frac{M_C}{M_L}))^{1.77}$$

where,

M_C	is mass of corrosion products on strainer per strainer area
M_L	is mass of fibrous debris on strainer per strainer area

If the approach velocity is decreased in any of the above equations, then head loss will decrease. If the accumulated debris or debris thickness is decreased in any of the above equations, head loss will also decrease. An increase in strainer surface area, according to the NUREG/CR-6224 parametric analysis, provides the greatest decrease in head loss. Because of spatial and dynamic loads constraints, some plants may not be able to increase their suction strainer surface area sufficiently to eliminate or reduce to acceptable levels the detrimental effects of debris accumulation on the suction strainers. BWRs that cannot install adequately larger strainers will need to take additional measures such as minimizing or eliminating operational debris, foreign materials, and LOCA generated debris that may migrate to the suction strainers. In response to this condition, the US industry (i.e., BWROG and PCI) has funded design and experimental programs to develop and test new passive suction strainers (e.g., the BWROG "star" and PCI stacked disk concepts) shown in Figures 6 and 7, and also self cleaning strainers. In addition the BWROG ECCS Suction Strainer Committee is developing a User Resolution Guidance (URG) document which would provide a structured analysis method to assist licensees in sizing strainers. At this time the BWROG has completed their experiments on alternate passive strainer designs which are designed to provide significantly increased strainer surface area while minimizing the spatial size envelope. A self cleaning suction strainer design is being evaluated by the BWROG. Although initial experimental results look promising, specific designs for plant application have not yet been submitted and testing is continuing.

There are two aspects to the potential strainer clogging issue. The first is the potential for clogging of ECCS suction strainers by debris and sludge which is present in

the pool during normal operation. This aspect of the issue is highlighted by the Perry and Limerick events, and is related to the LOCA debris issue because any debris present in the pool would contribute to the potential blockage of a strainer during a LOCA. However, debris present in the suppression pool during normal operation also represents a potential threat to the pumps used for suppression pool cooling mode for more common transients (e.g., stuck open SRV). The staff has also noted that the events at Perry and Limerick have raised concerns about the adequacy of licensee foreign material exclusion (FME) practices. Based on these considerations, NRC Bulletin 95-02 (Reference 8) was issued on October 17, 1995. The bulletin requested licensees to verify the operability of all pumps which draw suction from the suppression pool when performing their safety functions (e.g., ECCS, containment spray, etc.), based on an evaluation of suppression pool and suction strainer cleanliness conditions. In addition, the operability evaluation is requested to be confirmed through an appropriate test and strainer inspection within 120 days. Additional actions requested by the bulletin include establishing a program for suppression pool cleaning, evaluation of FME practices in the drywell and wetwell, correction of any identified FME weaknesses, and consideration of other ways to detect strainer clogging such as pump suction pressure trending and suppression pool water sampling. The staff is currently awaiting licensee responses to this bulletin.

The second aspect of the issue is the potential clogging of ECCS suction strainers by a combination of debris generated by a LOCA and debris and sludge which is present in the pool during normal operation. This issue has been under review by the staff and the BWROG. The staff issued a draft bulletin (Ref. 19) and proposed revision to RG 1.82, Rev. 1 (Ref. 20) for public comment on July 31, 1995. The public comment period has ended and the staff is currently addressing the comments. The staff concluded in the draft bulletin that there are three basic options for resolving this issue, although licensees are free to propose alternate solutions. The draft bulletin requests licensees to do one of the following: (1) install a large capacity passive strainer design of sufficient size that the worst expected debris loading would not cause the ECCS pumps to lose NPSH, (2) install a self-cleaning strainer design which continuously cleans the strainer surface and is capable of withstanding the worst case debris concentrations in the suppression pool, or (3) install a backflush system which can be actuated to clean the strainer surface and prevent the ECCS pumps from losing net positive suction head. Each of these options would also require supplementary actions by the licensee in order to comply with the intent of 10 CFR 50.46. For instance, a large capacity passive strainer would require actions by the licensee to ensure that the potential debris loading of the strainer never exceeds its design capacity. An example of a measure that may be required to ensure this is that a licensee may have to clean their suppression pool at certain intervals in order to ensure that sludge concentrations in the pool do not exceed the design basis of the strainer. This would then be a consideration for considering the frequency of pool cleaning. The final bulletin is scheduled to be issued in February 1996. The staff will incorporate resolution of any additional issues identified during the review of licensee responses to NRC Bulletin 95-02 in the February 1996 bulletin.

References

1. A.W. Serkiz, "Containment Emergency Sump Performance," NUREG-0897, Rev. 1, USNRC, Washington, DC, October 1985.

2. A.W. Serkiz, "USI A-43 Regulatory Analysis," NUREG-0869, Rev. 1,USNRC, Washington, DC, October 1985.

3. Regulatory Guide 1.82, Revision 1, "Water Sources for Long-Term Recirculation Cooling Following a Loss-of-Coolant Accident," USNRC, Washington, DC, November 1985.

4. Generic Letter 85-22, "Potential for Loss of Post-LOCA Recirculation Capability Due to Insulation Debris Blockage," USNRC, Washington, DC, December 3, 1985.

5. NRC Bulletin 93-02, "Debris Plugging of Emergency Core Cooling Suction Strainers," USNRC, Washington, DC, May 11, 1993.

6. OECD/NEA Workshop on the Barsebäck Strainer Incident in Stockholm, Sweden, January 26-27, 1994.

7. NRC Information Notice 95-47, "Unexpected Opening of a Safety/Relief Valve and Complications involving Suppression Pool Cooling Strainer Blockage," USNRC, Washington, DC, October 4, 1995.

8. NRC Bulletin 95-02, "Unexpected Clogging of a Residual Heat Removal (RHR) Pump Strainer While Operating in Suppression Pool Cooling Mode," USNRC, Washington, DC, October 17, 1995.

9. G. Zigler et al, "Parametric Study of the Potential for BWR ECCS Strainer Blockage due to LOCA Generated Debris, " NUREG/CR-6224, SEA No. 93-554-06-A:1, Washington, DC, December 1993. (DRAFT, UNPUBLISHED)

10. Hyvärinen, J. and Hongisto, Olli., "Metallic Insulation Transport and Strainer Clogging Tests," STUK-YTO-TR 73, Finnish Centre for Radiation and Nuclear Safety, Helsinki, Finland, June 1994.

11. Sandervåg, et. al., "Knowledge Base for Emergency Core Cooling System Recirculation Reliability," Organization for Economic Coorperation and Development/ Nuclear Energy Agency, Paris, September 1995. (DRAFT, UNPUBLISHED)

12. Blomquist, M. and Dellby, M., "Barsebäck 1 & 2, Oskarsham 1 & 2, Ringhals 1, Report from Tests Concerning the Effect of a Steam Jet on Caposil insulation at Karlshamm," SDC 93-1174, ABB Atom, June 1993.

13. Kegel, T., "Air Blast Destructive Testing of NUKON Insulation - Simulation of a Pipe Break LOCA," Colorado Engineering Experiment Station, October 1993.

14. Hoffmann, D. and Knapp, A., "RMI Debris Generation Testing, Pilot Steam Test with a Target Bobbin of Diamond Power Panels," NT34/95/e32, Siemens, Karlstein, Germany, July 3, 1995.

15. Trybom, J., "Metallic Insulation Jet Impact Tests (MIIJIT), GEK 77/95, Vattenfall Energisytem, June 1995.

16. ANSI/ANS-58.2-1988, "Design Basis for Protection of Light Water Nuclear Power Plants Against the Effects of Postulated Pipe Rupture," ANSI/ANS, October 1988.

17. "Karlshamn Tests 1992. Test report. Steam blast on insulated objects," RVE 92-205, ABB Atom, November 1992.

18. G. Zigler et al, "Parametric Study of the Potential for BWR ECCS Strainer Blockage due to LOCA Generated Debris, " NUREG/CR-6224, SEA No. 93-554-06-A:1, Washington, DC, August 1994. (DRAFT)

19. Proposed NRC Bulletin,"Potential Plugging of Emergency Core Cooling Suction Strainers by Debris in Boiling Water Reactors," USNRC, Washington, DC, July 21, 1995.

20. Draft Regulatory Guide DG-1038 (Proposed Revision 2 to Regulatory Guide 1.82, Rev. 1), "Water Sources for Long-Term Recirculation Cooling Following a Loss-of-Coolant Accident," USNRC, Washington, DC, July 1995.

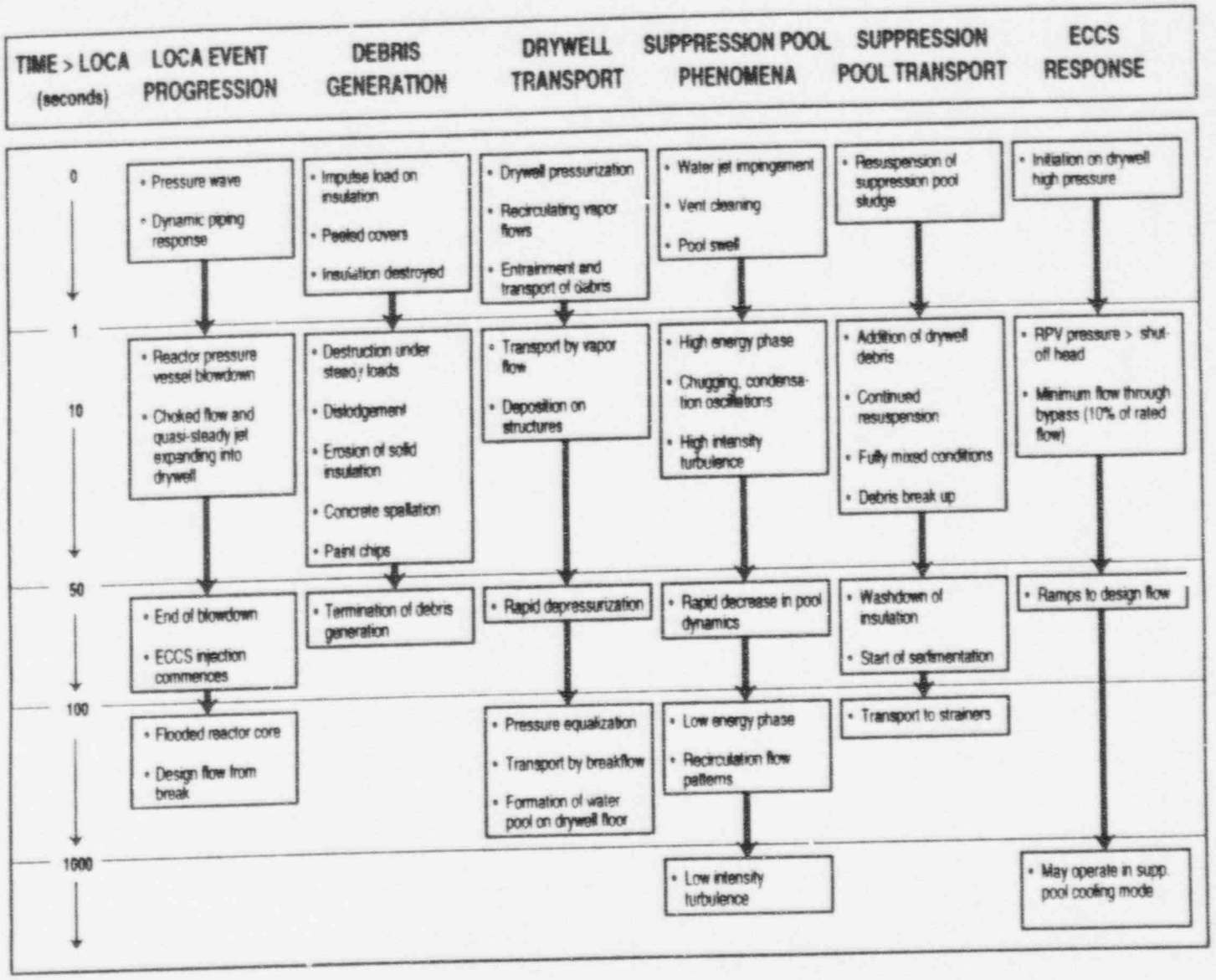

Figure 1 LLOCA Event Progression and Its Effect on Debris Generation and Transport

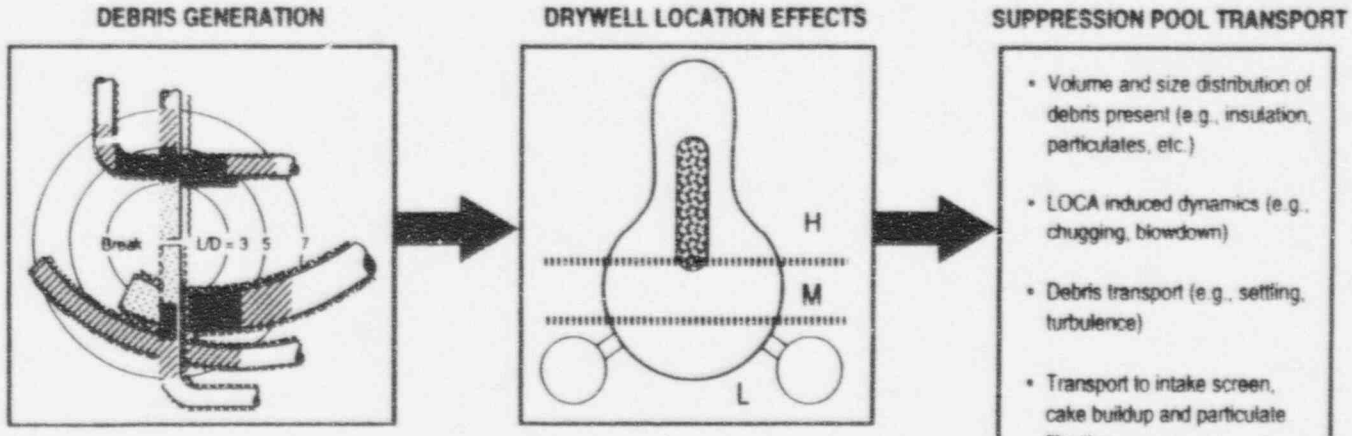

DESTRUCTION FACTORS

L/D	Fraction
3	0.75
5	0.6
7	0.4

DRYWELL TRANSPORT FACTORS

Region	Fraction
H	0.25
M	0.5
L	0.75

TERMINOLOGY

Destruction Factor: Fraction of insulation assumed to be destroyed and transportable (i.e., fines and shreds) by the break jet.

Drywell Transport Factor: Fraction of transportable debris that could travel from the drywell to the suppression pool due to a combination of blowdown and washdown.

Particulates: Very small non-insulation debris that is generated during a LOCA (drywell particulates) or exists prior to a LOCA (sludge).

Figure 2 A Pictorial Description of Important Elements of a Methodology for Analyzing BWRs

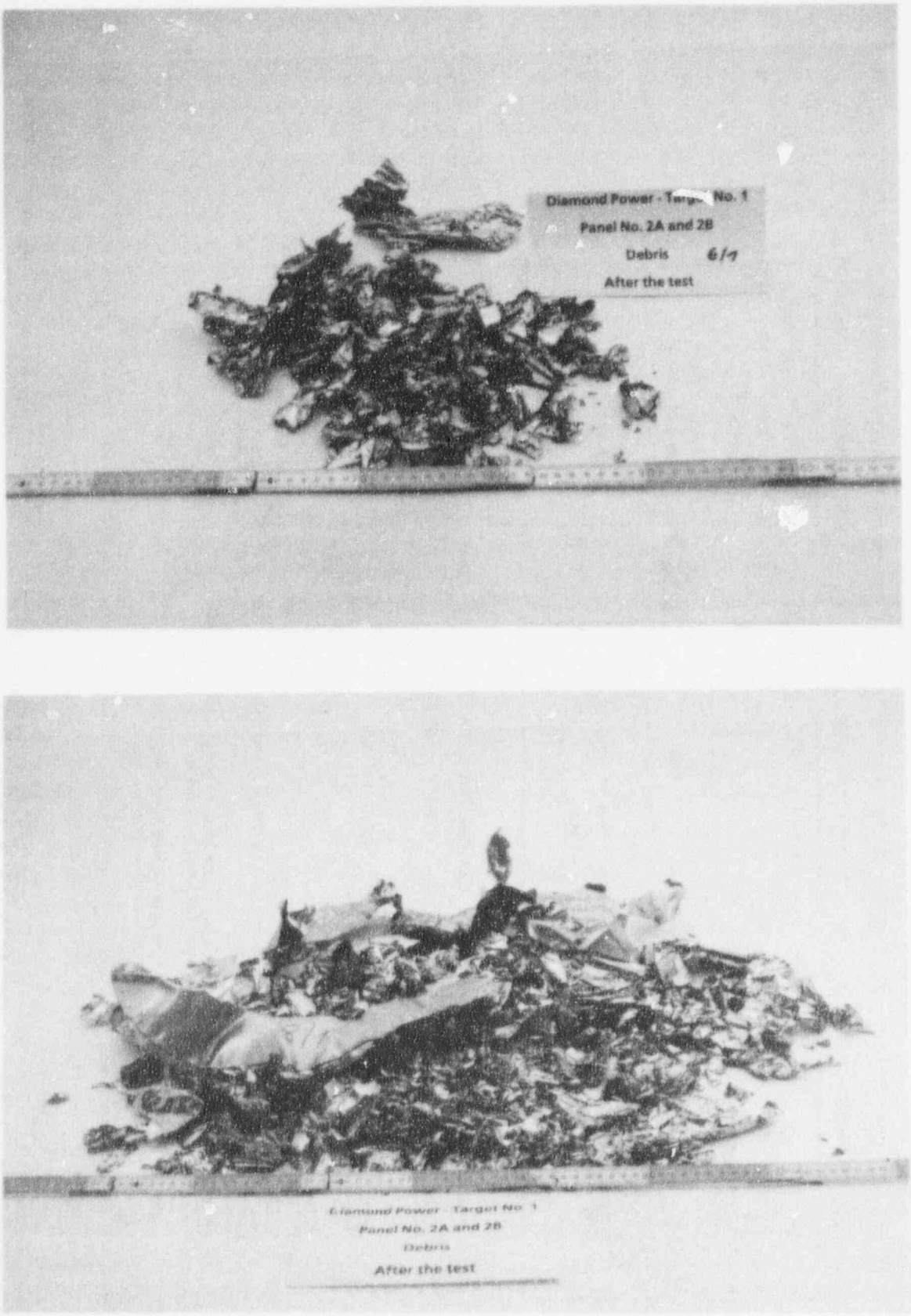

Figure 3 RMI Panels From Siemens KWU Steam Blowdown No. 1 Test (5/31/95)

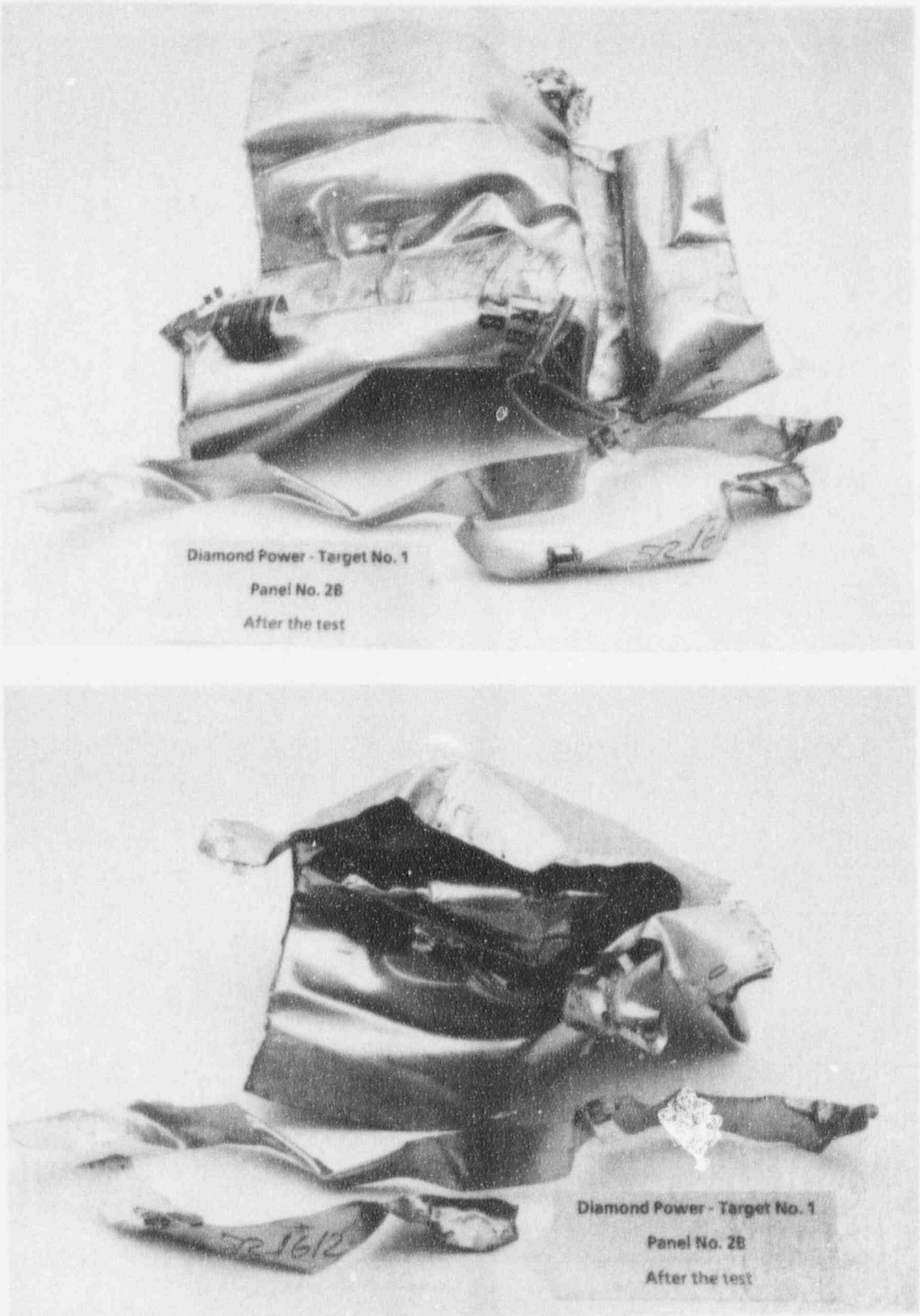

Figure 4 RMI Foil Debris From Siemens KWU Steam Blowdown No. 1 Test (5/31/95)

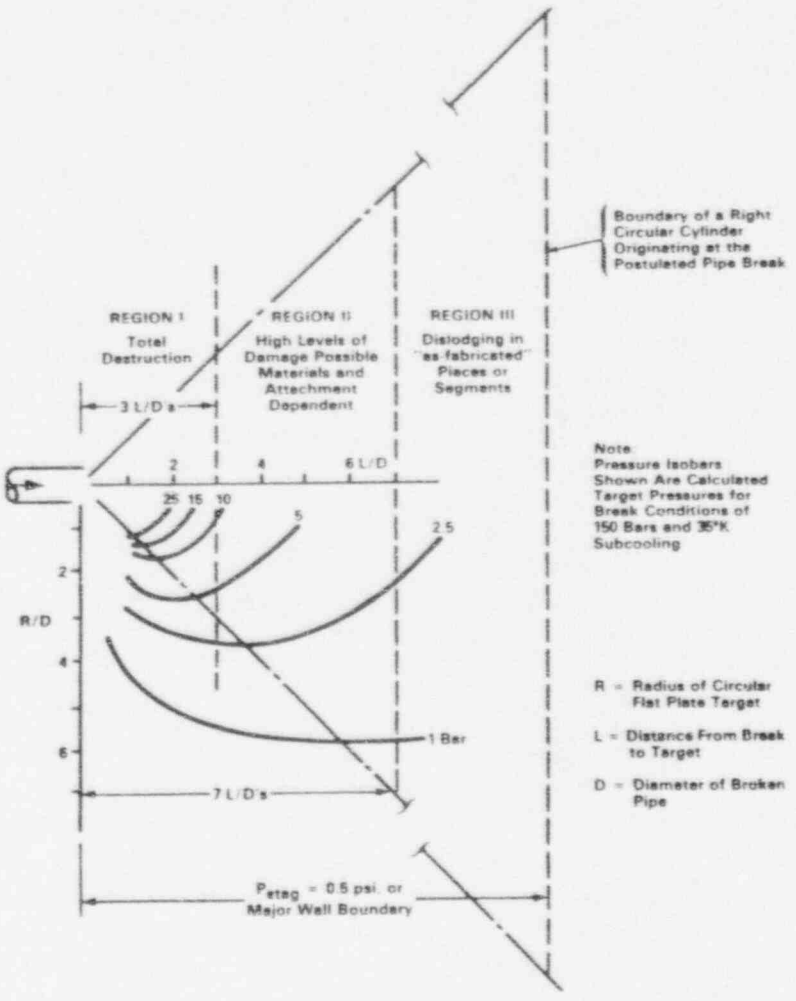

Figure 3.25 Multiple region insulation debris generation model

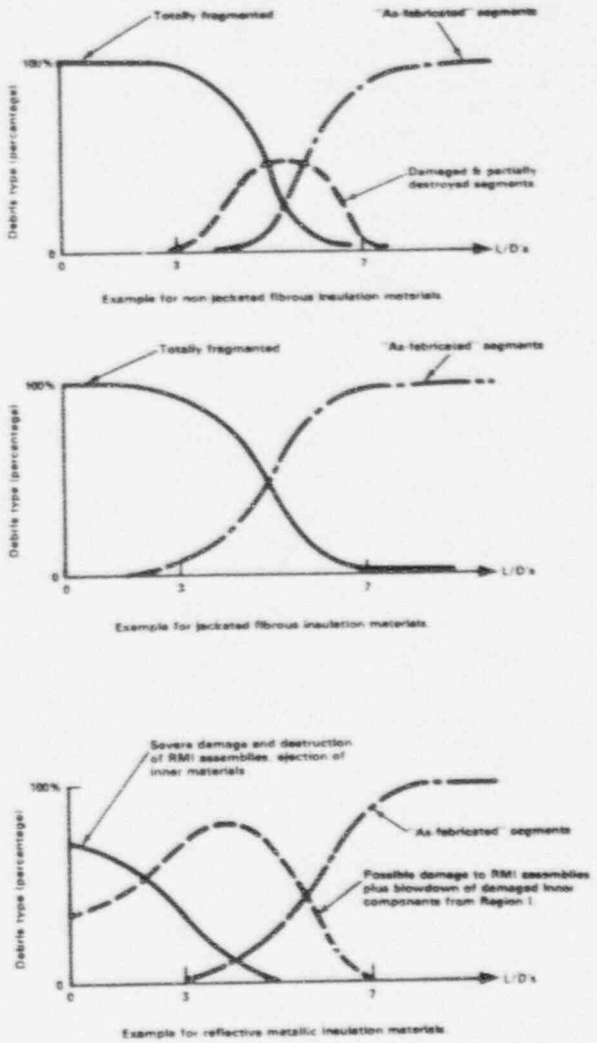

Figure 3.26 Possible variation of debris types and relative quantities in regions of the three-region jet model (see Figure 3.25)

Figure 5 History of Cone Model and Debris Generation Judgements

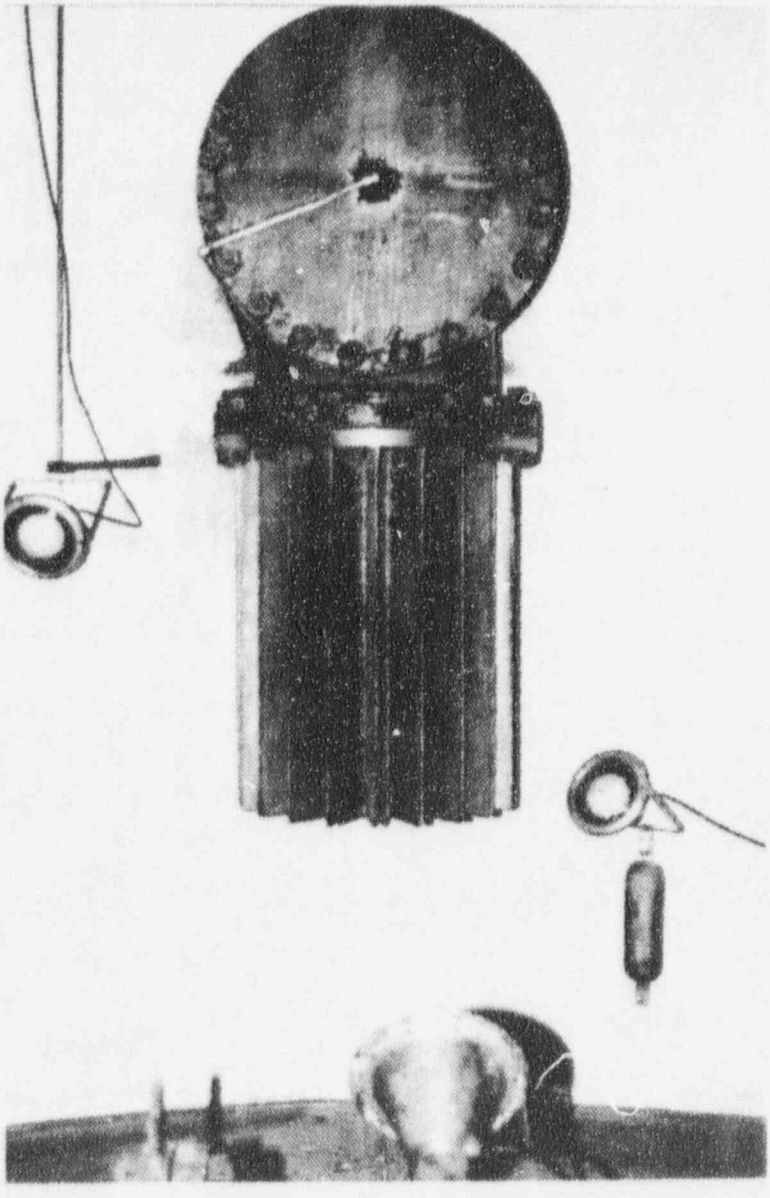

Figure 6 BWROG 20 Point STAR Strainer

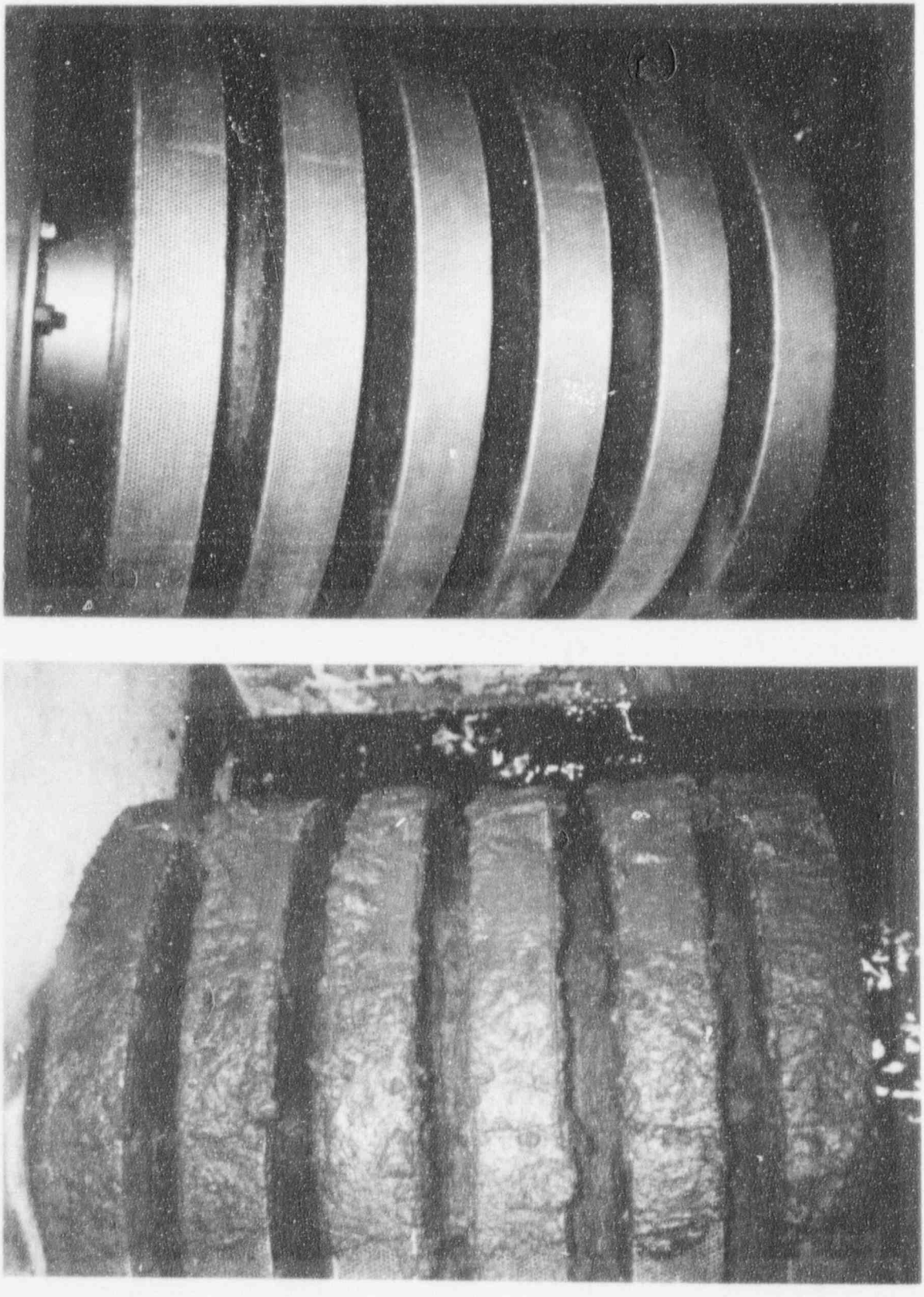

Figure 7 Performance Contracting Inc. (PCI) Scaled Stacked Disk Strainer

The CSNI/PWG-1 International Task Group on ECCS Reliability

Principal Authors[1]

O. Sandervåg (SKI, Sweden), T. Riekert (GRS, Germany),
A. Serkiz (USNRC, USA), J. Hyvärinen (STUK, Finland)

Background

On July 28, 1992 a steam line loss-of-coolant accident (LOCA) occurred when a safety relief valve inadvertently opened in the Barsebäck-2 nuclear power plant, a boiling water reactor (BWR) in Sweden. The steam jet stripped fibrous insulation from adjacent pipework. Part of that insulation debris was transported to the wetwell pool and clogged the intake strainers for the drywell spray system after about one hour. Although the incident in itself was not very serious, it revealed a weakness in the defense-in-depth concept which under other circumstances could have led to failure of the emergency core cooling system (ECCS) to provide water to the core.

Before the Barsebäck-2 LOCA, international regulators of nuclear power plants and the nuclear power plant industry had considered safety questions related to strainer clogging as resolved. Many European countries had followed the guidance for strainers in pressurized water reactors (PWRs) contained in United States Nuclear Regulatory Commission's (USNRC) Regulatory Guide 1.82, "Water Sources for Long Term Recirculation Cooling Following a Loss-of-Coolant Accident," 1974. However, data obtained from European experimental programs carried out in the late seventies to determine the performance of strainers indicated that this guide was not adequate.

In addition, Swedish plant owners had used this guidance to judge performance of emergency core cooling systems (ECCS) in their plants. Analyses at that time had indicated that strainer clogging, if occurring at all, would at least not occur during the first ten hours after a LOCA. Since operation of the ECCS would be needed for a long time, backflushing capabilities and monitors of pressure drop across the strainers were installed in older Swedish BWR plants with small strainer areas. These actions (particularly the backflushing capability) were judged to be adequate compliance with the revised USNRC Regulatory Guide 1.82, Rev. 1, issued in 1985. Safety questions related to strainer clogging were considered to have been resolved until the incident happened in Barsebäck-2, which showed that clogging and loss of net positive suction head (NPSH) margin could occur quickly.

The Barsebäck incident spurred immediate action on the part of regulators and utilities alike in several Organization for Economic Cooperation and Development (OECD) countries (e.g., Sweden, Finland, Germany, Switzerland and France). For example, the Swedish Nuclear Power Inspectorate (SKI) required that immediate measures to prevent strainer clogging

---

[1]This paper compiled by Mr. Sandervåg consist of excerpts from the CSNI/PWG-1 report, "Knowledge Base for Emergency Core Cooling System Recirculation Reliability," that was written by the principal authors listed above. The report has not been published yet.

should be taken for the five oldest Swedish BWRs which had strainers of small area before they were allowed to start again. Research and development efforts of varying intensity were launched in many countries and in several cases resulted in findings that earlier strainer clogging data was incorrect because essential parameters and physical phenomena (such as insulation aging) had not been recognized previously. Such efforts resulted in substantial backfitting being carried out for BWRs and some PWRs in several OECD countries.

To accelerate exchange of information and experience, and provide feedback of actions taken to the international community, a workshop on the strainer clogging issue was hosted by SKI in Stockholm, Sweden on January 26-27, 1994, under the auspices of Committee on the Safety of Nuclear Installations/Principle Working Group-1 (CSNI/PWG-1). The objectives of the workshop were (1) to give an overview of decisions and work performed recently on this issue, (2) to address the actual safety issues with regard to the reliability of ECC recirculation, and (3) to discuss further actions needed. The workshop revealed a rather confusing picture of the available knowledge base, examples of conflicting information and a wide range of interpretation of guidance provided in the USNRC Regulatory Guide 1.82, Rev. 1. Following this workshop, SKI requested formation of an international working group (IWG) under the auspices of CSNI/PWG-1 committee for establishing an internationally agreed-upon knowledge base for assessing the reliability of emergency core cooling water recirculation systems.

The specific tasks given to the group were:

1. Critical review and compilation of available experiments and other data related to the performance of ECC water recirculation systems, including formation and behavior of various types of debris contaminating the water.

2. Assessment of the applicability of the data base. Identification of major uncertainties, lack of information and data.

3. Proposal of additional research and experiments as well as pointing out those uncertainties which should be accommodated in terms of conservative design features.

The IWG, composed of participants from German (GRS), Swedish (SKI), Finnish (STUK), Japanese (NUPEC), and US (USNRC) regulatory authorities, the US BWR Owners Group (BWROG), insulation vendors (PCI and Transco Products, Inc.), Vattenfall Utveckling AB, and SEA (a NRC subcontractor), met initially in April 1994 in Stockholm, Sweden, and three additional meetings have been held.

Summary of the results of the International Working Group report

Two design approaches have emerged for dealing with LOCA generated debris - the robust design approach (the Nordic countries) and the "calculational" approach (United States). The robust design approach for minimizing effects of debris transport was devised in the Nordic countries in late 1992 and early 1993 following the Barsebäck-2 incident and was

discussed in detail at the Organization for Economic Cooperation and Development/Nuclear Energy Agency (OECD/NEA) workshop in January 1994. It consists of a few very simple assumptions that aim to make the strainer head loss evaluation very conservative and that is consistent with the licensing rationale of European countries that adopted this approach. The current U.S. approach is based on analytical models derived from separate-effects experiments designed to provide insights into debris generation and transport phenomena that would occur during the course of a LOCA.

Figure 1 illustrates LOCA considerations that should be addressed in the design of ECCS suction strainers.

For the robust design approach several processes were reviewed in order to quantify the amount of debris generated after a LOCA that would clog the strainers. The amount of material dislodged was estimated using a conservative model and assuming that all dislodged material was transported to the wetwell pool and that all this material could settle on the strainers of one train and should not cause loss of net positive suction head (NPSH) for the pumps. Conservative data for pressure drops was also used. This approach was considered consistent with the original Swedish licensing rationale and several other European countries had adopted this approach.

The first use of this principle applied pressure drop data for pure substances. Only later did experiments show that mixtures of particles and fibers gave rise to higher pressure drops than pure materials. To comply with the requirement of robustness, the Swedish plants were further modified by changeout of insulation materials, installation of even larger strainers, and protection of areas that could produce particulate material.

The U.S. calculational approach is based on analytical models derived from separate-effects experiments and the application of such models. This approach and the associated models were described in NUREG/CR-6224, "Parametric Study of the Potential for BWR ECCS Suction Strainer Blockage Due to LOCA Generated Debris." Many experiments were reviewed to provide insights in the basic mechanisms important for recirculation reliability and pressure drop associated with fibrous materials and their filtering of particulates. Additional insights regarding debris generation and transport were derived from the Marviken, HDR, and Karlstein experiments.

To facilitate review and evaluation, the considerations shown in Figure 1 were the basis for dividing this report into five major areas: Debris Generation, Drywell Transport, Suppression Pool Transport, Strainer Pressure Drop, and Related Issues. The last section was introduced to identify other safety considerations that should be reviewed in conjunction with ECCS recirculation performance evaluations and pursuit of backfit selections.

Debris Generation:

The major mechanisms for dislodging the material are the pressure wave associated with the pipe rupture, erosion by the fluid jet, and flow and pressure differences in narrow sections along the flow path. Conceptual and empirical models are identified that are

applicable to jet erosion and pressure differences. No model describing the first pressure wave has been identified. The models that are currently used to evaluate the amount of dislodged material seem to be mostly applicable to flashing water. Steam jets produce destruction zones that are much narrower and much longer than jets produced by flashing water. The observations at Barsebäck and experiments with steam jets seem to confirm that the destruction zone could be more extended than that anticipated for flashing water.

The various insulation materials used in nuclear power plants exhibit different behavior with respect to destruction. Materials such as mineral wool seem to disintegrate quicker than fiberglass material under impact from a jet. Destruction of fibrous insulation blankets can be considerably reduced if they are encapsulated by stainless steel jackets. Also fibrous insulation materials that have been subjected to realistic temperatures behave differently than new material. Aged material seems to clog strainers more effectively than new material. Reflective metallic insulation (RMI) has been used in many applications and experiments indicate that foils of RMI in the jet would be fragmented into small pieces. Larger RMI debris could form energetic missiles. Experiments have indicated that this potential also exists for fibrous insulation that is encapsulated by metal sheets. For this latter material the missiles are generally lighter because of the lower specific metal mass.

Most of the experimental studies have focused on estimating the amount of insulation debris generated by a postulated break. The amount is an important factor because it represents the fundamental source term for debris. However, considerations related to debris transportability and head loss revealed that factors such as size distribution of the debris and the content of the fine material, particles or fibers, could have a large effect on the head loss across the strainers. It has thus become equally important to identify the character of the debris, the amount of released fine particles, in the plant-specific safety assessments. A LOCA jet would also likely produce particles of concrete, paint chips, and corrosion products which could contribute to high strainer head losses. The database for the assessment of these issues is very limited.

For the debris generation the IWG concludes that plant-specific studies are needed.

Drywell Transport:

Debris is transported through the drywell by blast forces, blowdown forces and by washdown. Plant-specific analyses are needed to determine the retention in drywell. The uncertainty is high. Some separate-effects experiments have shown retention factors contradictory to what was observed in Barsebäck-2 incident. It is therefore difficult to draw conclusions of high confidence which are necessary for safety assessment from these experiments. Therefore, conservative assumptions are recommended regarding the fraction of the debris transported through the drywell. As a basis to future investigations, more research on how to perform meaningful experiments on drywell transport is regarded as necessary.

Wetwell Transport:

Debris transport in the wetwell pool is controlled by sedimentation and resuspension, which are dependent on parameters like character of the debris materials and turbulence levels present. Experiments simulating post-LOCA chugging and turbulence levels have shown that fibrous insulation materials which are subjected to pool turbulence during the high energy phase could be further fragmented and thereby remain suspended in the water for extended periods of time.

Note that different sedimentation characteristics between new and aged materials were partly responsible for the misleading conclusions on clogging times drawn from experiments in the seventies. In the old experiments, new mineral wool that had been mechanically cut to pieces had been tested. This material first floats on the water surface and thereafter rapidly sinks to the bottom. The new experiments using debris that was removed from the reactors or aged by temperature, showed that the material tended to remain suspended in the water and thus is available for strainer clogging.

Also, the resuspension of settled material could be higher than earlier indicated under more turbulent conditions. Resuspension of particulate material as, for instance, corrosion products could have a significant effect on strainer clogging. Another aspect is that particle size distributions may be significantly affected during pool transportation. Larger particles may settle quicker and an enrichment of smaller particles near the strainers may occur. Small particles, in combination with fibrous debris, would generally promote strainer clogging.

Strainer Pressure Drop:

The pressure drop over a debris bed is dependent on parameters like composition of the material and particle size distribution in the bed, thickness, approach velocity, and temperature. Predicting the behavior of pure materials is generally possible. The methodology for pressure drop prediction through beds of mixtures of fibrous and particulate debris has large uncertainties. These uncertainties primarily relate to the fact that present understanding related to filtration of particulate debris is incomplete. Additional factors that introduce uncertainties include: debris size distribution and method of debris bed formation. Caution has to be exercised when testing different types of debris so that the test and characteristics of the materials are representative of those expected in operating reactors after a LOCA.

Many experiments were performed on mixtures of fibers and particles. Generally, the pressure drops significantly increased for these mixtures as compared to pure materials. Experiments also showed that mineral wool aged at higher temperatures gave rise to higher pressure drops than new mineral wool and that the method for fragmentation of material could significantly influence the results. Mechanically cut samples gave generally much lower strainer pressure drop than material that had been fragmented by steam jets. This effect has been explained by differences in insulation size distributions. Experiments also showed that the regression curves used for fibrous insulation in the earlier guidelines were non-conservative.

Generally large pieces resulted in higher head losses compared to smaller pieces. A mixture of fibrous and RMI debris have been found to result in head losses that are higher than the sum of their pure constituents. However, these findings are based on a limited set of experiments and the results have been influenced by the manner that such experiments were conducted.

Related Issues:

A number of potential concerns for the recirculation operability were identified that encompass such issues as vent path clogging; generation of missiles; strainer penetration; potential for liquid flow restrictions in, for instance, spray nozzles and fuel bundles; and effects on pump operability. The safety relevance of such parameters should be assessed on a plant specific basis. Investigations of these areas have not been systematic, and the uncertainties could be significant.

Concluding Remarks:

Extensive research programs carried out since the January 1994 workshop have produced further insights. Results from such programs are still pending. Information that has been made available later than June 1995 has not been considered in preparing the CSNI/PWG-1 International Task Group on ECCS Reliability report.

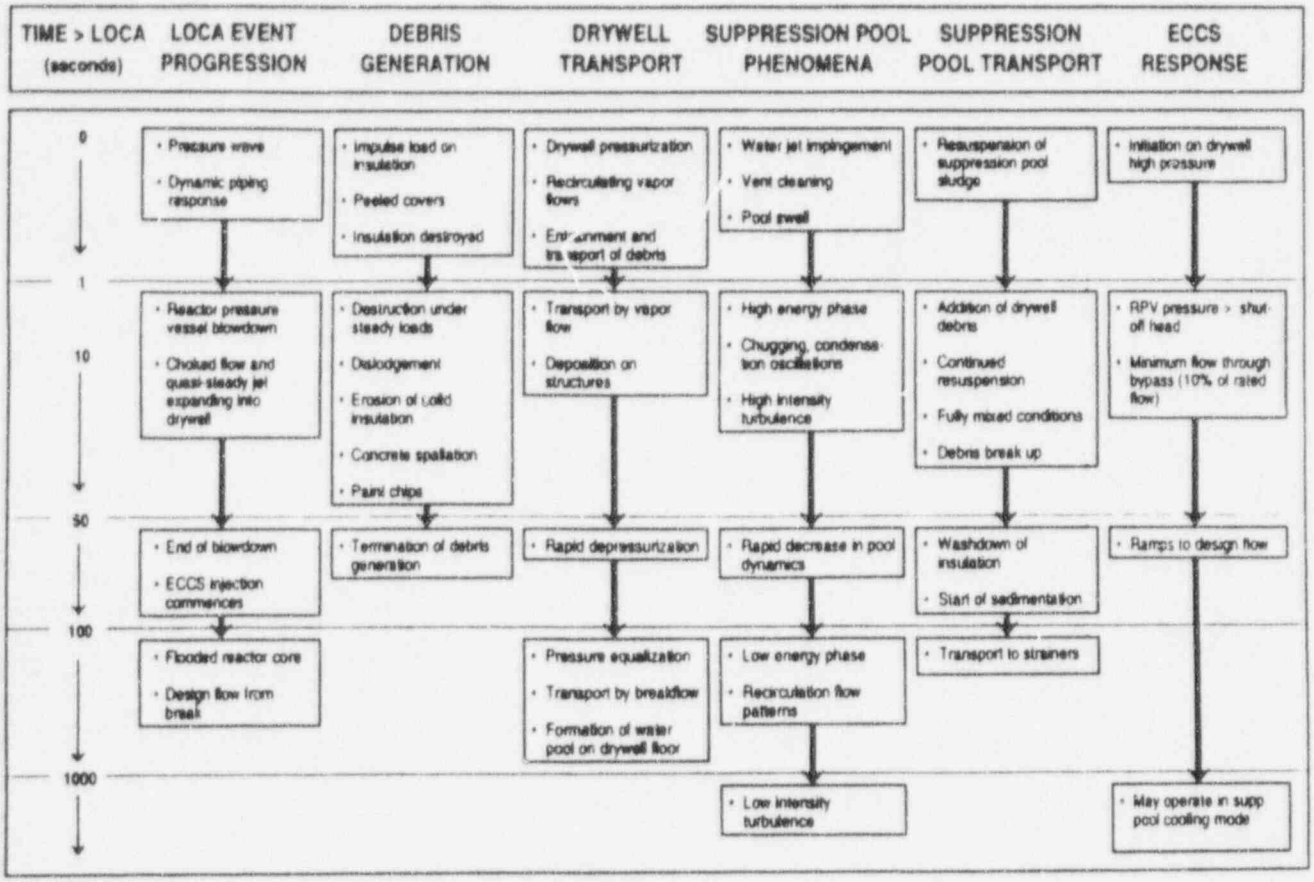

Figure 1: LOCA Event Progression and Its Effect on Debris Generation and Transport

EXPERIMENTS OF ECCS STRAINER BLOCKAGE AND DEBRIS SETTLING IN SUPPRESSION POOLS

by George E. Hecker, Alan B. Johnson, Prahlad Murthy, and M. Padmanabhan
Alden Research Laboratory, Inc.

If a rupture occurs in a nuclear power station pipe that leads to or from the reactor pressure vessel, the resultant Loss of Coolant Accident (LOCA) would initiate a chain of events involving complex flow phenomena. In a Boiling Water Reactor (BWR), the steam or liquid pipe break pressurizes the dry well, forcing the inert containment gases and steam through downcomers into the suppression pool, thoroughly mixing any particulates and pipe insulation debris carried with the gas flow to the pool. As the steam flow decreases, its unsteady condensation at the end of the downcomers ("Condensation Oscillation" and "Chugging") produces continued water motion in the suppression pool and downcomers. During the "blowdown" event, high pressure and then low pressure pumps automatically start injecting water from the suppression pool into the reactor to keep its temperature under control. Proper functioning of this Emergency Core Cooling System (ECCS) is critical for the first 30 minutes or so, before operators have time to consider and align alternative sources of cooling water.

A major concern for proper operation of the ECCS is the effect of fragmented insulation and plant particulates (oxidation products, concrete dust, paint chips, dirt, etc.) on the head loss at pump suction strainers. Sufficient loss could exceed the NPSH margin, causing cavitation with a resultant loss of pump capacity and longevity. The head loss increases with the mass of debris accumulated on the pump strainers (among other things), which in turn is dependent on the debris concentration versus time in the suppression pool.

This paper describes two sets of experiments that quantified the strainer head loss. One set of experiments considered the mixing and settling of fibrous insulation debris and fine iron oxide particles in the suppression pool during and after chugging. These tests used a reduced scale facility which duplicated the kinetic energy per unit water volume to define the concentration of the actual materials in the pool versus time. Such data allows calculation of the mass of debris on the strainer versus time.

The second set of experiments measured the head loss across a representative strainer plate for a range of masses of fibrous insulation debris and iron oxide particles. To allow the mass of oxide particles on the strainer plate to be estimated from pool concentrations, filtering efficiencies (trapping of the iron oxide particles by the fiber bed) were

also measured. Other parameters that influenced the head loss were the approach flow velocity and the water temperature.

The resulting data are being used as input to a computer code (developed by Science & Engineering Associates, Inc.) to predict strainer head loss versus time in the actual plant. The knowledge gained from these experiments allows the expected head loss to be calculated with greater confidence.

INTRODUCTION

During the critical 30 minutes after a potential Loss of Coolant Accident (LOCA) in a nuclear fueled power plant due to a break in one of the many piping systems connected to the reactor pressure vessel, various thermo-fluid phenomena occur and an Emergency Core Cooling System (ECCS) is automatically activated to keep core temperatures under control. In a Boiling Water Reactor (BWR), the initial heat sink is water stored in a suppression pool, and pumps would subsequently draw from this pool and inject the water into the core after its pressure is sufficiently reduced by the potential pipe break and system blowdown. The suction for the pumps is covered by strainers of perforated plate to protect critical system elements from various types of debris which would be created or transported by the pipe break discharge. Unfortunately, the collection of this debris on the strainer may cause a pressure drop sufficient to exceed the NPSH margin for the pumps, leading to cavitation and loss of pump performance. Although loss of the suppression pool as a source of water for the ECCS would not by itself lead to core damage, as other sources of water are available, the loss of redundancy and the need for operator action to make these other water sources available soon after a LOCA is of great concern.

This paper reports on a set of experimental studies to quantify the effects of some suppression pool flow phenomena on the behavior of debris in the pool and on the head loss across the pump suction strainers. Three basic types of debris were studied, fibrous thermal insulation fragmented by the pipe break energy, fragmented reflective metallic insulation (RMI), and rust particles (sludge) which accumulate over time in the suppression pool. Relevant geometric parameters, such as for the suppression pool, were modeled after BWR's with containments of the "Mark I" design. The two basic objectives of the study were a) to determine the extent of debris mixing and settling in the pool after system blowdown, such that the related concentration profiles are known for predetermined debris masses, and b) to determine the head loss across the pump suction strainers for various mass ratios of insulation debris and sludge retained on the strainer. Both of these variables are the inputs to a computer program which calculates the pump suction head loss versus time for the independently determined masses of various debris, pump flow, and strainer area for a given plant. The computer program was developed by Science and Engineering Associates, Inc. (SEA) and is described elsewhere (NUREG/CR-6224, 1994).

The approach to achieving these objectives included use of an analytical model to quantify the kinetic energy imparted to the pool after the initial system blowdown, a physical model of a portion of the toroidal Mark I suppression pool to study pool dynamics and debris motion, and a flow loop to measure the head loss produced by various masses of debris on a strainer in the loop's test section. The experimental facilities used the actual expected insulation debris and a simulated sludge, actual flow velocities, and the actual expected kinetic energy per water volume.

After a brief description of post LOCA thermo-fluid events, relevant features of the test facilities and procedures are explained, data of interest is summarized, and implications to future plant operation are projected.

POST LOCA EVENTS

A LOCA may occur due to the rupture of any of numerous steam or water pipes directly or indirectly connected to the core, and the breaks are postulated to occur at weld joints. Full scale studies (Serkiz, 1985) indicate that a sudden break in high pressure piping generates a pressure wave that appears responsible for removing typical protective shielding around fibrous pipe insulation and for disintegrating the fibrous insulation filler. Steam or super-heated water (which flashes to steam) discharges from the pipe break for several seconds to several minutes, depending on the break size, further eroding nearby exposed fibrous insulation. The discharge energy causes high velocity gas flows and mixing within the "drywell" containment, transporting the smaller insulation debris to the vents and "downcomers," which connect the drywell to the toroidal suppression pool, see Figure 1. Since steam is lighter than the inert gases of the drywell, the increase in drywell pressure initially forces mainly the inert gases and some fibrous debris down through the venting system, clearing the downcomers of water (NUREG/CR-6224, 1994). The resulting water jets, followed by a quasi-steady flow of non-condensable gas and debris, results in massive mixing and "swell" of the suppression pool water, increasing the pressure of the gases above the pool water surface. The high energy mixing causes resuspension of any (iron oxide) sludge which was previously on the pool floor, thus initially producing a highly turbulent pool with fully mixed insulation debris, sludge, and any other small drywell particulates (paint chips, spalled concrete, dust, etc.) vented to the pool.

With time, the inert drywell gases become depleted, and the vent (downcomer) flow transitions to more and more steam, which ultimately condenses due to heat absorption by the pool water. But as the steam flow decreases due to falling drywell pressure and increasing suppression pool pressure, unsteady condensation begins. For steam flow rates sufficient to prevent water from re-entering the vents, this unsteady process is called "condensation oscillations," producing pockets of steam near the end of the downcomers which vary quickly in volume and which may be torn off and move upward in the pool as the steam pockets collapse by condensation.

A further drop in differential pressure between the drywell and suppression pool allows water to periodically penetrate back up into the downcomers. Since steam is still being discharged from the original pipe break, the drywell pressure re-builds, forcing steam to penetrate from all downcomers (in phase) into the pool, where the bubbles implode simultaneously due to rapid condensation. This implosion forces water back up into the downcomers, repeating such cycles for a time depending on the initial pipe break size. The water mass involved, the compressibility of the drywell and suppression pool gases, and the rate of steam discharge from the original pipe break lead to rather periodic, in-phase, water motion into and from the downcomers, and this final phenomenon, called "chugging", occurs with a typical period of between 1.5 to 2.5 seconds (General Electric, 1979). During this phenomenon, large scale mixing of debris in the pool was thought probable, but was not quantified until this study.

Depending on the initial pipe break size (and system type), various pumps are started prior to and during "chugging" to inject water into the core, starting with the High Pressure Core Injection (HPCI), followed by Low Pressure Core Injection (LPCI) and Low Pressure Core Sprays (LPCS). This fills the reactor vessel to the point where the injected water flows out of the initial pipe rupture. Since the drywell is full

of steam, water flow from the pipe rupture onto the drywell floor causes large scale steam condensation and a rapid drop in drywell pressure. To prevent large reverse differential forces on floor and walls, vacuum relief valves open to equalize the pressure between the suppression pool non-condensible gases and the drywell steam.

This ends the high energy phase after a LOCA (lasting approximately 1 to 2 minutes for a large break and about 10 minutes for a medium break), but the injected water continues to recirculate down the vents to the suppression pool, perhaps washing down some additional debris, especially if the containment sprays have been turned on to reduce the containment pressure. In spite of the recirculating flow back to the pump suction in the pool, the pool turbulence decays, allowing some settling of the debris to the pool floor.

Long term heat removal from the system may be accomplished by heat exchangers downstream from the Residual Heat Removal (RHR) pumps, but this cooling mode is not needed until about 30 minutes after a LOCA. Operation of this recirculation system can again induce high levels of turbulence in the pool, leading to resuspension of any settled debris. Further insight on post-LOCA events is provided in NUREG/CR-6224, 1994.

SCOPE OF STUDY

This study concentrated on flow events prior to recirculation of the injected water or initiation of the RHR (pool cooling) system since it may not be needed for all break sizes and since the earlier head loss on the pump suction strainers must be addressed in any case. Also, the effects of flow recirculating from the pipe rupture to the suppression pool (and to the pump suction strainers) on the behavior of debris in the pool was not considered. Such recirculating flows would be dependent on the pool geometry, which is different between the Mark I, II and III BWR containment types. These factors may be considered later. No consideration was given herein to the volume of debris formed or the mechanisms which introduce it into the pool. Instead, this study concentrated on the suppression pool dynamics during and after chugging, which are more generic and which must be understood in any case.

In particular, pool kinetics were investigated experimentally, preceded by an analytical study to determine the amplitude of water-steam interface oscillations in the downcomers. This part of the study provided pool debris concentration versus time data so analyses of the mass flux to the strainer induced by the pump flow could be made. A separate phase of the study measured the head loss across a strainer plate for varying but known masses of fibrous insulation debris and fine iron oxide particles (sludge). Some data on the efficiency of the insulation debris in filtering the sludge was also obtained, as this is needed to calculate the mass of debris actually on the strainer.

For the study of pool kinetics, the insulation debris was heat treated, fragmented NUKON™ fiberglass blanket filler, commonly used to insulate nuclear piping and the reactor vessel, and fragmented Reflective Metallic Insulation (RMI). For the head loss study, both NUKON™ and Thermal Wrap™ insulation debris were used in separate test series. It was assumed that the debris would form a relatively uniform layer on the pump suction strainer as the flow to the strainer is reasonably uniform for cylindrically shaped strainers, and since the concentration gradients in the pool would be small during the high energy dynamics. For ease of understanding, the mass of fibrous insulation debris on the strainer was expressed as the equivalent thickness of "as manufactured" insulation filler on the strainer by using the (as

manufactured) bulk density of 2.4 lb/ft^3 for the insulation filler. This nominal thickness is not the actual thickness of the compressed insulation layer on the strainer.

The fibrous insulation was fragmented in a leaf shredder to small shreds designated Class 3&4 and Class 5&6 (see NUREG/CR-6224, 1994), whereas the RMI debris was generated by the rupture of an insulated high pressure steam pipe at the Siemens-KWU Large Valve Test Facility in Karlstein, Germany.

The sludge used in both experimental studies was commercially available iron oxide powder ranging in size from about 1 μm to about 10 μm in an unconglomerated suspension, similar to the size range reported for the actual plant sludge, but such material easily conglomerates to near spherical particles of 5 to 10 times this size. Such conglomeration may also occur with the actual plant sludge.

SUPPRESSION POOL KINEMATICS

ANALYSIS

A one dimensional transient flow analysis was made of the drywell and suppression pool volumes per downcomer, and the proportional connecting vent and downcomer was simulated by a single line, as shown in Figure 2. The compressibility of all fluids at their respective temperatures and pressures was included. Whenever the steam water interface reached the (lower) end of the downcomer, a sudden drop in steam volume was introduced, simulating an implosion caused by the sudden condensation of steam by the pool water. A steady inflow of steam to the drywell simulated the discharge from the initial pipe rupture. The sudden drop in steam volume and the steady steam inflow were adjusted so that this transient model yielded pressure variations in the pool water (at the downcomer exit elevation) similar in magnitude and frequency to those measured in a full scale test facility near the start, middle and end of chugging (General Electric, 1979). At that point, the analysis also yielded the magnitude and frequency of water steam interface oscillations in the downcomer, as shown in Figure 3, and these oscillations were scaled as inputs to the suppression pool model.

EXPERIMENTS

A 1:2.4 geometrically similar model of a section of a Mark I toroidal suppression pool was constructed, as shown in Figures 4 and 5. Four downcomers were included, and the motion of the steam water interface was simulated with pistons driven by a variable speed motor and a rotating crank system to produce the non-sinusoidal motion in Figure 3. The plane side walls were of plexiglass for viewing water and particle motion. Five sampling ports were at the center of the pool, between the four downcomers, their openings located to have minimal effects on particle motion from the false side walls.

To produce the full scale kinetic energy per unit water volume requires that model velocities be equal to actual (prototype) velocities, which is consistent with using actual insulation and sludge debris and their prototype fall velocities. Equal piston velocity indicates the piston amplitudes should be scaled to the length ratio, and the length and velocity ratio give the time ratio for the period (or frequency) of piston motion.

Tests were started with the debris on the pool floor, as it soon became apparent that simulated chugging produced rapid and complete mixing, so that the initial debris placement was not important.

Results for insulation debris only and for sludge only are shown in Figures 6 and 7, respectively. The upper left graph in each figure shows the time averaged material concentration during chugging for the lowest chugging energy tested, Case 3 of Figure 3, indicating complete mixing. The large scatter in the data for insulation debris only came from occasionally withdrawing larger than typical insulation fragments, and data scatter for the sludge only test was much less due to the very fine material used.

Vertical concentration profiles for selected times are shown in the top right hand graph on each figure, indicating the pool is vertically well mixed, even after chugging ceased. The decay of material concentration with time at each elevation after chugging ceased is shown in the lower left graph of each figure, also showing the fully mixed condition during chugging. It is evident that the sludge settled out faster than the insulation debris, but that a small fraction persists in the water column for a longer time. In either case, about 50% of the material settled in about 20 minutes after chugging stopped, about the time for the entire pool volume to have been recirculated once through all pumps. Recall, however, that any dynamic effects in the pool of recirculating flows have not been included.

Changes in vertical concentration profiles with time may be transposed to graphs of material settling velocities, as shown in the lower right hand graphs of Figures 6 and 7. By testing different mass ratios between insulation debris and sludge, the family of settling velocity curves shown on Figure 8 was obtained. The dashed lines were obtained by prorating results from the insulation debris only and sludge only tests based on the relative masses when both materials were tested simultaneously. Due to the agreement between experimental and predicted curves, it may be concluded that the materials act independently and do not combine or trap each other to form an alternative material with different properties.

The RMI debris behaved quite differently, in that not all the material was in suspension during simulated chugging and the particles settled much faster after chugging ceased. The fraction of debris in suspension during simulated chugging was estimated visually by comparing the amount on the floor with the amount in suspension. For the same (low) simulated chugging energy used for the tests of Figures 6 and 7, from about 1/3 to 1/2 of the RMI debris remained in suspension, see Figure 9, whereas for a more typical (higher) simulated chugging energy from about 1/2 to 3/4 of the debris remained in suspension. Settling times after simulated chugging ceased was not affected by the chugging energy or by the concentrations tested (from about 1 to 5 gm/ft^3), and all debris settled to the floor in about two minutes.

These data may be used to find the debris concentration in the suppression pool versus time based on some initial mass of insulation debris and sludge which enters the pool. Such concentrations and the known pump flows allow calculation of the mass flux to the strainers.

STRAINER HEAD LOSS

A closed flow loop was constructed, as shown in Figure 10, to hold a piece of BWR strainer plate in a vertical section of 12 inch pipe. The remaining pipe was 4 inches in diameter to prevent material from settling out. A range of flows was produced by a variable speed pump and measured by a calibrated venturi meter. Elevated water temperatures were produced by heating tapes. Pressure ports were located above and below the strainer to obtain the differential pressure of interest versus the approach velocity to the strainer. The material caught on the strainer was determined from the material added minus the material suspended in the water, as measured from water samples withdrawn from the loop.

As actual debris, actual approach velocities, and the actual BWR strainer perforated plate were used, the resulting pressure differentials are those that would occur in the actual plant if the strainer were loaded with the same mass per unit strainer area as tested. However, the differential pressure rise versus time is not indicative of the actual plant, since the arbitrary mass flux to the strainer and the concentration of mass in the test loop is different from that which would be in the suppression pool for the same ultimate mass on the strainer. Therefore, only the steady state head losses were of interest.

Debris was introduced at the top of the 12 inch pipe while the valve at the stand pipe bottom was closed, fixing the water level irrespective of increasing head losses. After the top of the 12 inch pipe was sealed, the stand pipe valve was opened to provide some compliance to the system and to prevent low pump suction pressures. Based on structural limits of the plexiglass used to allow visualization of insulation debris collecting and compressing on the strainer, the maximum allowable differential pressure head in the loop was about 60 ft of water. The iron oxide (sludge) particles were added first and allowed to mix well in the loop at an approach velocity of 1.5 ft/sec, to be followed by all the insulation debris added at one time (introduced at an approach velocity of 0.15 ft/sec) so that a time of collection of the debris layer on the strainer could be established. After a steady head loss was achieved, the flow (approach velocity) was increased in steps. Exploratory tests showed that this procedure produced essentially the same head loss as if the material had been introduced at the higher approach velocity. The flow loop was thoroughly cleaned between tests. A matrix of test parameters was established to determine the effects of insulation debris size (within a limited range), water temperature, the mass ratio of sludge to insulation debris, and the "as manufactured" insulation thickness used in each test. For each combination of variables tested, head loss was obtained as a function of approach velocity until the maximum pressure for the loop was reached (unless this occurred during material introduction). A summary of the data for NUKON™ is shown in Figure 11, intended as a visual indicator of the number of test points available for analysis. A similar series of tests was conducted with Thermal Wrap™.

By comparing test data for conditions where only one parameter of interest was varied, the effect of that parameter on head loss was determined. Only effects of importance are discussed herein. For example, Figure 12 shows a comparison of pairs of tests conducted with NUKON™ and water at about 50° F versus at about 125° F, with and without sludge. Statistical analyses of these results showed that the effect of the elevated temperature expected in the suppression pool is to lower the head loss by an average factor of about 2.2. This reduction is consistent with the expected effect of reduced water viscosity on head loss. Due to this major effect, most tests were conducted with water at about 125° F. Of greater significance was the effect of sludge, as shown in Figure 13, which gives the ratio of head losses between tests with NUKON™ for varying mass ratios of sludge to insulation debris compared to tests with only insulation debris. The data for all velocities of a given test were averaged to obtain these trends. For mass ratios around 10, multiplication factors of up to about 100 were obtained for "as manufactured" insulation thicknesses on the strainer of 0.5 to 1.0 inches. This could lead to high head losses across the strainer; for example, about 50 ft of loss was measured for an approach velocity of only 0.15 ft/sec to a strainer with 1 inch of insulation and a sludge to insulation mass ratio of 7.5.

A summary of all the head loss data for NUKON™ is presented in Figure 14, wherein the contour lines are dimensionless values of head loss divided by the nominal insulation thickness. For a known approach velocity (pump flow divided by gross strainer area), insulation debris mass or "as manufactured" thickness (from the pump flow and pool concentration, integrated over time) and the mass of sludge trapped or filtered out in the insulation debris on the strainer (from the pump flow, pool concentration, and filtering efficiency), the data of Figure 14 allows the head loss at a given time to be calculated. This

is more easily accomplished by the computer code, BLOCKAGE, developed by SEA, which makes use of these data to calibrate equations that account for the various physical processes involved.

The additional factor needed for such calculations is the extent of sludge filtering, so that the mass of sludge actually on the strainer may be determined. By measuring water concentrations upstream and downstream from the strainer versus time during the first flow cycle in the loop (before the upstream concentration and particle size distribution has been affected), the drop in particle concentration across the strainer was used to calculate a filtering efficiency for various test conditions. Figure 15 shows that the filtering efficiency for NUKON™ decreased slightly with increasing approach velocity (higher velocities increasing the head loss and compression of the insulation, leading to less void volume) and increased slightly with increasing nominal insulation debris thickness (greater voids).

Head losses with Thermal Wrap™ were compared to those with NUKON™ for the same test conditions, and a summary of that comparison is shown in Figure 16. The upper graph, Figure 16A, shows a direct comparison of head loss with NUKON™ to head loss with Thermal Wrap™. The lower graph, Figure 16B, shows a frequency distribution of the ratios of head losses, the left hand portion of Figure 16B being for comparable tests where the head loss with Thermal Wrap™ was greater than with NUKON™, and vice versa for the right hand portion of the figure. On the average, it is evident that head losses with Thermal Wrap™ were essentially equal to those with NUKON™, the average increase of 11% for Thermal Wrap™ compared to NUKON™ not being of practical significance. Filtration efficiencies with Thermal Wrap™ varied from about 20% to 60%, depending on the insulation mass and approach velocity, a range similar to that obtained with NUKON™.

At this point, all information needed to predict strainer head loss for a plant is known for given pool debris masses, assuming the limitations of phenomena included in this study.

APPLICATIONS AND FUTURE NEEDS

Application of the knowledge gained from the studies described herein to a typical BWR plant by use of the SEA computer code BLOCKAGE (NUREG/CR-6224, 1994) indicates the NPSH margin is lost within minutes after the pumps reach their maximum flow in response to a large or medium sized LOCA. Operator action would be required to manually realign the suction of certain ECCS pumps (by changing various valves) to draw water from other sources outside the containment, such as the condensate storage tank, to use emergency service water, or to provide core cooling via the condensate/feedwater system. Timing of various events associated with ECCS strainer blockage may be an important consideration in determining whether or not core cooling by alternative means can be successfully accomplished.

Therefore, hardware fixes are being considered for certain BWR plants to increase the ECCS reliability. Possible schemes include larger strainers of the same type (to reduce the approach velocity), multi-sided, irregularly shaped strainers to increase their area, "self-cleaning" strainers (driven by the pump flow), and backflush systems using air or water. Studies by the Boiling Water Reactor Owner's Group (BWROG) address these possibilities.

Another avenue would be to minimize the debris volume which could be transported to the suppression pool by gas flows during the reactor vessel blowdown, and during the subsequent washdown by the recirculating injection flow and containment sprays. This approach addresses means of trapping debris in the drywell, such as by using finer grating over the vents to the suppression pool. The effect of plant

specifics may also be relevant; for example, flow from the horizontal vent endings just above the pool floor in a Mark III design may re-entrain settled debris during recirculation of the injected flows.

The studies described herein will be shared with the International Working Group on ECCS Recirculation Reliability. This international working group was formed to further the understanding and exchange of information concerning ECCS strainer blockage.

ACKNOWLEDGEMENTS

This study by the Alden Research Laboratory, Inc. (ARL) was funded by the U.S. Nuclear Regulatory Commission, and the guidance and practical insights provided by Al Serkiz and Michael Marshall of the Generic Safety Issues Branch were critical in achieving useful results. D.V. Rao and Gil Zigler of Science and Engineering Associates, Inc. (SEA) provided many technical insights and helpful project management, respectively.

REFERENCES

General Electric, "Mark I Containment Program, Full Scale Test Program, Final Report", NEDE-24539-P, Class III, April 1979.

NUREG/CR-6224, "Parametric Study of the Potential for BWR ECCS Strainer Blockage Due to LOCA Generated Debris", Draft Report for Comment, Science and Engineering Associates, Inc., August 1994.

Serkiz, A.W., "Containment Emergency Sump Performance", U.S. Nuclear Regulatory Commission, NUREG-0897, Rev. 1, October 1985, Appendix C and F.

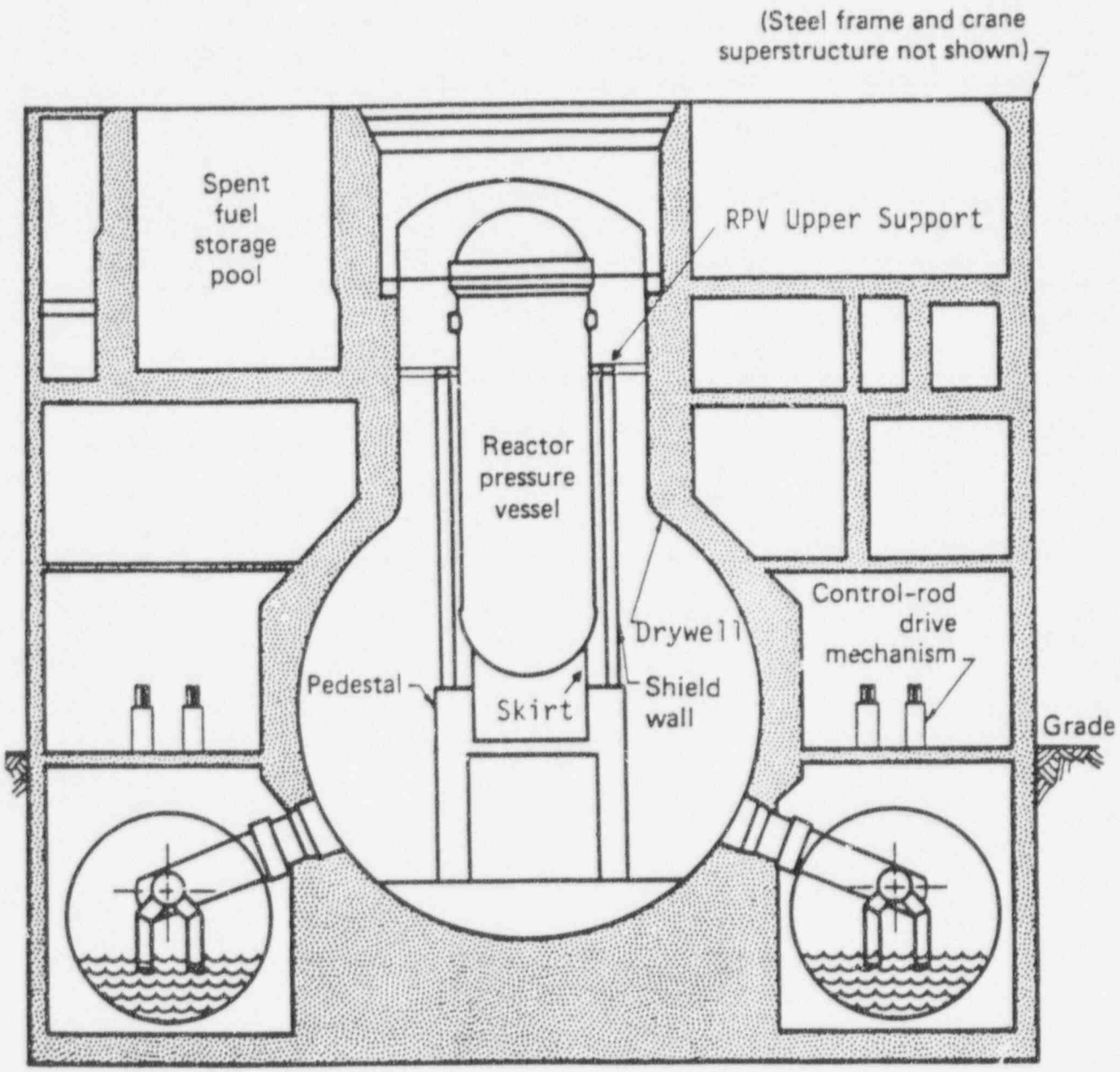

FIGURE 1 TYPICAL MARK I - BWR CONTAINMENT
(PIPING IN DRYWELL NOT SHOWN)

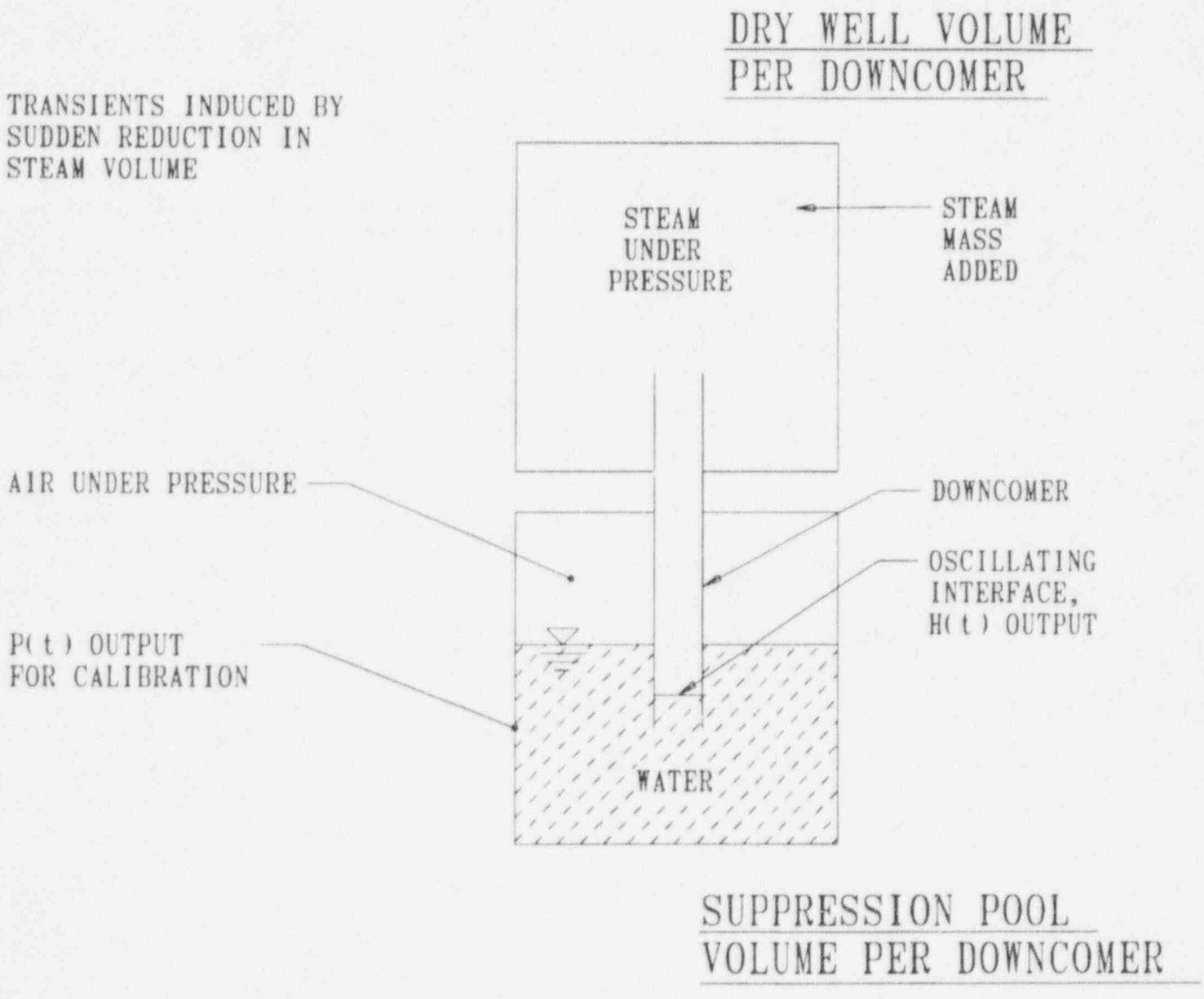

FIGURE 2 ONE DIMENSIONAL CLOSED CONDUIT TRANSIENT ANALYSIS

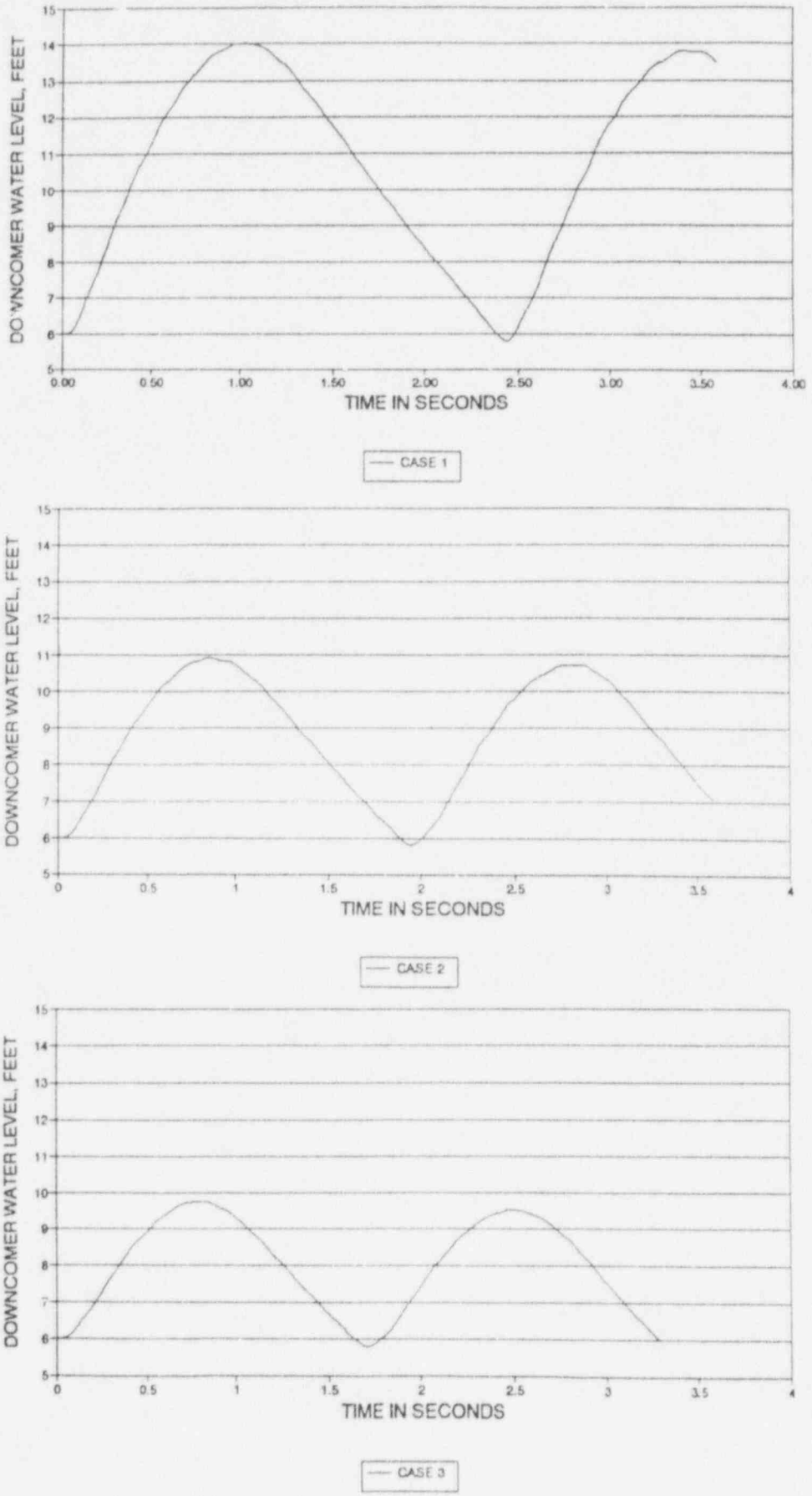

FIGURE 3 DOWNCOMER INTERFACE OSCILLATIONS DURING CHUGGING - FROM TRANSIENT ANALYSIS

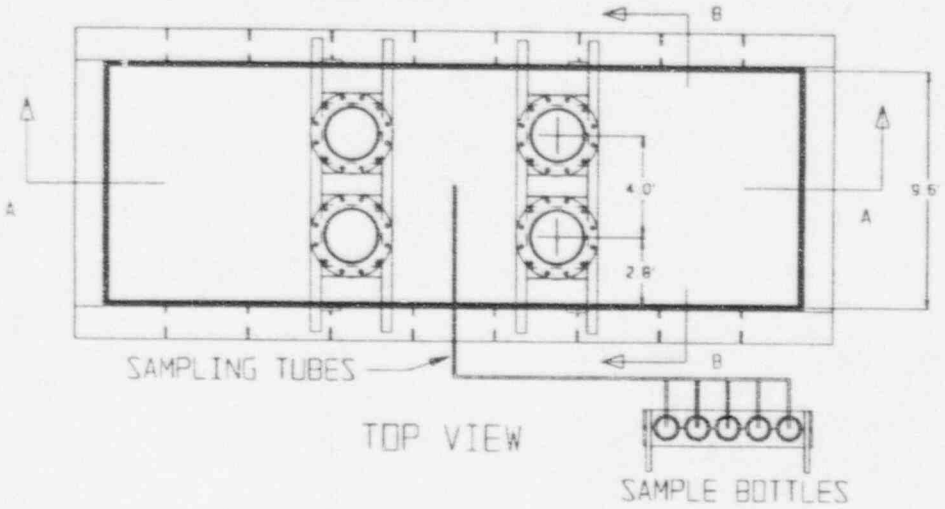

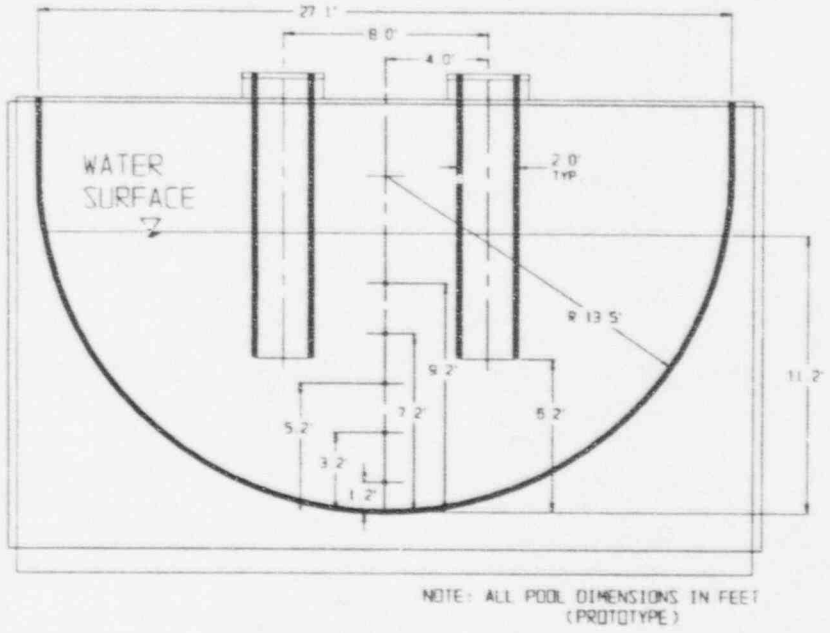

SECTION A-A

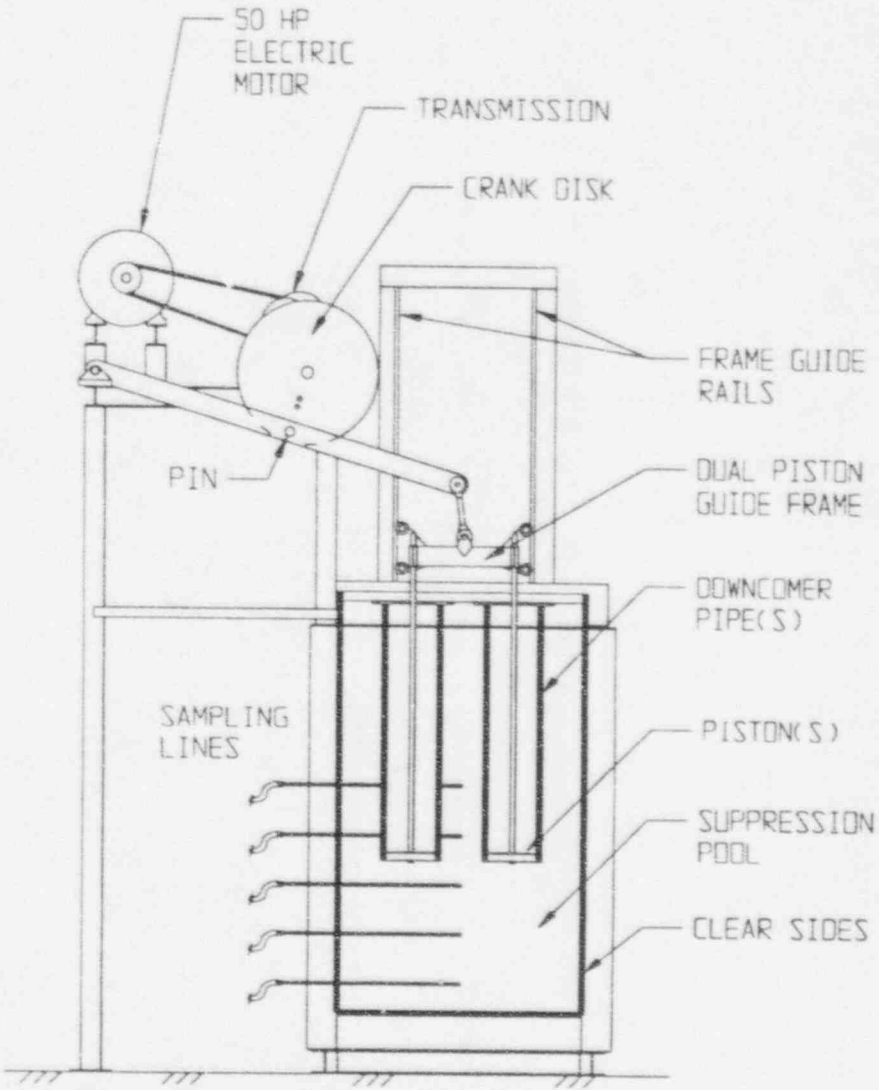

SECTION B-B

FIGURE 4 BASIC FEATURES OF 1:2.4 SUPPRESSION POOL MODEL

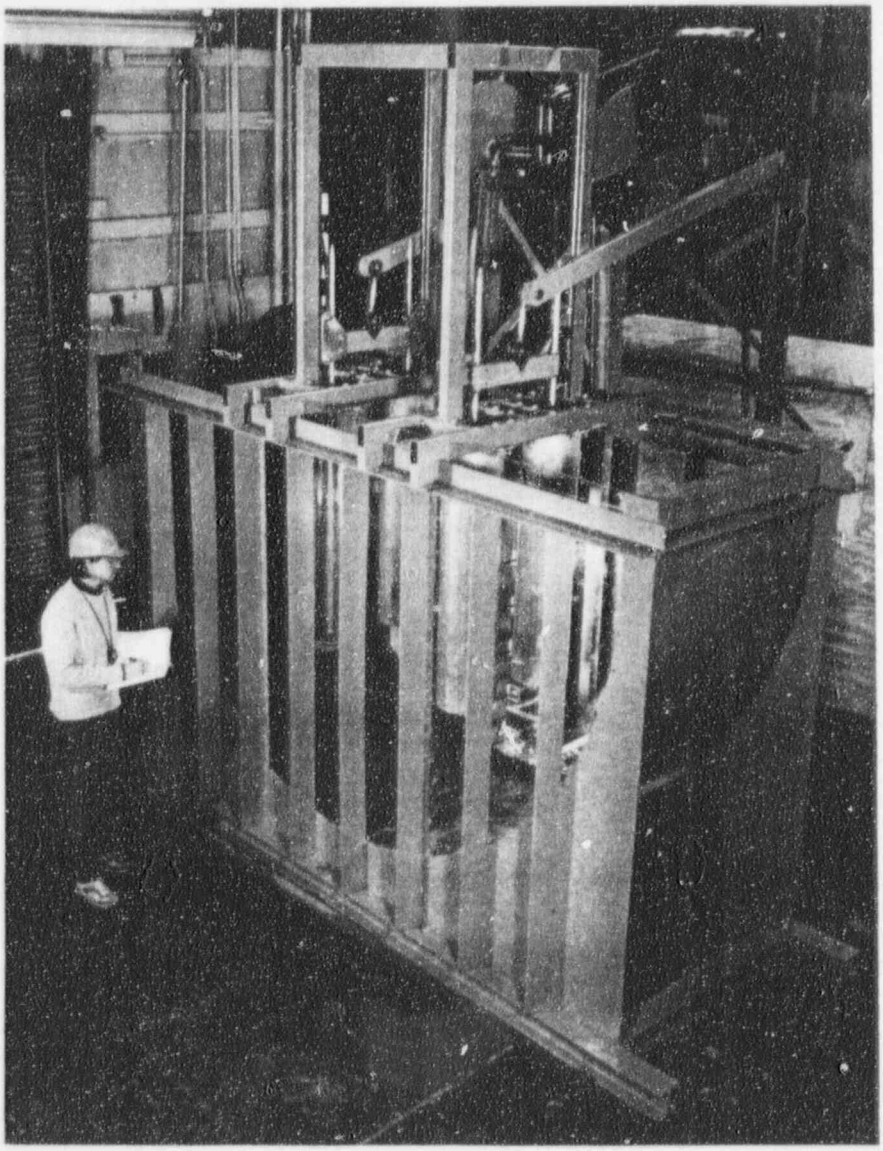

FIGURE 5 1:2.4 SCALE SUPPRESSION POOL SEGMENT MODEL

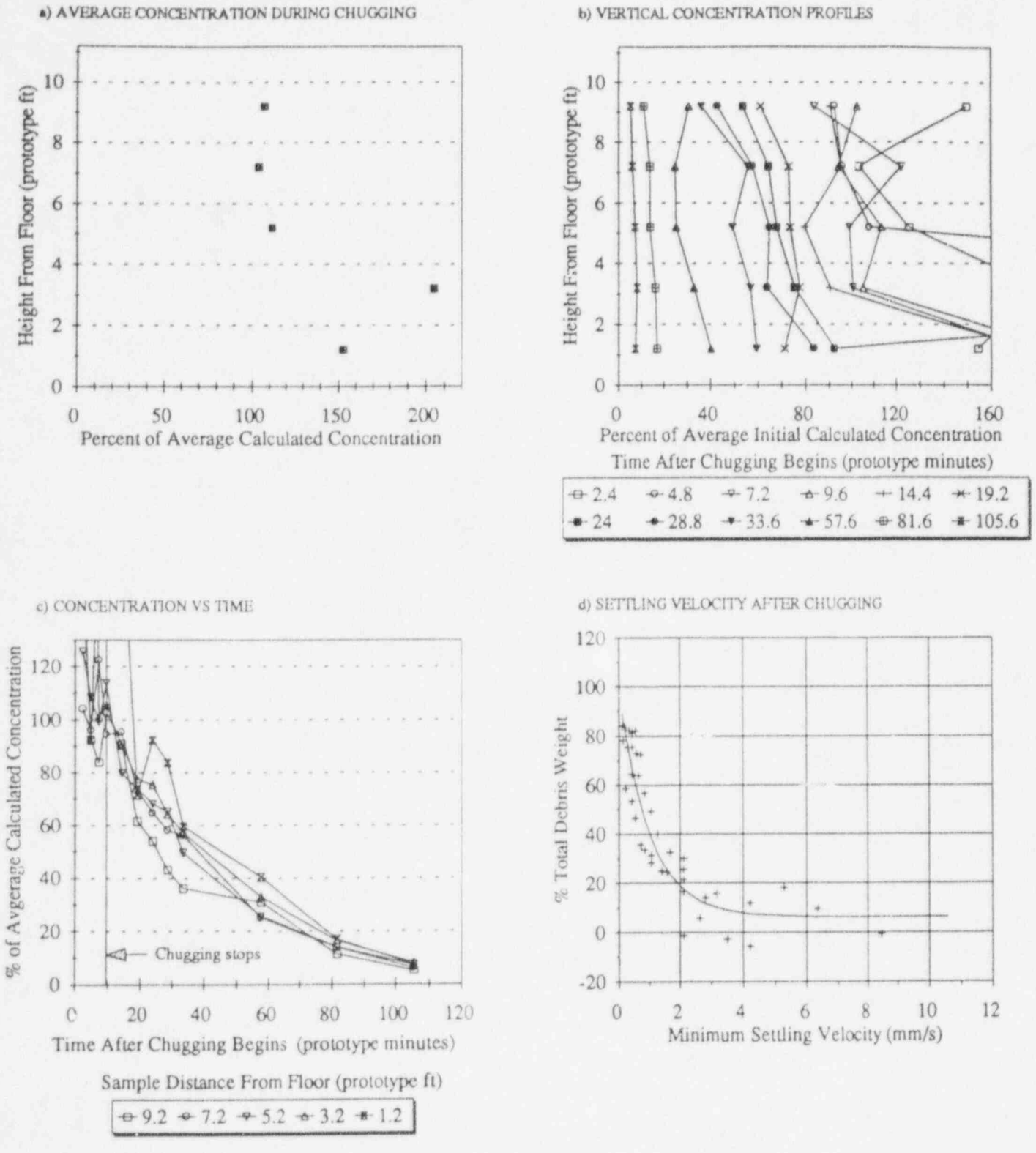

FIGURE 6 KINEMATICS OF FIBROUS INSULATION DEBRIS IN SUPPRESSION POOL (TEST A-1R1; 3.8 FT, 1.6 SEC; NUKON 0.003%, SLUDGE 0%)

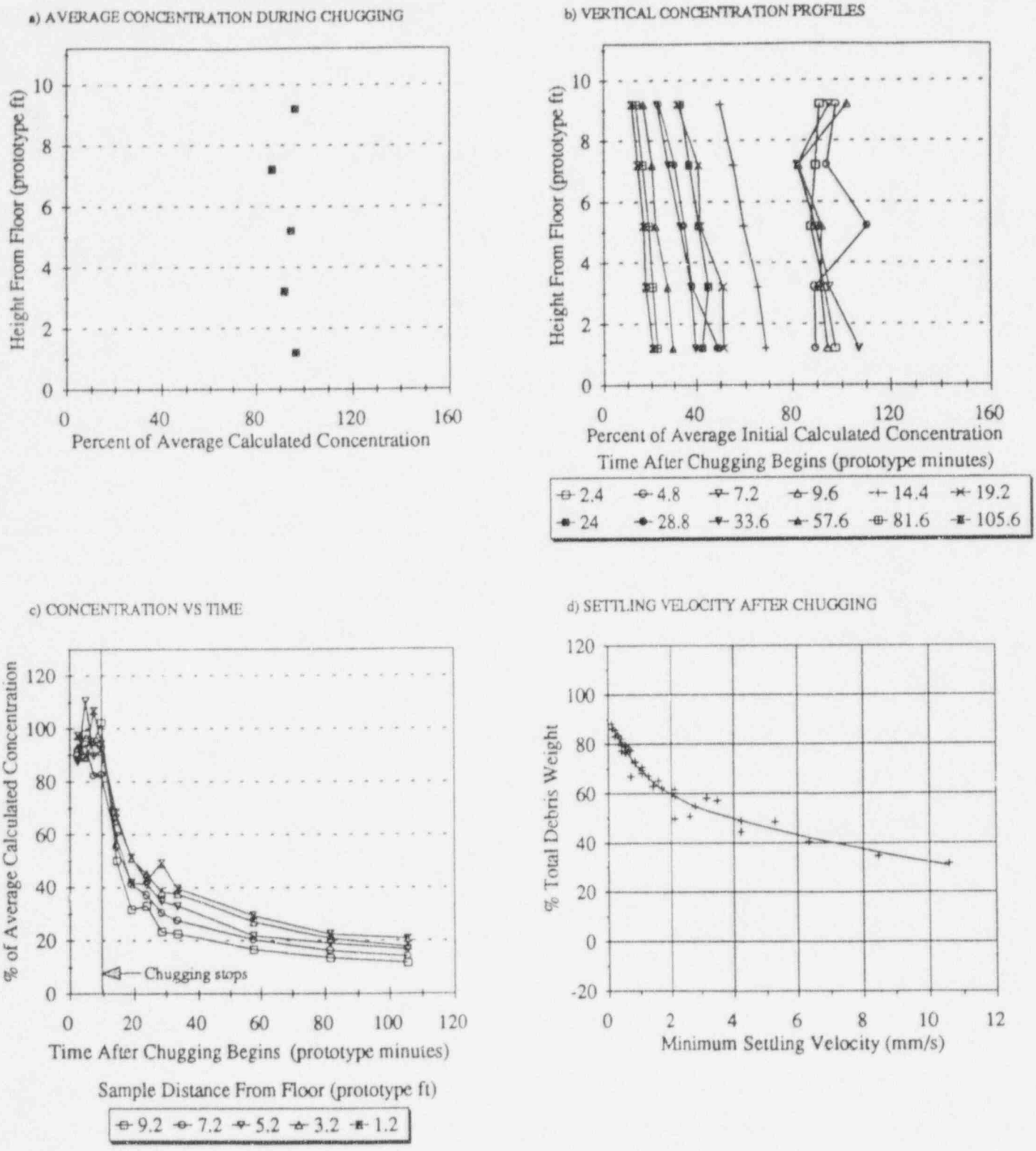

FIGURE 7 KINEMATICS OF SLUDGE IN SUPPRESSION POOL
(TEST A-3R1; 3.8 FT, 1.6 SEC; SLUDGE 0.02%, NUKON %)

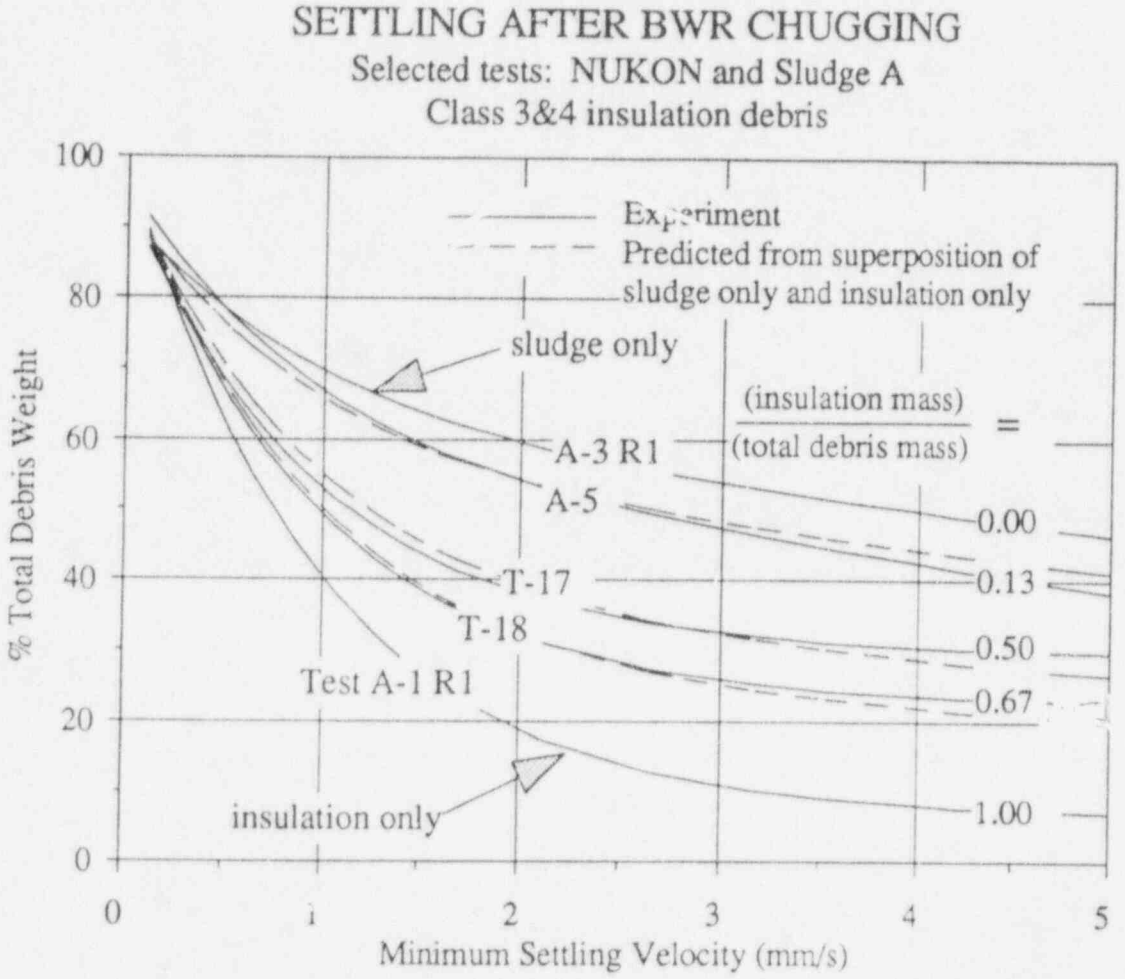

FIGURE 8 SUPERPOSITION OF SETTLING RATES FOR INSULATION DEBRIS AND SLUDGE

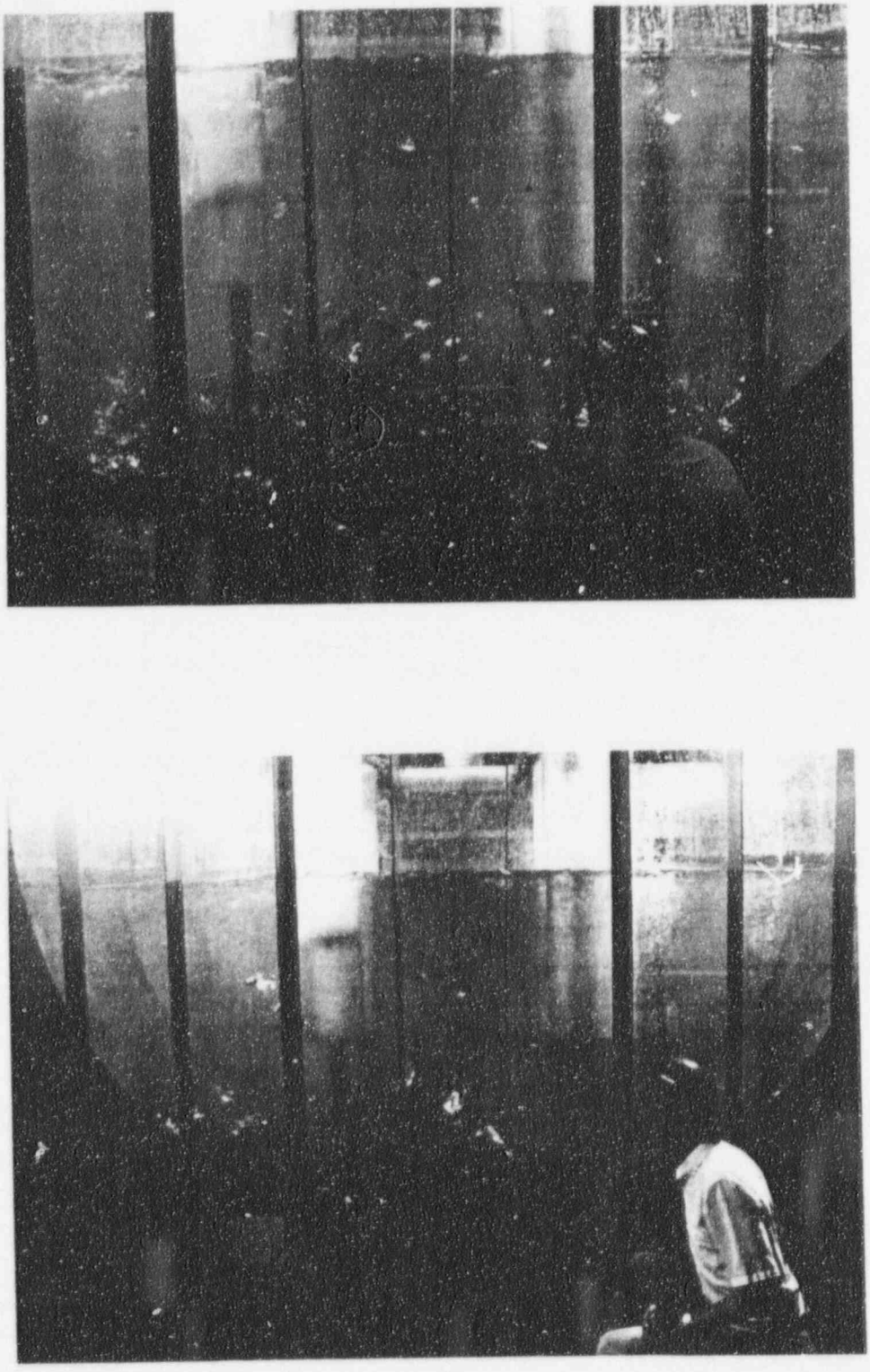

FIGURE 9 RMI DEBRIS DURING CASE 3 CHUGGING
(3.8 FT, 1.6 SEC)

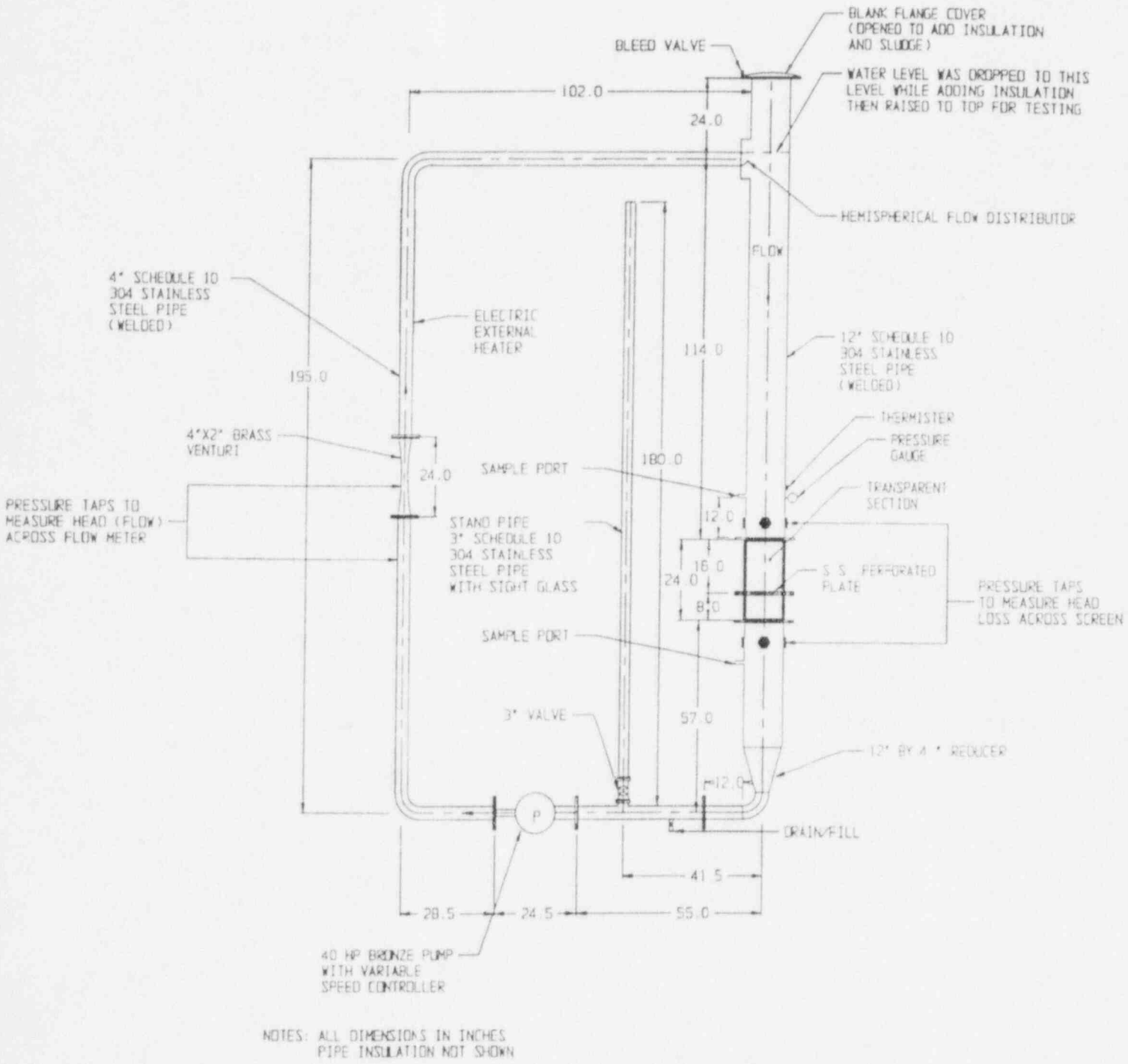

FIGURE 10 FLOW LOOP FOR HEAD LOSS TESTING

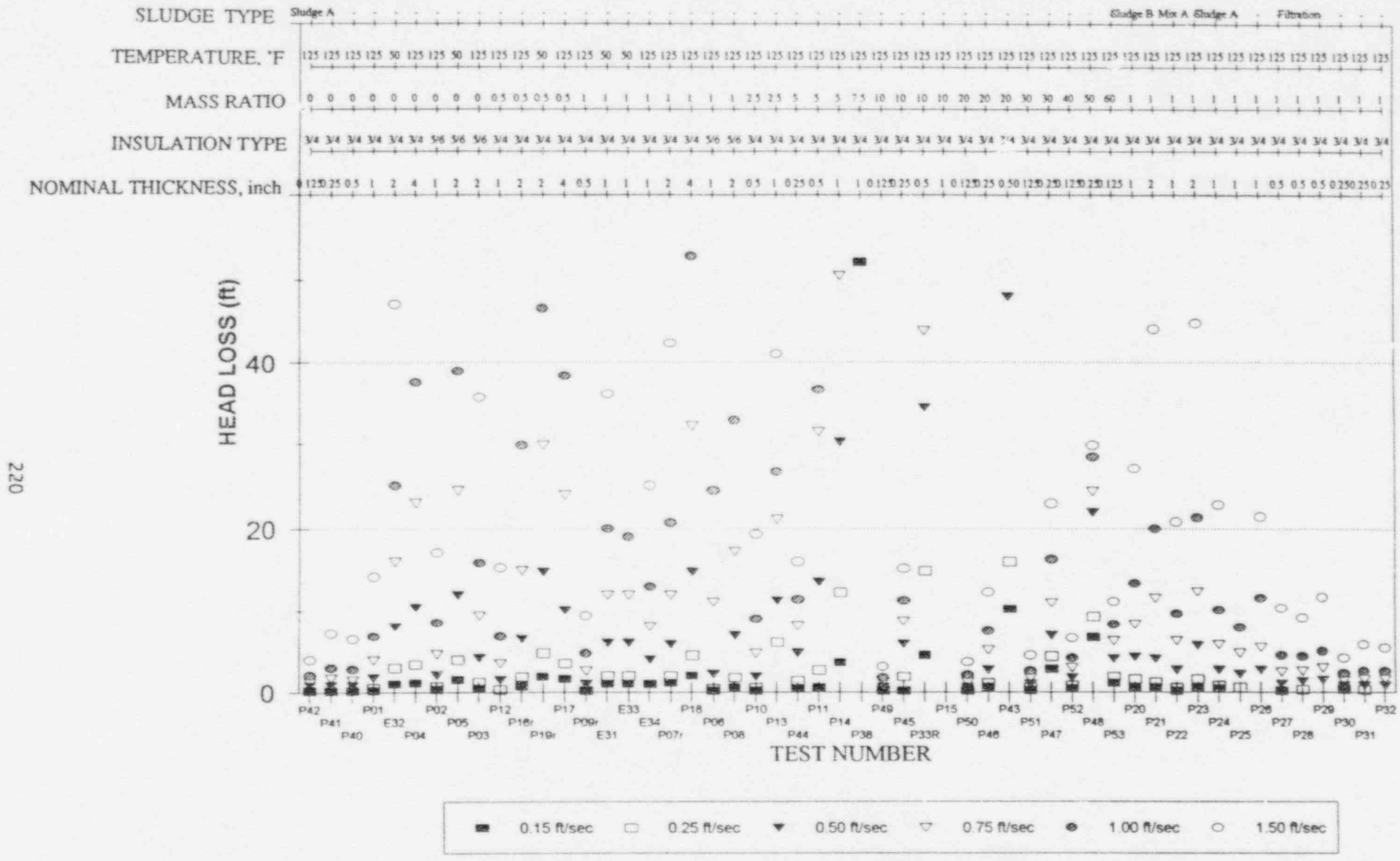

FIGURE 11 GRAPHICAL SUMMARY OF HEAD LOSS DATA FOR NUKON™

EFFECT OF TEMPERATURE
50°F vs 125°F

Note: Numbers over symbols are Head Loss in feet @ 125° F

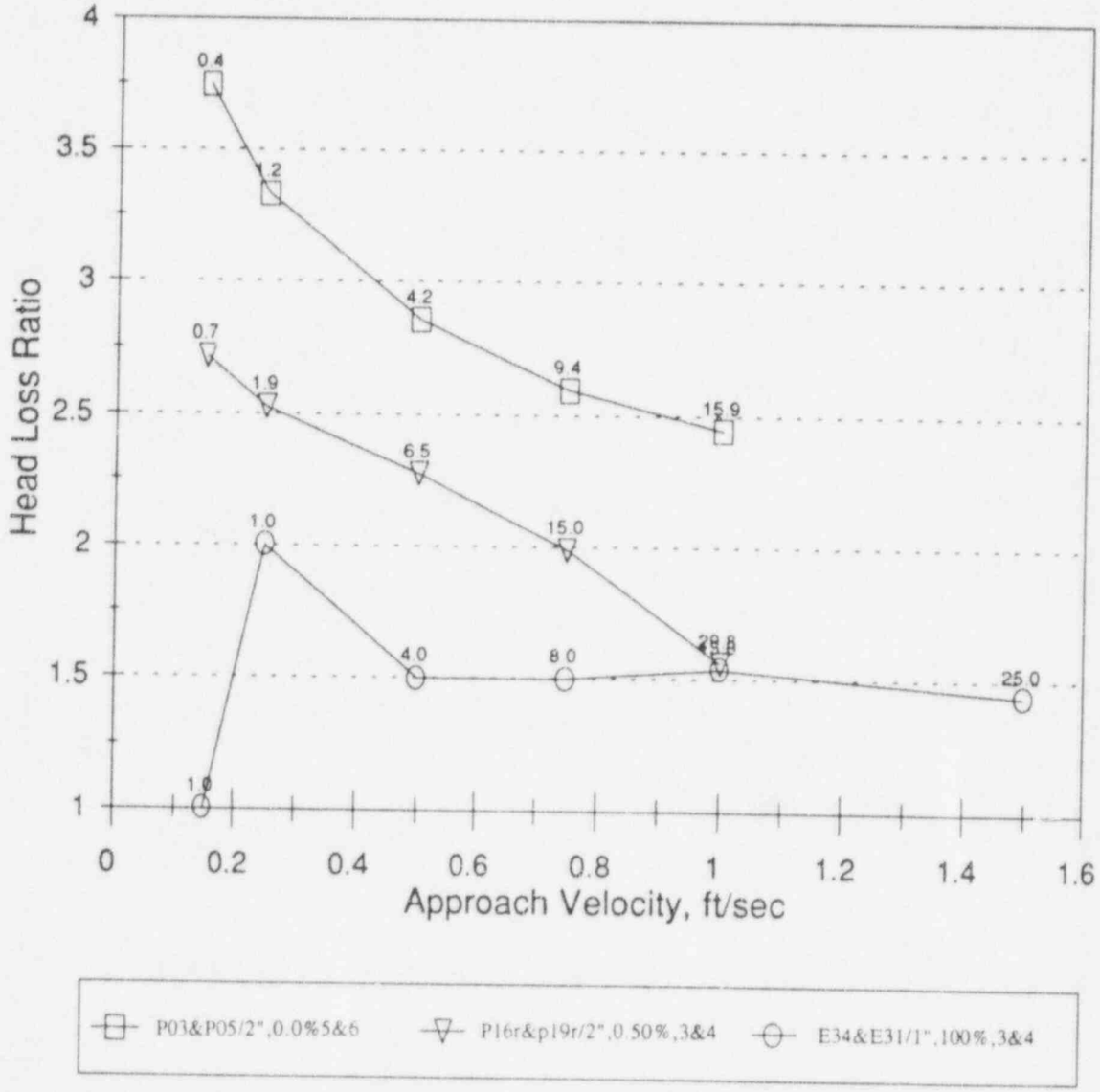

$$\text{Head Loss Ratio} = \frac{\text{Head Loss at } 50°\text{F}}{\text{Head Loss at } 125°\text{F}}$$

FIGURE 12 RATIO OF HEAD LOSSES FOR NUKON™
AT TWO WATER TEMPERATURES

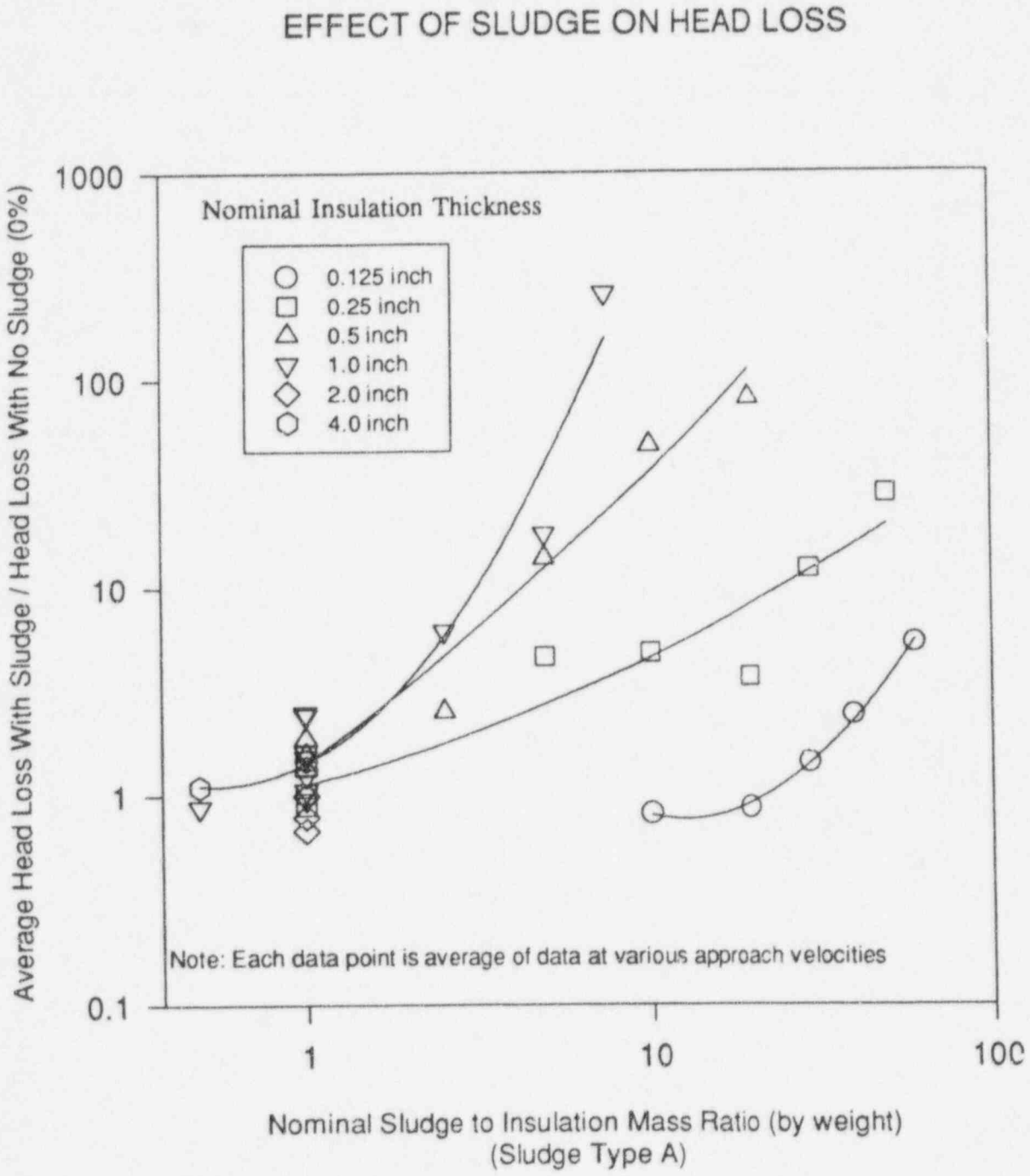

FIGURE 13 RATIO OF HEAD LOSSES FOR NUKON™ WITH SLUDGE TO WITHOUT SLUDGE

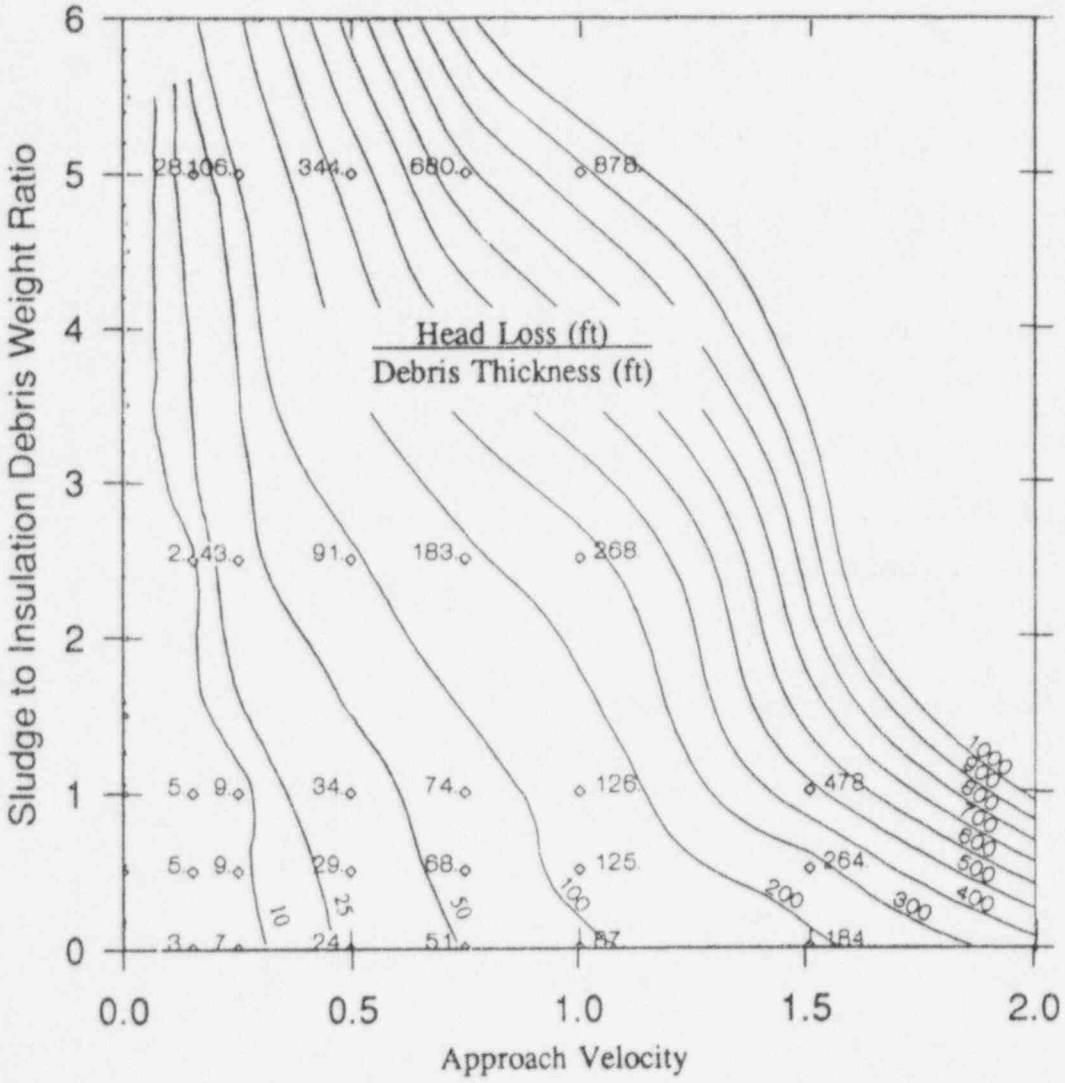

FIGURE 14 SUMMARY OF DIMENSIONLESS HEAD LOSSES FOR NUKON™

Note: 1) Contour Lines Are Constant Values of Head Loss/Nominal Insulation Thickness
2) Data Only For Thickness > 0.5
3) Data Only For 125°F Tests

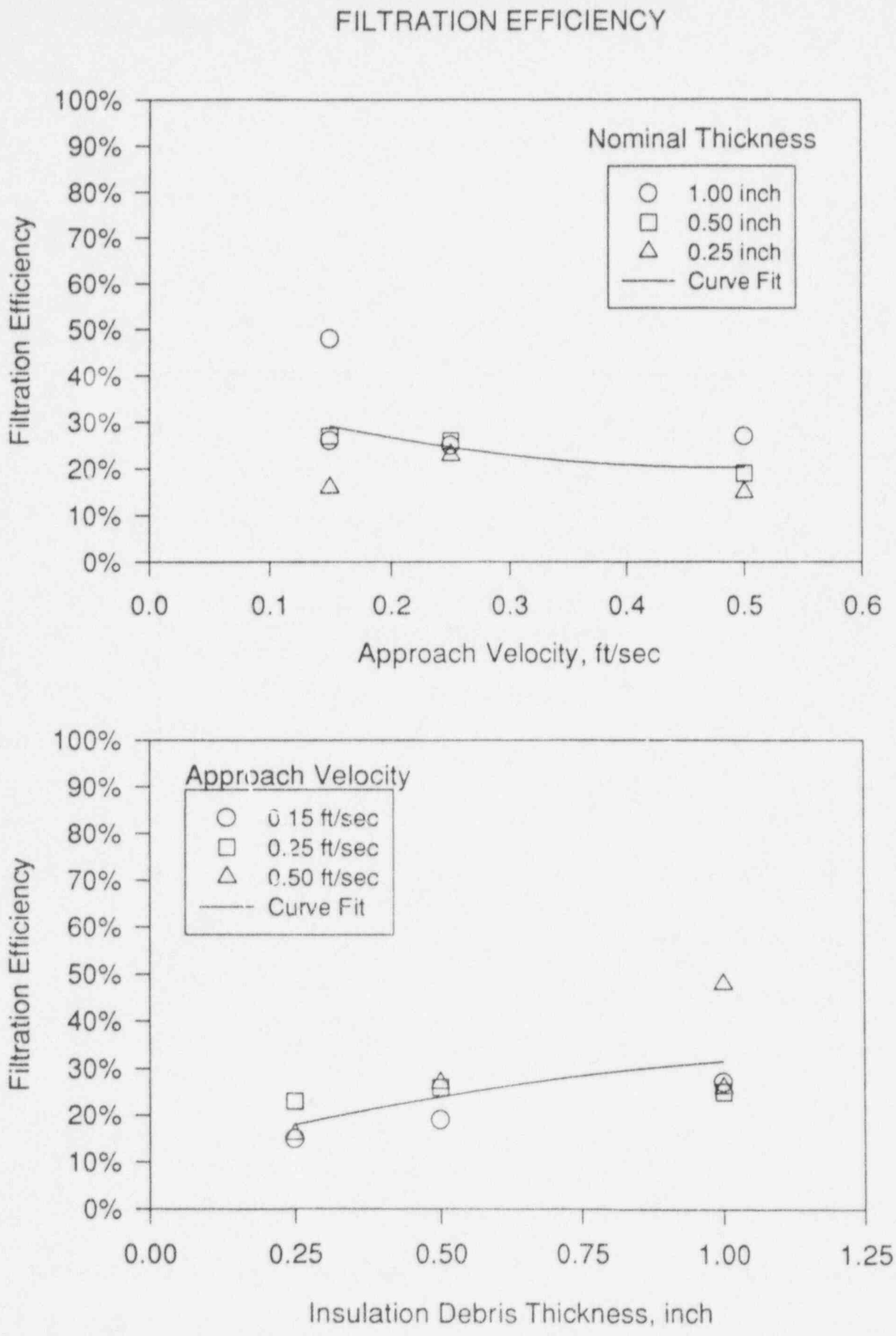

FIGURE 15 FILTRATION EFFICIENCY (PERCENT SLUDGE TRAPPED WITHIN NUKON™ INSULATION DEBRIS LAYER)

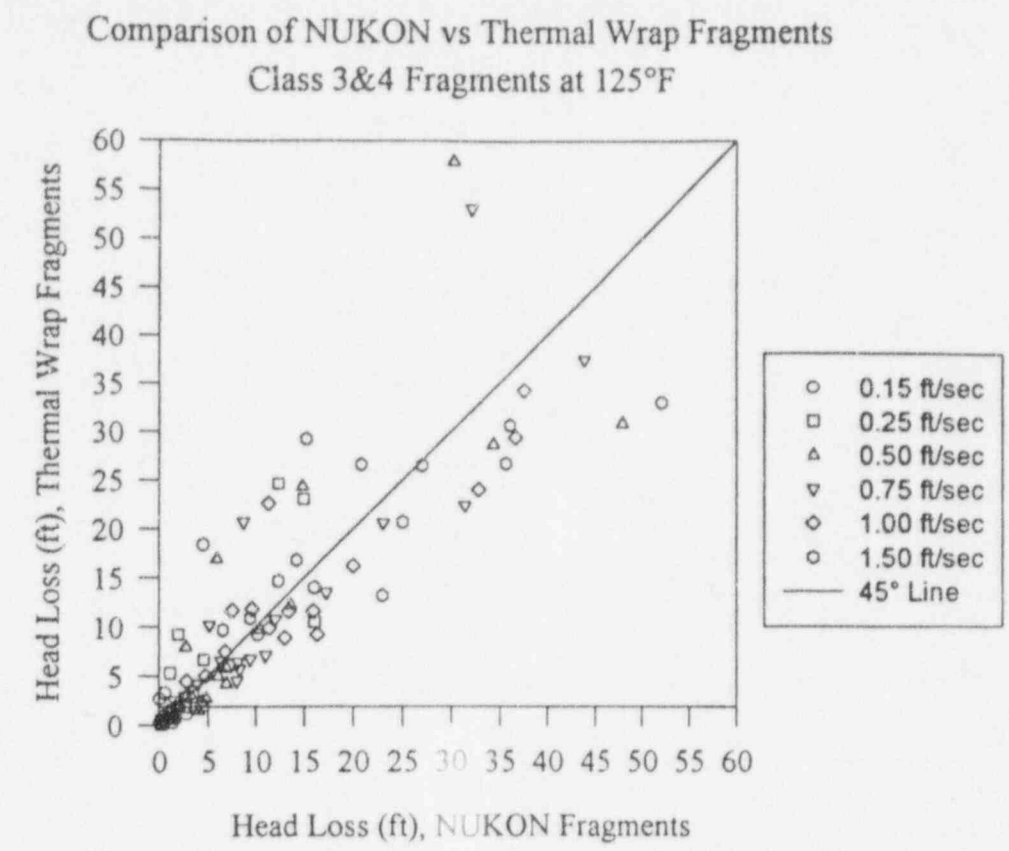

A) Raw Data

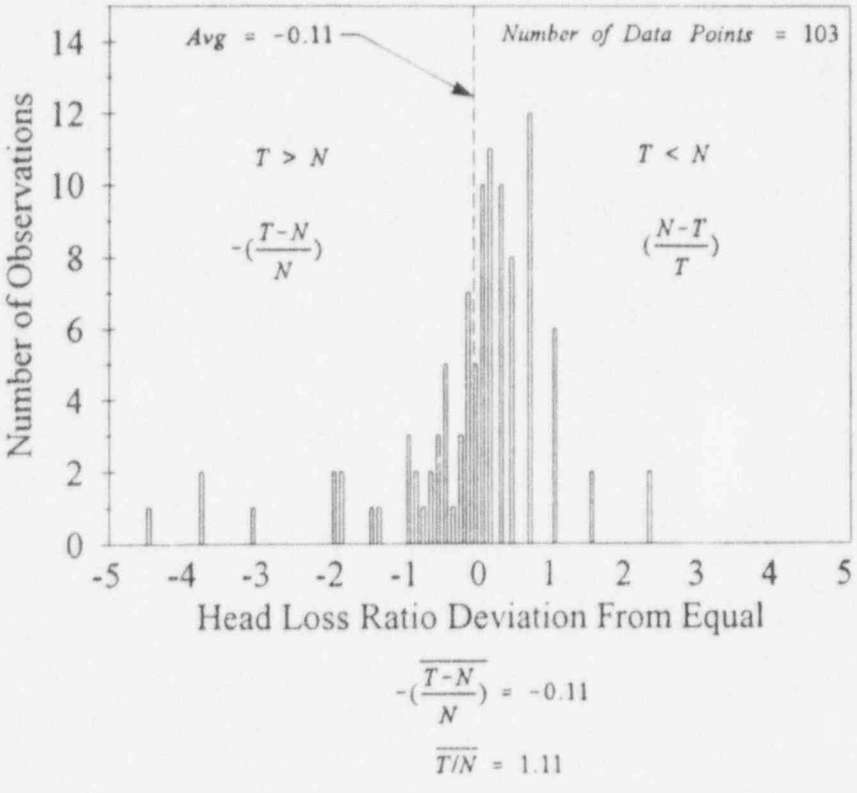

$$-\left(\frac{\overline{T-N}}{N}\right) = -0.11$$

$$\overline{T/N} = 1.11$$

B) Histogram

FIGURE 16 COMPARISON OF THERMAL WRAP™ AND NUKON™ HEAD LOSS TEST RESULTS

The Strainer Blockage Assessment Methodology Used in the BLOCKAGE Code

Gilbert L. Zigler
D.V. Rao

Science and Engineering Associates, Inc.
Albuquerque, New Mexico

On July 28, 1992 a spurious opening of a safety valve at Barsebäck Unit 2 in Sweden resulted in clogging of the Containment Vessel Spray System strainers in less than one hour. Instances of ECCS strainer clogging have occurred in U.S. BWRs. Given these precursors the USNRC staff initiated analyses to estimate the potential for loss of NPSH of the ECCS pumps in BWRs due to clogging of suction strainers by a combination of fibrous and particulate material. The BLOCKAGE code was developed in support of NUREG/CR-6224, a probabilistic scoping analysis of a BWR/4 with a Mark 1 containment. This paper addresses the key elements of the methodology used in the BLOCKAGE code to assess head loss across ECCS strainers. The debris generation model, the debris drywell transport, and the suppression pool models are discussed briefly. NUREG/CR-6224 provides in-depth discussions of the models used in BLOCKAGE. Additionally, user interface features of BLOCKAGE are discussed.

Several incidents of suction strainer blockage due to debris accumulation that challenged Emergency Core Cooling System (ECCS) function have occurred at operating boiling water reactors (BWRs). On July 28, 1992, a spurious opening of a safety valve at Barsebäck Unit 2, a Swedish BWR with a containment similar to a Mark II, resulted in clogging of the Containment Vessel Spray System pump suction strainers within one hour after the accident. At the Perry plant, a U.S. BWR/6 with Mark III containment, fibers from air filters inadvertently dropped into the suppression pool were transported to the strainer and were found to have filtered corrosion products and dust particles. The resultant increase in pressure deformed the strainers and highlighted the important role played by suppression pool sludge, heretofore not evaluated in detail. Given these precursors and the safety implications of loss of ECCS soon after a loss-of-coolant accident (LOCA), the U.S. Nuclear Regulatory Commission (USNRC) initiated analyses to estimate the potential for loss of net positive suction head (NPSH) margin of the ECCS pumps in a BWR due to clogging of suction strainers by a combination of fibrous and particulate debris, either generated by the LOCA or previously present inside the containment.

Science and Engineering Associates, Inc. (SEA) was selected by the USNRC to perform a comprehensive study on the reliability of the ECCS due to LOCA generated debris. The SEA study is documented in NUREG/CR-6224 entitled, "Parametric Study of the Potential for BWR ECCS Strainer Blockage Due to LOCA Generated Debris", October 1995. NUREG/CR-6224 concluded that

for the reference plant, a BWR 4 with a Mark 1 containment whose dry well piping is essentially all insulated with steel jacketed fibrous material, considerable potential exists for loss of the ECCS pumps due to strainer clogging by the LOCA generated debris. It was further concluded that very thin insulation debris layers are sufficient to induce pressure drops that are in excess of available NPSH margin for most BWRs.

A strainer blockage assessment methodology was developed as part of NUREG/CR-6224. Since NUREG-6224 was a scoping probabilistic study, the models, parameters and methodology were developed to yield point estimates and are not necessarily "conservative" or "worst case". The NUREG/CR-6224 methodology was codified in a computer code named BLOCKAGE. The elements of the methodology developed for BLOCKAGE to evaluate the effect on head loss across strainers due to debris introduced into the suppression pool as a result of a LOCA follows the key LOCA event progression phenomenology delineated in figure 1. A LOCA event can be effectively divided in two phases for the purpose of BLOCKAGE analysis: (1) the short term phase, starting with the actual weld failure and ending with the drywell de-pressurization and (2) the long term phase which ends when the ECCS and long term residual heat removal functions are no longer necessary. BLOCKAGE can be effectively set-up to analyze both phases of a LOCA event.

A BLOCKAGE user friendly interface is currently under development. As depicted in figure 2, there are three main interfaces: data is input through data entry dialogs and the results of BLOCKAGE calculations can be viewed as either tabular reports or time-dependent plots. The main user interface is the control panel depicted in figure 3. The control panel allows for selection of the sub-menus indicated for either inputting data or viewing the output. An error list is also provided to alert the user of possible errors such as debris mass balance out of tolerance for a particular weld.

The LOCA event starts with a hypothetical circumferential weld failure associated with a pressurized pipe in the drywell. The drywell pressurized piping contains either steam or saturated water at a nominal 80 bar pressure. Based on other LOCA assessment studies, a pressure wave was presumed to be generated following the instantaneous weldment failure. Depending on the medium in the pipe, this pressure wave would have different amplitudes and duration (impulse). This pressure wave was presumed to cause destruction of piping insulation and dislodgment of drywell debris. Following the pressure wave, jets of either steam or saturated water would exit from the weld break. Depending on the degree of restraint of the pipe, these jets would be mainly perpendicular to the pipe axis (highly restraint pipe) or parallel to the pipe axis (marginally restraint pipe). Given the scoping nature of NUREG/CR-6224, which precluded a detail piping restraint analysis for each weld and taking into account the congested layout of the drywell, a spherical zone of influence debris destruction model was developed. The NUREG/CR-6224 debris generation model was further generalized to encompass both steam and water lines. A 3 region level of destruction concept was also incorporated into the model to account for lesser damage at further distance from the weld failure. Considerable engineering judgment was then used to extrapolate the very sparse debris generation data, mostly air blast data, to arrive at the destruction factors used in NUREG/CR-6224. The codification of the NUREG/CR-6224 debris generation model in BLOCKAGE consisted of allowing the user to define the three zones of destruction based on L/D ratios and to enter different destruction factors for each of the three zones of destruction. Figure 4 depicts the data entry screen to input pipe lengths, diameters, and insulation thickness and type for calculation of the debris volume estimated to be generated by each break. As an option, BLOCKAGE also allows the user to enter an estimated total debris volume for a given hypothetical pipe break.

Following the debris generation in a LOCA, the debris could be transported to the suppression pool during blow down and during washdown. Given the tortuous path which debris need to follow between the dry well and the suppression pool, a debris transport model was developed for

NUREG/CR-6224 based on the premises that the fraction of debris reaching the suppression pool from a weld failure at a higher elevation would be lower than that from a weld failure at a lower elevation. As in the debris generation model, the NUREG/CR-6224 does not differentiate between steam and water pipes for estimating debris transport in the drywell. As shown in figure 5, the NUREG/CR-6224 model was codified in BLOCKAGE by allowing the user to define three elevation and the transport factors associated with each elevation. BLOCKAGE then tracks the elevation of the hypothetical weld failure and associates it with the appropriate transport factor. BLOCKAGE also allows the user to enter an estimate of debris volume not associated with piping insulation which could be transported to the suppression pool both during blow down and during washdown. Finally, as a separate entity, the estimate of the quantity of "sludge" present in the suppression pool to be modeled is entered.

Figure 6 depicts BLOCKAGE data entry screen used to characterize the suppression pool volume, the average suppression pool temperature during the calculations, the strainer area, the available NPSH, and the maximum ECCS flow. As shown in Figure 7, BLOCKAGE allows the user to define the properties of the different kinds of debris such as strand densities and settling velocities. Furthermore, given the probabilistic nature of NUREG/CR-6224, BLOCKAGE also requires entries of weld break probabilities for the different type of welds and weld diameter in order to perform the NPSH head loss probabilistic calculations.

The modeling of the suppression pool phenomena incorporated into BLOCKAGE entails definition of ECCS pump operating times and flow regimes as well as defining the times for the end of blowdown and washdown for the two different types of LOCAs - LLOCA and MLOCA. Figure 8 depicts the data entry screen for input of the event scenario profiles. During the blowdown time period, BLOCKAGE uses a settling velocity of zero for all debris, given the turbulence associated with the anticipated chugging and condensation oscillations. During washdown, as in the NUREG/CR-6224 model, BLOCKAGE uses the still water settling velocities entered as an attribute to each type of debris. BLOCKAGE then performs a time dependent calculation of the head loss across the strainer for each one of the welds entered into the weld data base using the NUREG/CR-6224 head loss correlation. Figures 9 and 10 depict representative report and plotted outputs available for the user to interpret the results of BLOCKAGE calculations.

BLOCKAGE can also be configured to estimate strainer head losses caused by suppression pool debris not originating from a LOCA. The blowdown phase can be bypassed, and the recirculation is modeled with appropriate flows, temperatures, strainer area, etc. To account for the re-suspension caused by the ECCS recirculation flows, the settling velocities should also be lowered. The recent Limerick event was modeled by BLOCKAGE which confirmed that small quantities of fibrous material deposited as a thin layer on a strainer in the presence of particulates could result in head losses approaching the available NPSH in less than one hour.

BLOCKAGE is currently in the process of being updated to allow for further flexibility in estimating the pressure drops across ECCS strainers. Additional features under development include modeling of each ECCS train to include modeling of each train flow rate, NPSH, and strainer area; allowing user specified head loss correlations to be used in lieu of the NUREG/CR-6224; and enhanced user interfaces. A user interface to the BLOCKAGE code is currently being developed by SoftwareEdge as a WINDOWS application. A fully tested version of the BLOCKAGE WINDOWS application is currently scheduled for public release in February 1996.

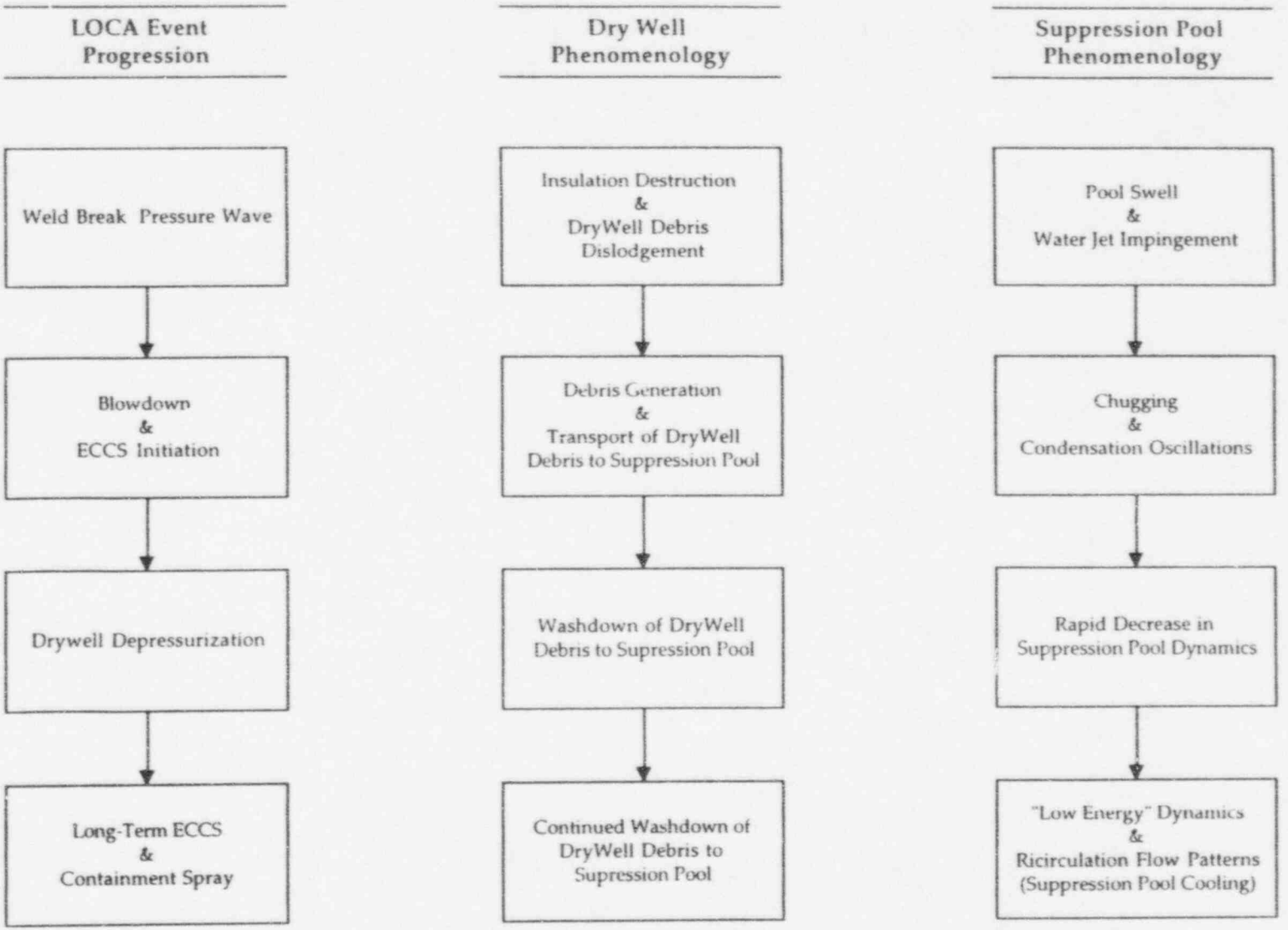

Figure 1: L & MLOCA Event Progression Phenomelogy

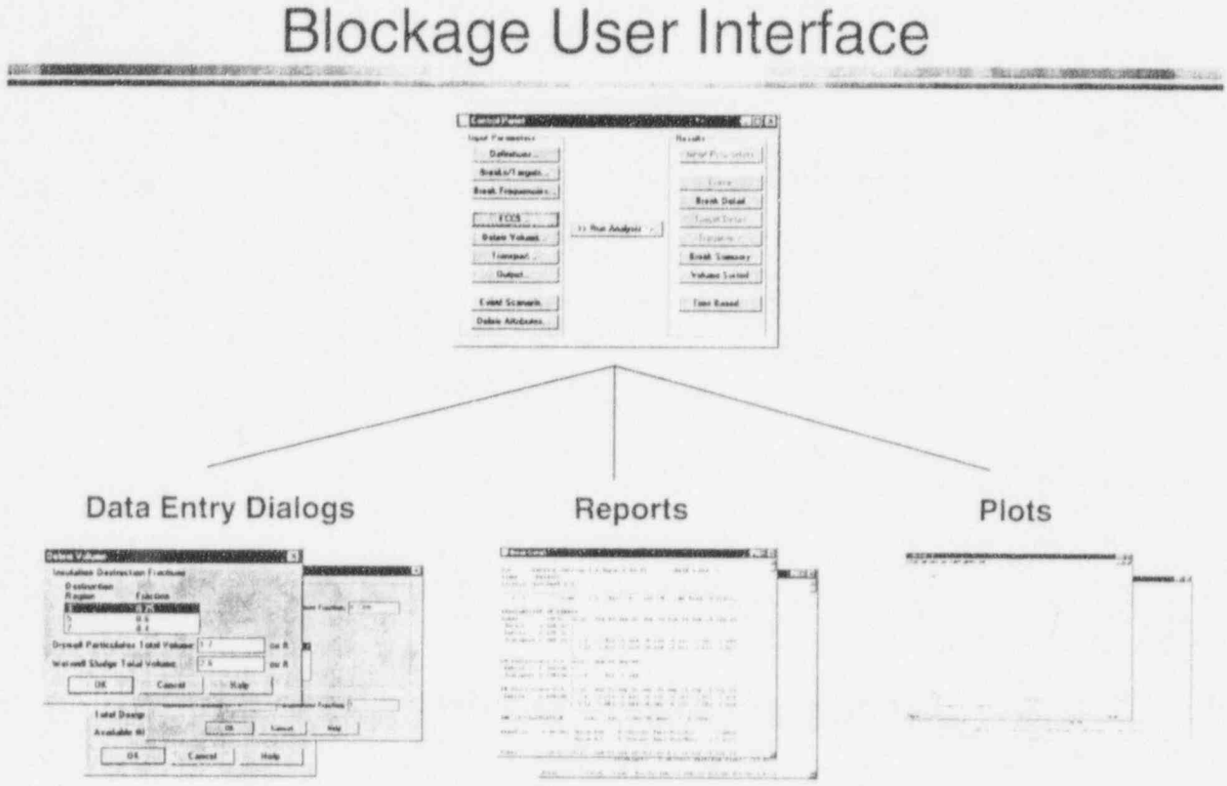

Figure 2: Blockage User Interface

Control Panel

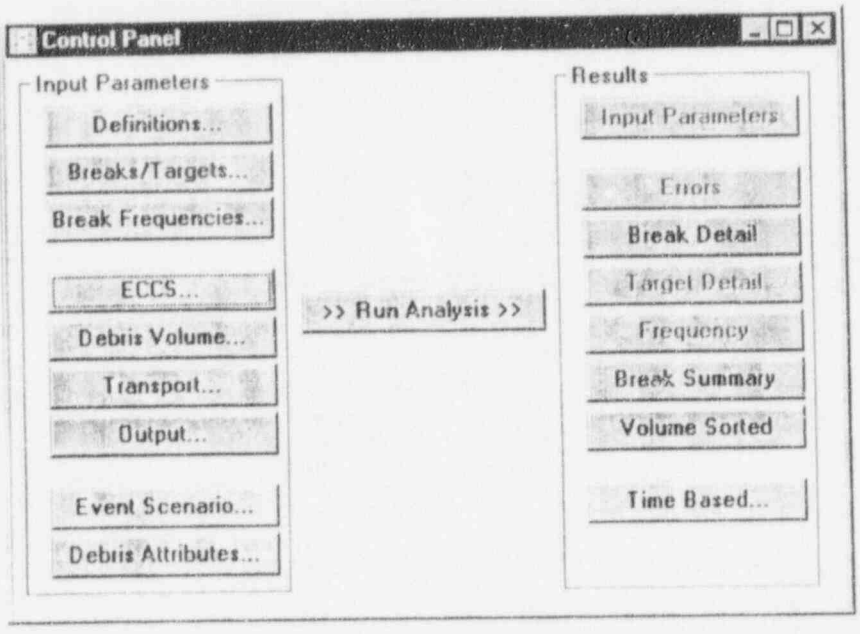

Figure 3: Control Panel

Break / Target Specification

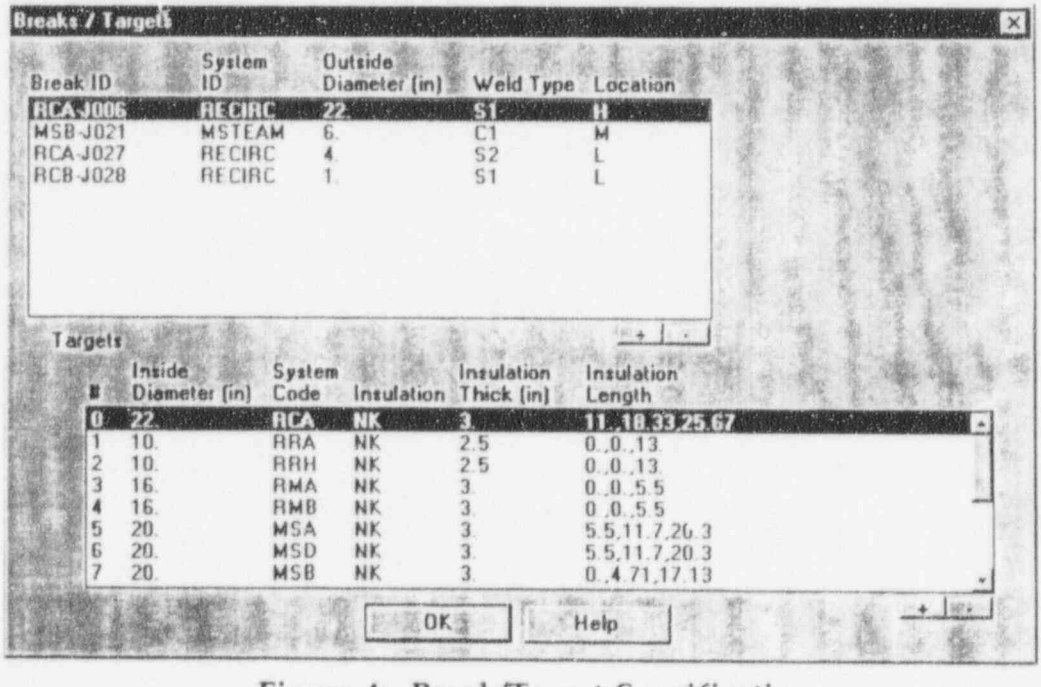

Figure 4: Break/Target Specification

Transport

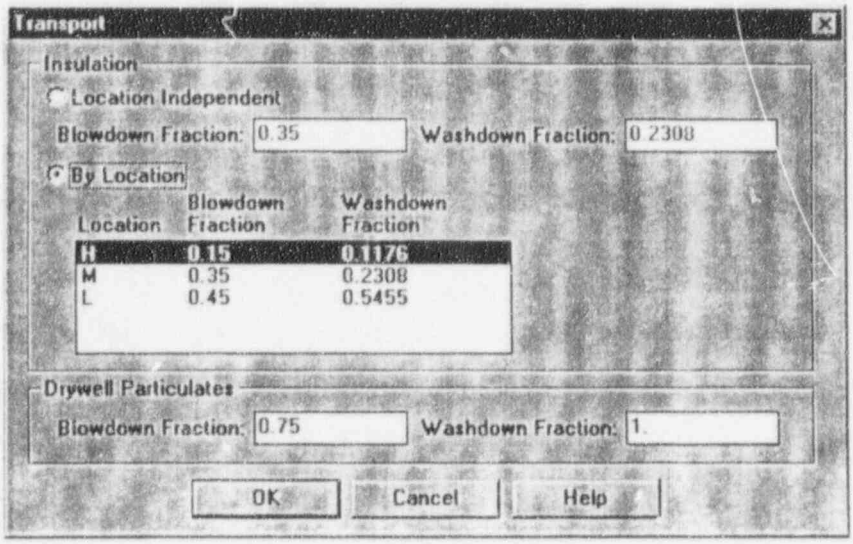

Figure 5: Transport

ECCS Specifications

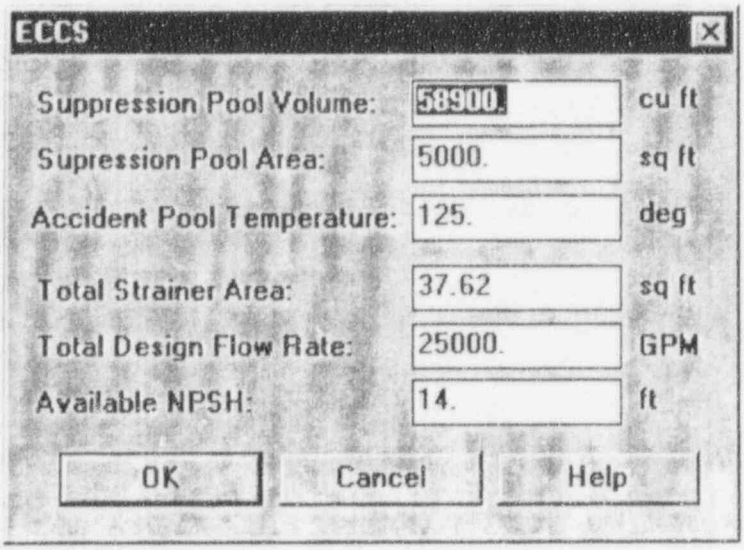

Figure 6: ECCS Specifications

Debris Attributes

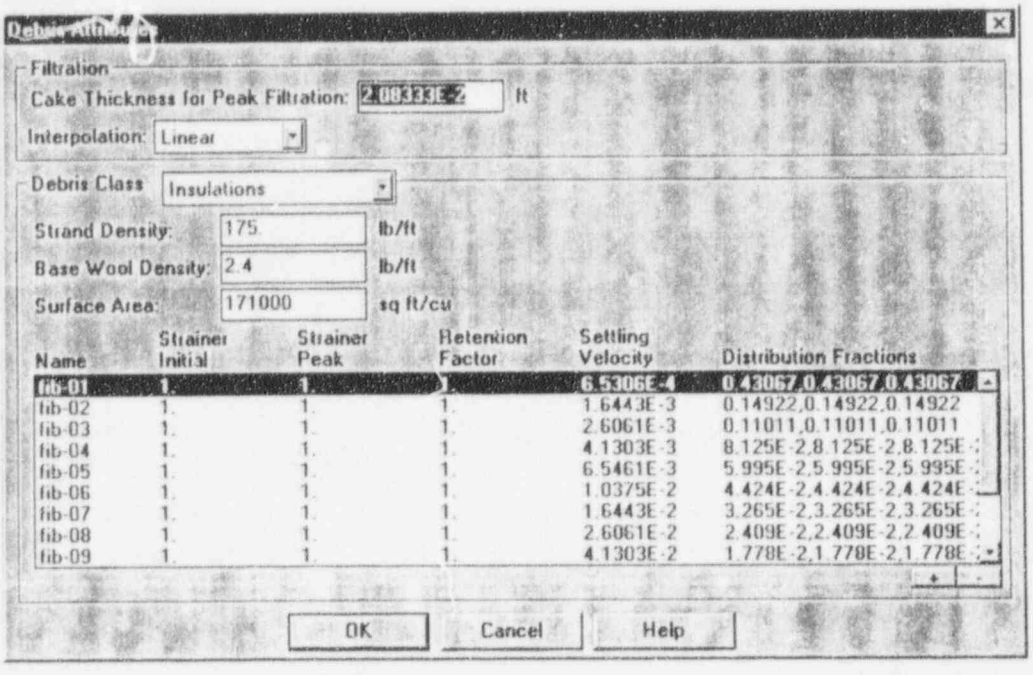

Figure 7: Debris Attributes

Event Scenario Profiles

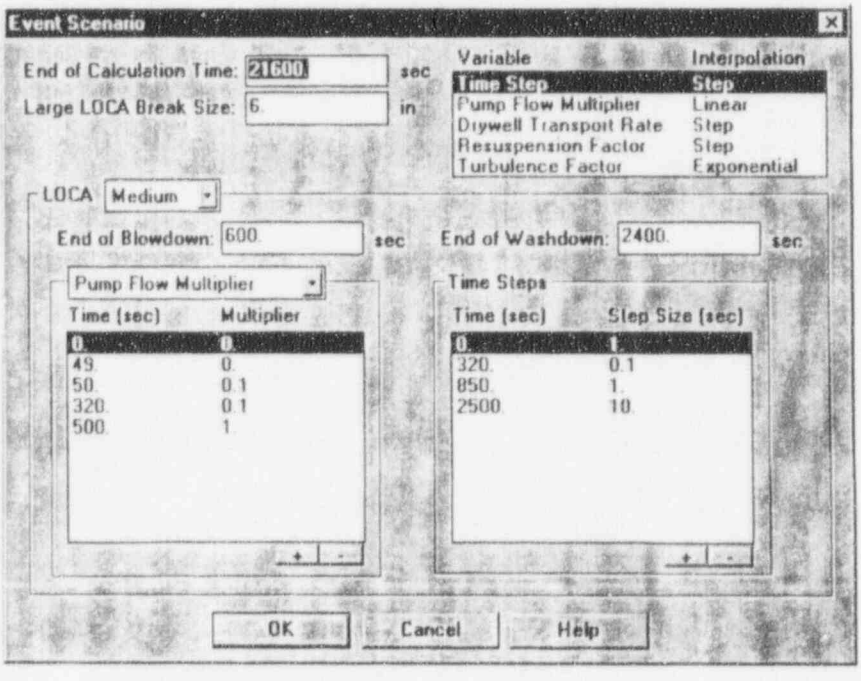

Figure 8: Event Scenario Profiles

Reports

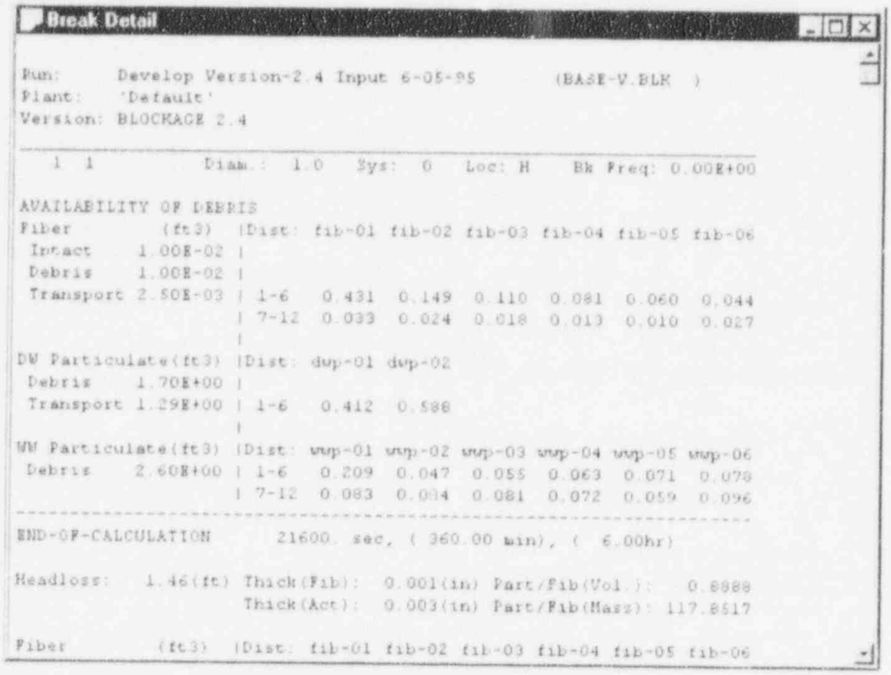

Figure 9: Reports

Time-Based Variable Plots

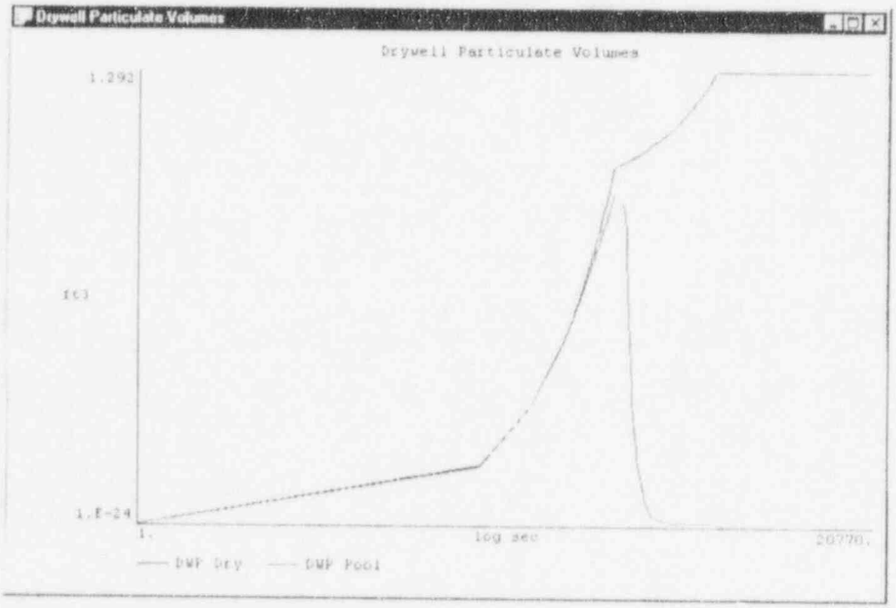

Figure 10: Time-Based Variable Plots

NRC FORM 335 (2-89) NRCM 1102, 3201, 3202

U.S. NUCLEAR REGULATORY COMMISSION

BIBLIOGRAPHIC DATA SHEET

(See instructions on the reverse)

1. REPORT NUMBER (Assigned by NRC. Add Vol., Supp., Rev., and Addendum Numbers, if any.)

NUREG/CP-0149

Vol. 3

2. TITLE AND SUBTITLE

Proceedings of the Twenty-Third Water Reactor Safety Information Meeting

Structural & Seismic Engineering, Primary Systems Integrity, Equipment Operability and Aging, ECCS Strainer Blockage Research & Regulatory Issues

3. DATE REPORT PUBLISHED

MONTH: March YEAR: 1996

4. FIN OR GRANT NUMBER

A3988

5. AUTHOR(S)

Compiled by Susan Monteleone, BNL

6. TYPE OF REPORT

Conference Proceedings

7. PERIOD COVERED (Inclusive Dates)

October 23-25, 1995

8. PERFORMING ORGANIZATION – NAME AND ADDRESS (If NRC, provide Division, Office or Region, U.S. Nuclear Regulatory Commission, and mailing address; if contractor, provide name and mailing address.)

Office of Nuclear Regulatory Research
U.S. Nuclear Regulatory Commission
Washington, DC 20555-0001

9. SPONSORING ORGANIZATION – NAME AND ADDRESS (If NRC, type "Same as above"; if contractor, provide NRC Division, Office or Region, U.S. Nuclear Regulatory Commission, and mailing address.)

Same as Item 8 above.

10. SUPPLEMENTARY NOTES C. Bonsby, NRC Project Manager
Proceedings prepared by Brookhaven National Laboratory

11. ABSTRACT (200 words or less)

This three-volume report contains papers presented at the Twenty-Third Water Reactor Safety Information Meeting held at the Bethesda Marriott Hotel, Bethesda, Maryland, October 23-25, 1995. The papers are printed in the order of their presentation in each session and describe progress and results of programs in nuclear safety research conducted in this country and abroad. Foreign participation in the meeting included papers presented by researchers from France, Italy, Japan, Norway, Russia, Sweden, and Switzerland. The titles of the papers and the names of the authors have been updated and may differ from those that appeared in the final program of the meeting.

12. KEY WORDS/DESCRIPTORS (List words or phrases that will assist researchers in locating the report.)

BWR type reactors-reactor safety, international organizations-meetings, PWR type reactors-reactor safety, water cooled reactors-proceedings, Human Factors, Reactor Control Systems, Reactor Instrumentation, Probabilistic Estimation, Risk Assessment

13. AVAILABILITY STATEMENT

Unlimited

14. SECURITY CLASSIFICATION

(This Page) Unclassified

(This Report) Unclassified

15. NUMBER OF PAGES

16. PRICE

Federal Recycling Program

UNITED STATES
NUCLEAR REGULATORY COMMISSION
WASHINGTON, D.C. 20555-0001

OFFICIAL BUSINESS
PENALTY FOR PRIVATE USE, $300

SPECIAL FOURTH-CLASS RATE
POSTAGE AND FEES PAID
USNRC
PERMIT NO. G-67